Arcjet Thruster Research And Technology

Contract NAS 3-24842
Final Report - NASA CR-180865
February 1988

Prepared For:
NASA/Lewis Research Center
Cleveland, Ohio 44135

Aerojet TechSystems Company

Technion Incorporated

ARCJET THRUSTER RESEARCH AND TECHNOLOGY

Contract NAS 3-24842

FINAL REPORT
NASA CR-180865

February 1988

Prepared for:

NASA/Lewis Research Center
Cleveland, OH 44135

Prepared by:

Darby B. Makel
Aerojet TechSystems Company
P.O. Box 13222
Sacramento, CA 95813

Gordon L. Cann
Technion Inc.
17751-F Sky Park East
Irvine, CA 92714

RPT/BB0642

ABSTRACT

The design, analysis, and performance testing of an advanced lower power arcjet is described. Aerojet TechSystems Company and Technion, Inc. in conjunction with NASA Lewis Research Center have conducted a research program to study a high impedance, vortex stabilized 1-kw class arcjet. A baseline research thruster has been built and endurance and performance tested. This advanced arcjet has demonstrated long life time characteristics, but lower than expected performance. Analysis of the specific design has identified modifications which should improve performance and maintain the long life time shown by the arcjet.

FOREWORD

This program is conducted under Contract NAS 3-24842 for the NASA/Lewis Research Center, Auxiliary Propulsion Branch. NASA Program Manager is Jim Stone. The program is conducted by Aerojet TechSystems Company, Research and Technology Department, Rich LaBotz, Director. Aerojet Program Manager is Don Jassowski, and the Project Engineer is Darby Makel. Technion, Incorporated, is a major participant in the program, with extensive participation by Gordon Cann, President and Program Manager. Involvement of Technion includes conceptual and detailed design, fabrication, and Series I testing of the arcjet. Interpretation of test results, formulation of conclusions and recommendations, and preparation of the final report are by Aerojet TechSystems Company.

EXECUTIVE SUMMARY

This contract is a result of the NASA Lewis Research Center RFP 3-142500, entitled "Arcjet Thruster Research and Technology." The objective of the program is to advance and demonstrate the state of the art for arcjet thrusters. Specific technology goals for the program were an Isp of 400 seconds, an efficiency of 40% and a 3000 hour life. A thruster has been designed to operate with storable propellants over the power range of 0.5 to 3.0 kW.

The program consists of two phases. This report summarizes the work done during the Phase I of the program. The first task of Phase I was an assessment of the state-of-the-art technology utilizing ongoing literature studies at Aerojet TechSystems Co. and Technion Inc. Information was assembled into a state-of-the-art summary report to NASA, drawing together the available information from the literature, workers in the field, and our experience. The results of the Technion 1 kW thruster development program were included.

The available data and models were compared with those required in order to identify areas needing further research. From this, a detailed program of model development and empirical data collection was prepared. Research in pertinent subjects has been performed. Topics in the study include analysis and testing of arc-gas physics, electrode design, low Reynolds number nozzles, and electrical characterization. This research has utilized a nominal 1 kW thruster for experimental studies. The arcjet thruster was built in a flight-like prototype configuration, so that the studies would be directly applicable to a flight hardware program. The results of the experimental and analytical efforts have provided a definition of problem areas which must be resolved to develop a 1 kW class arcjet thruster.

The baseline arcjet thruster designed and tested during Phase I of the program is shown in Figure 1. With the goal of a 3000 hour life time as a major driver, the Aerojet/Technion team determined that major design innovations would be required. With this in mind, this arcjet represents a radical

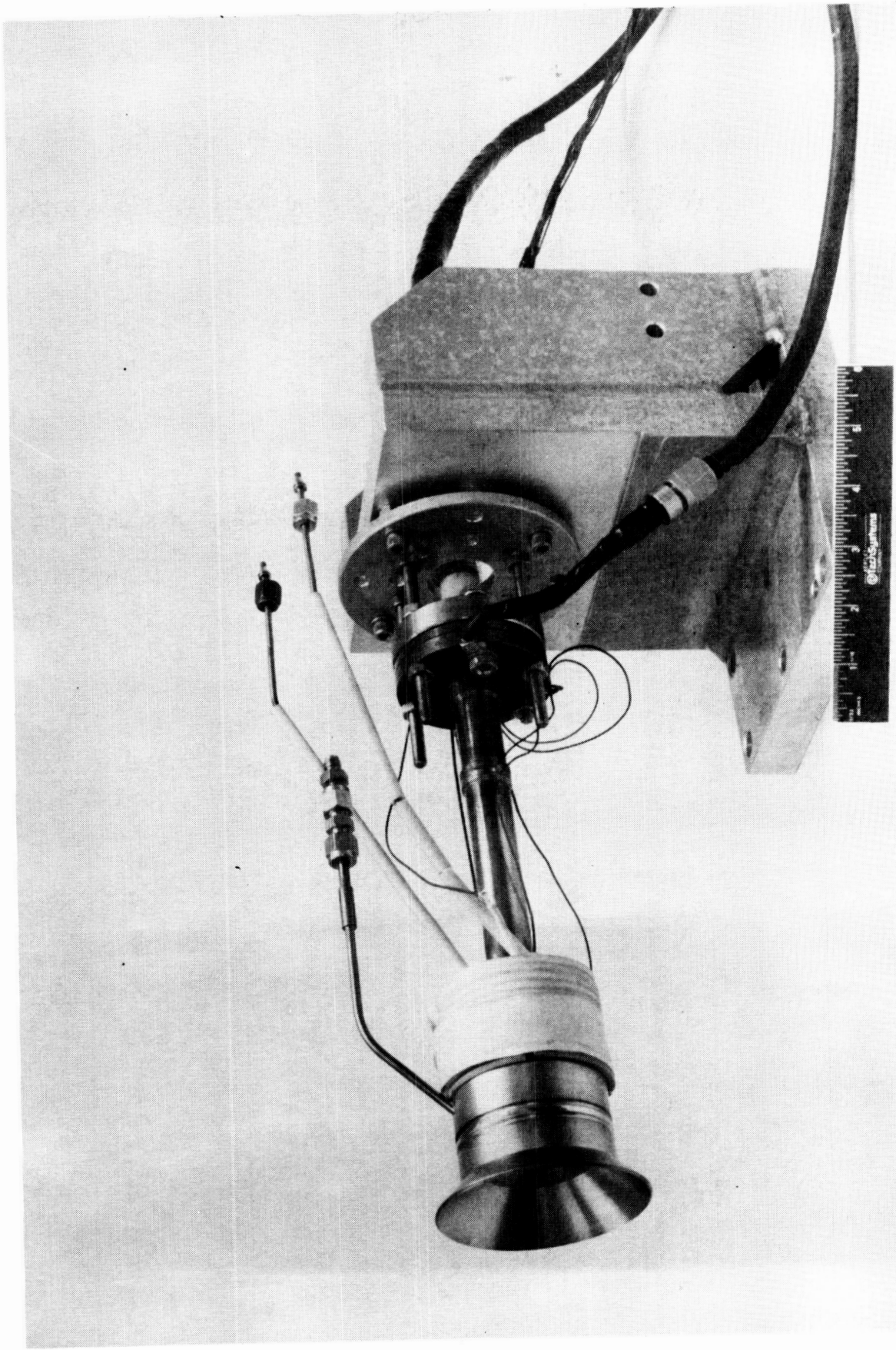

Figure 1. Advanced 1 KW Arcjet Research Thruster

departure from the constricted arc type arcjets investigated during the 1960's. This arcjet has been designed with advanced features for improved life, increased efficiency, and low plume contaminants and RFI. These improvements are achieved by the use of an arc where the anode attachment is upstream of the nozzle in the high pressure region. In addition a mixing chamber upstream of the nozzle is used to promote recombination of ionized and dissociated species. Since this arcjet is estimated to operate at lower currents than constricted arc arcjets of the 1960's and lower arc centerline temperatures (estimated to be 10,000-12,000 K compared to 30,000-40,000 K for constricted arcjets) electrode losses should be reduced and electrode life increased.

The initial investigation of the advanced arcjet concept was concentrated in the thruster design and experimental characterization tasks at Technion Inc. During this part of the program analytic models of arc/vortex gas interaction were studied along with the results of a joint Aerojet/Technion 1 kW arcjet IR&D program. From this work resulted the design of the advanced 1 kW class arcjet thruster. The thruster was built at Technion and the initial test series (i.e., Test Series 1) was performed in the Technion bell jar test facility. During this test series, the arc stability, electrode erosion, current/voltage relation, and arc initiation with propellant were all investigated. In all, over 100 hours of operation were accumulated including 284 starts and over 70 thermal cycles of the hardware. The results of the testing at Technion verified the feasibility of using the advanced vortex-stabilized/magnetically-driven arc in a thruster configuration. Without optimizing electrode geometry, erosion rate measurements indicate that this thruster's life characteristics are capable of achieving a 3000 hour life goal.

The second part of the Phase I test program consisted of performance mapping the baseline thruster and establishing the data base required to develop the thruster into a flight-like unit. The performance testing was performed in Aerojet's Arcjet Test Facility. The thrust levels produced by the arcjet (less than 25 gm) required precise measurement to determine the

specific impulse and thrust efficiency of the unit. The best performance that could be achieved was Isp of 310 sec and thrust efficiency of 22%.

There are three possible causes for the lower than expected performance. First, convective heat transfer from the gas to the thruster body in the mixing chamber lowered the specific enthalpy of the gas prior to expansion through the nozzle. Viscous losses and inefficient expansion of the arc heated gas through the nozzle contributed significant momentum losses. Finally, the most significant cause is that 40% of the propellant mass flowrate was injected in the mixing chamber and did not pass through the arc. The intent of the gas injection in the mixing chamber is to promote mixing, and to provide film cooling in the nozzle throat. The design flow split was 75% of the total flow through the arc and 25% of the total propellant flow injected in the mixing chamber. The flow split is not variable in the research thruster as currently designed. It has been concluded that the flow split must be optimized before high performance can be achieved. Analysis subsequent to the fabrication of the thruster and borne out by the experimental results indicate that there was excessive mixing and excessive film cooling.

In addition to performance testing and evaluation of the thruster during the second half of the program, design and analysis of flight-like features was performed. A permanent magnet (using high temperature, rare earth colbalt) was designed and built for the thruster but was not tested. Also built was a high capacity hydrazine gas generator for extended duration tests with liquid hydrazine propellant which was also not used. In all, no hardware design problems were encountered that would prevent the development of the research thruster into flight-like hardware.

Continued development of the advanced 1 kW arcjet thruster at the research thruster level is required before the concept is ready for development into flight hardware. Optimization of the features of the advanced arcjet such as the mix chamber, anode attachment location, and flow-split will yield potentially useful levels of performance.

TABLE OF CONTENTS

LIST OF TABLES

LIST OF FIGURES

LIST OF FIGURES (cont.)

LIST OF FIGURES (cont.)

LIST OF FIGURES (cont.)

LIST OF FIGURES (cont.)

LIST OF FIGURES (cont.)

LIST OF FIGURES (cont.)

1.0 INTRODUCTION

This contract is a result of the NASA/Lewis Research Center RFP 3-142500, entitled "Arcjet Thruster Research and Technology." The objective of the program is to advance and demonstrate the state of the art for arcjet thrusters. Specific technology goals for the program are an Isp of 400 seconds, an efficiency of 40%, and a 3000-hour life. Storable propellants were used. The power range goal was 0.5 to 3.0 kW.

The Phase I program consisted of two major tasks. Task 1.0 provided an assessment of the state-of-the-art of arcjet technology utilizing ongoing literature studies at Aerojet TechSystems Co. and Technion Inc. Information was assembled into a state-of-the-art summary report to NASA, drawing together the available technology information from the literature, workers in the field, and our experience. The results of the Technion 1 kW thruster development program were included. The results of Task 1.0 were published in Ref. 1.

The available data and models were compared with those required in order to identify areas needing further research in Task 2.0. From this, a detailed program of model development and empirical data collection was prepared. Research in pertinent subjects was planned. Topics in the study included analysis and testing of low Reynolds number nozzles, arc-gas physics, electrode design, and electrical characterization. This research used a nominal 1 kW thruster for experimental studies. The thruster was configured into a flight-like prototype configuration, but with a water cooled magnet, so that the studies would be directly applicable to a flight hardware program. The results of our experimental and analytical efforts have been used to develop the data base needed to evolve the arcjet into a flight-type design.

The task descriptions for Phase I are summarized as follows:

PHASE I - ARCJET TECHNOLOGY DEVELOPMENT

Task 1.0 - State-of-the-Art Assessment

1.0, Introduction (cont.)

Task 2.0 - Research and Technology Assessment

This task consisted of five subtasks:

Task 2.1 - Design and Analysis
Task 2.2 - Fabrication Support
Task 2.3 - Testing
Task 2.4 - Data Analysis
Task 2.5 - Final Design and Performance Prediction

Task 5.0 - Reports

The following sections describe the activities of the above tasks. In addition recommendations are made based upon the conclusions of the program.

2.0 STATE-OF-THE-ART ASSESSMENT

The first task of the program consisted of an assessment of the state of the art of technology important to arcjet research. The ongoing literature studies at Aerojet and Technion served as the basis for this assessment. Available information on arcjets and related technologies such as arc physics, propellants, power conditioning units, viscous gas dynamics, and arc flow interactions have been reviewed and summarized as they relate to arcjet development. The State-of-the-Art Assessment was submitted as a report at the conclusion of Task 1.0 in February, 1986 [1]. The report included an extensive bibliography with abstracts. The following section summarizes the scope and topics covered in that report.

2.1 SUMMARY OF IMPORTANT TOPICS REVIEWED IN STATE-OF-THE-ART ASSESSMENT

Arcs have existed in concept since the turn of the century. Arcs were used to heat gases to extreme temperatures. Small, high-speed wind tunnels in the 1950's used arc heating. Because the specific impulse of a propulsive device can be related to temperatures which at the core of an electric arc discharge may be as high as 50,000 K, it was natural that the electric arc was looked upon as a means of heating a propellant considerably above the 3000K range available chemically [2].

There was a significant effort during the early 1960's to develop high-Isp arcjets[3,4,5,6]. Most of the efforts were at higher power levels than the present program and focused on the constricted arc approach where the anode attachment region is in the nozzle downstream from the throat. The various arcjet efforts encountered the same basic problems; namely,

1) discharge erosion of the nozzle,

2) low efficiency due to thermal losses and frozen flow losses, and

3) cathode erosion.

2.1, Summary of Important Topics Reviewed in State-of-the-Art Assessment (cont.)

The projects were terminated due to changes in mission requirements and lack of available power sources.

During the late 1960's and through the 1970's, much of the high-pressure arc research was oriented toward arc heaters[7,8,9]. Designs evolved from the constricted arcs to coaxial arc heaters to vortex-stabilized arc heaters. Significant effort went into finding ways to increase the enthalpy of the gas and to extend the lifetime of equipment. Efficiency became an issue with the megawatt arc heater systems.

Recent trends have changed the applicability of arcjet propulsion. High efficiency, high power, solar arrays are being developed with substantially improved power/mass ratio compared with those that than have been used on prior spacecraft. Satellites are evolving from fractional kilowatt capability to multikilowatt systems, with large-capacity battery storage. By careful management of on-board power, the power may be "free" for arcjet propulsion. Nuclear electric systems are under development with excellent power/mass properties. Interplanetary missions are now feasible that could not be undertaken with chemical systems.

Arcjets are being considered for missions requiring high efficiency, high Isp, and low to moderate thrust. The missions fall into two categories; stationkeeping and primary propulsion. The use of arcjets for these missions requires consideration of not only the thruster, but the entire propulsion system. An arcjet propulsion unit consists of the thruster, propellant supply system, power conditioning, power source and controls. The state-of-the-art assessment report covered each of these areas as they pertain to low power (0.5 to 3.0 kW) arcjets. The chapter headings of the report are:

1. Missions and Applications
2. Space Power Sources
3. Power Conditioning
4. Arc/Gas Flow Interactions
5. Cathode Phenomena

2.1, Summary of Important Topics Reviewed in State-of-the-Art Assessment (cont.)

6. Anode Attachment
7. Magnets
8. Mixing Chambers
9. Nozzles
10. Propellants
11. Hydrazine Gas Systems
12. Materials
13. Vehicle Interactions, Plumes, and RFI
14. Testing

3.0 TASK 2.0 RESEARCH AND TECHNOLOGY

3.1 SCOPE AND OBJECTIVES

Task 2.0 consisted of arcjet model development, construction and testing of a high impedance, vortex stabilized arcjet, and empirical research on critical issues identified in the Task 1.0 State-of-the-Art Assessment. This work has covered the following topics.

1. Analytical modeling of vortex flow/arc interaction.

2. Performance estimates for a high impedance, vortex stabilized arcjets.

3. Testing of low Reynolds number nozzles.

4. Design, construction, and testing of a baseline research arcjet thruster.

Work on the baseline research thruster comprised the majority of effort in Task 2.0.

The baseline thruster is a nominal 1 kW unit designed, constructed, and characterized at Technion and later performance tested at Aerojet. The testing of the thruster consisted of two parts, Series 1 testing at Technion and Series 2 testing at Aerojet. The Test Series 1 consisted of establishment of the thrusters operating characteristics, such as current, voltage, electrode gap, and propellant mass flowrate. During Test Series 1 the thruster was operated for over 100 hours with 284 starts and 70 thermal cycles. The Series 2 testing consisted of the performance testing of the thruster with the intent of obtaining a sufficient data base to develop the baseline thruster into a flight-like thruster. During the Series 2 testing the thruster was operated for 5 hours with 26 starts and 8 thermal cycles.

The following sections describe the design of the baseline thruster, including model development, supporting analysis, and the activities of Series 1 and 2 testing.

3.2 DESIGN OF BASELINE THRUSTER AND COMPONENTS

- Thruster Design

The baseline research thruster was designed with as many flight-like features as possible so data would be directly applicable to an actual thruster. The following requirements were imposed on the design of the thruster:

1. Radiation cooled
2. Use of high temperature materials
3. Hard seals (i.e, welds) wherever possible
4. Easily disassembled for inspection of internal parts and electrodes
5. Usable for performance measurements.

Design features of the thruster are shown in Figure 2. Figure 3 shows the assembled thruster and components.

The vortex stabilized arc extends from the cathode on the centerline of the thruster, to an annular anode. Rotation of the anode attachment spot is accomplished with a magnet. An electromagnet was used for the testing, but can be replaced with a permanent magnet. The propellant flow enters the thruster through a feedline connected to the nozzle as shown and is distributed in an annular manifold. The manifold allows the flow to be split between the arc chamber and the mixing chamber. Approximately 75 percent of the propellant flow is designed to be injected tangentially into the arc chamber to provide a vortex flow. Downstream of the anode is a mixing chamber, where the remainder of the propellant flow is injected to provide film

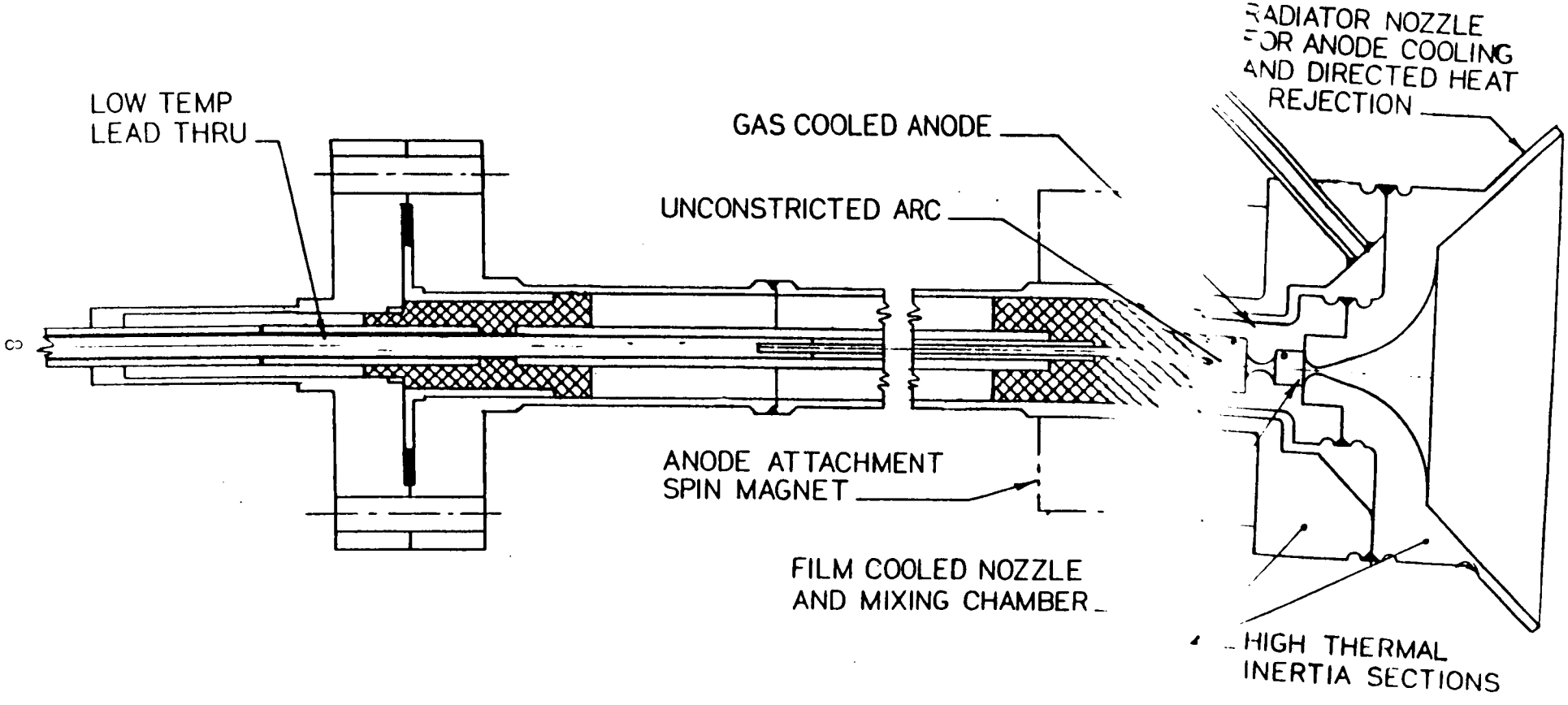

Figure 2. Design Features of Baseline Arcjet

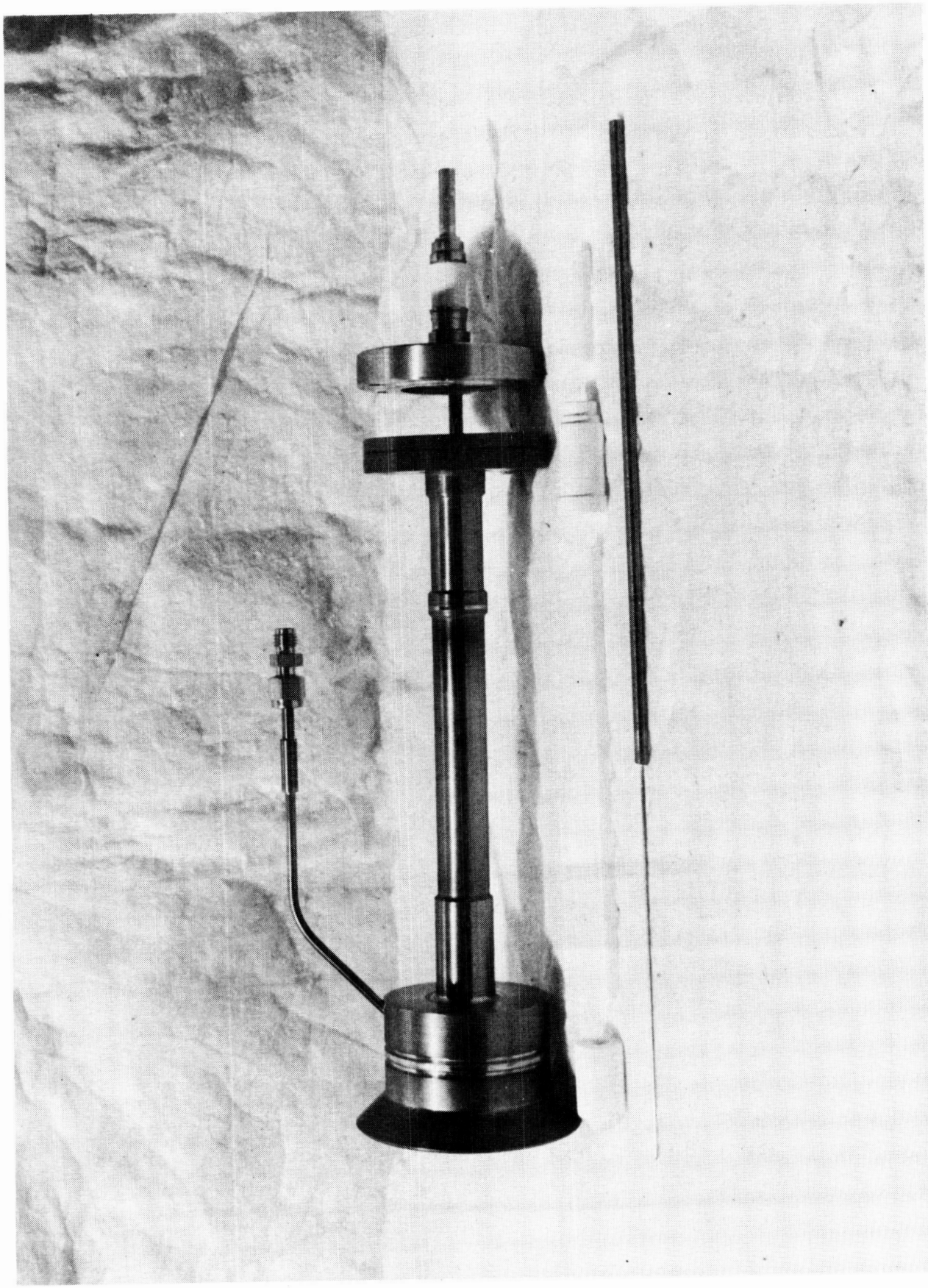

Figure 3. Assembled Arcjet Thruster and Components

3.2, Design of Baseline Thruster and Components (cont.)

cooling in the nozzle. The nozzle is a high area-ratio, trumpet design based on Technion's high performance resistojet experience. The thruster was designed with large thermal masses to provide sufficient conduction cooling of hot surfaces in the thruster interior.

The thruster's body is extended to provide a thermal stand off for the stainless steel mounting flange and low temperature ceramic/metal electrical leadthrough. The cathode, which passes through the vacuum electrical feedthrough is insulated by boron nitride spacers and alumina tubing to prevent electrical breakdown to the thruster body. The nozzle and outer thruster body are made of TZM moly and are welded to the thoriated tungsten anode. A complete list of the thruster components is given below.

Part	Material
Nozzle	TZM moly
Propellant Feed Tube	TZM moly
Anode	Thoriated Tungsten
Cathode	Thoriated Tungsten
Aft Body	Stainless Steel
Arc Chamber Insulator	Boron Nitride
Cathode Insulator	Alumina
Aft Insulator	Boron Nitride
Rear Seal/Electrical Feed Through	Stainless Steel and Ceramic
Electromagnet	Copper Tubing

Drawings of individual components are given in Figures 4 through 22.

During Test Series 2, a minor modification to the rear flange assembly was required to ensure against a damaging electrical breakdown to the arcjet body. Figure 23 shows the flange/feed through with the aft insulator cemented in place and an alumina tube inserted into the aft insulator. In order to ensure proper alignment of the cathode through the new rear flange assembly, the shank portion of the cathode, in the region of the new assembly, was reduced in diameter from 0.475 cm to 0.424 cm.

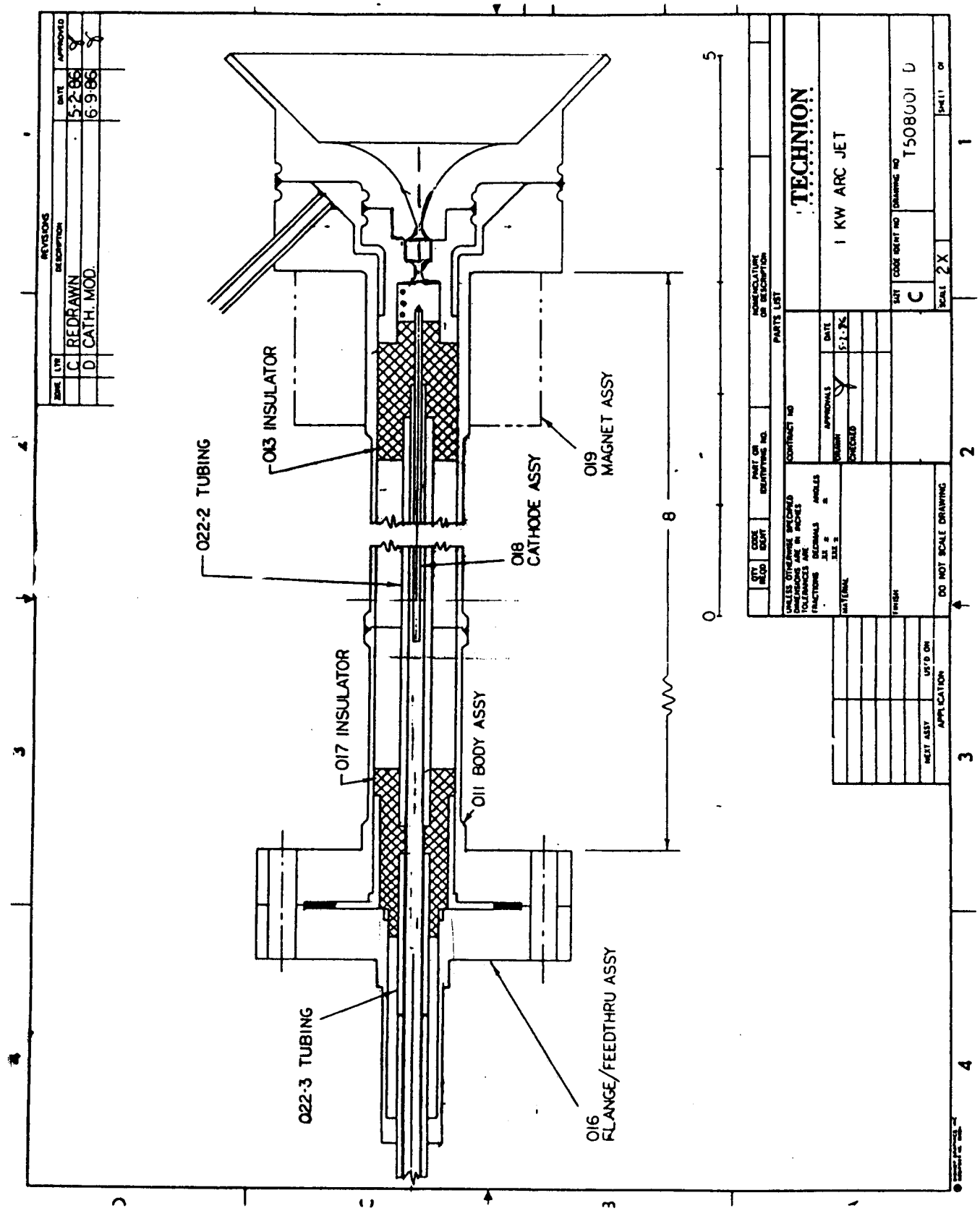

Figure 4. Asembly Drawing of 1 KW Arcjet

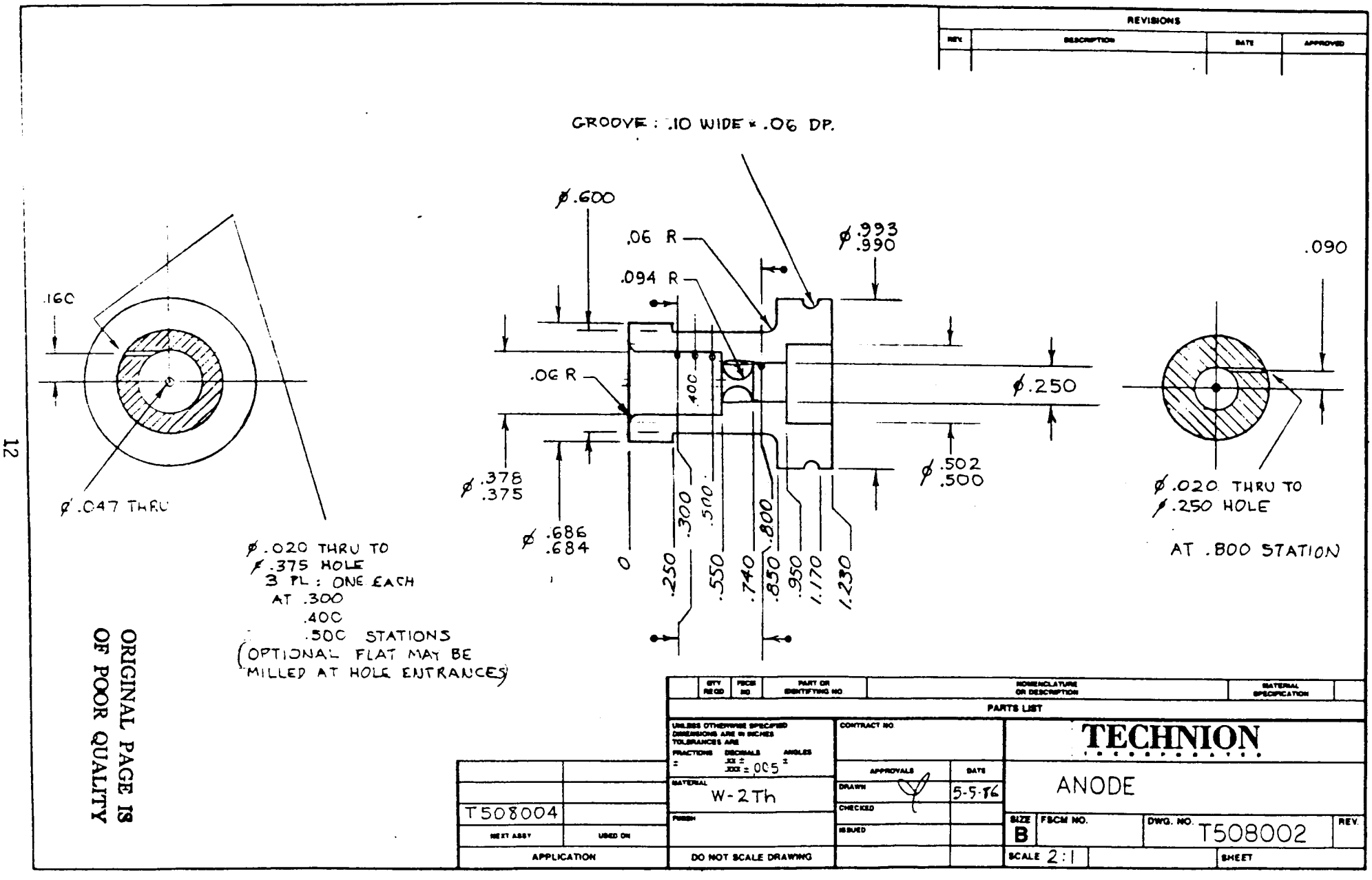

ORIGINAL PAGE IS
OF POOR QUALITY

Figure 5. Anode

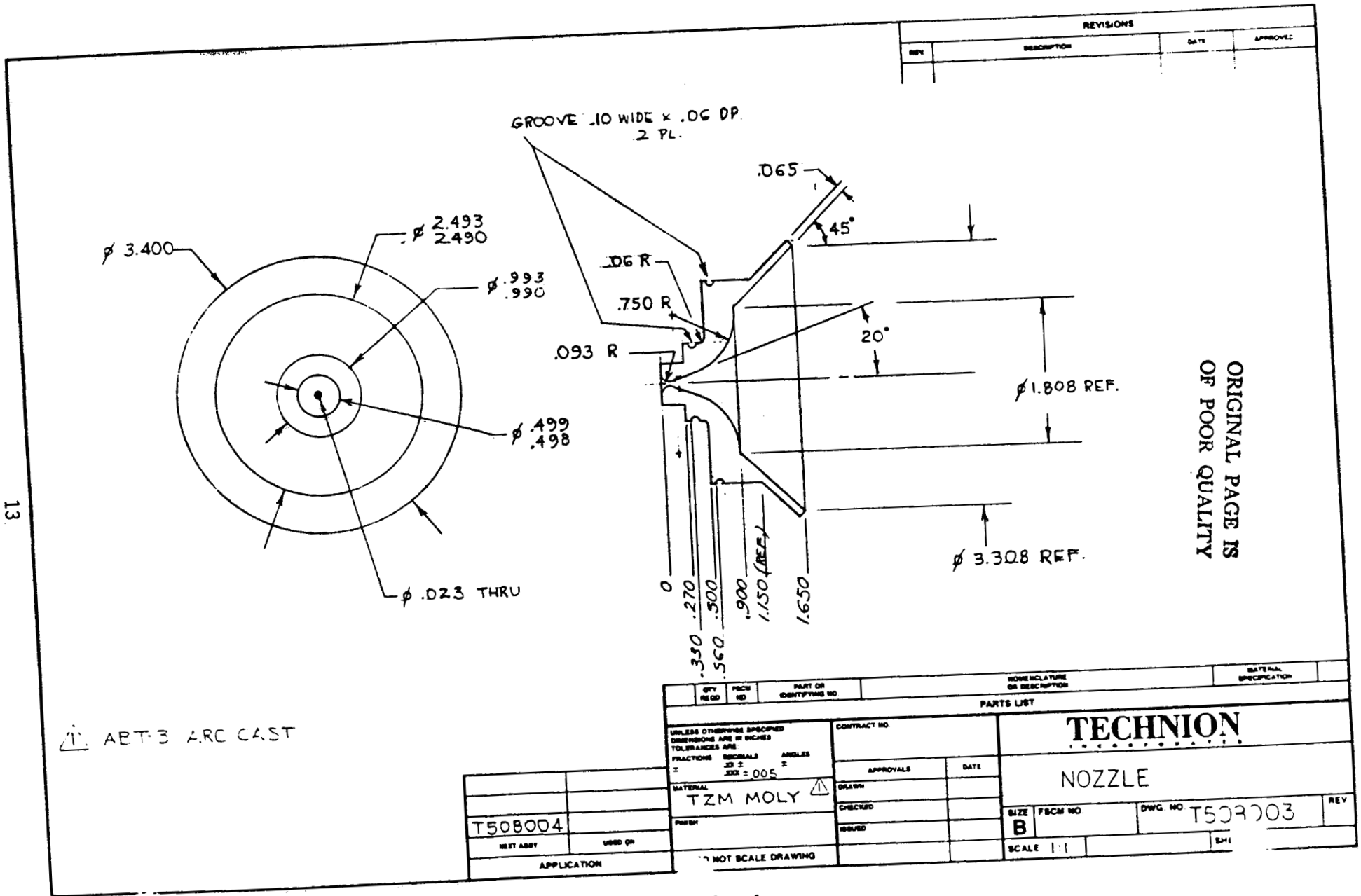

Figure 6. Nozzle

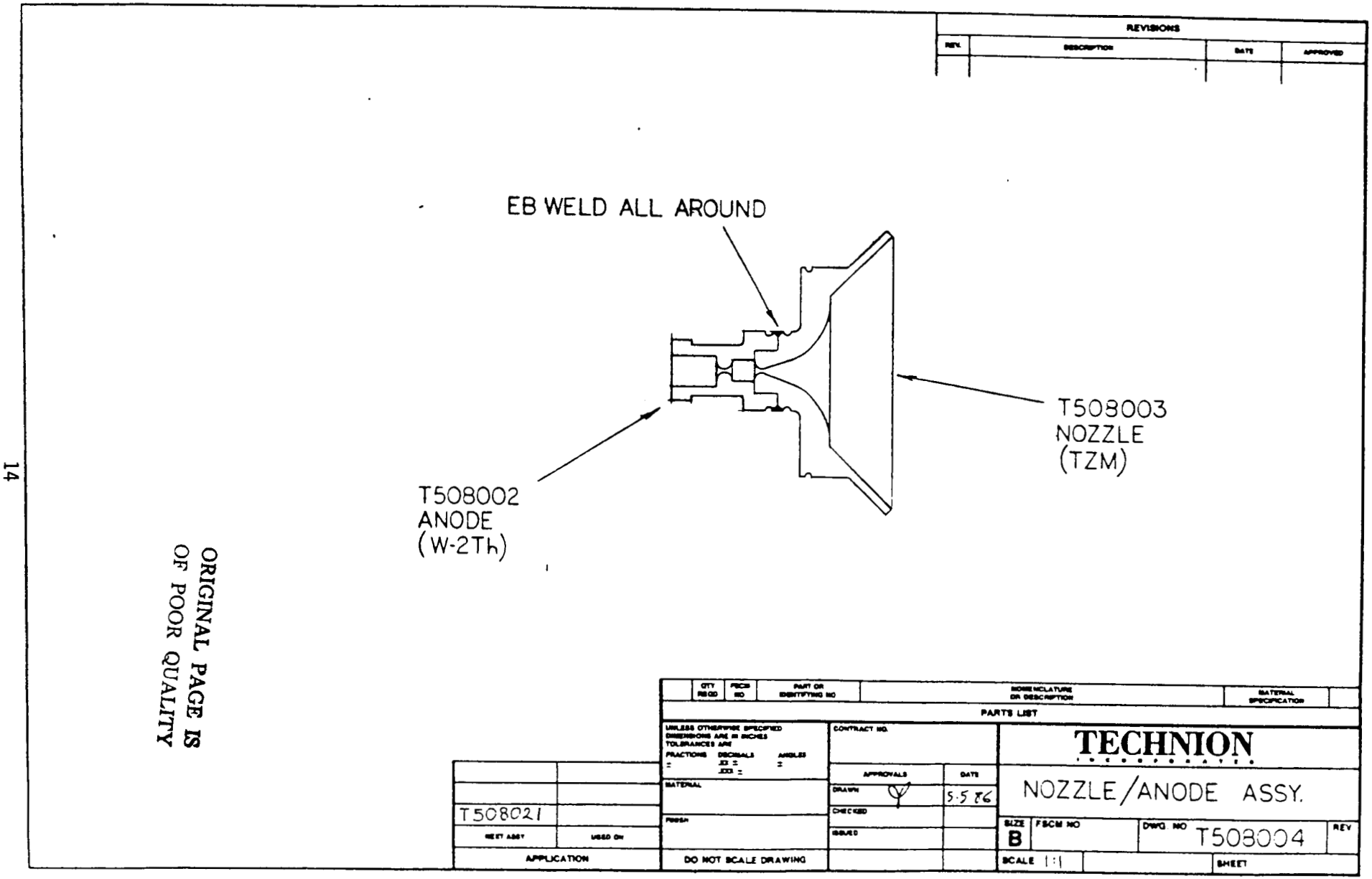

Figure 7. Nozzle/Anode Assy

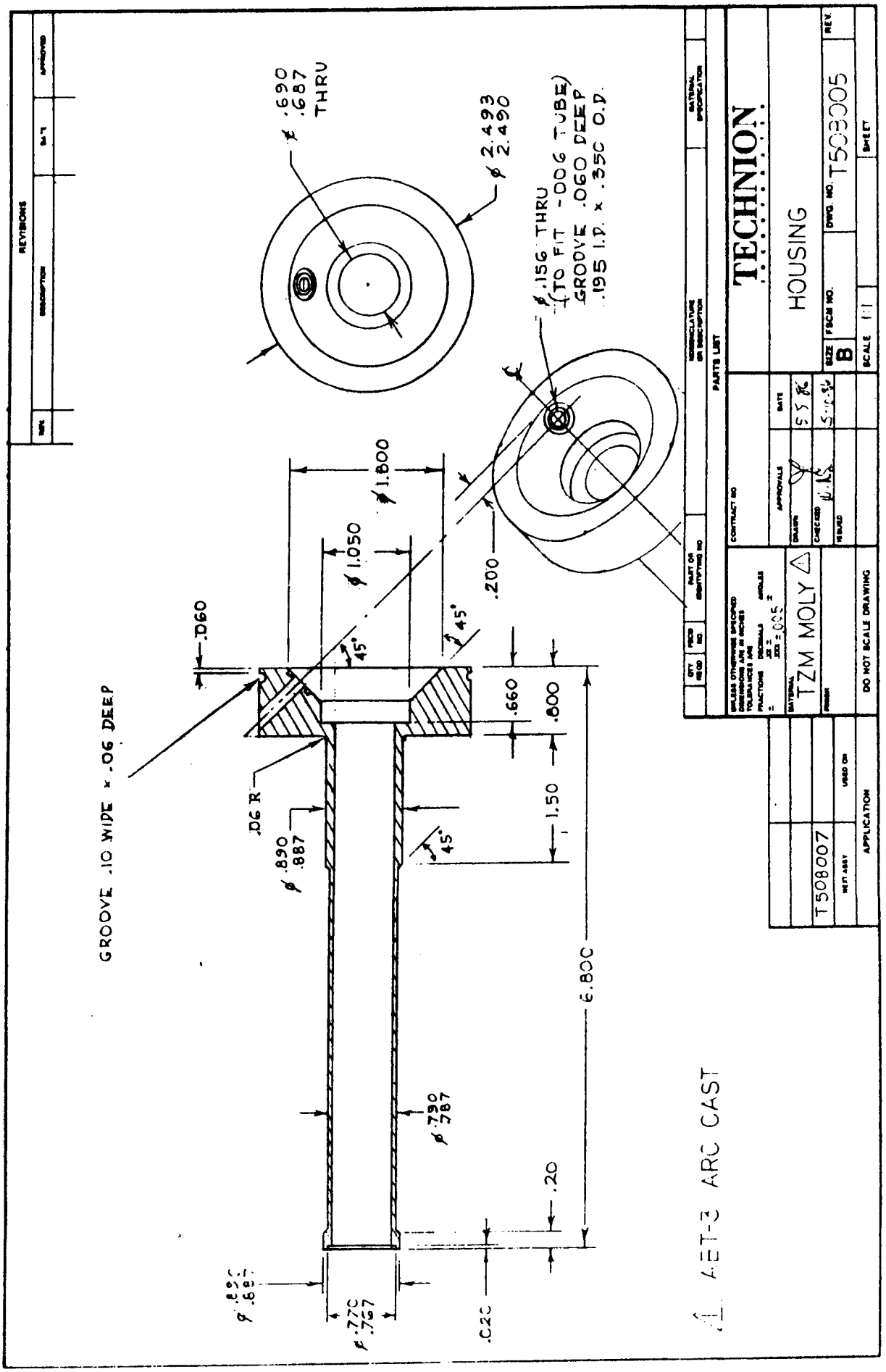

Figure 8. Housing

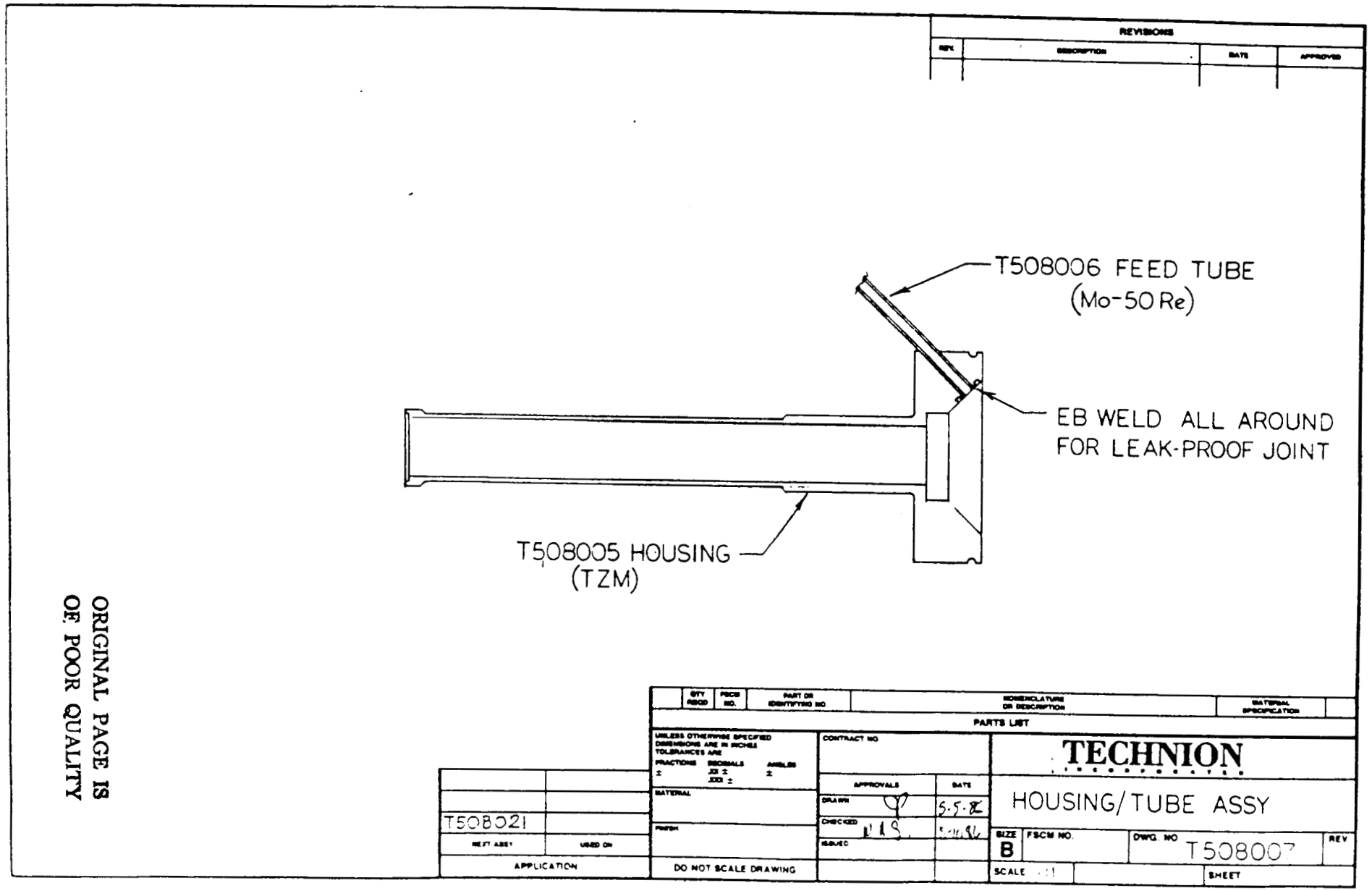

Figure 9. Housing/Tube Assy

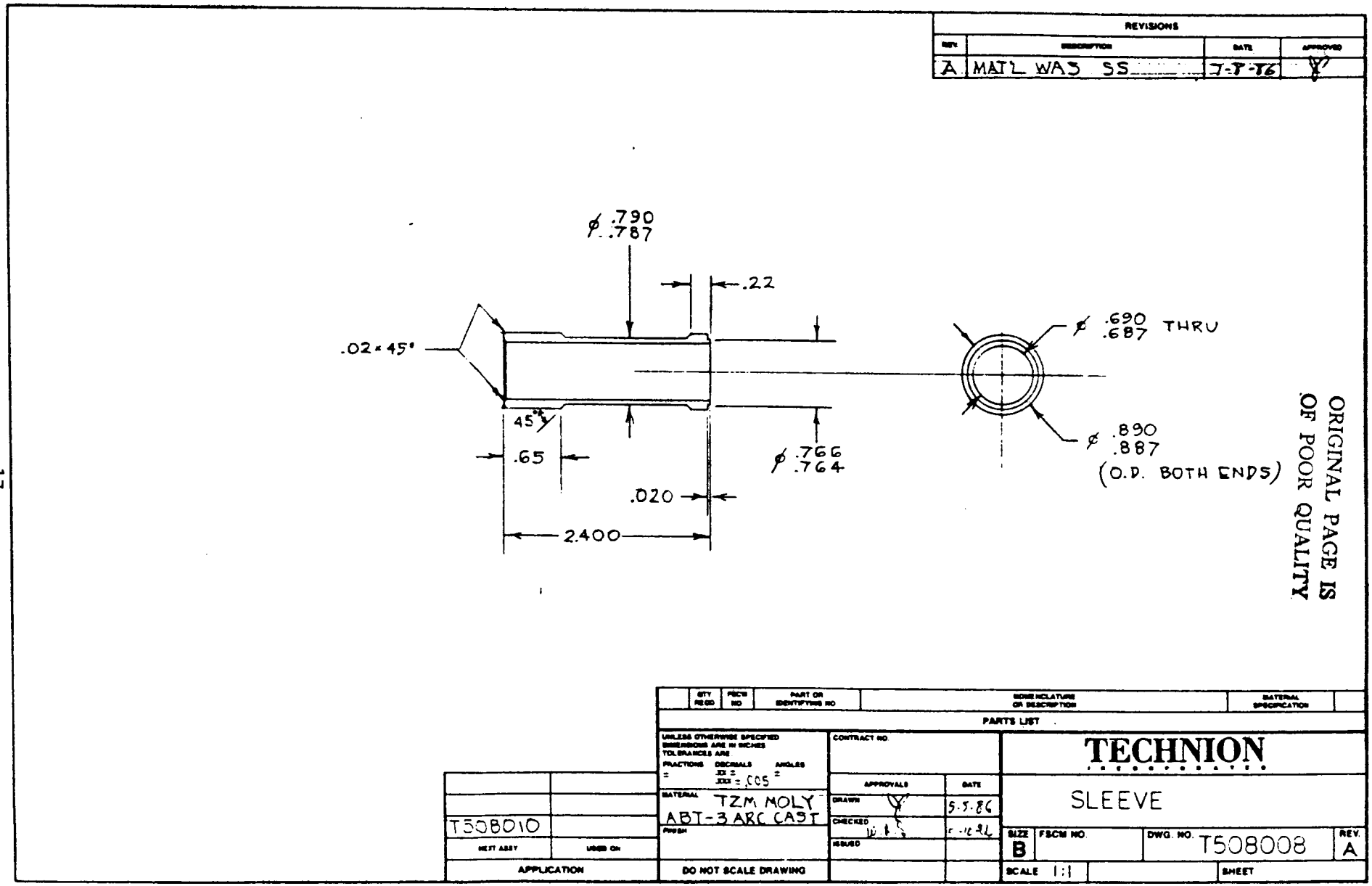

Figure 10. Sleeve

REVISIONS			
REV	DESCRIPTION	DATE	APPROVED
A	.100 WAS .200	7-8-86	

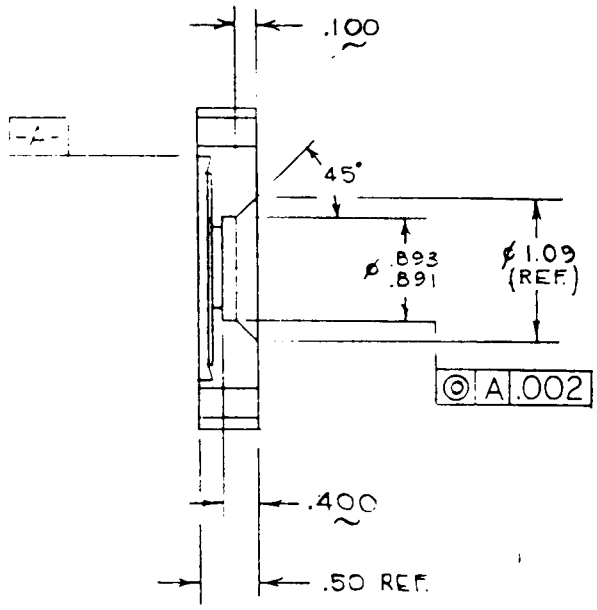

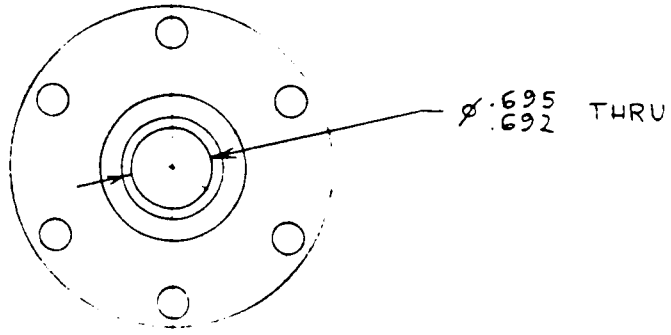

MODIFY 2-3/4 CF BLANK FLANGE AS SHOWN
(NORCAL 275-000 OR SIM.)

QTY REQD	FSCM NO	PART OR IDENTIFYING NO.	NOMENCLATURE OR DESCRIPTION	MATERIAL SPECIFICATION
			PARTS LIST	

UNLESS OTHERWISE SPECIFIED DIMENSIONS ARE IN INCHES
TOLERANCES ARE
FRACTIONS ± DECIMALS .XX ± .XXX ± .005 ANGLES ±

CONTRACT NO.

APPROVALS	DATE
DRAWN	5.5.86
CHECKED	5-6-86
ISSUED	

MATERIAL

FINISH

DO NOT SCALE DRAWING

T508010

NEXT ASSY | USED ON

APPLICATION

TECHNION
INCORPORATED

FLANGE

SIZE B | FSCM NO. | DWG. NO. T503009 | REV A

SCALE 1:1 | SHEET

Figure 11. Flange

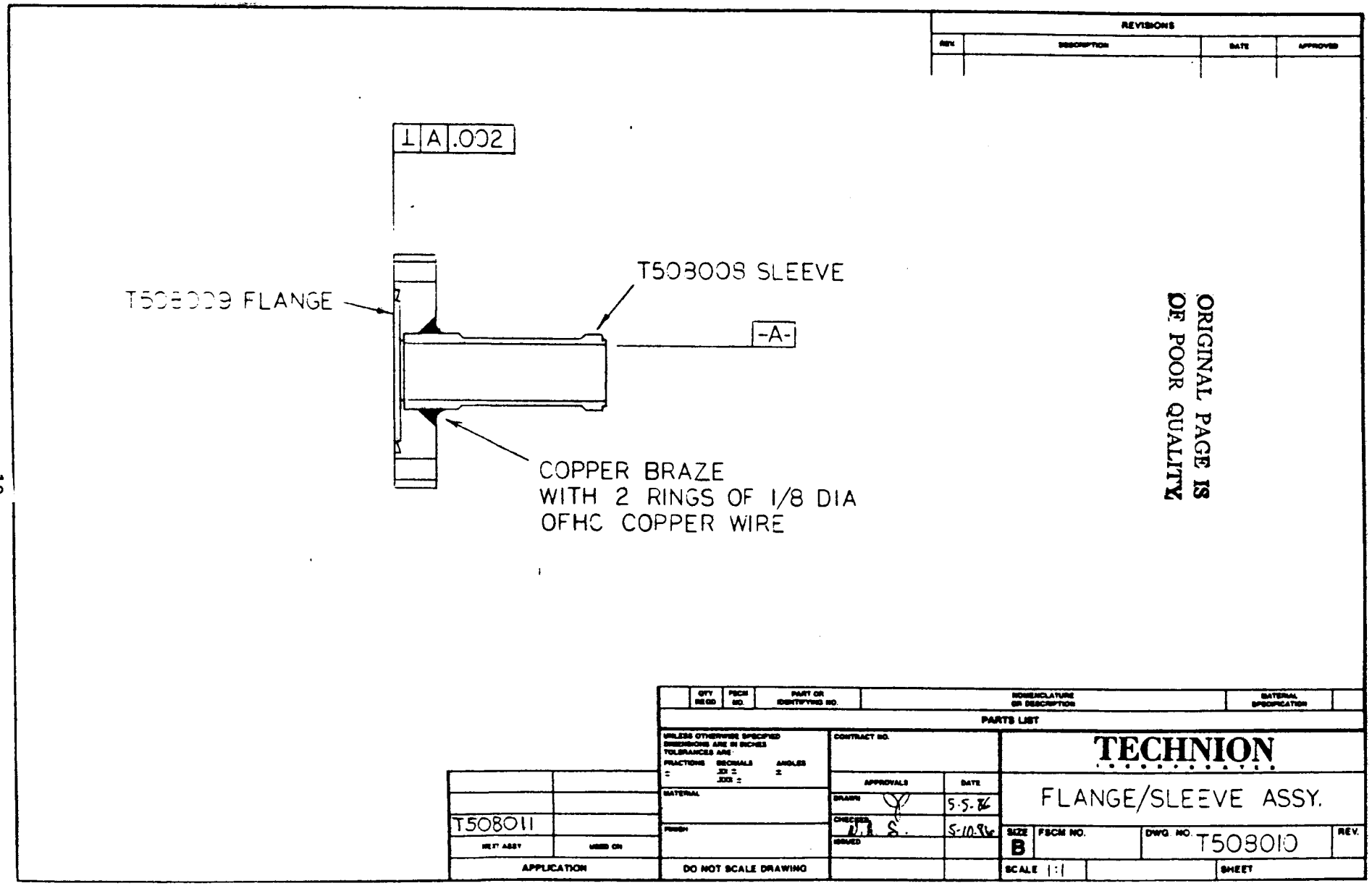

Figure 12. Flange/Sleeve Assy

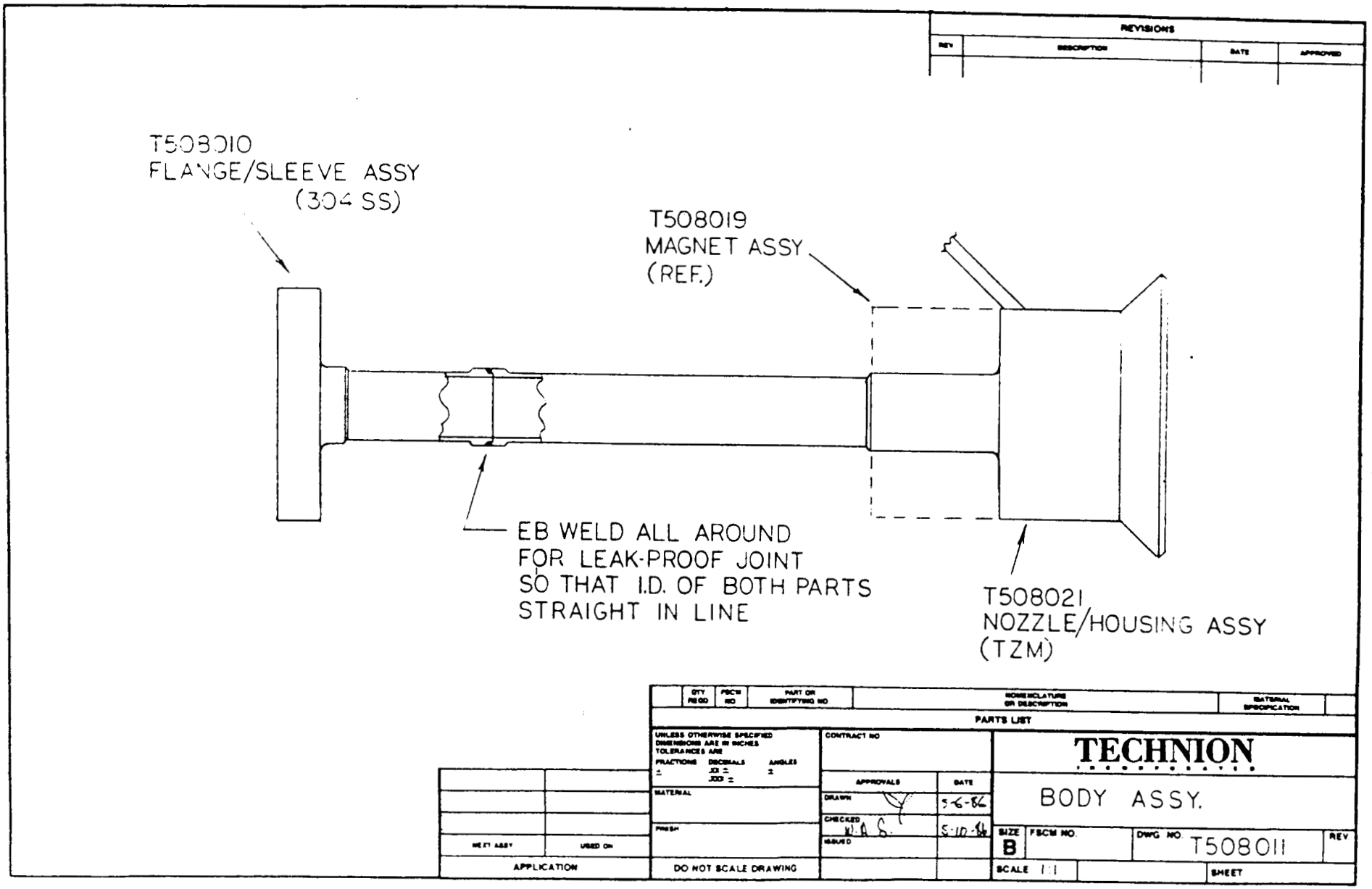

Figure 13. Body Assy

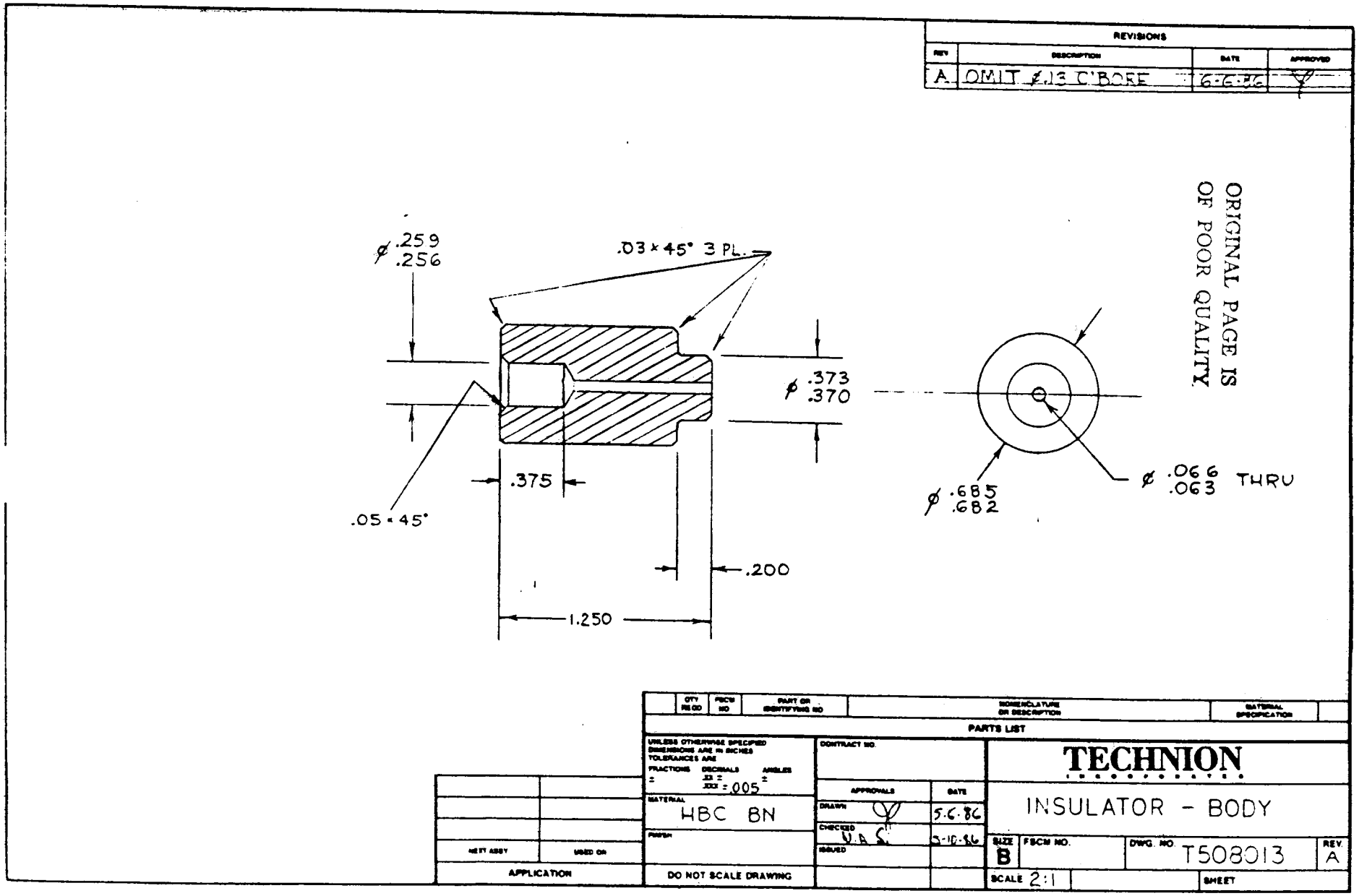

Figure 14. Insulator - Body

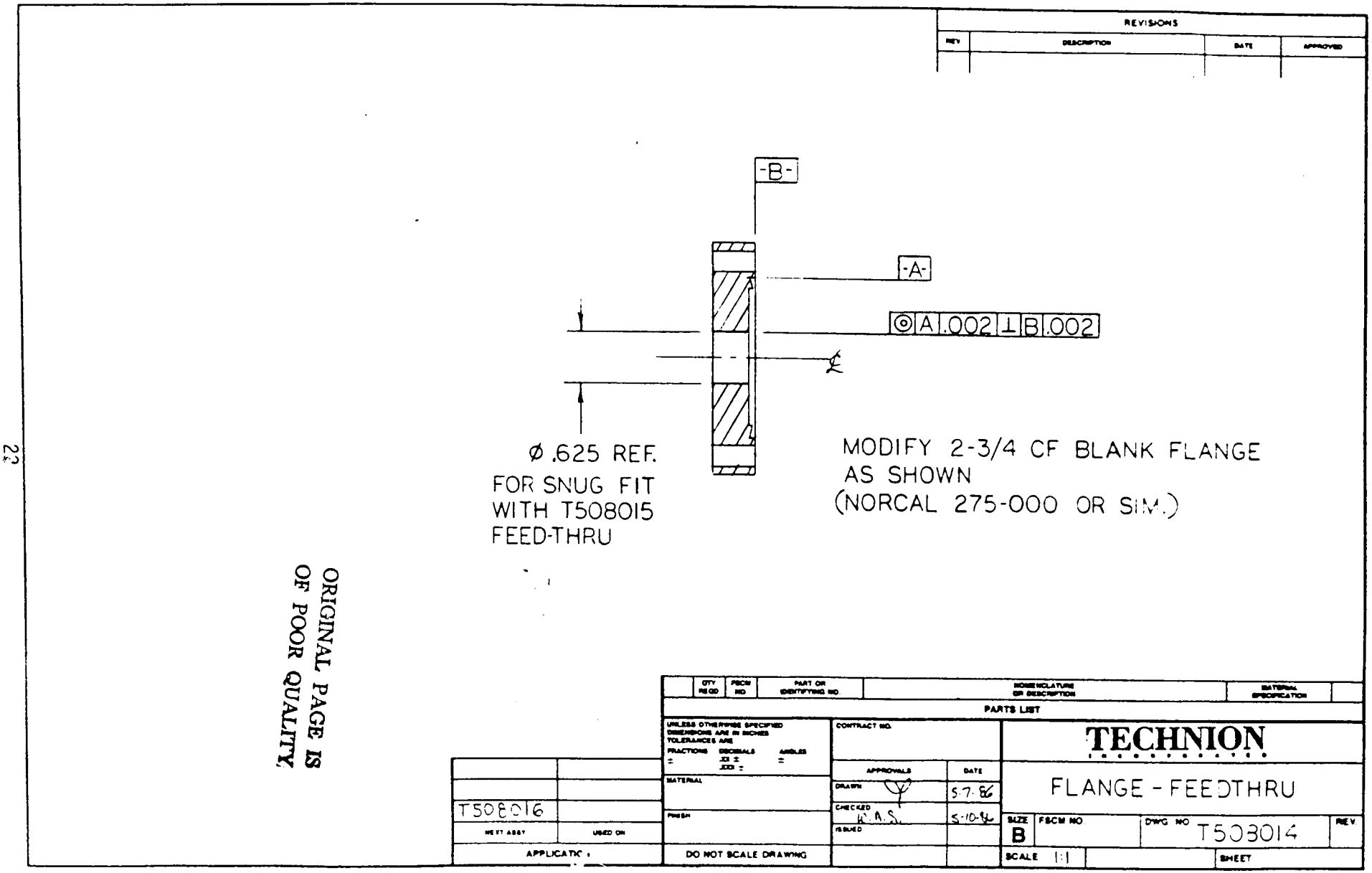

ORIGINAL PAGE IS
OF POOR QUALITY

Figure 15. Flange - Feed-Thru

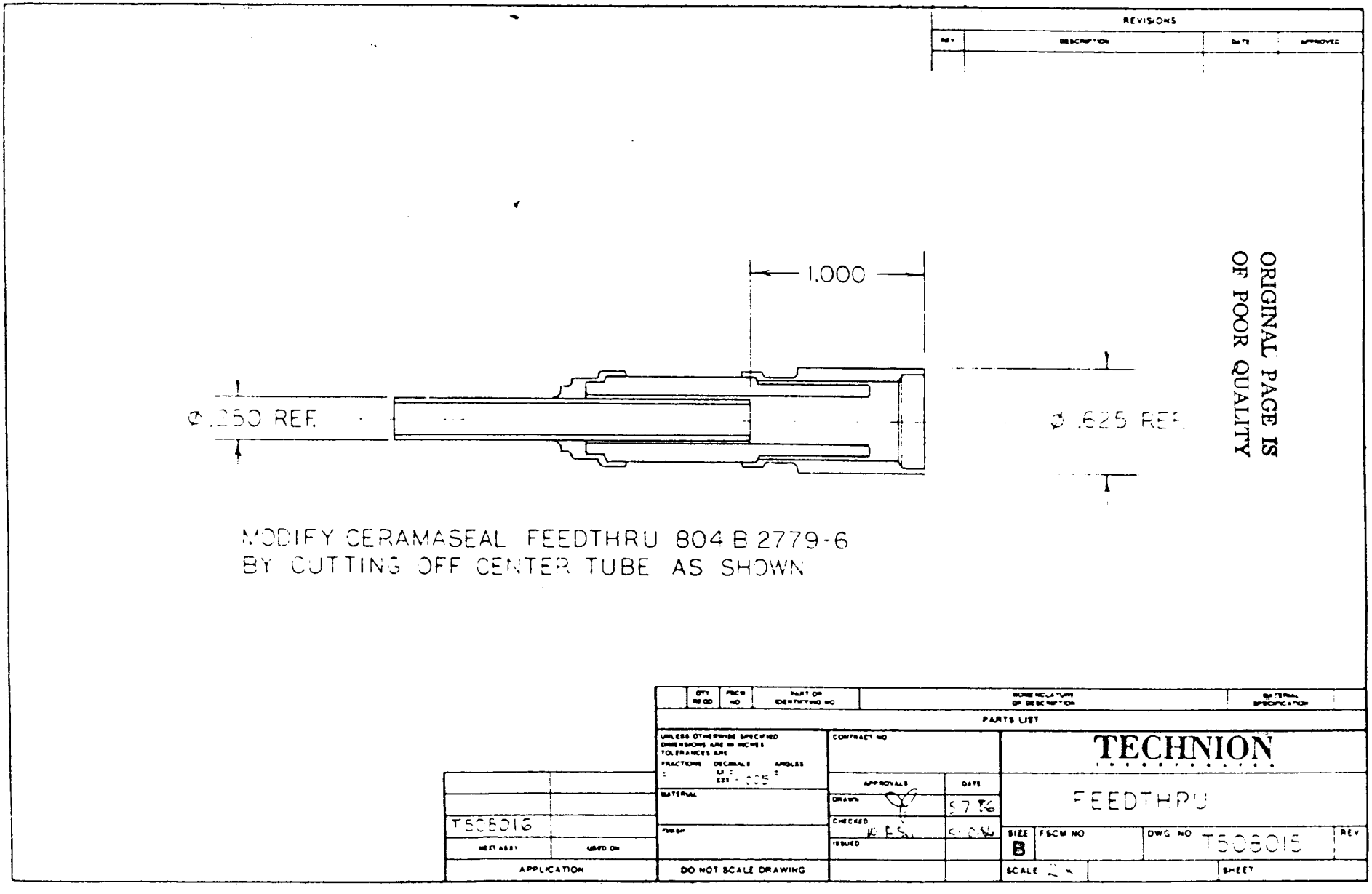

Figure 16. Feed-Thru

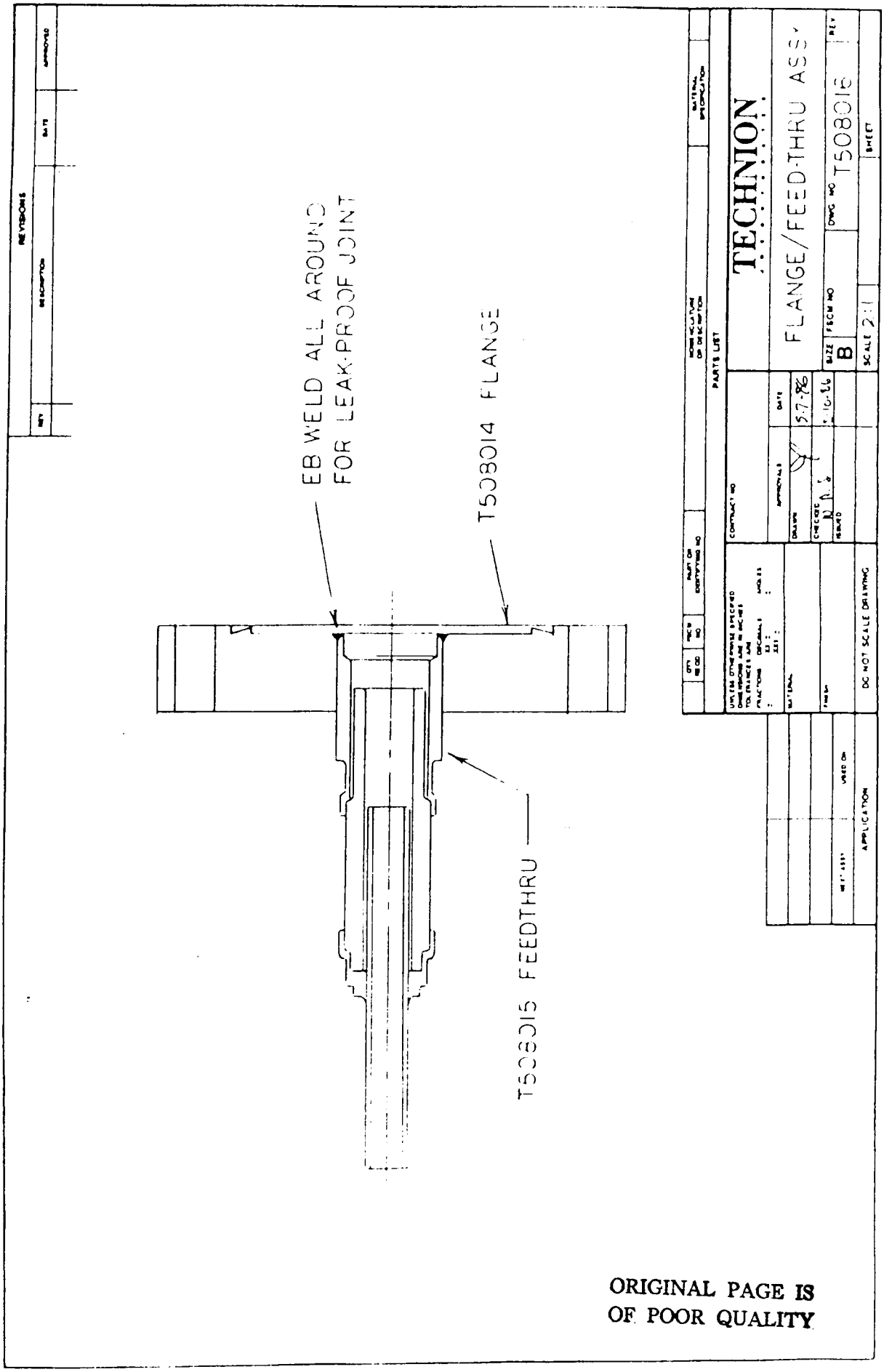

Figure 17. Flange/Feed-Thru Assy

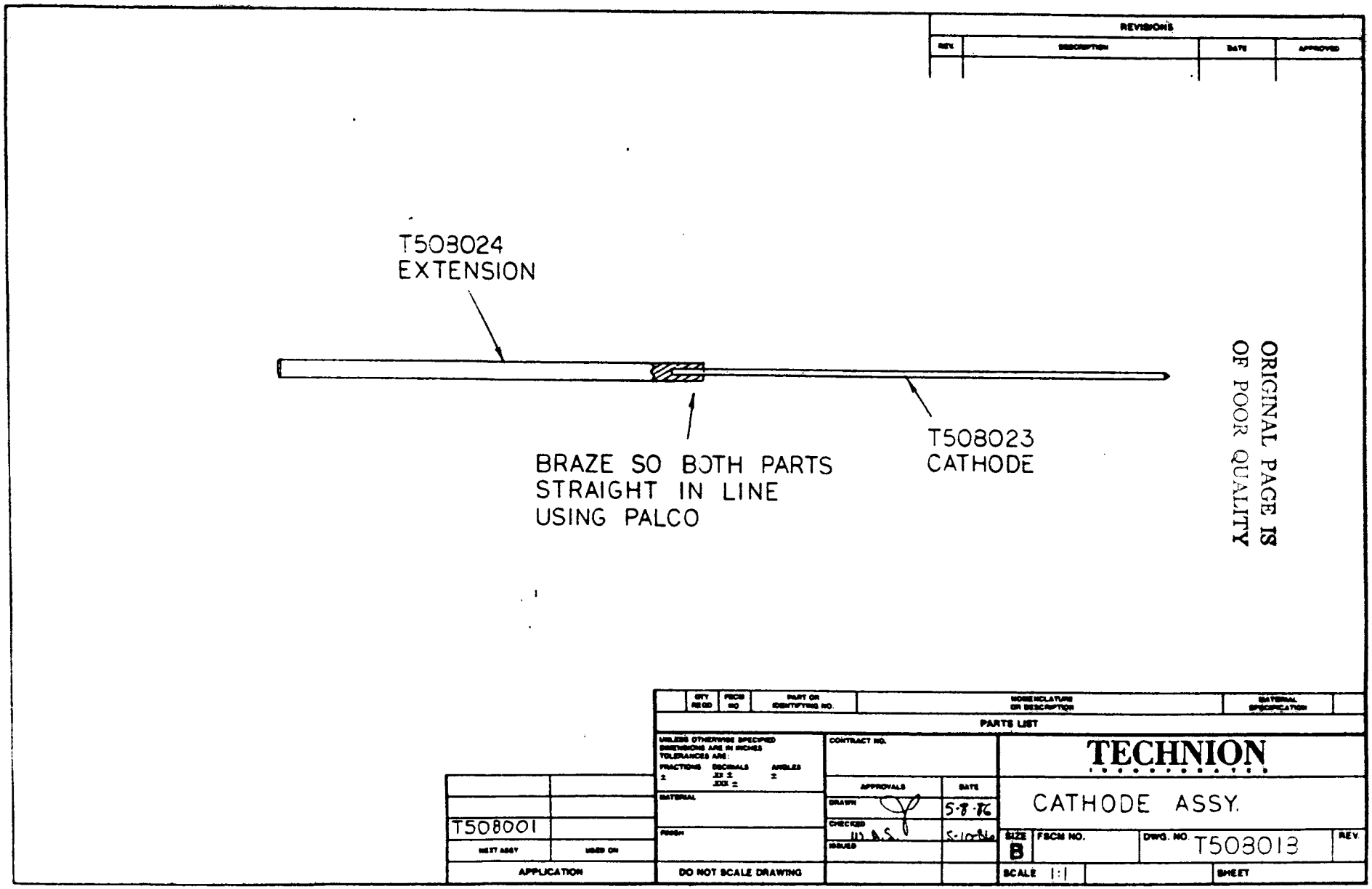

Figure 18. Cathode Assy

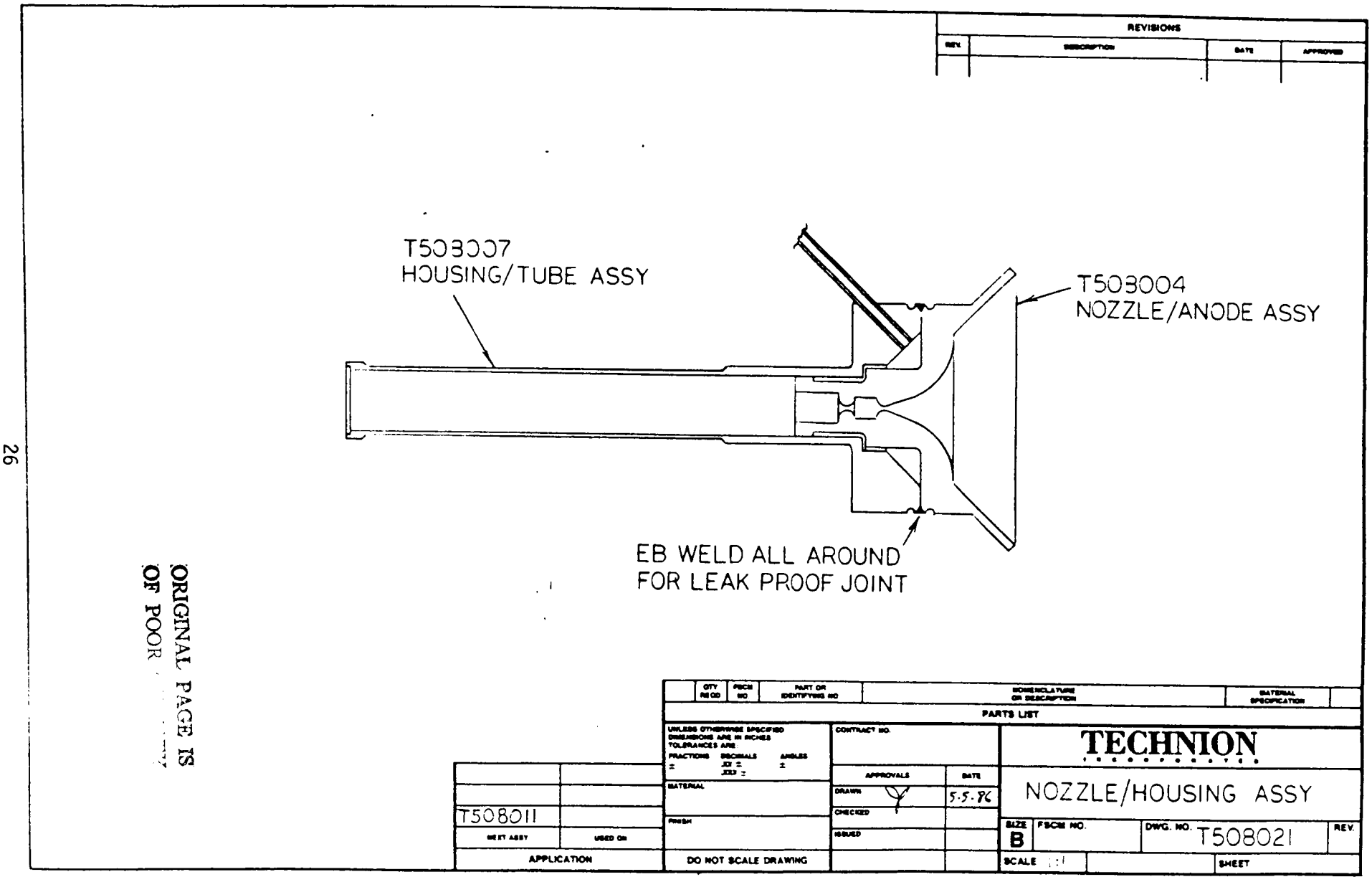

Figure 19. Nozzle/Housing Assy

REVISIONS			
REV	DESCRIPTION	DATE	APPROVED
A	OMIT -1	6-12-86	

ALUMINA ROUND SINGLE BORE TUBING

PART NO	ID	OD	LENGTH REQD ⚠1	SOURCE & CAT. NO.	NO REQ'D / ASSY
T508022-1	.062	.125	6.760	McDANEL AXRS-0732	(OMIT)
-2	.187	.250	6.435	" AXRS-0753	1
-3	"	"	1.490	" " "	1

⚠1 LENGTH TO BE VERIFIED AFTER FABRICATION OF BODY AND FEEDTHRU ASSYS

QTY REQD	ITEM NO	PART OR IDENTIFYING NO	NOMENCLATURE OR DESCRIPTION	MATERIAL SPECIFICATION
PARTS LIST				

UNLESS OTHERWISE SPECIFIED DIMENSIONS ARE IN INCHES
TOLERANCES ARE
FRACTIONS ± DECIMALS .XX ± .XXX ± .005 ANGLES ±

CONTRACT NO

APPROVALS	DATE
DRAWN	5 8 86
CHECKED	
ISSUED	

MATERIAL

FINISH

DO NOT SCALE DRAWING

T508001	
NEXT ASSY	USED ON
APPLICATION	

TECHNION
INCORPORATED

TUBING

SIZE	FSCM NO	DWG NO	REV
B		T508022	A

SCALE SHEET

Figure 20. Tubing

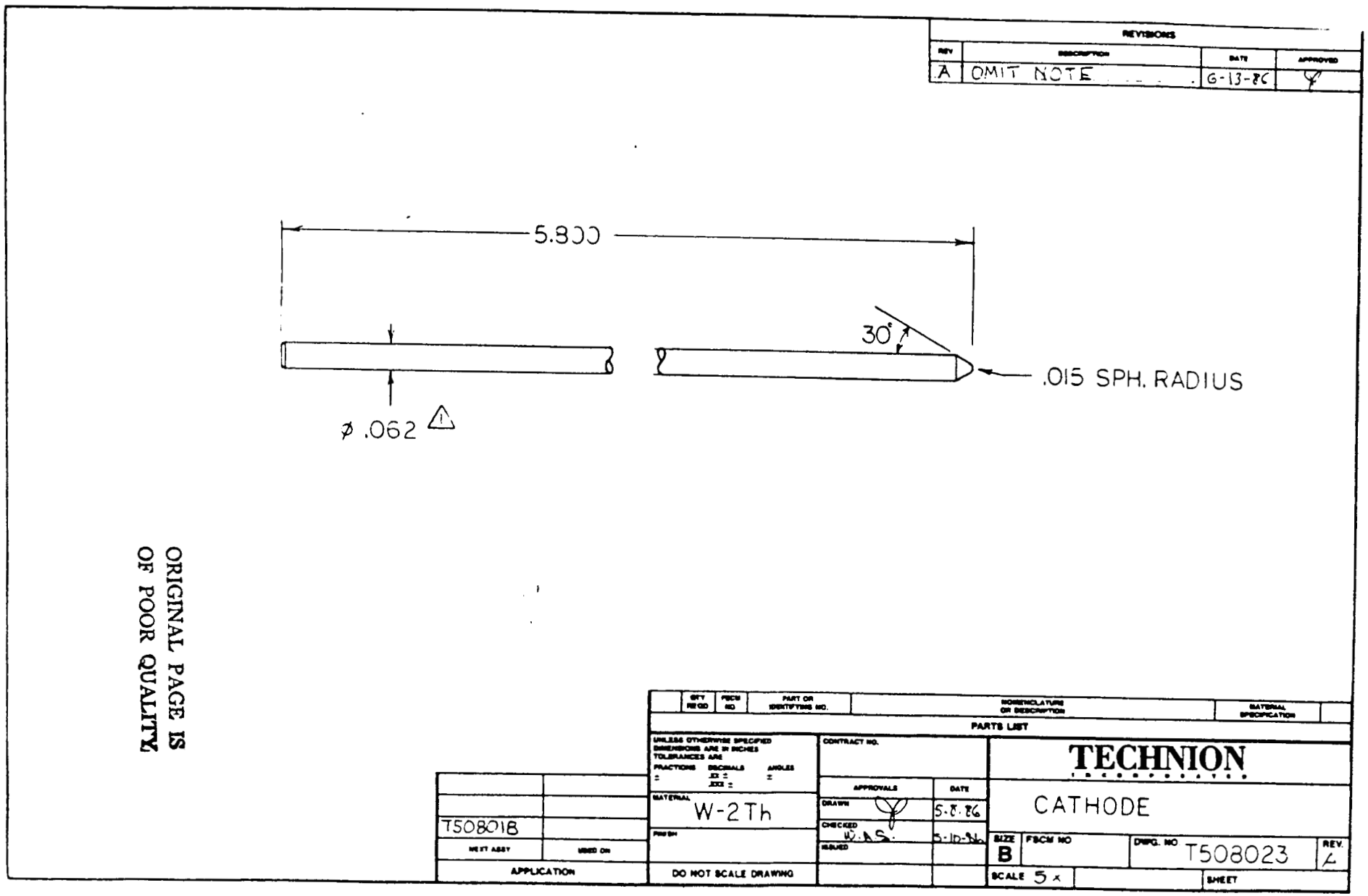

Figure 21. Cathode

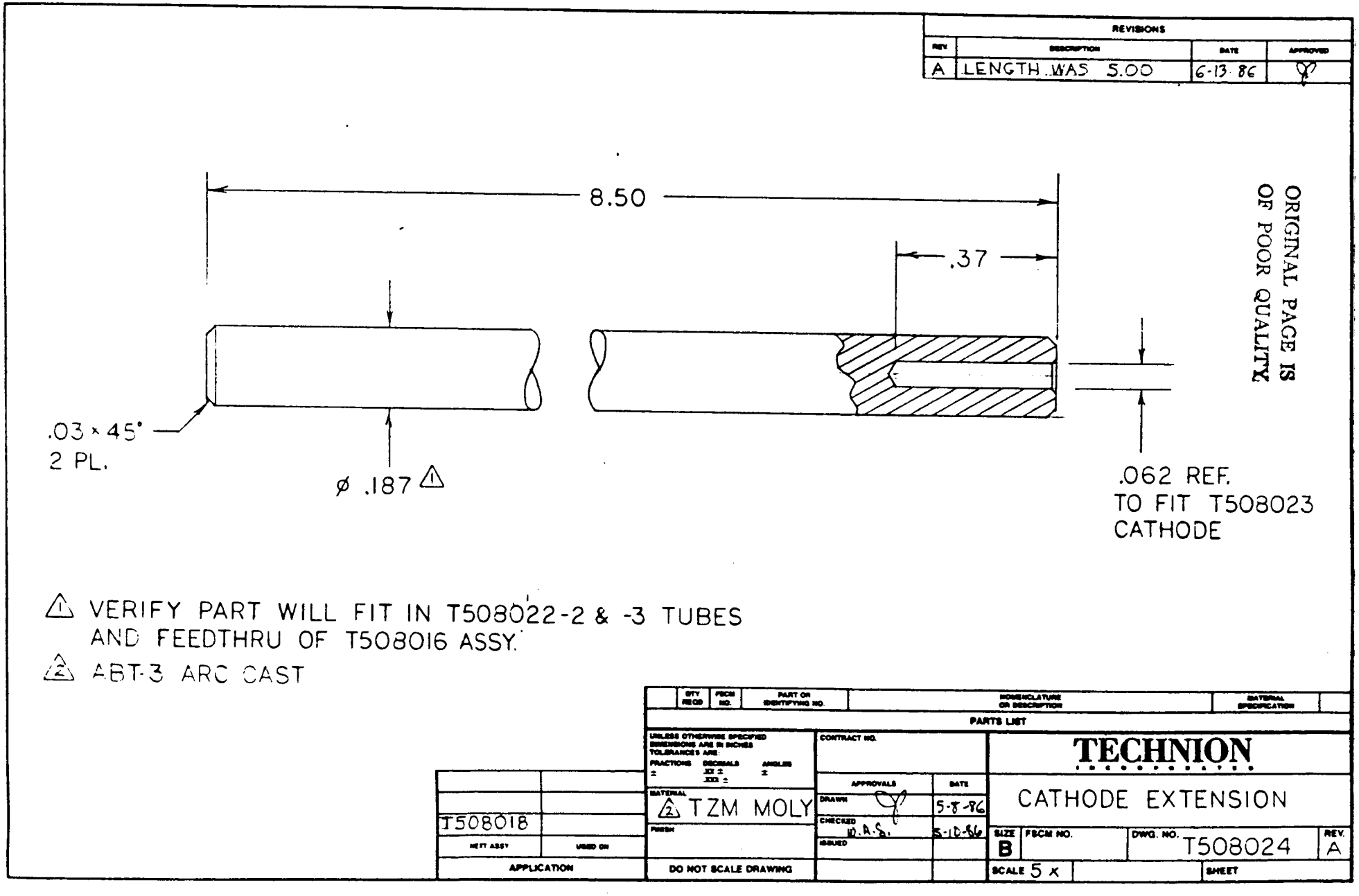

Figure 22. Cathode Extension

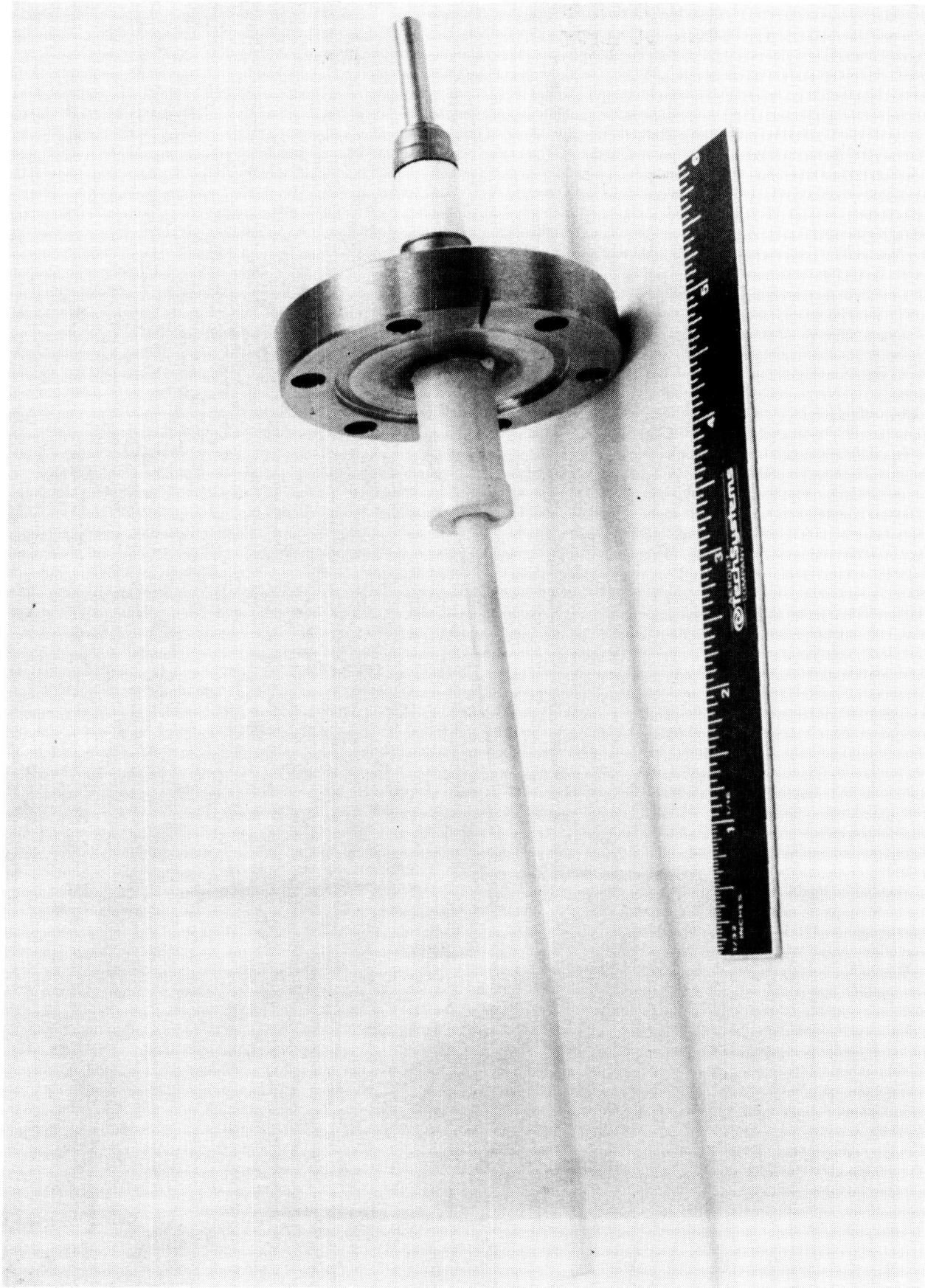

Figure 23. Improved Aft Insulator Assembly

3.2, Design of Baseline Thruster and Components (cont.)

- Permanent Magnet Design

The design of the permanent magnet intended for 1 kW arcjet Series 2 testing is shown in Figures 24, 25 and 26. The purpose of incorporating the permanent magnet into the Series 2 is to demonstrate that a permanent magnet, properly insulated from the thruster, can provide a stable magnetic field. The nominal design field strength is 500 gauss. This value is not considered an optimal value, but is typical of the field strengths generated with the electromagnet (the nominal Series 1 magnetic field strength was 400 gauss). A 25% safety factor has been added in case temperature effects on the magnet are greater than expected.

The maximum operating temperature of the rare earth cobalt magnet material, Recoma 28, is 350 C. The magnet is insulated from the thruster with zirconia felt insulation. Figure 27 shows the required thermal conductivity of the insulation layer (approximately 0.2 inch thick for our design) as a function of arcjet body temperature for maximum magnet temperatures of 350, 250, and 150 C. Also shown is the thermal conductivity of candidate insulation materials. The design point with an estimated arcjet body temperature of 1500 K is shown for reference. The maximum magnet temperature is expected to be approximately 200 C and the magnet is adequately insulated for arcjet body temperatures as high as 2200 K. The maximum arcjet body temperature, when operating with a water-cooled electromagnet, has been measured at 700 C. Energy balance considerations limit the theoretical maximum outer-body temperature to less than 1800K and axial conduction in the thruster housing reduces local hot spots in the region of the magnet.

Figure 28 shows the power dissipated through the magnet for given maximum (inner diameter) magnet temperatures. For the worst possible case, T_m = 350 C, a total of 81.0 watts would be dissipated. Ideally, thruster body should operate at as low a temperature as possible to increase the thermal efficiency of the thruster. To accomplish this, the anode region must be conduction cooled by coupling it to the nozzle region, rather than allowing conduction to the outer-body housing.

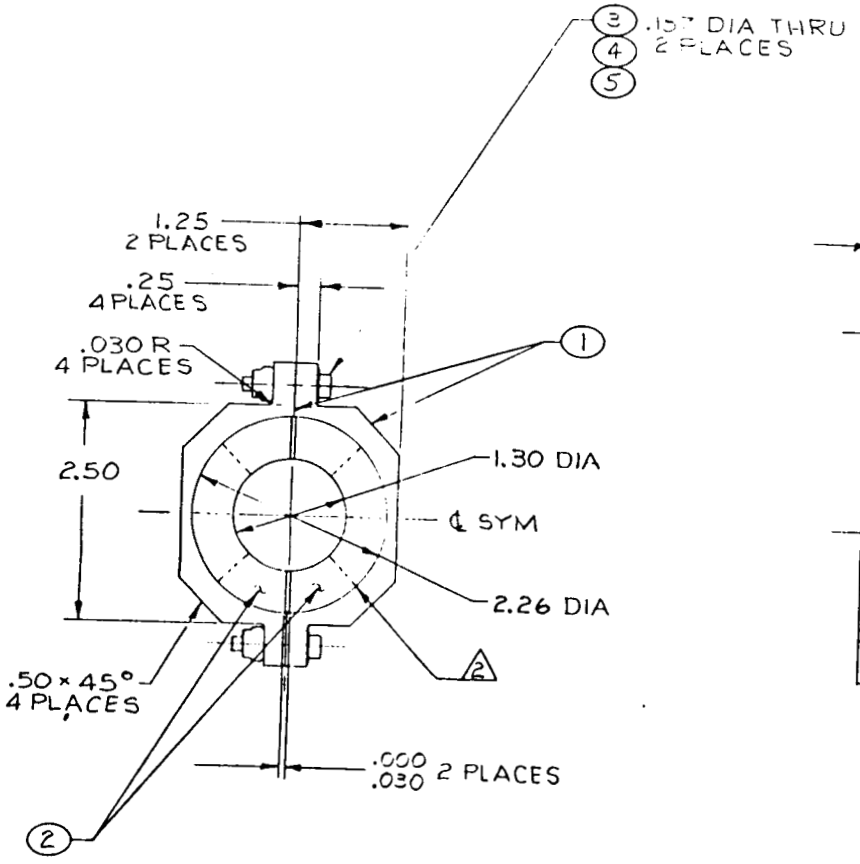

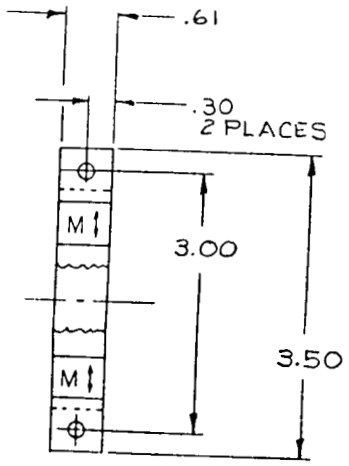

	2		AN960C8L	WASHER		5
	2		MS21044C08	NUT	#8-32UNC CRES	4
	2		MS16995-29	SCREW	#8-32UNC×.87 LONG S.H. CRES	3
5	2		-2	MAGNET	RARE EARTH COBALT	2
	2		-1		CRES 400 SERIES	1
	-9	FSCM NO.	PART OR IDENTIFYING NO.	NOMENCLATURE OR DESCRIPTION	MATERIAL SPECIFICATION	ITEM NO.
QTY REQ'D PER ASSY				PARTS LIST		

Figure 24. Permanent Magnet Design

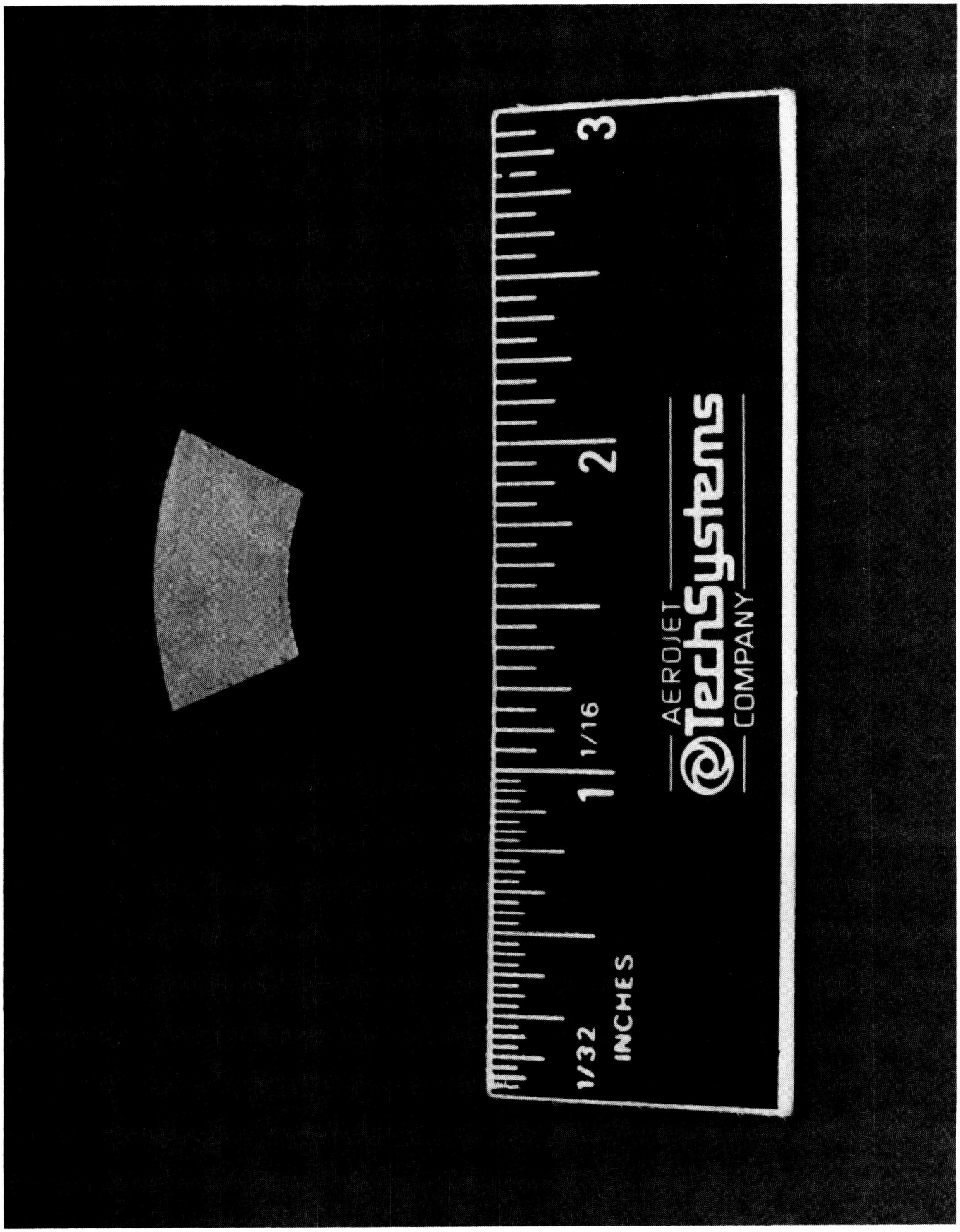

Figure 25. Individual Sector of Arcjet Permanent Magnet

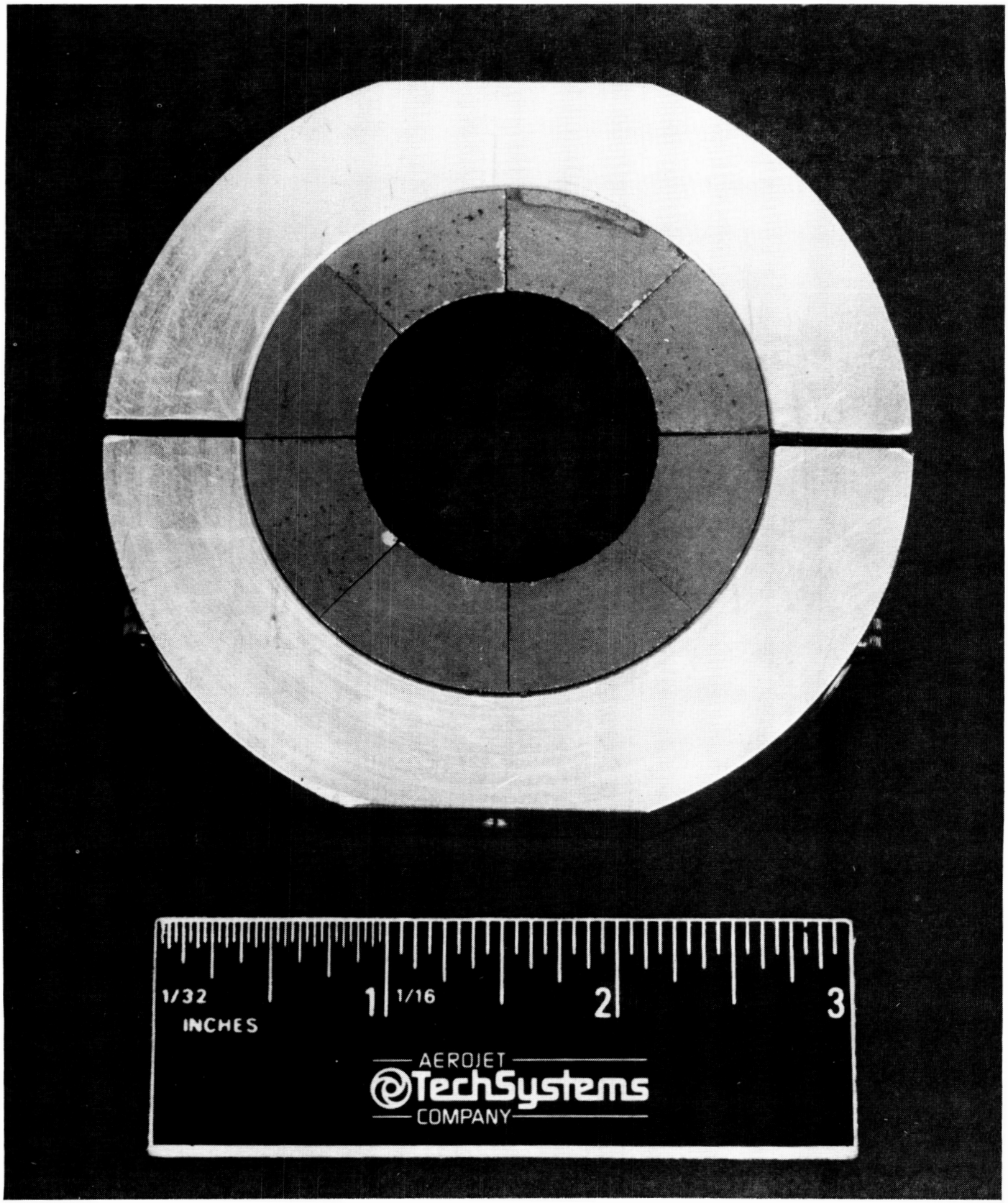

Figure 26. Arcjet Permanent Magnet Assembly

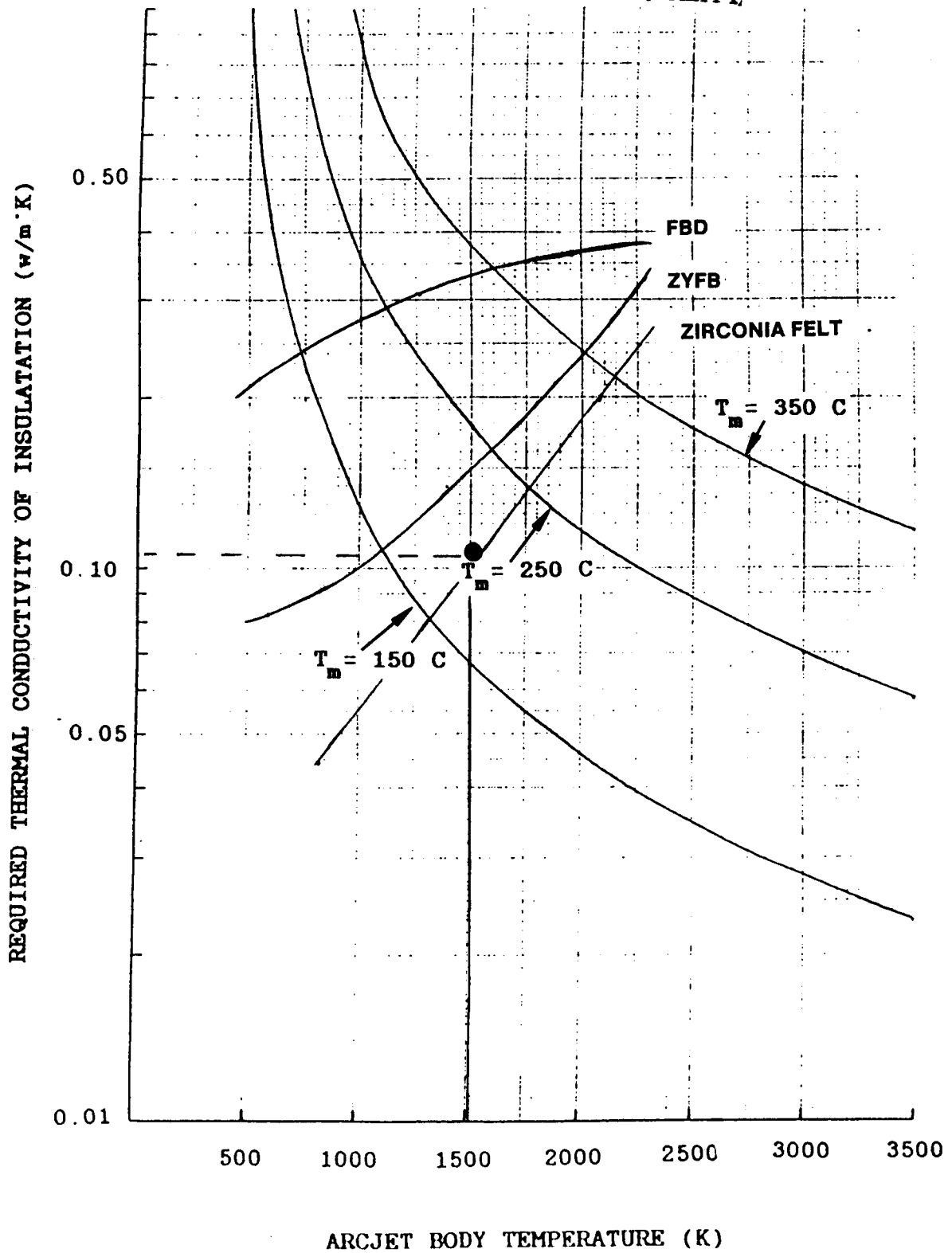

Figure 27. Thermal Characteristics of Permanent Magnet Design

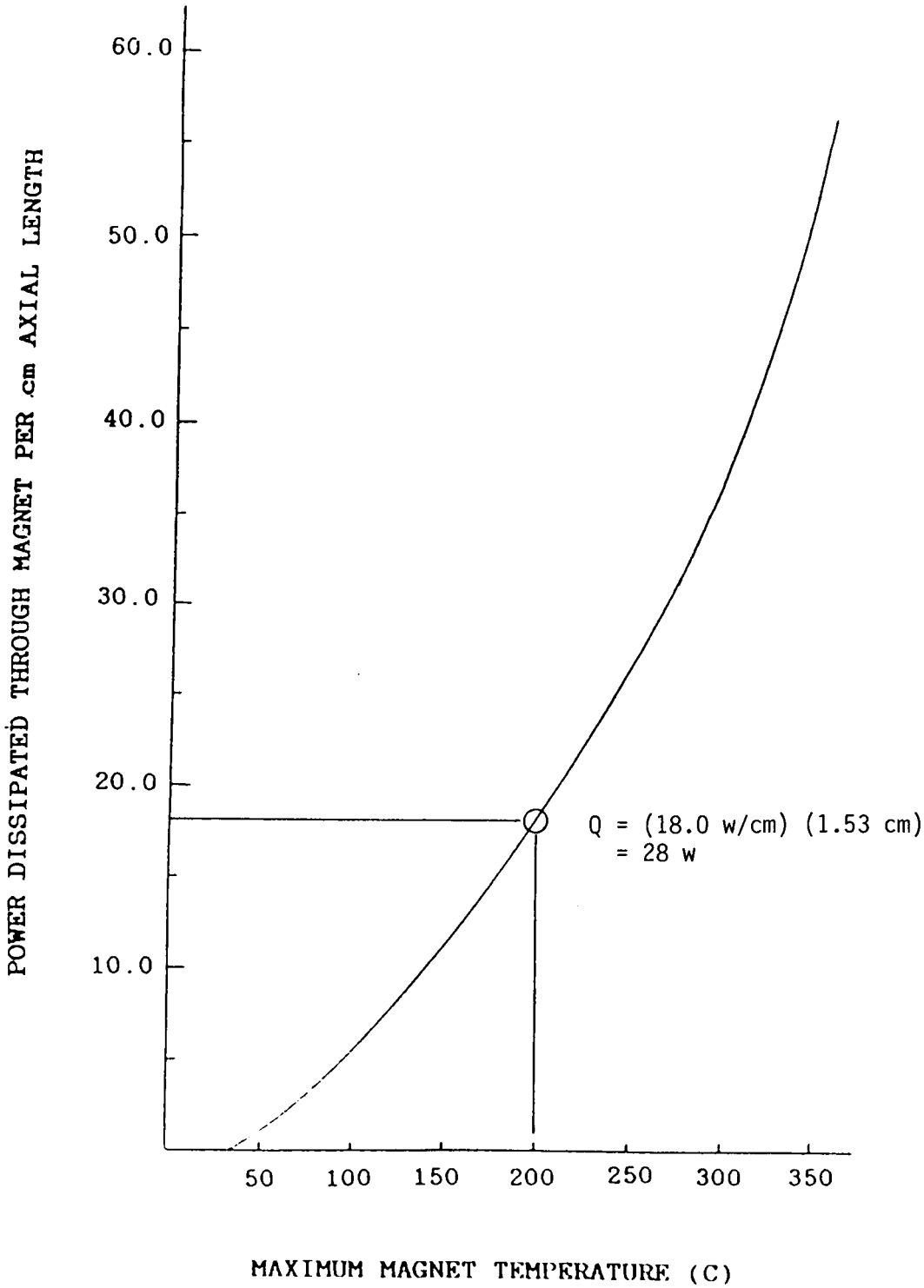

Figure 28. Energy Loss through Magnet

3.2, Design of Baseline Thruster and Components (cont.)

Figure 29 shows a comparison of the magnetic fields for the electromagnet and the permanent magnet. The field strengths were measured with a gauss meter. The magnet field strength in the arc region can be varied with the permanent magnet by changing its position along the thrust axis.

- Facility Gas Generator

Figure 30 shows the design of the facility gas generator. No tests were conducted on this device. The inlet end is a tube with an 0.0254 cm I.D. to provide a high inlet velocity and to reduce the possibility of thermal decomposition of the liquid hydrazine prior to it entering the catalyst bed. The catalyst bed material is Shell 405 granules.

This design of the facility gas generator closely resembles a flight-type unit. To ensure proper startup of the unit, the catalyst bed can be heated to 550 K before the hydrazine is injected into the bed. The catalyst bed temperature is monitored by a thermocouple (not shown) mounted on the body of the gas generator. The enlarged catalyst bed is to ensure stable generator performance during long-duration arcjet testing. The extended startup and shutdown transients associated with a larger catalyst bed will not be a problem during arcjet testing.

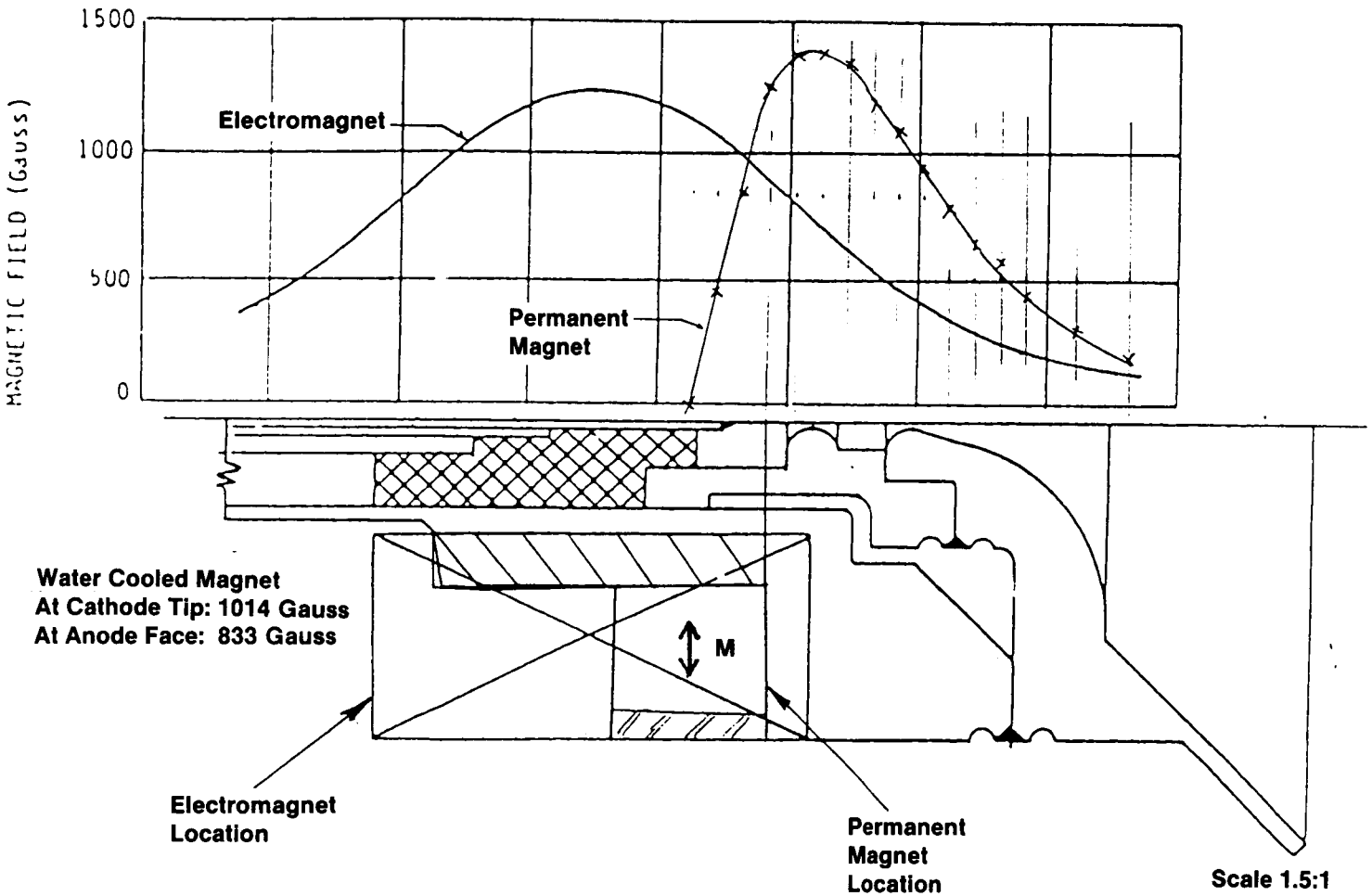

Figure 29. Comparison of Magnetic Fields for Permanent Magnet and Electromagnet

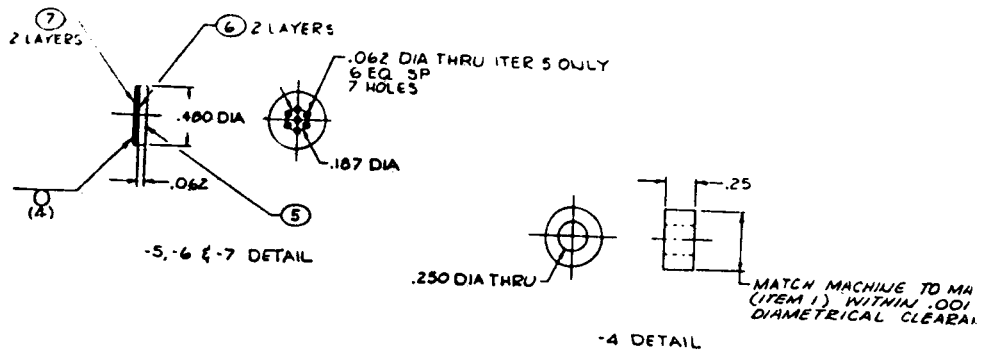

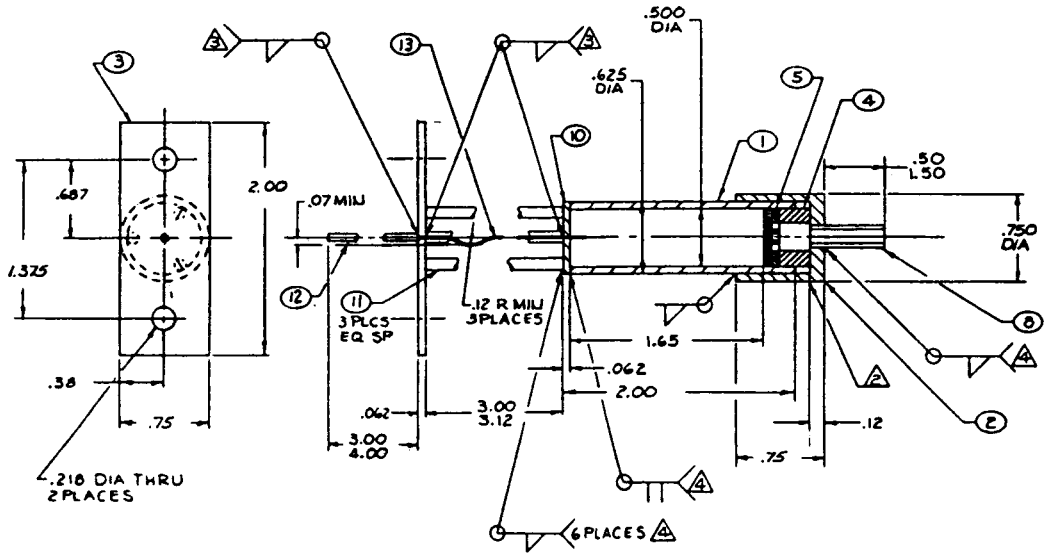

						19
	AR			WELD ROD	AMS 5837	18
	AR			WELD ROD	MIL-R-5031, CL 12	17
						16
						15
						14
	1		-13	TUBE	.020 O.D. x .00525 WALL TUBING CRES 304L	13
	1		-12	TUBE	.062 O.D. x .016 WALL TUBING CRES 304L	12
	3		-11	TUBE	.094 O.D. x .016 WALL TUBING INCONEL	11
	1		-10	CAP	INCONEL 625	10
						9
	1		-8	TUBE	.187 O.D. x .03 WALL TUBING INCONEL 625	6
	2		-7	SCREEN	150 MESH INCONEL 625 OR HASTELLOY X	7
	2		-6	SCREEN	20 MESH INCONEL 625 OR HASTELLOY X	6
	1		-5	SPACER		5
	1		-4	LOAD SPACER		4
	1		-3	PLATE	INCONEL 625	3
	1		-2	CAP		2
	1		-1	HOUSING		1
	-9	ITEM NO.	PART OR IDENTIFYING NO.	NOMENCLATURE OR DESCRIPTION	MATERIAL SPECIFICATION	ITEM NO.
QTY REQ'D PER ASSY				PARTS LIST		

Figure 30. Facility Hydrazine Gas Generator

3.3 SUPPORTING ANALYSES

Analyses were performed in several areas in order to aid the design and development of the advanced arcjet. The analyses conducted can be grouped in three categories:

1. Basic arc-gas interaction

2. Overall scaling and performance estimates

3. Detailed hardware thermal/stress analysis

The studies of the first two types provide a model of the physics and the gross characteristics of the device. Analysis of the third type was used to ensure the integrity of the research thruster.

1. Basic Arc-Gas Interactions

A study of arc/laminar gas flow interaction for a vortex stabilized arc was conducted to determine limitations on the coupling of arc power into a vortex flow. The details of the analysis are contained in Appendix A. The conclusion of the analysis was that a limit exists on the total mass flux that can pass through a vortex due to the viscosity variations of an arc heated propellant.

The second basic gas-arc interaction studied was definition of the applicable plasma flow equations for arcjet. The distinction between the compressible and incompressible Navier-Stokes equations was clarified. The incompressible equations are applicable to the low Mach number regions of the arc chamber and the compressible equations are required to describe the plasma flow through the nozzle. A detailed discussion is contained in Appendix B.

3.3, Supporting Analysis (cont.)

2. Overall Scaling and Performance Predictions

The approach taken in developing the advanced arcjet is based on the scaling of the physics of large arc heaters. Appendix C contains an assessment of the scaling and identified weaknesses. Due to limitations in both experimental data and analytical techniques, extrapolation of arc heater data to low power arcjets must be performed with care.

The baseline research thruster can be used with ammonia, hydrogen, or hydrazine decomposition products as the propellant. The anticipated performance for each of these propellants is shown in Figures 31 through 33. A typical design point for each propellant is shown in Table I. The estimates were prepared with the procedure described in Appendix D. The research thruster has been design operated at a chamber pressure less than 1 MPa. The design point used for the research thruster is shown on Table II.

3. Thermal/Stress Analysis

Thermal and stress analyses have been conducted on the engine design shown in Figure 34. One dimensional calculations for conduction heat transfer and stress were used to design the thruster. The thermal design has been made deliberately very conservative so that all critical components will run cooler than is necessary or desirable in a flight design. The size of components and material were choosen so to minimize stress and ensure no failure due to mechanical loading or thermal stresses. This has been done so that parametric tests can be conducted without undue damage occurring to the components. Also, the long (20 cm) extension between the feed-throughs and the vortex chamber, required to ensure that the feed-throughs do not overheat, would be greatly shortened in a flight model by folding the tube. Folding was not incorporated into the design, since it would interfere with access to components in the vortex chamber and the anode. Some temperature and heat flux estimates are displayed in Figure 34.

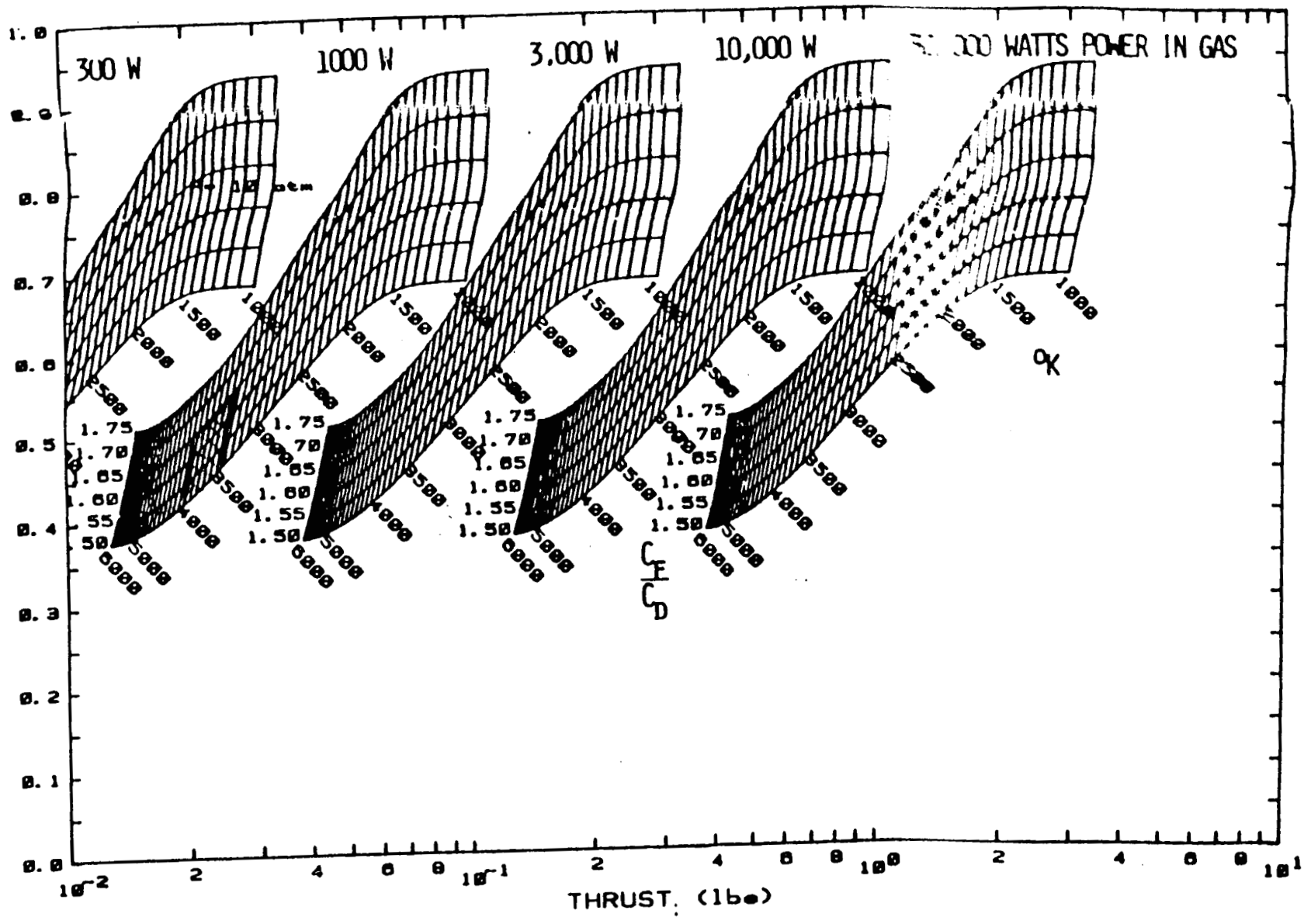

Figure 31. Propellant Efficiency Vs. Thrust for H_2 at Pressure - 10 Atmospheres

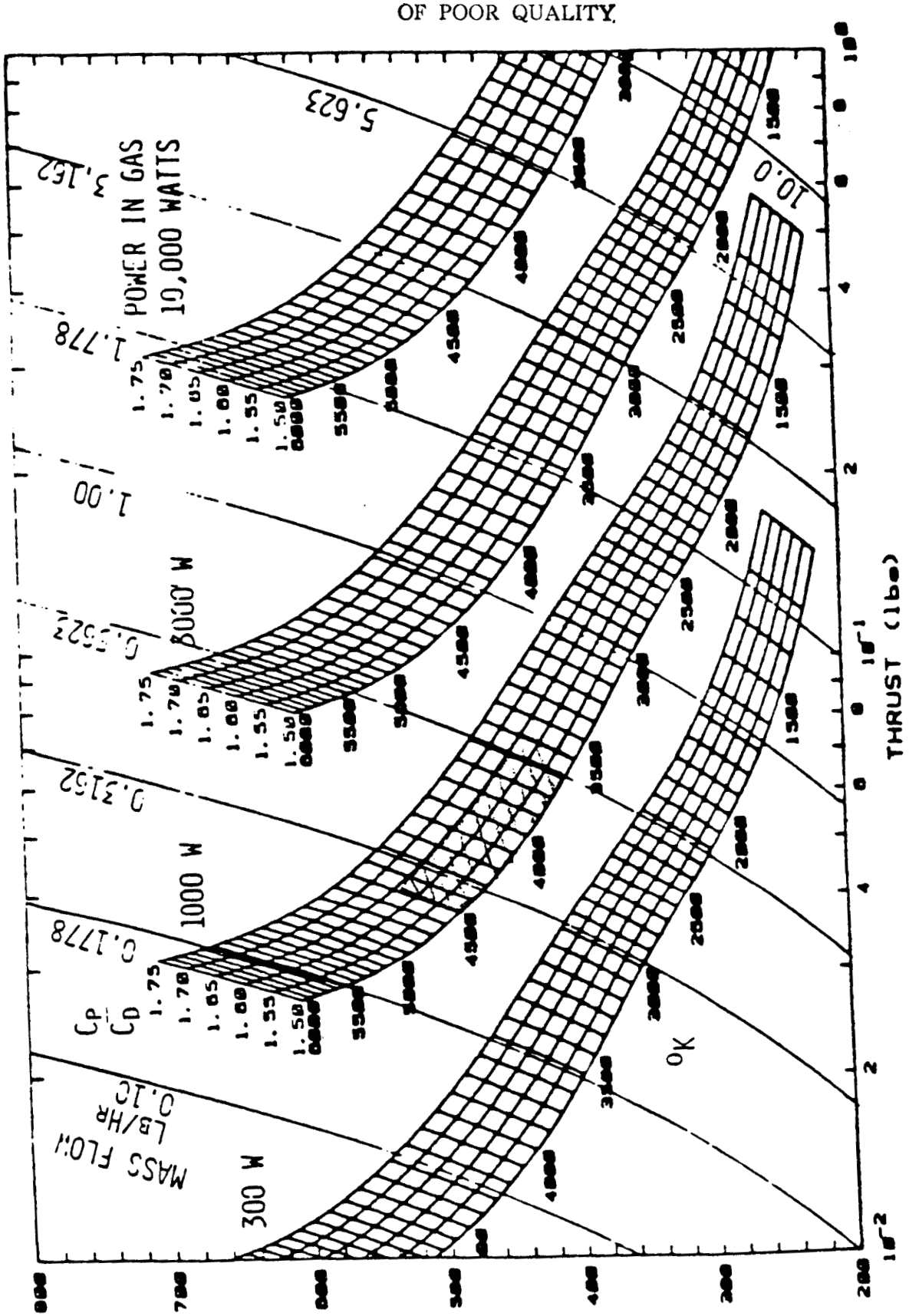

Figure 32. N_2H_4 Isp Vs. Thrust at Pressure - 10 Atmospheres

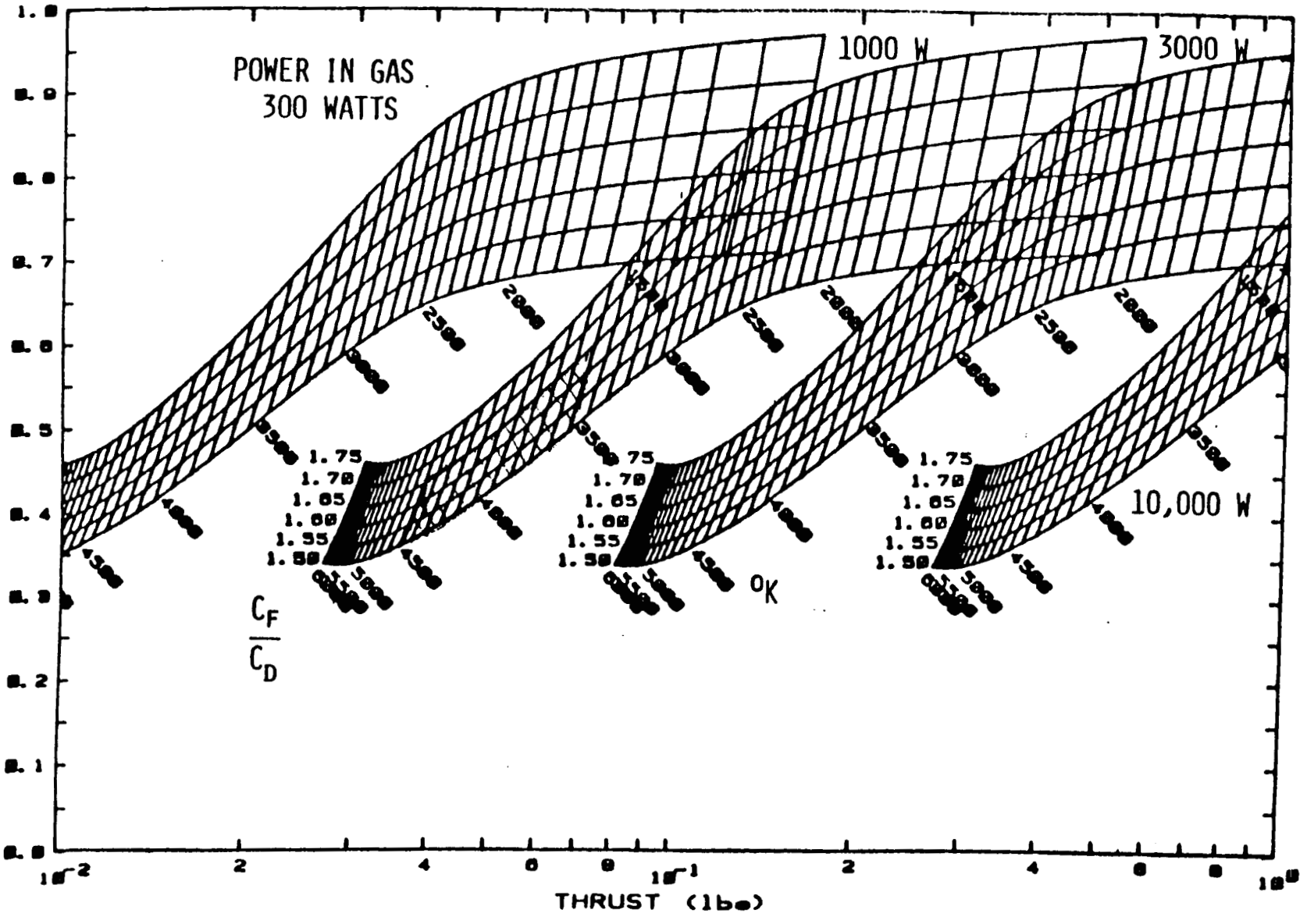

Figure 33. Propellant Efficiency Vs. Thrust for N_2H_4 at Pressure - 10 Atmospheres

TABLE I

ESTIMATED PERFORMANCE FOR TYPICAL PROPELLANTS IN THE 1-KW ARC ENGINE

	N_2H_4 Products	NH_3	H_2
Pg watts	1057	1000	1000
$\dot{m}$ /min	2.4	1.4	.53
$\bar{T}$ ^{o}K	4300	4150	4000
V volts	150	170	200
I amps	8	6	6
F mlb	43	30	20
I_{sp} sec	488	583	1027
η% -	35	31	40
Re^{*} -	905	547	338

TABLE II

1 kW ARCJET DESIGN POINT

Power Input:	1200 watts
Discharge Voltage:	130-160 volts
Thermal Efficiency:	80-90%
Propellant:	Simulated N_2H_4
Mass Flow Rate:	0.04 gm/sec
Isp:	500 sec
Overall Efficiency:	34-40%
Average Gas Temperature:	4300 K
Thrust:	0.191 N_3
Thrust-to-Discharge Coefficient:	1.60
Throat Reynolds Number:	900

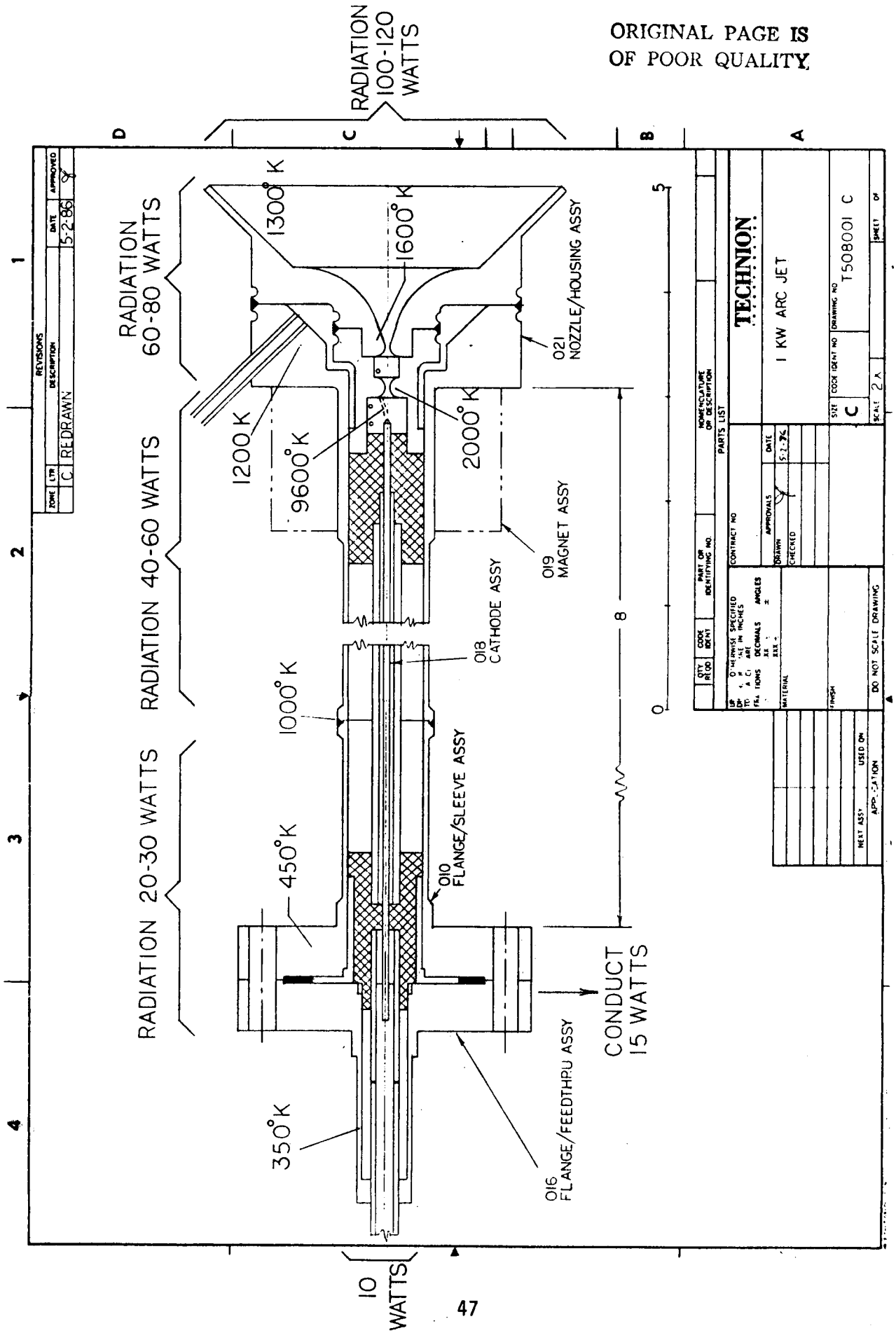

Figure 34. 1-kw Arcjet - Preliminary Thermal Analysis

3.4 NOZZLE DESIGN AND TESTING

One of the technology development subtasks of Task 2.0 was an investigation of the behavior of low thrust, low Reynolds number nozzles. The typical throat Reynolds number for a 1 kW-class arcjet thruster is in the 1200 to 800 range. Previous investigators have noted a reduction in measured thrust coefficients due to test chamber background pressure and due to viscous flow effects in the nozzles[10,11]. In addition to the effect of large boundary layers occupying a large portion of the total flow area in the supersonic portion of the nozzle, the presence of a large swirl component to the flow can effect nozzle performance[12.13]. The purpose of this subtask was to evaluate the performance of candidate nozzle designs for use on a flight-like thruster.

Originally, a numerical study of nozzle performance using the VNAP-2 computer code [14] was planned. Initial results indicated that the VNAP-2 code was too costly to use for performance predictions in the straight flow (no swirl) case due to lack of knowledge of the thermal boundary conditions. The code is not applicable to flows with swirl, because it does not calculate a circumferential velocity component. In conjunction with the numerical study, it was planned to conduct an experimental investigation to test candidate nozzle designs. The experimental investigation was conducted using interchangeable nozzles on a modified Technion resistojet. The resistojet is capable of simulating arcjet flow Reynolds numbers under certain operating conditions. The tests were conducted at NASA/LeRC in the Tank 5 test facility. The Tank 5 facility was chosen because low background pressures could be maintained.

3.4.1 Nozzle Design

Six candidate nozzle configurations were selected for study at arcjet flow conditions. The nozzle geometries were chosen based on designs in available literature and previous experience with low thrust nozzles. The nozzles were tested using a modified Technion resistojet shown in Figure 35

ORIGINAL PAGE IS
OF POOR QUALITY

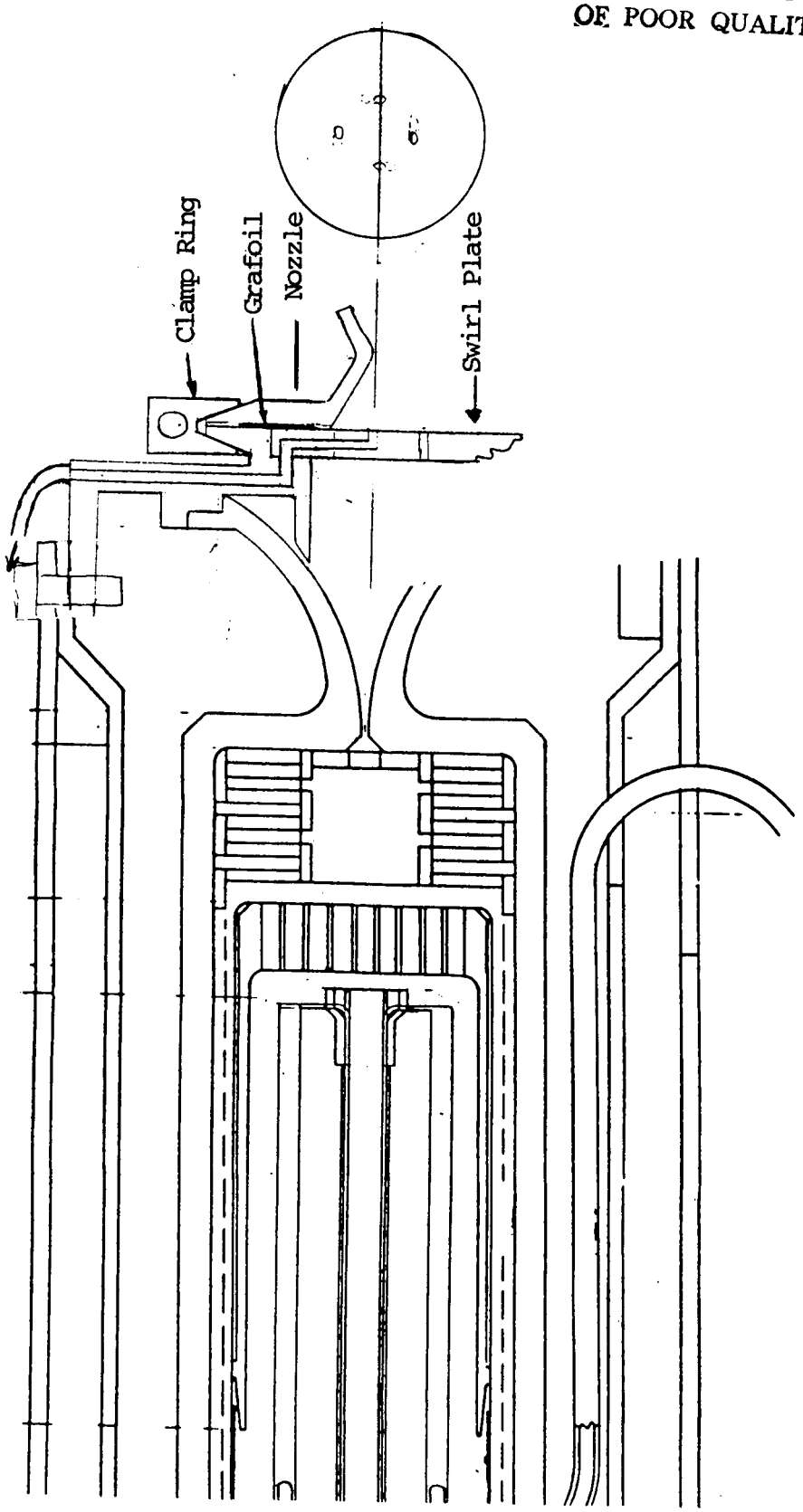

(a) Schematic

Figure 35. Modification of Technion Resistojet for Nozzle Experiments

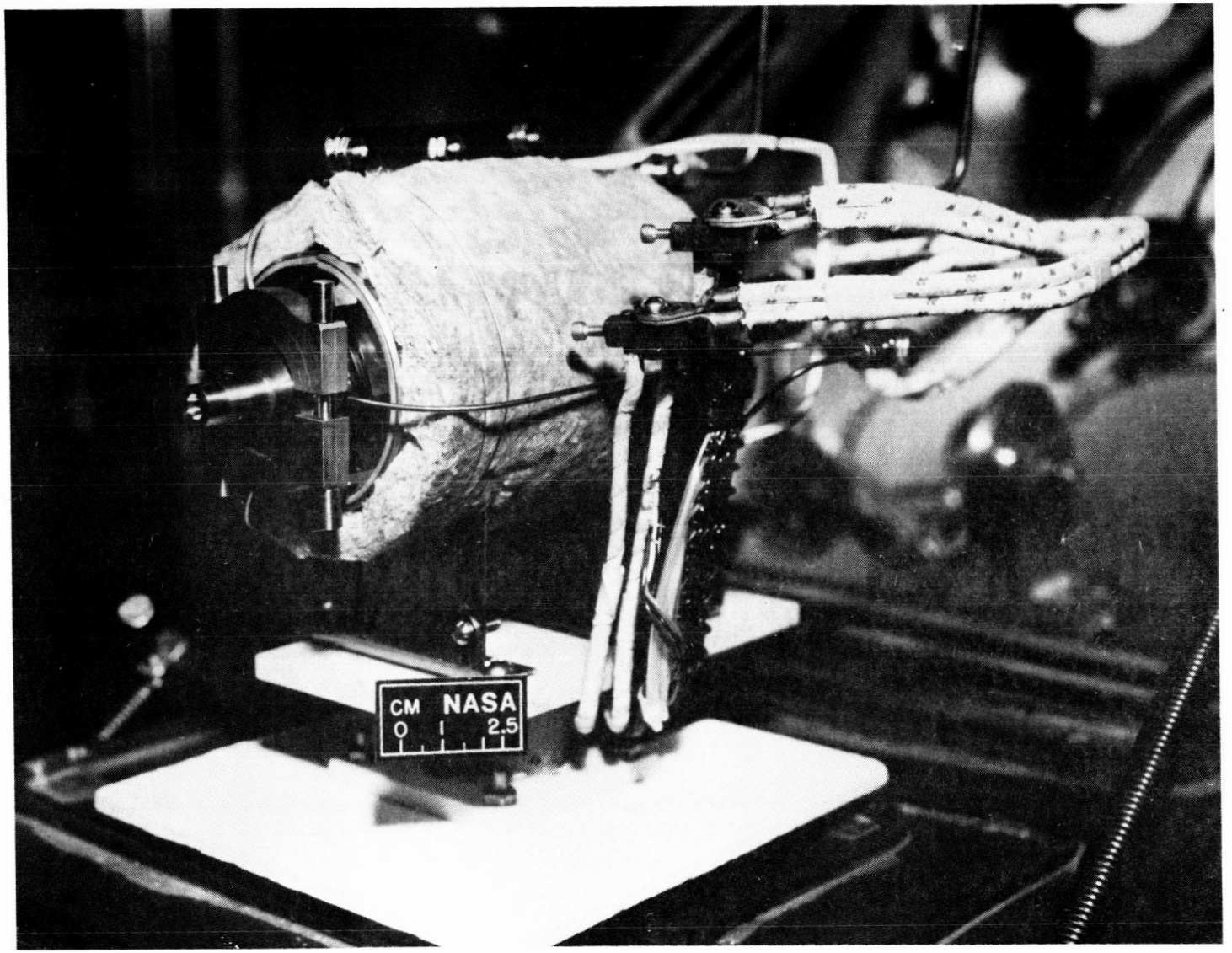

(b) Photograph of Installation on NSAS LeRC Thrust Stand

Figure 35. Modification of Technion Resistojet for Nozzle Experiments (cont)

3.4, Nozzle Testing (cont.)

The adapter hardware was designed to allow interchangeable nozzles. The bell and the cone nozzle are shown in Figures 36, 37, and 38. The nozzle skirts are shown in Figures 38, 39, and 40. A cone and tulip skirt allow numerous experimental configurations. These include:

Geometry	Area Ratio
Cone	50:1
Bell	50:1
Cone-Cone	100:1
Cone-Tulip	100:1
Bell-Cone	100:1
Bell-Tulip	100:1

A swirl plate was fabricated, which can impart a circulation of 1 m^2/sec; a second plate was fabricated which can provide an axial flow with no circulation. Potential test combinatins include:

Swirl or Axial	X	6 Nozzle Combinations	X	500-2000 Reynolds Number	X	Various Back Pressures

Due to the difficulty in instrumenting nozzles with such small dimensions, local heat flux or pressure measurements were not feasible. In addition, the hardware associated with multiple pressure taps would substantially increase the thrust stand tare, reducing the accuracy of the thrust measurements. Only thrust levels in the 10-15 millipound range could be attained using the Technion resistojet.

An operating space for the resistojet was defined as follows:

$P_c > 100$ kPa
$T_c < 1500$ K
$d^* > 0.051$ cm

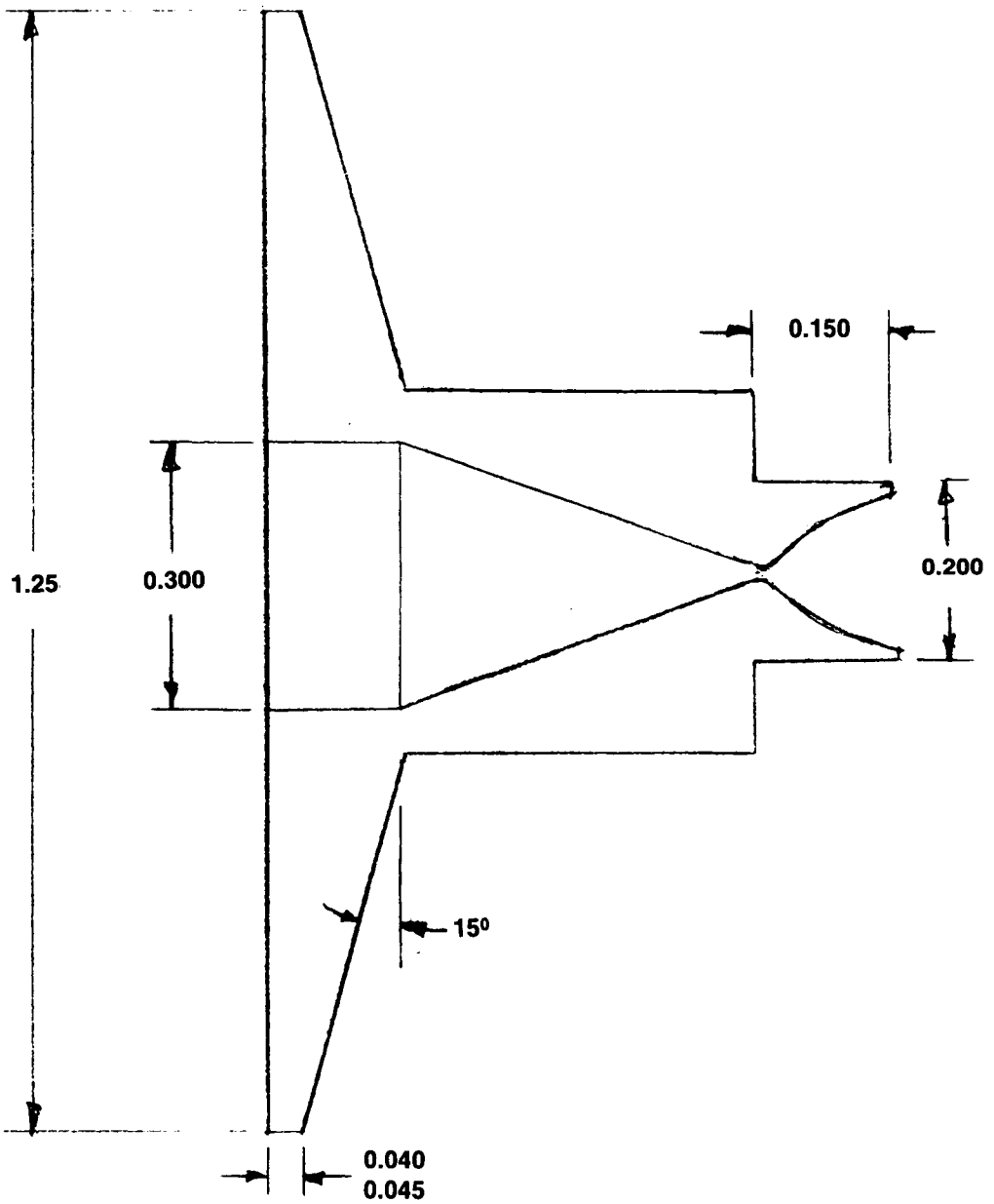

Figure 36. Bell Nozzle (Dimensions in Inches)

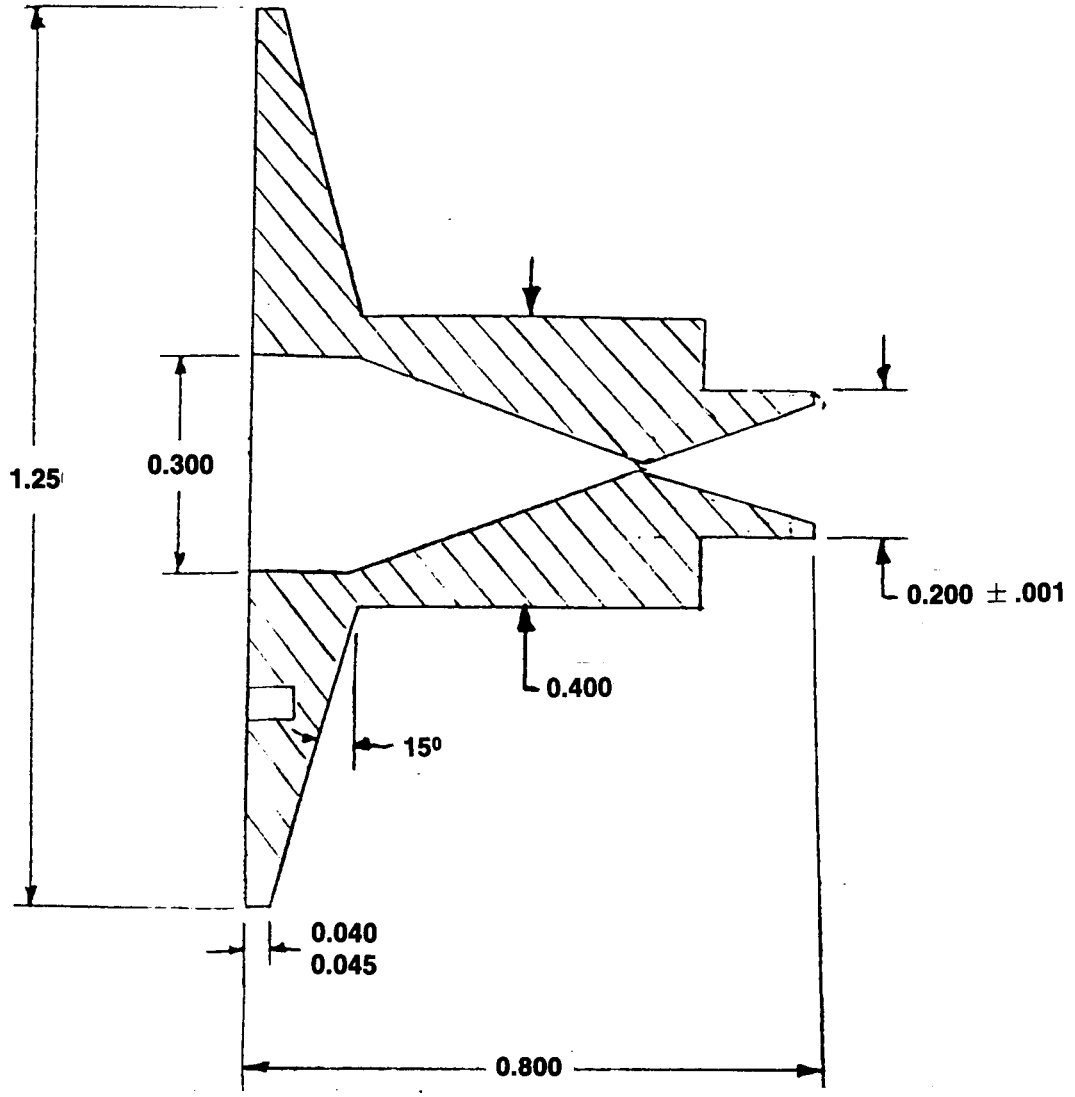

Figure 37. Cone Nozzle (Dimensions in Inches)

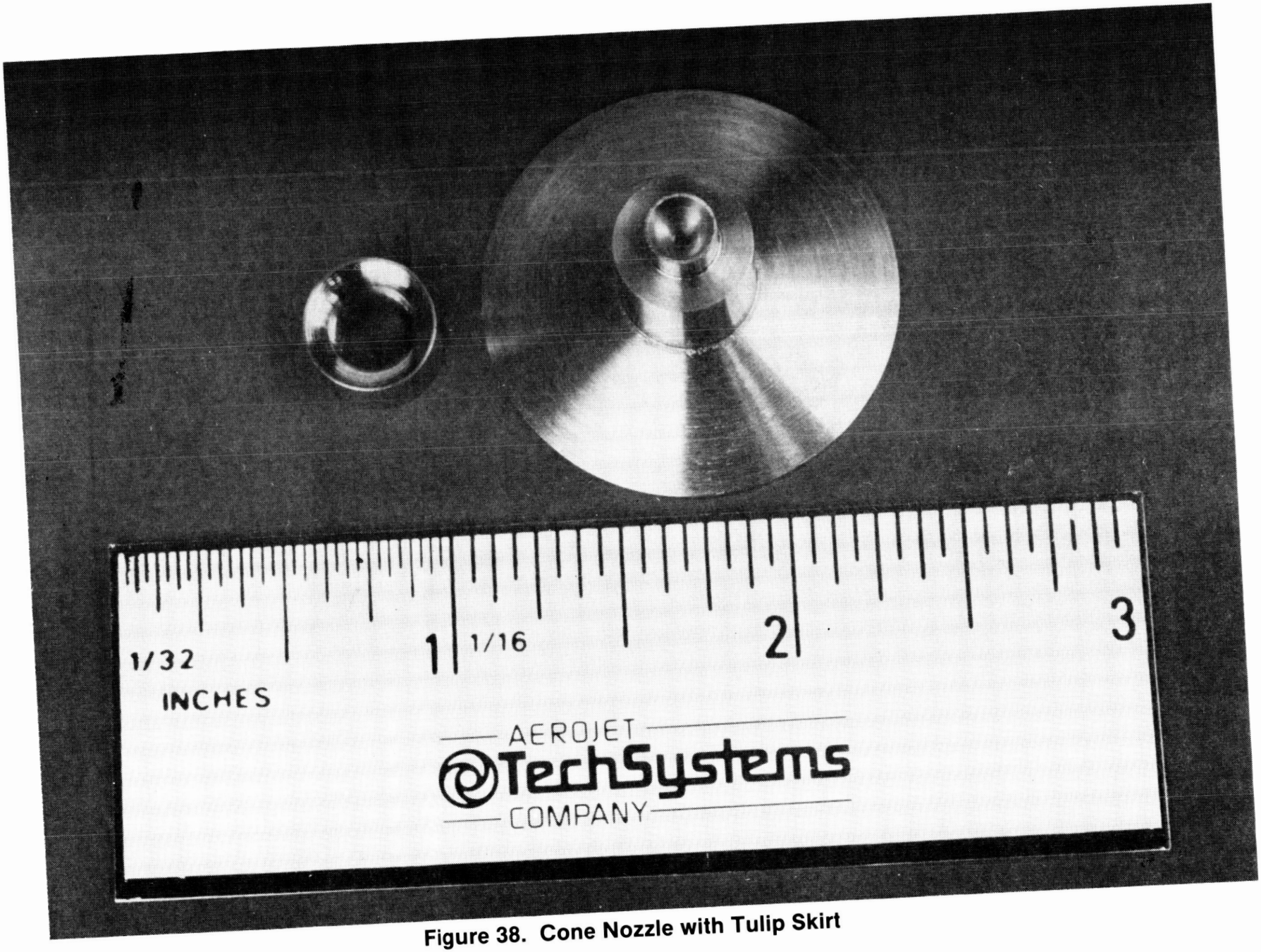

Figure 38. Cone Nozzle with Tulip Skirt

Figure 39. Tulip Nozzle with Cone Skirt Attached

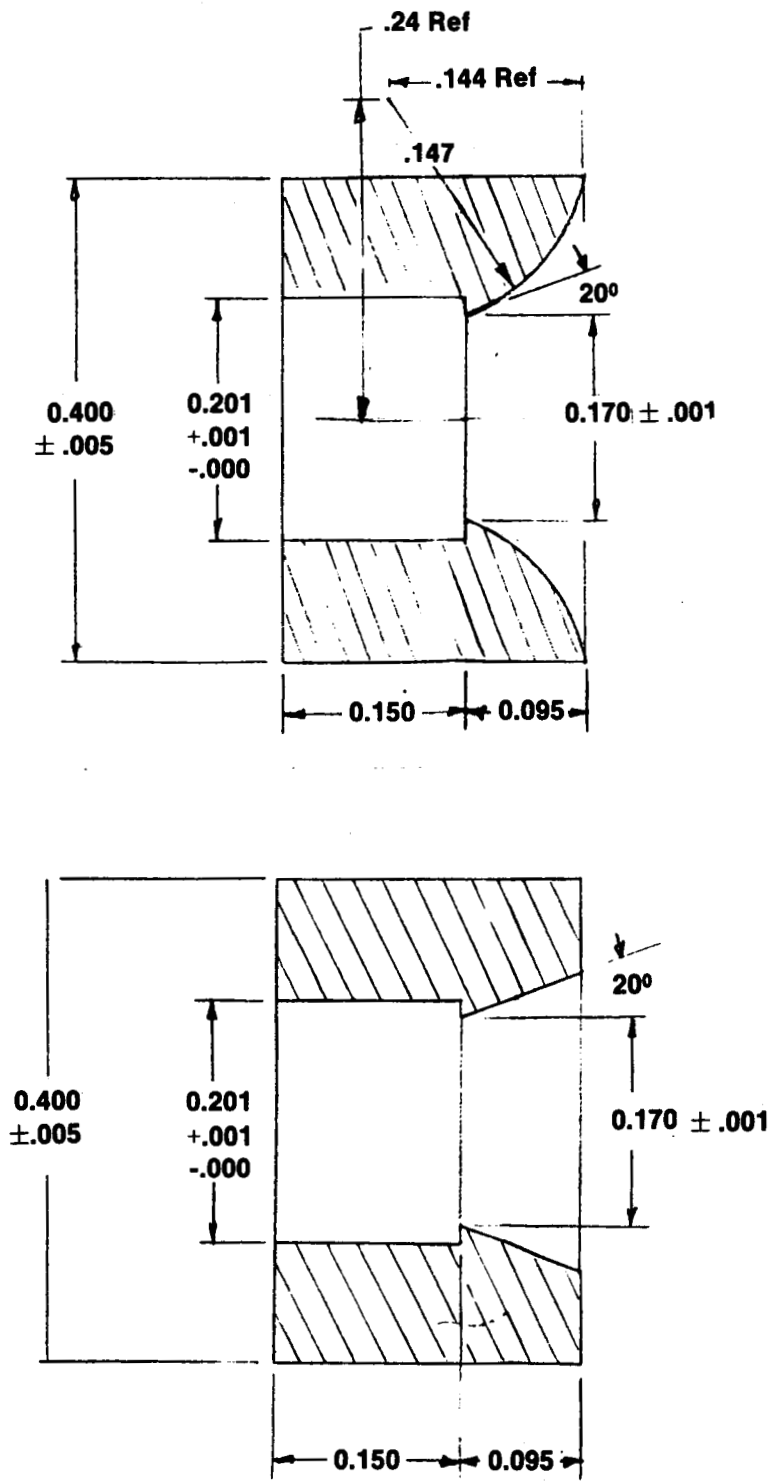

Figure 40. Tulip and Cone Skirts (Dimensions in Inches)

3.4, Nozzle Testing (cont.)

Evaluating the potential parameters to achieve a Reynolds number in the 500-2000 range, a limited combination is available. Nitrogen is not feasible. Throat diameters of approximately 5 mils would be required to achieve the low Reynolds number. Hydrogen is the only feasible diatomic gas. The operating parameters are:

T_c = 1400 K
P_c = 100 kPa
d* = 0.061 cm
$\dot{m}$ = 5-20 milligrams/sec
P = 100-1000 watts

The power was adjusted to achieve the required enthalpy for a set mass flow rate. T_c was varied by changing $\dot{m}$ and P to evaluate thrust at various Reynolds numbers.

3.4.2 Test Results

Nozzle testing was limited due to leaking from braze joints of one of the chamber pressure taps during assembly. The leaks were not discovered prior to assembly of the hardware at NASA/LeRC. Facility scheduling precluded rebrazing the leading pressure tap. Since repair was not feasible, the hole was closed by installing a tantalum plug and peening to seal off the hole. Leaks were encountered in the braze between the original nozzle and the nozzle adaptor, and at the Grafoil seal in the nozzle.

Significant drift (~10%) in the thrust stand occurred in the course of 2-3 hours. The thrust stand zero was sensitive to vibration of the raised platform. Significant noise was encountered in the thrust measurements. The thrust stand was frequently recalibrated to reduce the calibration errors.

3.4, Nozzle Testing (cont.)

A hot run was performed using hydrogen propellant. When the chamber temperature reached 1140°C, the pressure dropped significantly, indicating a significant leak. Upon inspection, the second chamber pressure tube was found to have failed. The appearance was that of a grain boundary failure in the braze region. Therefore, a decision was made to discontinue hot runs and to pursue cold tests. Rubber gaskets were made to seal the nozzle and the swirl plate. Leak rate measurements indicated values less than the minimum measurable level.

An insulation plate was removed from the thrust stand, decreasing the weight. The thrust stand operated in a more stable mode with virtually no calibration change and minimal zero shift.

Due to the loss of both chamber pressure taps, an inlet pressure measurement was used for chamber pressure. The conductance drop between the line pressure gage and the chamber was calibrated by flowing gas with the nozzle removed, thus bringing the chamber pressure to ambient. A series of measurements was made to determine the conductance losses at various mass flow rates.

A series of cold-flow tests was performed in which the mass flow rate was set at various levels and the thrust and chamber pressures were measured. These experiments were performed with hydrogen, nitrogen, nitrogen-hydrogen mix, and helium. The cone and bell nozzles were tested without a skirt and the cone was tested with the cone skirt. An additional series was performed using a rotational flow in the chamber to simulate the swirl in the arcjet. Table III summarizes the configurations and conditions of the tests.

The results are inconclusive as to the effect of swirl on nozzle performance. There appears to be no significant effect of geometery on thrust coefficient at the Reynolds numbers tested. The results indicate a decrease in thrust coefficient with decreasing Reynolds number.

TABLE III

SUMMARY NOZZLE COLD FLOW TESTS

NOZZLE CONFIGURATION	FLOW	GAS	THROAT Re	THRUST COEFFICIENT
BELL no skirt	NO SWIRL	HYDROGEN	1739	1.61
"	"	NITROGEN	4576	1.31
"	SWIRL	HYDROGEN	4243	1.30
"	"	NITROGEN	4717	1.55
CONE no skirt	NO SWIRL	HYDROGEN	3986	1.17
"	"	NITROGEN	1407	1.32
"	"	HELIUM	2801	1.42
"	"	HYD / NIT	3410	1.35
CONE w/ CONE SKIRT	NO SWIRL	HYDROGEN	932	1.21
"	"	NITROGEN	1342	1.45
"	"	HELIUM	4376	1.51
"	"	HYD / NIT	2345	1.55

59

3.5 SERIES 1 TESTING

The initial testing on the advanced arcjet research thruster was performed at Technion Inc. The prime objectives of the test program were:

1) To establish the envelope of stable operation of a 1 kW arc thruster that is radiation and regeneratively cooled and operates with a minimum arc temperature.

2) To establish the validity of mechanisms, operational modes, and scaling laws predicted from the analysis of the arc-vortex interaction.

3) To ensure that the electrodes, seals, and/or feed-throughs survive for the required lifetime (~1000 hr) and number of thermal cycles (over 500). This is to be established with chemically inert propellants (a mixture of hydrogen, nitrogen, and ammonia) in the proper ratios to simulate the decomposition products of pure hydrazine.

To accomplish these objectives, the test plan shown in Table IV was implemented. In order to obtain the required data from the tests, the measurements shown in Table V were made. The instrumentation was calibrated prior to use to ensure accurate measurements. A correction factor was applied to the rotometer readings to account for the different gases. The rotometer was subsequently calibrated after the test series with the actual gases to check the correction factor.

Test Procedures and Results

The assembly shown in Figure 41 was used to adapt the arcjet to Technion's existing bell jar. This equipment has previously been used for 30 kW arcjet testing. The existing data acquisition system, gas system, calorimeter, vacuum system, and utilities were used for the 1 kw experiment. The principal effort required was to build the adapter assembly and connect an existing power supply.

TABLE IV

1 KW ARCJET TEST PLAN - TEST SERIES 1

TEST GROUP	TEST PURPOSE	HARDWARE CONFIG.	POWER, KW	PROPELLANT	DURATION MINUTES	PROPELLANT FLOW RATE, GM/MIN	ARC GAP, CM	MAGNETIC FIELD TESLA	TOTAL TESTS	EXPECTED RESULTS
1.1	COLD FLOW CHECKOUT									
1.1.1	PROOF TEST	BASELINE	-	N_2	-	-	-	-	AR	CHARACTERIZE INITIAL CONDITION/SUITABLILTY OF BASELINE HARDWARE & CALIBRATE AS FUNCTIONS OF TEST VARIABLES.
.2	LEAK CHECK		-	N_2	-	-	-	-		
.3	FLOW FOR KW		-	N_2	-	-	0.2-1.0	-		
.4	ARC/MIX CHAMBER FLOW SPLIT		-	N_2	-	0-4	-	-		
.5	IMPEDANCE & BREAKDOWN VOLTAGE		-	N_2	-	-	0.2-1.0	-		
.6	MAGNETIC FIELD INTENSITY		-	AIR	-	-	-	0-0.1		
1.2	IGNITION SEQUENCE									
1.2.1	NITROGEN START		0-1.0	N_2	1.0	0-4	0.2-1.0	.05	AR	DEVELOP STARTING SEQUENCE FOR MAXIMUM STABILITY & MINIMUM EROSION; SET INITAL ARC LENGTH & MAGNETIC FIELD.
.2	NITROGEN + HYDROGEN START		0-1.0	N_2*N_2	1.0	0-4				
.3	NITROGEN + HYDROGEN + AMMONIA START		0-1.0	N_2*N_2*NH_3	1.0	0-4				
.4	OPTIMUM START SEQUENCE		0-1.0	N_2*N_2*NH_3	1.0	0-4	BASELINE	BASELINE		
1.3	OPERATING POINT TESTS								6	LOOK FOR EVIDENCE OF LIFE LIMITING EFFECTS
1.3.1	THERMAL EQUILIB/COMPONENT ENDURANCE		1.0(NOM.)	N_2*N_2*NH_3	20	2.0	AR	AR	6	LIFE LIMITING EFFECTS
1.3.2	SET BEST OPERATING ENTHALPY		1.0	N_2*N_2*NH_3	20	BEST	BASELINE	BASELINE	6	OPTIMIZE ELECTRODE GAP
1.3.3	SET BEST ELECTRODE SPACING		1.0			BEST	BEST	BASELINE	6	OPTIMIZE MAGNETIC FIELD
1.3.4	SET BEST MAGNETIC FIELD		1.0			BEST	BEST	BEST	6	ADJUST BEST OPERATING POINT
1.3.5	RE-OPTIMIZE VARIABLES		1.0		20	BEST	BEST	BEST	6	DETERMINE EFFECT OF POWER LEVEL
1.3.6	POWER LEVEL EFFECTS		0.5-1.5		20	50-150%	BEST	BEST		
1.4	ENDURANCE EVALUATION									
1.4.1	EXTENDED DURATION		1.0	N_2*N_2*NH_3	60	BEST	BEST	BEST	10	EVALUATE HARDWARE LIFE
1.4.2	LONG DURATION		1.0	N_2*N_2*NH_3	3000	BEST	BEST	BEST	2	100 HR ENDURANCE

Table V.

Measurements Made During Test Series No. 1

Measurement	Instrument
Current	Hall Effect Ammeter
Voltage	Voltage Divider and Digital Voltmeter
Mass Flow Rate	Rotometer
Arc Length	Cathode Position
Magnetic Field Strength	Magnet Current and Calibration
Arc Temperature	Estimate from Ohn's Law
Throat Tempertaure) Nozzle Temperature) Body Temperature)	Thermocouples
Power-In Gas	Calorimeter

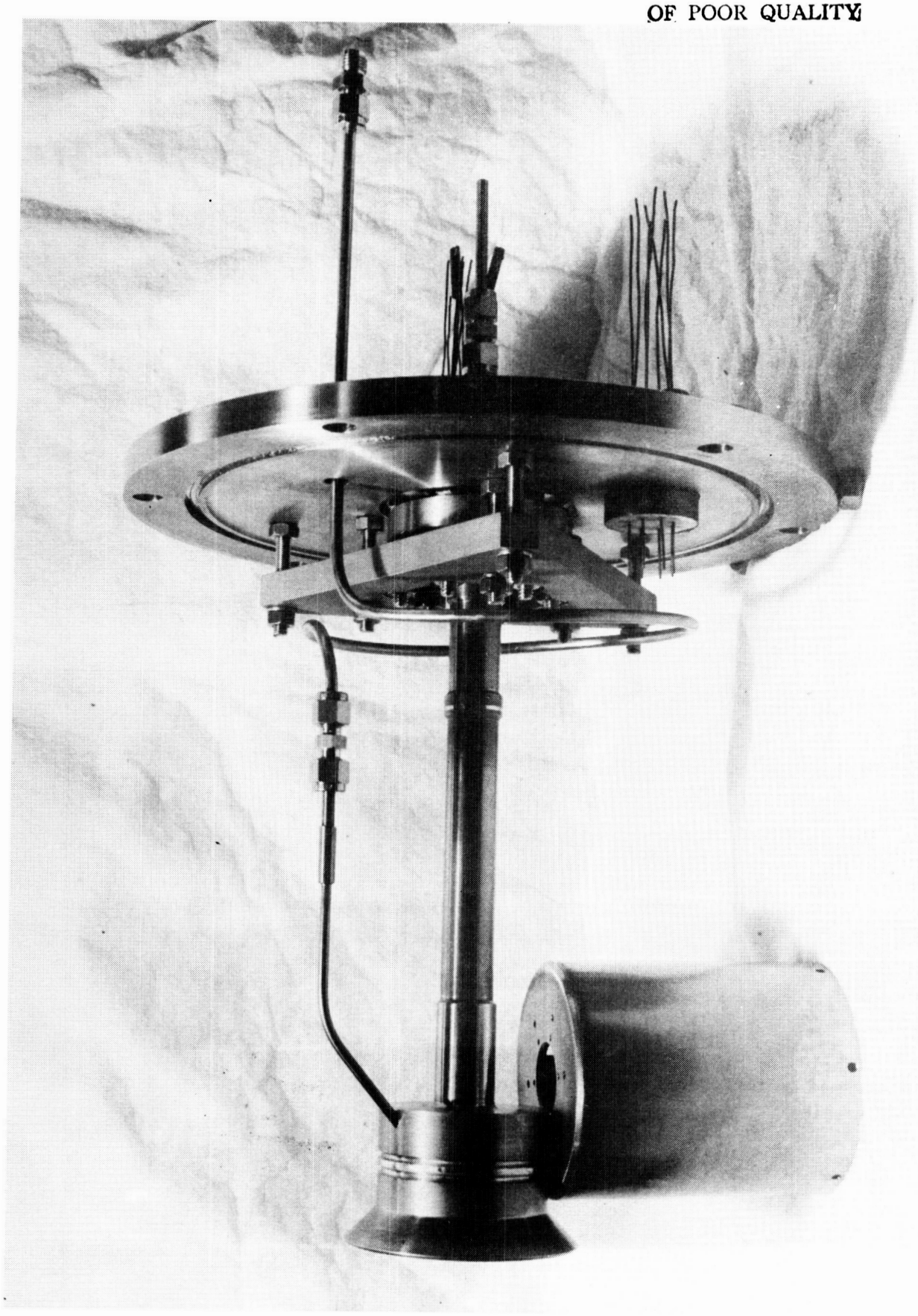

Figure 41. Research Arcjet Mounted to Bell Jar Adaptor (the Nozzle is Supported by a Cylinder which is not Part of the Thruster or Bell Jar Adaptor)

3.5, Test Series 1 Testing (cont.)

A schematic drawing of the test facility is shown in Figure 42. The electric schematic is shown in Figure 43. Optional series resistors (3), each 245 ohm have been used instead of the ten 50 ohm resistors. A gas flow schematic is presented in Figure 44. This system was used for the engine characterization tests except that no preheating of the gas was done. For the characterization tests a water-cooled copper electromagnet was used. The target calorimeter was also used. The cooling water circuits for the colorimeter and electromagnet as well as the thermocouple locations for measuring the temperature of the engine body, are shown in Figure 45.

The axial magnetic field strength on the axis of the solenoid has been computed and is shown in Figure 46, for a current of 100 amperes passing through the solenoid.

The cathode was located by bringing it forward until it touched the anode and then retracting it a fixed amount. Tests have been conducted with three cathode locations, shown in Figure 47.

Table VI summarizes the results for the first 50 starts. Table VII shows summary test data for starts 51 through 77. Many starts did not result in a run for the following reasons:

1) The operating volatge of the arc required more than the power supply was capable of producing.

2) The sudden flow of N_2-H_2 propellant blew the arc out. Operation at that flow rate could be established in many cases by starting with argon and slowly introducing the nitrogen-hydrogen mixture.

The first 18 tests conducted where data has been acquired while the engine was running on a mixture of hydrogen and nitrogen are summarized in Table VII.

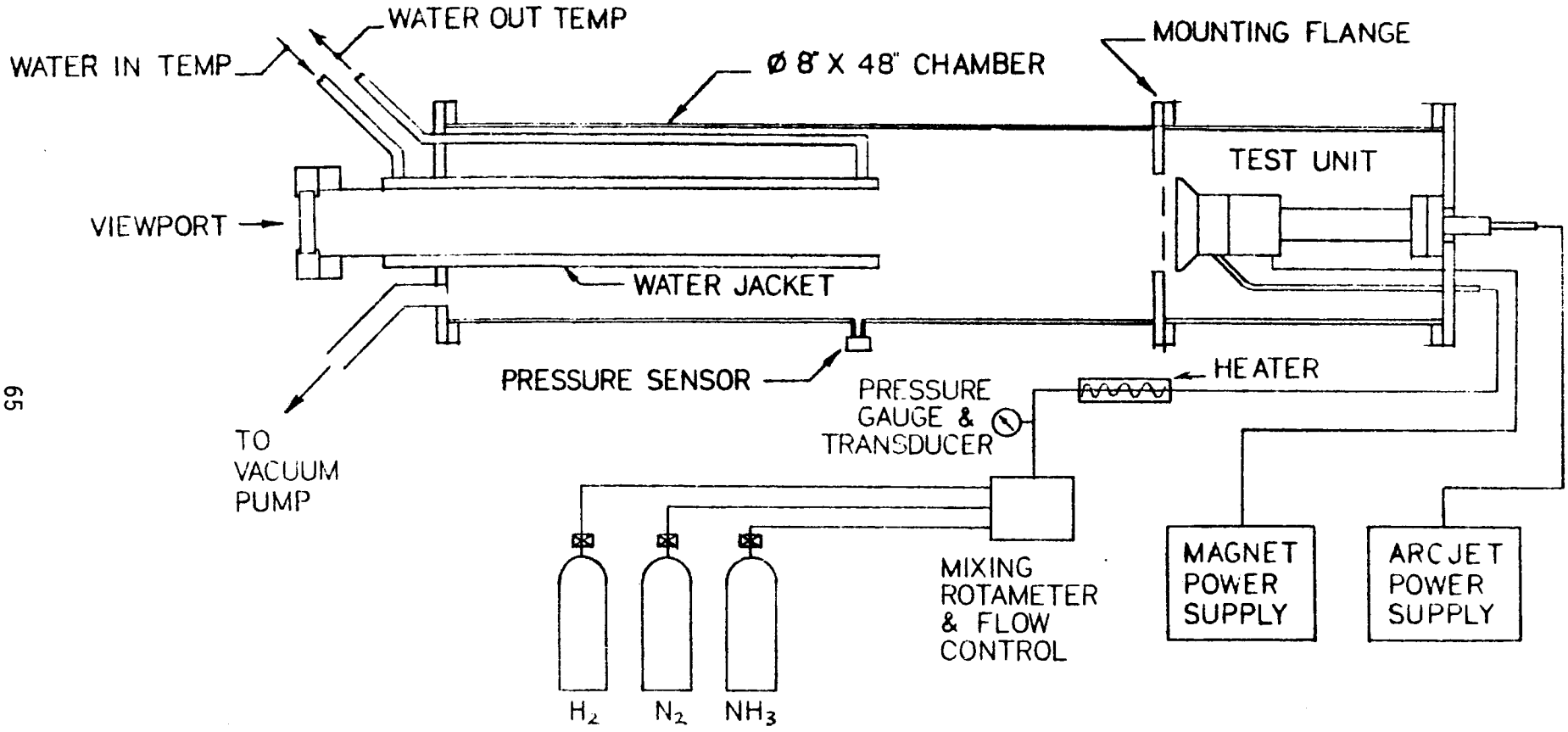

Figure 42. Schematic of Series I Test Facility

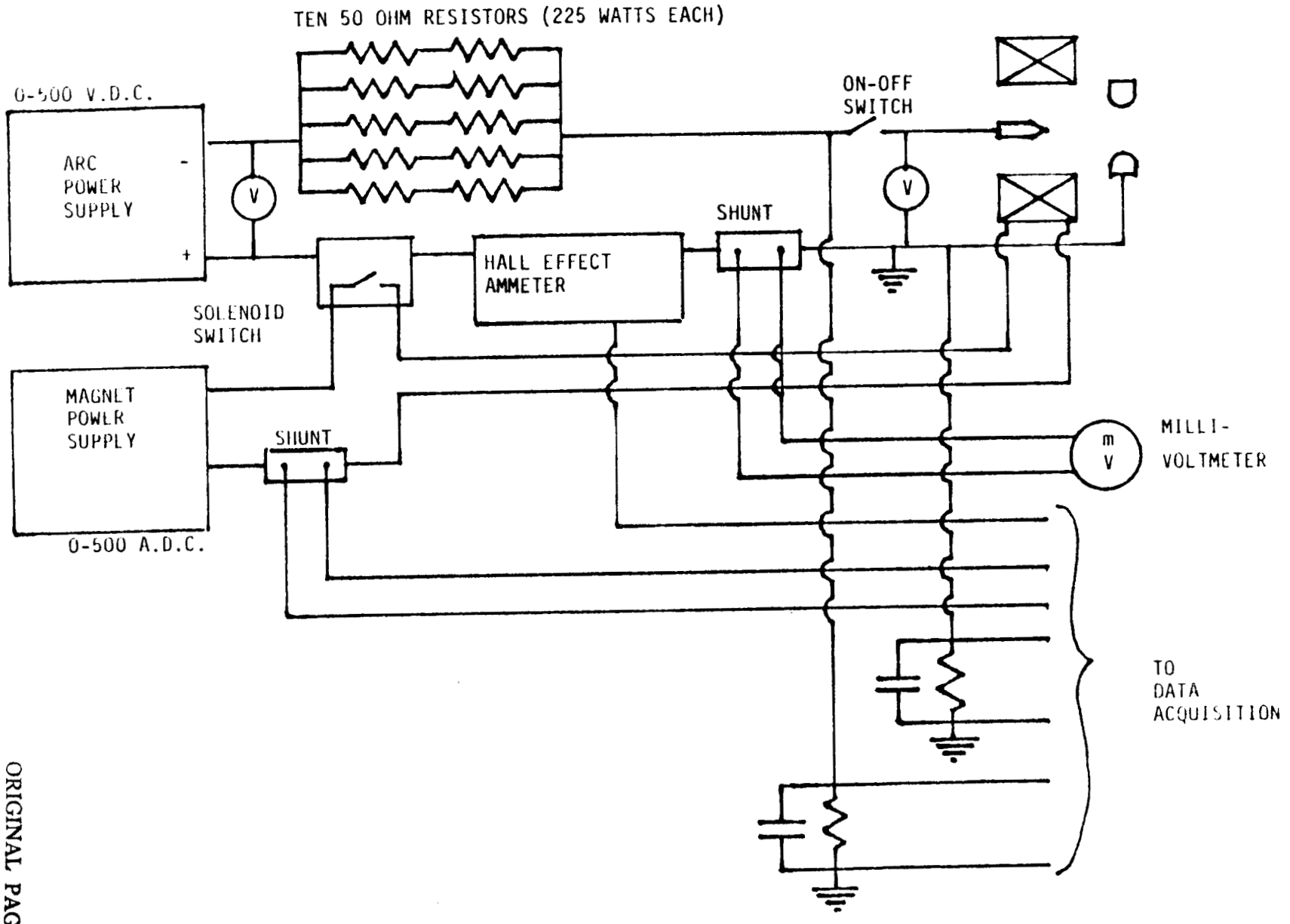

Figure 43. Electrical Wiring Schematic

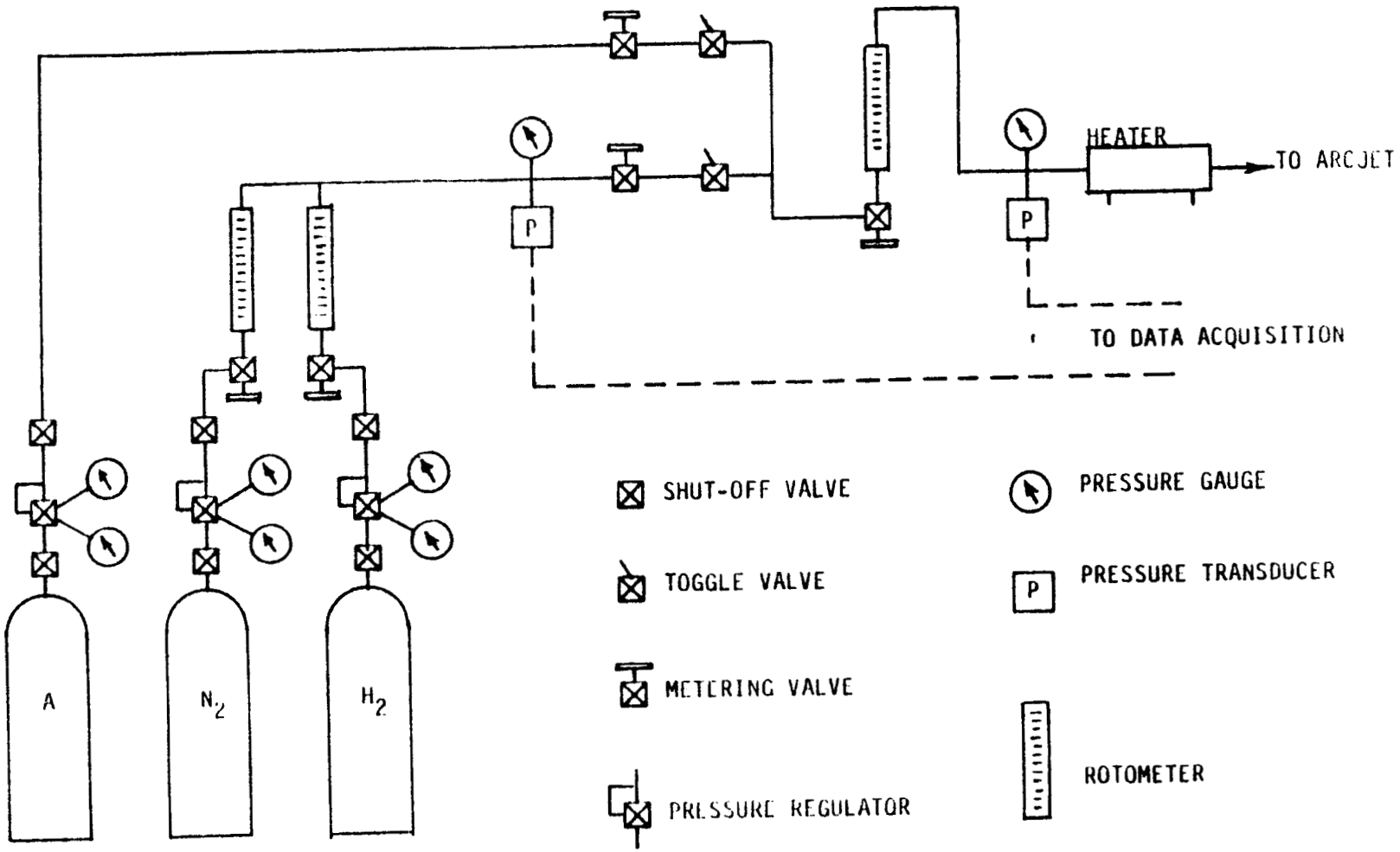

Figure 44. Propellant Supply Schematic

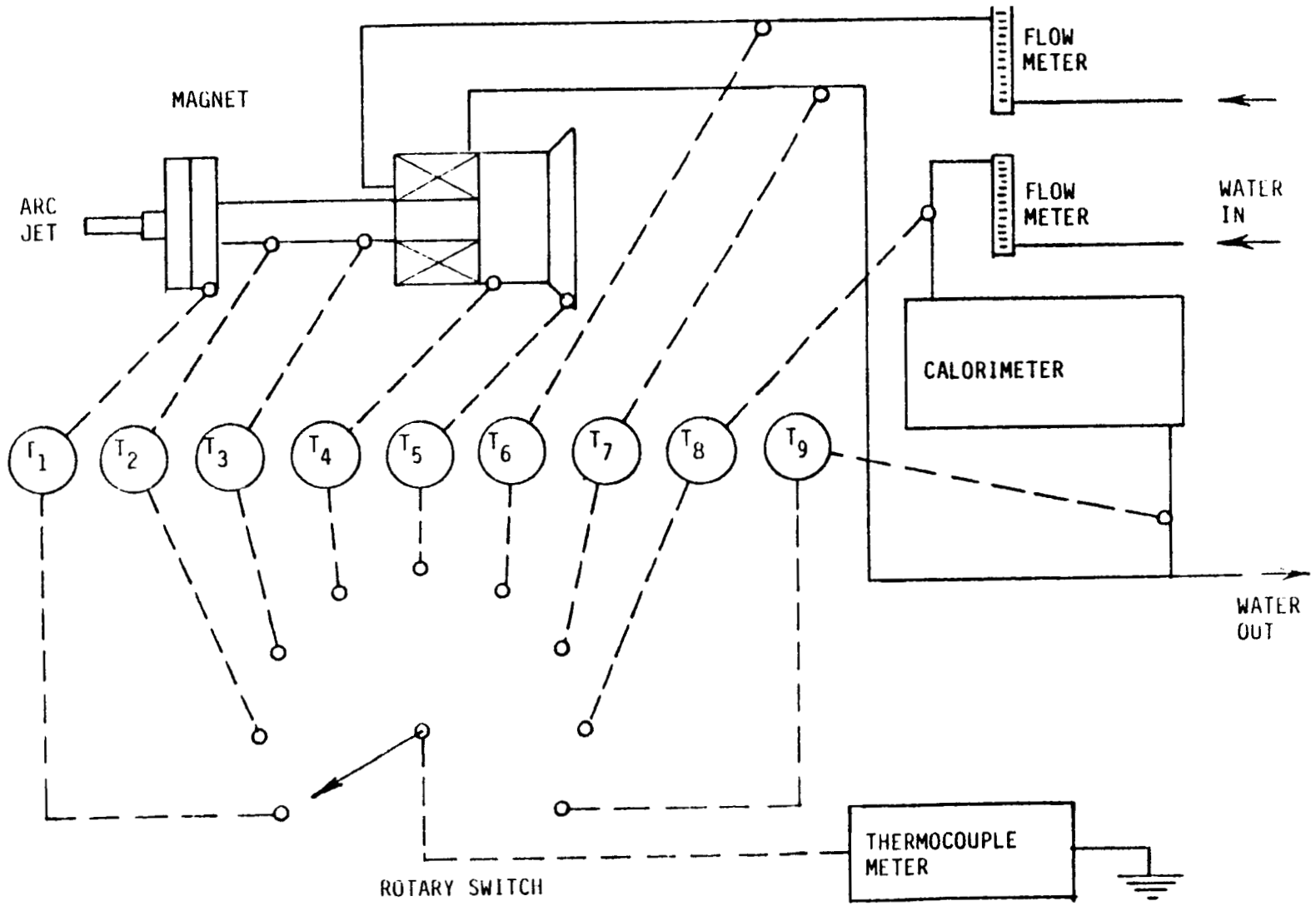

Figure 45. Water Flow and Thermocouple Schematic

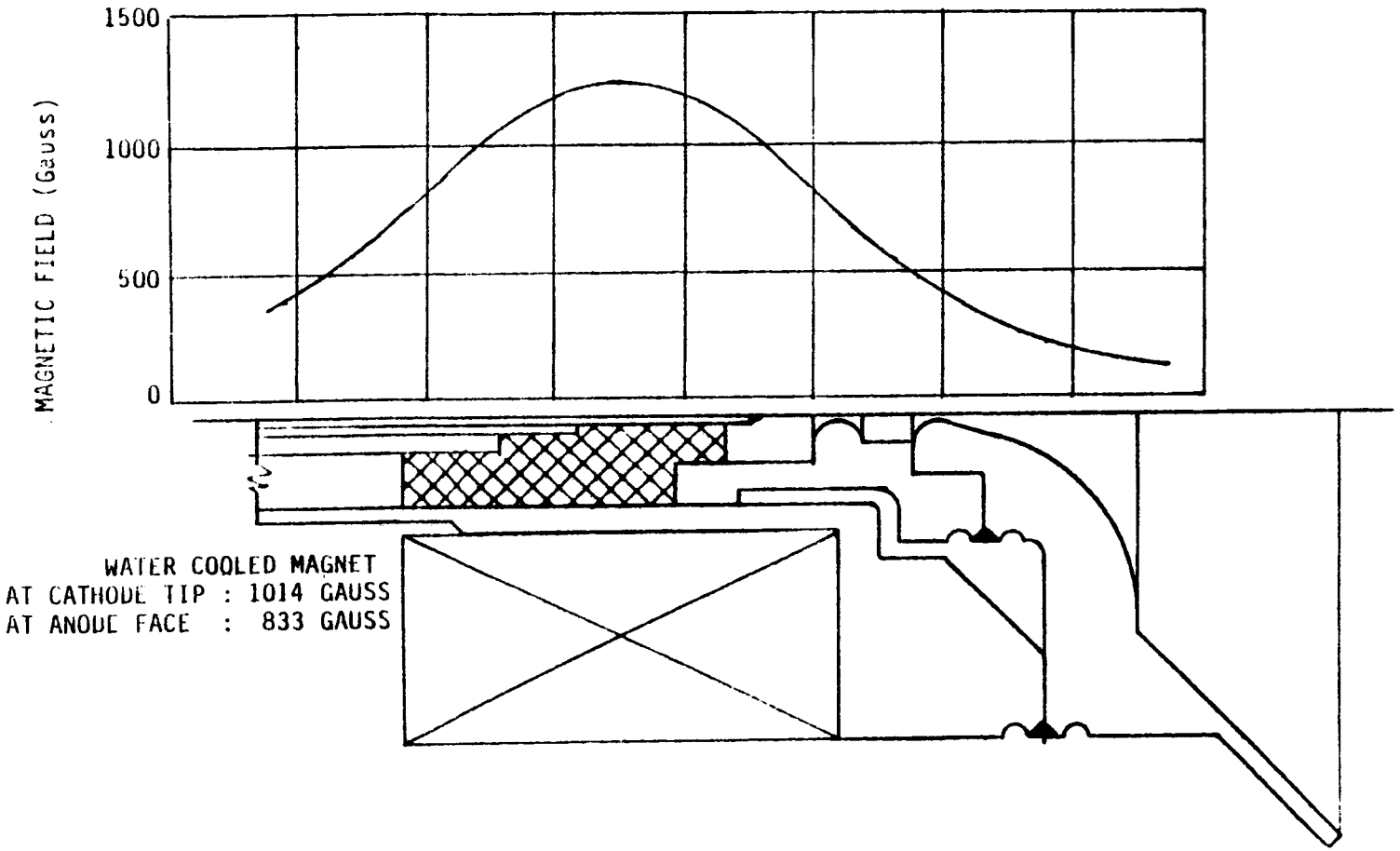

Figure 46. Magnetic Field Strength

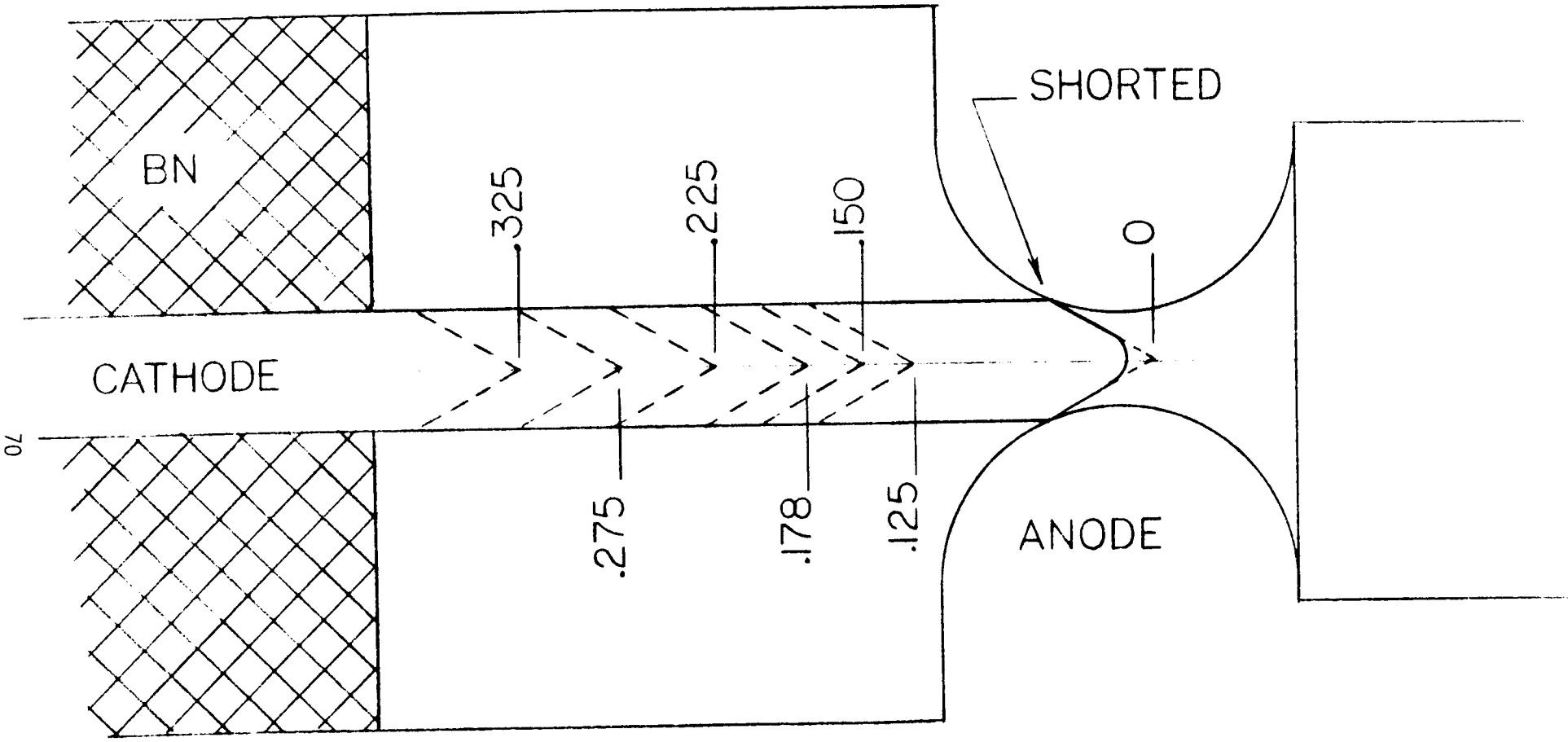

Figure 47. Cathode Location

TABLE VI

ARCJET PRELIMINARY TESTS

TEST RUN NO.	TEST TYPE/PURPOSE	RESULTS
1-7	FACILITY ACTIVATION, DATA ACQUISITION CHECKOUT	FACILITY/DATA ACQUISITION PROBLEMS RESOLVED, POWER SUPPLY SENSITIVITY IDENTIFIED.
8-13	ARGON FIRING TESTS	STARTING PROCEDURE DEVELOPED, TEMPERATURE INSTRUMENTATION CHECKED OUT, EFFECT OF MAGNETIC FIELD EVALUATED.
14-38	IGNITION TESTS, N_2/H_2	DEFINE IGNITION ENVELOPE AND SENSITIVITY TO POWER SUPPLY PARAMETERS, OPEN CIRCUIT VOLTAGE, ARC GAP, MAGNETIC FIELD.
39-50	ARGON START - TRANSITION TO N_2/H_2	DEVELOPED START TRANSITION PROCEDURE, SHORT DURATION N_2/H_2 OPERATION

TABLE VII

1 KW ARCJET TEST SUMMARY

TEST		ARC					MAGNET			GAS			REDUCED DATA				
No.	DURATION H/M/S	SERIES RESIST ohms	GAP SETTING inch	V-OC volts	Ia amps	Va volts	SERIES RESIST. ohms x10	FIELD GAUSS	I amps	P_{arg} Psia	P_{reg} Psia	P_c Psia	$\dot{m}$ mg/sec	P_A watts	C* m/sec	$\sqrt{P_a/\dot{m}}$ m/sec	T_{av} (η_{th}=.75) °K
51*	0/0/47	49	.125	50	8.76	25	0.6	343	40	47	- -	33					
	0/4/06	49	.125	500	6.77	226	0.6	343	40	--	62.6	27.5	22.7	1530	2238	8210	5900
		Next: Repeat Argon start, Argon off low N_2-H_2 flow, off as increase															
52*	0/0/37	49	.125	500	8.60	25	0.6	343	40	47	- -	32					
		Next: Repeat Argon start, Argon off low N_2-1h flow, off as increase															
53*	0/0/37	49	.125	500	8.60	25	0.6	343	40	47	- -	33.8					
	0/0/48				5.73	273				--	62.5	29.5	22.7	1564	2400	8301	6000
		Next: Installed capacitors in P.S.; Increased magnetic field															
54*	0/0/33	49	.125	500	7.07	22	0.6	509	60	31.2	- -	31.2					
55		Argon start; gradual to H_2-N_2									48.0						
	0/4/40		.125		7.21	89.6					48.0	44.4	44.2	646	1856	3823	3200
		Next: Try N_2-H_2 start															
56*	0/1/0	49	.125	500	632	108	0.6	509	60		51.0	49.0	50.3	683	1799	3685	3100
		N_2-H_2 start															
		Next: Increase magnetic field															
57*	0/1/0	49	.125	500	6.16	102	0.6	597	70	--	50.1	48.1	49.9	628	1781	3548	3000
		N_2-H_2 start															
	0/1/0	Increase I_a			6.64	100	0.6	597	70	--	50.3	48.6	49.9	664	1799	3648	3100
		Next: Reduce magnetic field															
58*	0/1/0	49	.125	500	6.20	122	0.6	423	50	--	52.7	51.2	47.7	756	1983	3981	3300
59*	0/1/0	Increase im			6.11	129	0.6	423	50		75.1	73.6	81.7	788	1664	3106	2700
		N_2-H_2 start, increasing in blew out arc															
		Next: Repeat															

TABLE VII (cont.)

TEST		ARC					MAGNET			GAS			REDUCED DATA				
No.	DURATION H/M/S	SERIES RESIST ohms	GAP SETTING inch	V-OC volts	Ia amps	Va volts	SERIES RESIST. ohms x10	FIELD GAUSS	I amps	P_{arg} Psia	P_{reg} Psia	P_c Psia	$\dot{m}$ mg/sec	P_A watts	C* m/sec	$\sqrt{P_a \dot{m}}$ m/sec	T_{av} (η_{th} = .75) °K
61*	0/1/0	49	.125	500	5.97	102	0.6	423	50	--	39.2	38.2	41.8	609	1688	3817	3200
		N_2-H_2 start															
		Next: Increase gap															
62*	0/1/0	49	.125	500	5.81	109	0.6	423	50	--	46.8	45.6	49.7	633	1695	3569	3100
	0/1/0	Increase I			6.11	109	0.6	423	50	--	48.8	47.7	49.7	666	1773	3661	3200
63, 64, 65			.178	No start													
66	0/0/20	49	.178	500	6.72	26	0.6	419	50	39.7	- -	- -					
		Argon start - out with N_2-H_2															
67	0/0/23	49	.178	500	8.34	23	0.6	420	50	36.3							
*		Argon start, gradual switch to N_2-H_2															
*	0/1/40	49	.178		6.16	12.1	0.6	421	50	--	46.7	45.1	48.5	745	1718	3919	3300
		Arc OUT, increasing magnetic field to 461 gauss															
		Next: Reduce arc length and increase magnetic field															
68*	0/1/0	49	.148	500	6.16	102	0.6	506	60	--	45.7	44.0	48.2	628	1686	3610	3100
	0/6/03	49	.148 Raise Ia		6.62	106	0.6	507	60	--	47.3	45.8	48.2	702	1755	3816	3200
		Next: Increase magnetic field															
		Repeat															
70*	0/1/10	49	.148	500	6.15	109	0.6	596	70	--	46.2	44.8	49.0	670	1689	3698	3200
*	0/4/20	49	.148 Lower B-field		6.16	108	0.6	507	60	--	47.9	46.7	49.4	665	1746	3669	3200
*	0/2/26	49	.148 Increase Ia		6.65	108	0.6	507	60	--	49.9	48.6	49.8	718	1803	3797	3200
*	0/1/40	49	.148 "	"	7.19	106	0.6	508	60	--	50.1	48.8	50.2	762	1796	3896	3300
*	0/1/40	49	.148 "	"	7.66	102	0.6	508	60	--	50.4	49.1	50.6	781	1792	3929	3300

TABLE VII (cont.)

TEST No.	DURATION H/M/S	ARC: SERIES RESIST ohms	ARC: GAP SETTING inch	ARC: V-OC volts	ARC: Ia amps	ARC: Va volts	MAGNET: SERIES RESIST. ohms X10	MAGNET: FIELD GAUSS	MAGNET: I amps	GAS: Parg Psia	GAS: Preg Psia	GAS: Pc Psia	REDUCED DATA: $\dot{m}$ mg/sec	REDUCED DATA: PA watts	REDUCED DATA: C* m/sec	REDUCED DATA: $\sqrt{Pa/\dot{m}}$ m/sec	REDUCED DATA: Tav (Mth = .75) °K
*	0/1/48	49	.148	Increase Ia	8.12	102	0.6	507	60	--	51.4	50.3	51.0	828	1822	4029	3400
*	0/1/20	49	.148	" "	8.66	99	0.6	507	60	--	51.4	50.3	51.4	857	1808	4083	3400
		P.S. Fuse blew															
74*	0/1/0	49	.225	500	8.2	23.0	0.6	430	60	30				DATE: 8/8/86			
		Argon start good - transitioned to H_2-N_2															
	0/7/38	49	.225	500	7.4	156.5	0.6	430	60	--	63.07	63.1	53.4	1158	2183	4657	3700
77*	0/0/45	49	.225	500	8.2	not reading	0.6	428	60	46	- -						
		Argon start good - transitioned to H_2-N_2															
	0/3/12		.225		8.17	145	0.6	428	60	--	62.7	62.3	53.5	1185	2151	4706	3700
		Increase B - field															
	0/0/54	49	.225		8.12	148	0.6	463		--	63.4	63.1	53.0	1202	2199	4762	3800
		Increase B - field															
	0/1/52	49	.225		8.08	149	0.6	508		--	64.0	63.7	52.6	1204	2237	4784	3800
		Decrease mass flow rate															
	0/5/0	49	.225		8.18	137	0.6	507		--	61.5	61.2	52.6	1137	2149	4649	3700
		Increase magnetic field (B-field)															
	0/1/0	49	.225		8.18	137	0.6	580		--	61.1	60.8	52.7	1121	2131	4612	3700
		Increase magnetic field															
	0/1/54	49	.225		8.16	138	0.6	598			61.2	61.0	52.8	1126	2134	4618	3700
		Decrease magnetic field															
	0/8/40	49	.225		8.15	141	0.6	509			61.9	61.6	52.8	1149	2155	4665	3700
		Adjust mass flow rate upward															
77	0/1/6	49	.225		7.81	182	0.6	510			70.9	70.5	60.4	1421	2156	4850	3800
		P.S. capacitor failed															

3.5, Test Series 1 Testing (cont.)

- Parametric Tests

The No. 1.3 series of tests which involved filling in a matrix of arc current, mass flow rate, magnetic field, and anode-to-cathode gap were completed in Tests 78 through 104. Power supply limitations severly restricted the range of the variables over which useful data could be obtained. Test data were obtained over the following ranges of variables.

Arc Current	6 - 9.5 amperes
Mass Flow Rate	30 - 50 mg/sec
Centerline Magnetic Field Strength at the Anode	330 - 580 gauss
Arc Gap	0.343 - 0.572 cm

Evaluating the data, the following nominal ranges of the variables were picked for an endurance test.

Arc Current	8 - 8.5 amperes
Electrode Gap	0.343 - 0.381 cm
Mass Flow Rate	35 - 50 mg/sec
Axial Magnetic Field Strength	417 - 500 gauss

In Series 1.4, endurance testing, the initial tests were partly a search for power supply characteristics that permit long-term testing. Seventy-five starts were necessary to obtain the first 47.5 hours of hot operating time extending over Tests 105 through 181. During these tests, the engine was thermally cycled 37 times. A thermal cycle is defined as a run that lasts 10 minutes and is off long enough to permit the peak thermocouple temperature to fall below 300 C.

The parametric tests are summarized in Table VIII. In the course of the testing, several improvements were made to the data acquisition. The nitrogen and hydrogen flow meter tubes were replaced with smaller units in order to increase the scale readings for the typical flow range and to provide better accuracy. The ammonia branch was added to the flow system

TABLE VIII

SUMMARY OF TESTS

TEST No.	VIDEO CAMERA	MAGNETIC FIELD CURRENT (amps)	PURPOSE P=Parametric, E=Endurance	ARC POWER SUPPLY T=Technion E=Eratron	CAPACITANCE (uf)	RESISTANCE (Ohms)	STARTING GAS	START	TRANSITION TO PROPELLANT GAS	GAP (inches)	OFF *	OUT *	MODE	TEST DURATION (Minutes)	COMMENTS	ARC VOLTAGE (VOLTS)	ARC CURRENT (AMPS)
78	No	60	P	E	0	0	A	Yes	No	.220	-	Yes	-	-	Bring the Eratron power supply on line	320	8.20
79	"	"	"	"	"	"	"	"	"	"	"	"	"	"	" " " " "		
80	"	"	"	"	"	"	"	"	"	"	"	"	"	"	" " " " "		
81	"	"	"	"	"	"	N_2/H_2	No	N.A.	"	"	-	"	"	" " " " "		
82	"	"	"	"	"	"	A	Yes	No	"	"	Yes	"	"	" " " " "		
83	"	"	"	"	"	24.5	A	"	Yes	"	"	"	"	1/2	" " " " "		
84	"	"	"	"	"	"	"	"	"	"	Yes	-	H.V.	3	" " " " "		
85	"	"	"	"	"	"	"	"	No	"	-	Yes	-	-	Try I=7.5		
86	"	"	"	"	"	"	"	"	"	"	-	"	-	-	Try I=7.0		
87	"	"	"	"	"	49	"	"	"	"	"	"	"	"	" " " " "		
88	"	"	"	"	"	"	"	"	Yes	"	-	"	H.V.	2½	Check Flow System Corrected Leak		
89	"	"	"	"	"	"	"	"	No	"	-	"	-	-			
90	"	"	"	"	"	24.5	"	"	Yes	"	Yes	-	H.V.	16½		265	7.20
91	"	"	"	"	"	"	"	"	No	-	-	Yes	-	-	Try 6 Amps		
92	"	"	"	"	"	"	"	"	Yes	"	Yes	-	H.V.	9	Try 8 Amps	310	7.80
93	"	"	"	"	"	"	"	"	No	"	-	Yes	-	-			
94	"	"	"	"	"	"	"	"	"	"	"	"	"	"			
95	"	"	"	"	"	"	"	"	"	"	"	"	"	"			
96	"	"	"	"	"	"	"	"	"	"	"	"	"	"	Examine Cathode		
97	"	"	"	"	"	"	"	"	"	"	"	"	"	"			

*"Off" Test Terminated Manually; "Out" Arc Extinguished

TABLE VIII (cont.)

TEST No.	VIDEO CAMERA	MAGNETIC FIELD CURRENT (amps)	PURPOSE P=Parametric, E=Endurance	ARC POWER SUPPLY T=Technion E=Eratron	CAPACITANCE (uf)	RESISTANCE (Ohms)	STARTING GAS	START	TRANSITION TO PROPELLANT GAS	GAP (inches)	OFF	OUT	MODE	TEST DURATION (Minutes)	COMMENTS	ARC VOLTAGE (VOLTS)	ARC CURRENT (AMPS)
98	No	60	P	E	9000	24.5	A	-	-	22.7	-	-	-	-	Blew capacitor		
99	"	"	"	"	2250	"	"	Yes	Yes	"	Yes	-	-	-	Changed capacitor from parallel to series		
100	"	"	"	"	"	"	"	"	"	"	"	"	"	½	Inst. problem		
101	"	"	"	"	"	"	"	"	"	"	"	"	"	1	" " " " "		
102	"	60-72	"	"	"	"	"	"	"	.154	-	Yes	L.V.	26	Dismantled engine, New feed thru	133	4.19
103	"	60	"	"	"	"	"	"	"	.173	Yes	-	"	9	Arc extinguished. Start using ~5% ammonia		
104	"	"	"	"	"	"	"	"	"	"	-	Yes	"	1½	Arc extinguished.		
105	"	"	E	"	"	"	"	"	"	"	Yes	-	"	121	Examine cathode	140	8.00
106	Yes	"	"	"	"	"	"	"	No	"	-	Yes	-	-	-		
107	"	"	"	"	"	"	"	"	Yes	"	"	"	"	2			
108	"	"	"	"	"	"	"	"	"	"	"	"	"	1	Problem with computer acquisition &		
109	"	"	"	"	"	"	"	"	"	"	"	"	"	2	Problem on fully opening gas flow		
110	"	"	"	"	"	"	"	"	"	"	"	"	"	2			
111	"	"	"	"	"	"	"	"	"	"	"	"	"	2	" " " " "		
112	"	"	"	"	"	"	"	"	"	"	"	"	"	1½	" " " " "		
113	"	"	"	"	"	"	"	"	"	"	"	"	"	2	" " " " "		
114	"	"	"	"	"	"	"	"	"	"	"	"	"	1½	" " " " "		
115	"	"	"	"	"	"	"	"	"	.148	"	"	"	2½	" " " " "		
116	"	"	"	"	"	"	"	"	"	"	"	"	"	3½	" " " " "		
117	"	"	"	"	"	"	"	"	"	"	"	"	"	-	" " " " "		
118	"	"	"	"	"	18.46	"	"	"	"	"	"	"	2	" " " " "		
119	"	"	"	"	"	"	"	"	"	"	"	"	"	3	" " " " "		
120	"	"	"	"	"	33	"	"	"	"	"	"	"	10	" " " " "		
121	"	"	"	"	"	"	"	"	"	"	"	"	"	14	" " " " "	143	8.54
122	"	"	"	"	"	"	"	"	"	.202	"	"	"	9	" " " " "		

TABLE VIII (cont.)

TEST No.	VIDEO CAMERA	MAGNETIC FIELD CURRENT (amps)	PURPOSE P=Parametric, E=Endurance	ARC POWER SUPPLY T=Technion E=Eratron	CAPACITANCE (uf)	RESISTANCE (Ohms)	STARTING GAS	START	TRANSITION TO PROPELLANT GAS	GAP (inches)	OFF	OUT	MODE	TEST DURATION (Minutes)	COMMENTS	ARC VOLTAGE (VOLTS)	ARC CURRENT (AMPS)
123	Yes	60	E	E	2250	33	A	Yes	Yes	.202	-	Yes	L.V.	2			
124	"	"	"	"	"	"	"	"	"	.145	Yes	-	-	127	Removed and Examined Cathode Photos.	150	8.12
125	"	"	"	"	"	"	"	"	"	"	-	Yes	"	22.5		150	8.02
126	"	"	"	"	"	"	"	"	"	"	"	"	"	-	Eratron Supply Dead		
127	"	"	"	T	2250	"	"	"	No	.145	-	"	-	-			
128	"	"	"	"	"	"	"	"	Yes	"	"	"	L.V.	3	Arc extinguishes		
129	"	"	"	"	"	"	"	"	"	"	"	"	"	4	" " " " "		
130	"	"	"	"	"	"	"	"	"	"	"	"	"	5	" " " " "		
131	"	"	"	"	"	"	"	"	"	"	"	"	"	5	" " " " "		
132	"	"	"	"	"	"	"	"	"	"	"	"	"	8½	" " " " "		
133	"	50	"	"	"	"	"	"	"	"	"	"	"	36	" " " " "	142	8.00
134	"	"	"	"	"	"	"	"	"	.135	"	"	"	6½	" " " " "		
135	"	"	"	"	"	"	"	"	"	"	"	"	"	30	Try going to 8½ amps from 8 amps	137	8.46
136	"	"	"	"	"	24.5	"	"	No	"	"	"	"	2	Arc extinguishes		
137	"	"	"	"	"	"	"	"	Yes	"	"	"	"	2½	" " " " "		
138	"	"	"	"	"	37	"	"	"	"	"	"	"	2			
139	"	"	"	"	"	"	"	"	"	"	"	"	"	61	" " " " "		
140	"	"	"	"	"	42.2	"	"	"	"	"	"	"	218	" " " " "	140	8.40
141	"	"	"	"	"	"	"	"	"	"	"	"	"	66	" " " " "	144.5	8.36
142	"	"	"	"	"	"	"	"	"	"	"	"	"	54	" " " " "	139	8.40
143	"	"	"	"	"	"	"	"	"	"	"	"	"	44		152	8.00
144	"	"	"	"	"	"	"	"	"	"	"	"	"	68	" " " " "	144	8.36
145	"	"	"	"	"	"	"	"	"	"	"	"	"	102	" " " " "	146	8.48
146	"	"	"	"	"	"	"	"	"	"	"	"	"	32	" " " " "	144	8.5

TABLE VIII (cont.)

TEST No.	VIDEO CAMERA	MAGNETIC FIELD CURRENT (amps)	PURPOSE P=Parametric, E=Endurance	ARC POWER SUPPLY T=Technion E=Eratron	CAPACITANCE (uf)	RESISTANCE (Ohms)	STARTING GAS	START	TRANSITION TO PROPELLANT GAS	GAP (inches)	OFF	OUT	MODE	TEST DURATION (Minutes)	COMMENTS	ARC VOLTAGE (VOLTS)	ARC CURRENT (AMPS)
147	Yes	50	E	T	2250	42.2	A	Yes	Yes	.135	-	Yes	L.V.	35	Arc extinguishes	146	8.48
148	"	"	"	"	"	"	"	"	"	"	"	"	"	87	" " " " "	143	8.50
149	"	"	"	"	"	"	"	"	"	"	"	"	"	95	Examined cathode		
150	"	"	"	"	"	"	"	"	"	"	"	"	"	-	" " " " "		
151	"	"	"	"	"	"	"	"	"	"	"	"	"	8	" " " " "		
152	"	"	"	"	"	"	"	"	"	"	"	"	"	2	" " " " "		
153	"	"	"	"	"	"	"	"	"	"	"	"	"	5	" " " " "		
154	"	"	"	"	"	"	"	"	"	"	"	"	"	63	No ammonia	147	8.08
155	"	"	"	"	"	"	"	"	"	"	"	"	"	108	Arc extinguishes	142	8.48
156	"	"	"	"	"	"	"	"	"	"	"	"	"	13	" " " " "		
157	"	"	"	"	"	"	"	"	"	"	"	"	"	19	" " " " "		
158	"	"	"	"	"	"	"	"	"	"	"	"	"	74	" " " " "	154	9.00
159	"	"	"	"	"	45.6	"	"	"	"	"	"	"	48	" " " " "	153	8.08
160	"	"	"	"	"	"	"	"	"	"	"	"	"	37	" " " " "	143	8.50
161	"	64	"	"	"	"	"	"	"	"	"	"	"	101	" " " " "	156	8.08
162	"	"	"	"	"	"	"	"	"	"	"	"	"	87	" " " " "	156	8.56
163	"	"	"	"	"	"	"	"	"	"	"	"	"	41	" " " " "		
164	"	63	"	"	"	"	"	"	"	"	"	"	"	34	" " " " "	156	8.02
165	"	64	"	"	"	"	"	"	"	"	"	"	"	30	" " " " "	156	8.0
166	"	60	"	"	"	"	"	"	"	"	"	"	"	2	" " " " "		
167	"	"	"	"	"	42.2	"	"	"	"	"	"	"	6	" " " " "		
168	"	"	"	E	"	24.5	"	"	"	"	"	"	"	-	" " " " "		

TABLE VIII (cont.)

TEST No.	VIDEO CAMERA	MAGNETIC FIELD CURRENT (amps)	PURPOSE P=Parametric, E=Endurance	ARC POWER SUPPLY T=Technion E=Eratron	CAPACITANCE (uf)	RESISTANCE (Ohms)	STARTING GAS	START	TRANSITION TO PROPELLANT GAS	GAP (inches)	OFF	OUT	MODE	TEST DURATION (Minutes)	COMMENTS	ARC VOLTAGE (VOLTS)	ARC CURRENT (AMPS)
169	Yes	60	E	E	2250	24.5	A	Yes	Yes	.135	-	Yes	L.V.	½	Arc Extinguishes		
170	"	"	"	"	"	"	"	"	"	"	"	"	"	8	" " " " "		
171	"	0	"	"	"	"	"	"	"	"	Yes	-	"	2	No magnetic Field		
172	"	60	"	"	"	"	"	"	"	"	-	Yes	"	7	Took apart, took photos	135	8.04
173	"	"	"	"	"	"	"	"	"	"	"	"	"	28	Arc extinguishes	128	8.04
174	"	70	"	"	"	"	"	"	"	"	"	"	"	11	" " " " "		
175	"	54	"	"	"	"	"	"	"	"	"	"	"	47	" " " " "	120	8.06
176	"	60	"	"	0	29.5	"	"	"	"	"	"	"	1	" " " " "		
177	"	"	"	"	"	"	"	"	"	"	"	"	"	11	" " " " "		
178	"	"	"	"	9000	24.5	"	"	"	"	"	"	"	1	" " " " "		
179	"	"	"	"	"	"	"	"	"	"	"	"	"	93	" " " " "	144	8.12
180	"	60	E	E	9000	36.8	A	Yes	Yes	.135	-	Yes	L.V.	135	" " " " "	142	8.04
181	"	"	"	"	"	"	"	"	"	"	Yes	-	"	604	Took apart; took photos	138	8.10

3.5, Test Series 1 Testing (cont.)

starting with Test No. 103. This provides for more complete simulation of hydrazine decomposition products. Ammonia flow was adjusted to correspond to a hydrazine reactor ammonia dissociation level of 80-85%.

The operational procedure adopted was as follows:

Starting

Vacuum breakdown was chosen as the preferred technique because, in the Technion engine configuration this represents a soft start. Typically an open circuit voltage of 500 volts was used, but, in a few tests the open circuit voltage was raised to 600 volts.

Starts were first tried by pumping down to under 10 microns in the chamber, applying the voltage to the arc electrodes and then opening the gas feed valves for the hydrogen-nitrogen mixture. When the arc did not ignite, the same procedure was adopted except argon was substituted for the hydrogen-nitrogen. Once an arc was established, then the valve feeding the hydrogen-nitrogen would be slowly opened while the valve feeding the argon was slowly closed. Attempts were made to ensure that the injection gauge pressure never fell below 237 kPa.

A solenoid switch was placed in the power lead to the arc so that arc current would activate a switch that turned on the magnet current. This was done since initially it had been observed that the magnetic field interfered with the vacuum breakdown. At the end of Test Series I, the soleniod switch was removed and starts with the magnet on were conducted. All tests in Test Series II were started with the magnet on.

At the conclusion of Test Series 1.0, starts with propellant gas were made using the following procedure.

3.5, Test Series 1 Testing (cont.)

Checkout Prior to Test

1) Retract the cathode from a shorted position to the cathode to the desired amount, between 0.30 - 0.36 cm.

2) Ensure that there is no leak through the seal to the cathode rod.

3) In vacuum environment, ensure that cathode rod external to the engine and the lead is adequately insulated.

4) Ensure that cathode-to-anode resistance is >10,000 ohms.

5) Ensure that gas feed-tube joint does not leak.

6) Ensure that a water flow rate greater than 4 gm/sec passes through the electromagnet.

7) Check the resistance of the magnet coil by passing 20-50 amperes with water flowing. With the engine cold, R $\simeq$0.038 ohms. When the engine is hot, ~0.040 ohms.

8) When passing 35 milligrams per second of simulated hydrazine through the cold engine, with no arc, the injection pressure should be over 169 kPa.

Startup

1) With water flowing through the electromagnet, increase the magnet current to 50 amperes. The voltage across the magnet should be 1.90 ± 0.02 volts.

2) Current control should be set to establish arc current between 7-8 amperes.

3) If argon start, argon flow rate should be set to give an injection pressure of 237 - 304 kPa with no arc.

3.5, Test Series 1 Testing (cont.)

4) If starting with to use simulated hydrazine products, flow rate should be about 35 milligrams/sec at injection pressure of about 414 - 440 kPa.

5) Eratron OCV should be set at minimum (740 volts) for starting to prevent breakdown before gas is injected.

Note: On numerous occasions at Technion, breakdown occurred before the gas was injected when using the Eratron power supply. Immediately opening the argon gas valve led to the normal arc start mode.

6) If an argon start is used, the argon valve can be opened to permit full flow at start.

7) A normal start is characterized by:

a) Luminosity is seen through the throat.
b) The ammeter registers a constant current.
c) The voltage across the arc should be 20-40 volts.

8) With an argon start, once conditions noted in No. 7 are met, the gas simulating hydrazine products should be introduced slowly into the flow. Once the full flow of this gas is established (~35 milligrams/sec), the argon can be turned off abruptly.

9) It may be desirable to ramp up the ignition voltage to see if it prevents the arc from extinguishing.

10) If a start using simulated hydrazine products is attempted, a valve can be opened to permit full gas flow after the power supply is energized.

3.5, Test Series 1 Testing (cont.)

OPERATIONAL PROCEDURES

A) It will take 10-15 minutes for the thruster to reach thermal equilibrium.

B) Using a Simpson Model 260 or equivalent, an arc potential drop of 130-170 volts should be displayed once the arc is running on the simulated hydrazine gas mix. This voltage may increase 5-10 volts during the 10-15 minutes while the engine is heating up.

C) As the engine heats up, the voltage drop across the electromagnet will increase to slightly over 2.0 volts with 50 amperes flowing in the circuit.

D) With ~35 milligrams/sec flow of simulated hydrazine gas products, the injection pressure should be between 410 and 473 kPa.

The cathode was inspected visually during the course of the testing. The engine was completely disassembled, and the condition of the critical parts documented photographically at three points during the testing. Figures 48 through 59 show the condition of the cathode, anode, and insulator after Test Runs 124, 172, and 181. Accumulated run time at these points was 5 hours, 32 hours, and 48 hours, respectively.

Test Series 1.4 was concluded at the end of the 100-hour endurance testing. A total of 120 starts and 63 thermal cycles were accumulated during the endurance tests. Including all test series, the engine to this point had 214 starts and had been subjected to 68 thermal cycles. A summary of the test conditions is presented in Table IX. The engine was disassembled after Tests 218 and 235. Photographs of the components are shown in Figures 60 through 67. It should be emphasized that these are all the original components which have been used for all 253 tests which include the parametric tests, the endurance tests, and the starting tests.

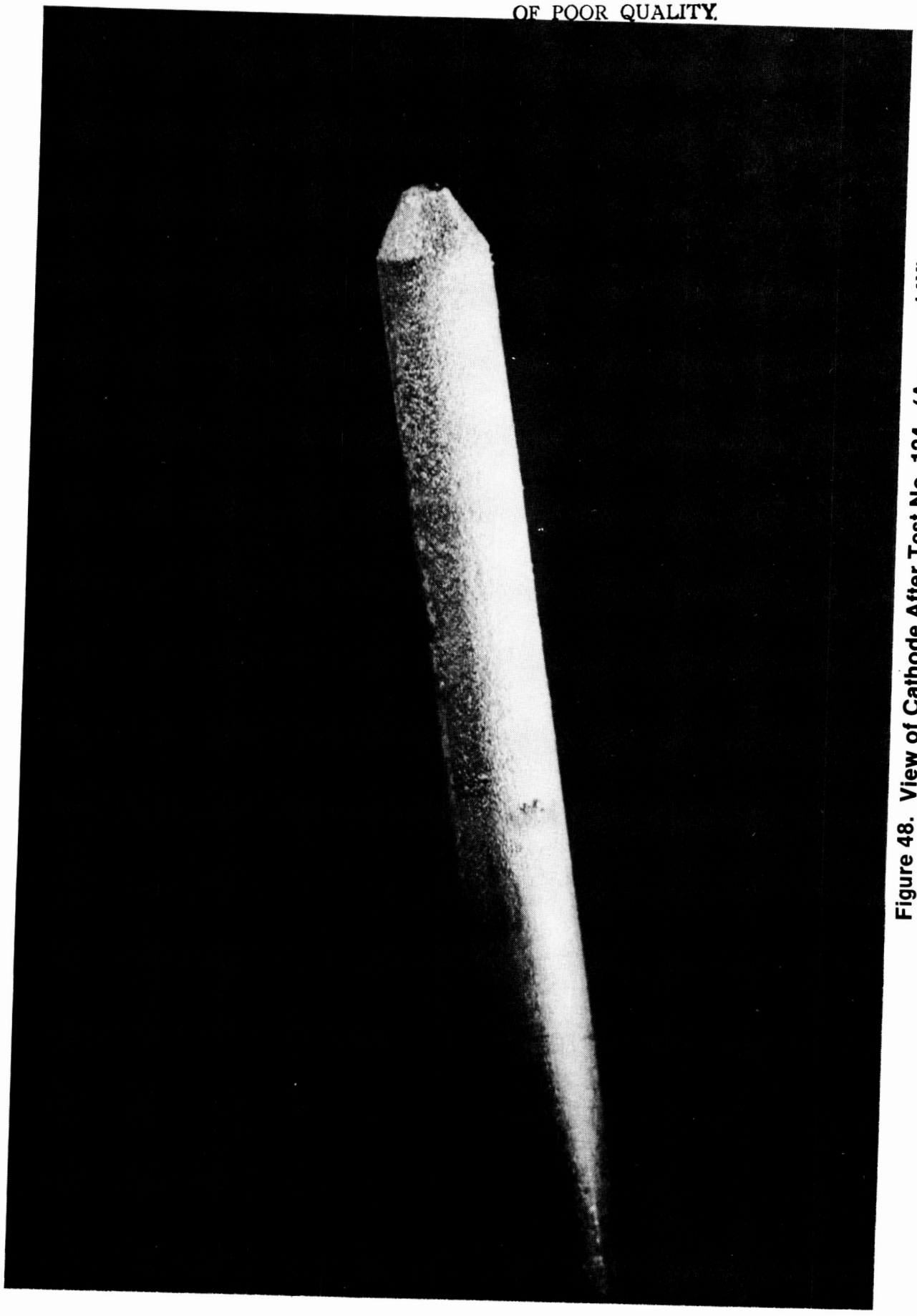

Figure 48. View of Cathode After Test No. 124 (Approx. 14X)

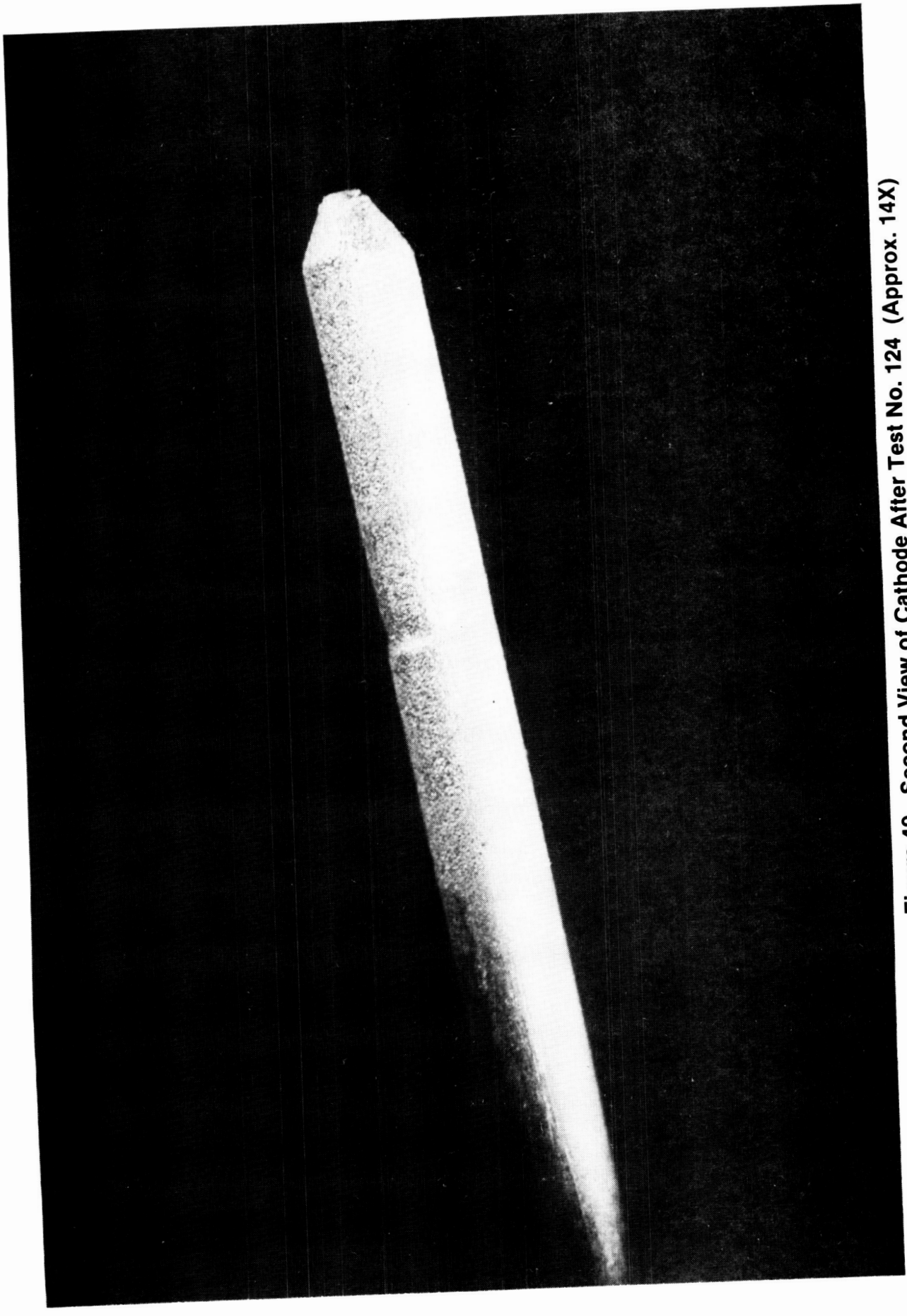

Figure 49. Second View of Cathode After Test No. 124 (Approx. 14X)

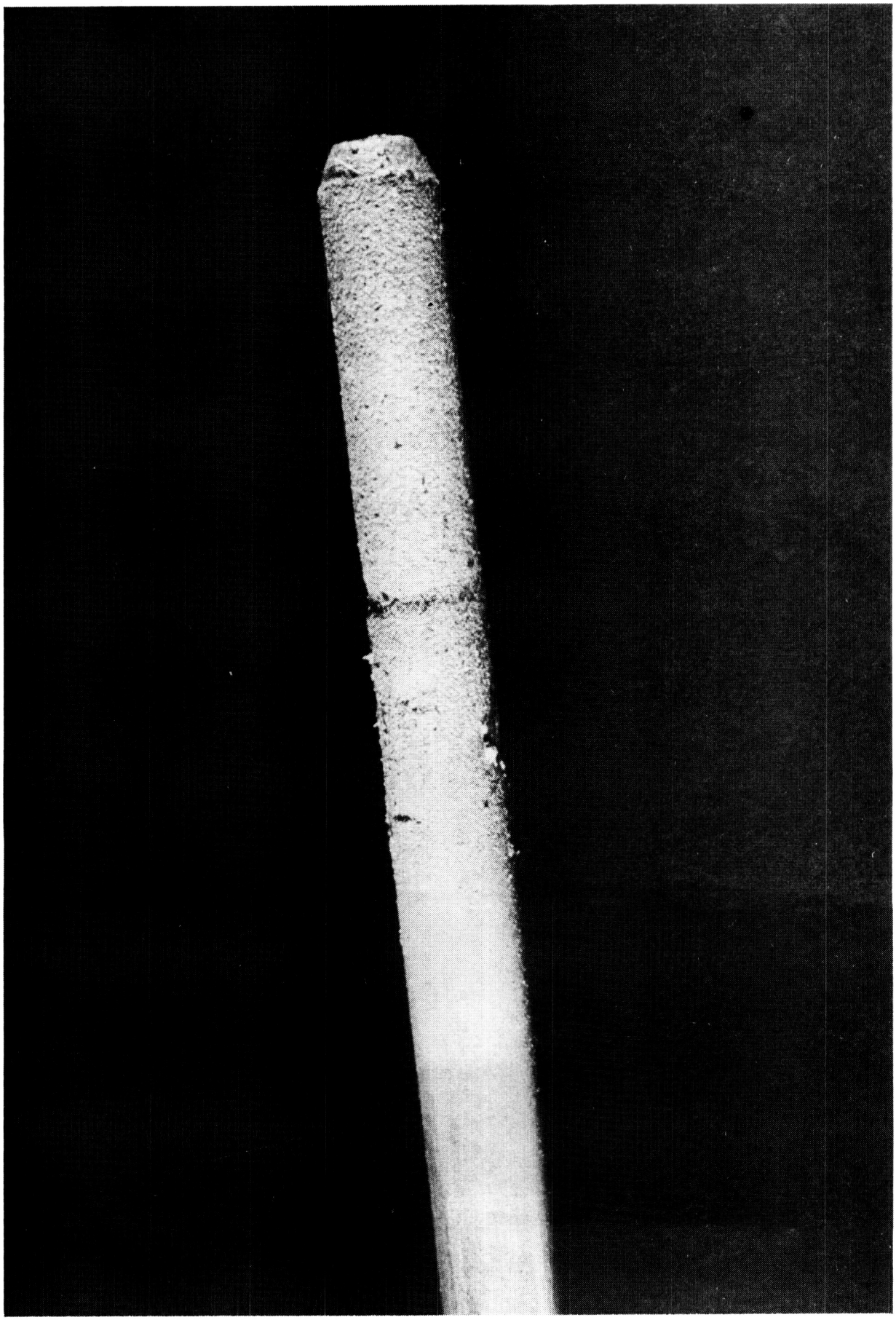

Figure 50. View of Cathode After Test No. 172 (Approx. 14X)

Figure 51. Second View of Cathode After Test No. 172 (Approx. 14X)

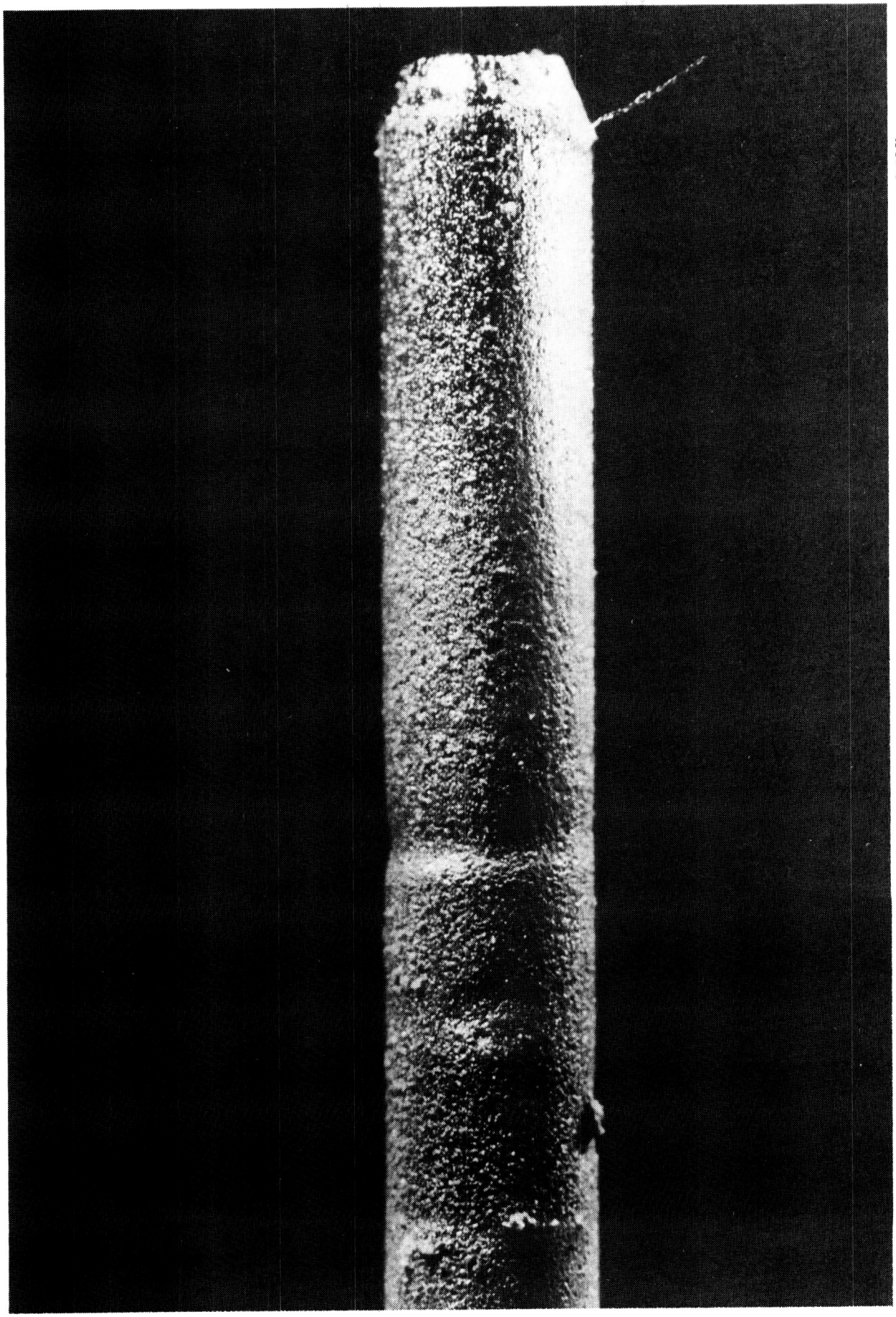

Figure 52. View of the Cathode After Test No. 181 (≈ 50 Hrs.) (Approx. 24X)

Figure 53. Second View of the Cathode After Test No. 181 (≈ 50 Hrs.) (Approx. 35X)

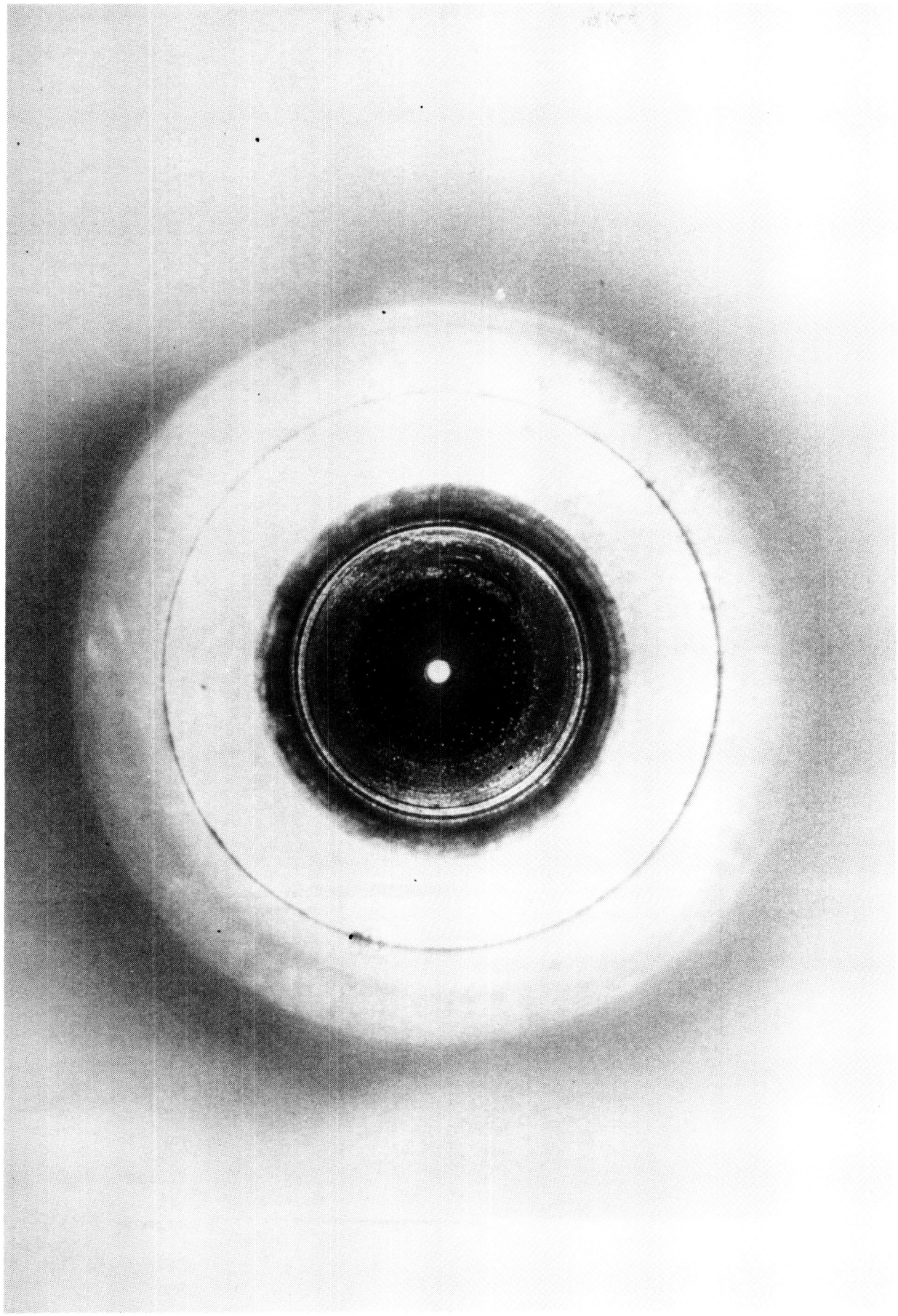

Figure 54. View of Anode Face After Test No. 124 (Approx. 5X)

Figure 55. View of Anode Face After Test No. 172 (Approx. 6X)

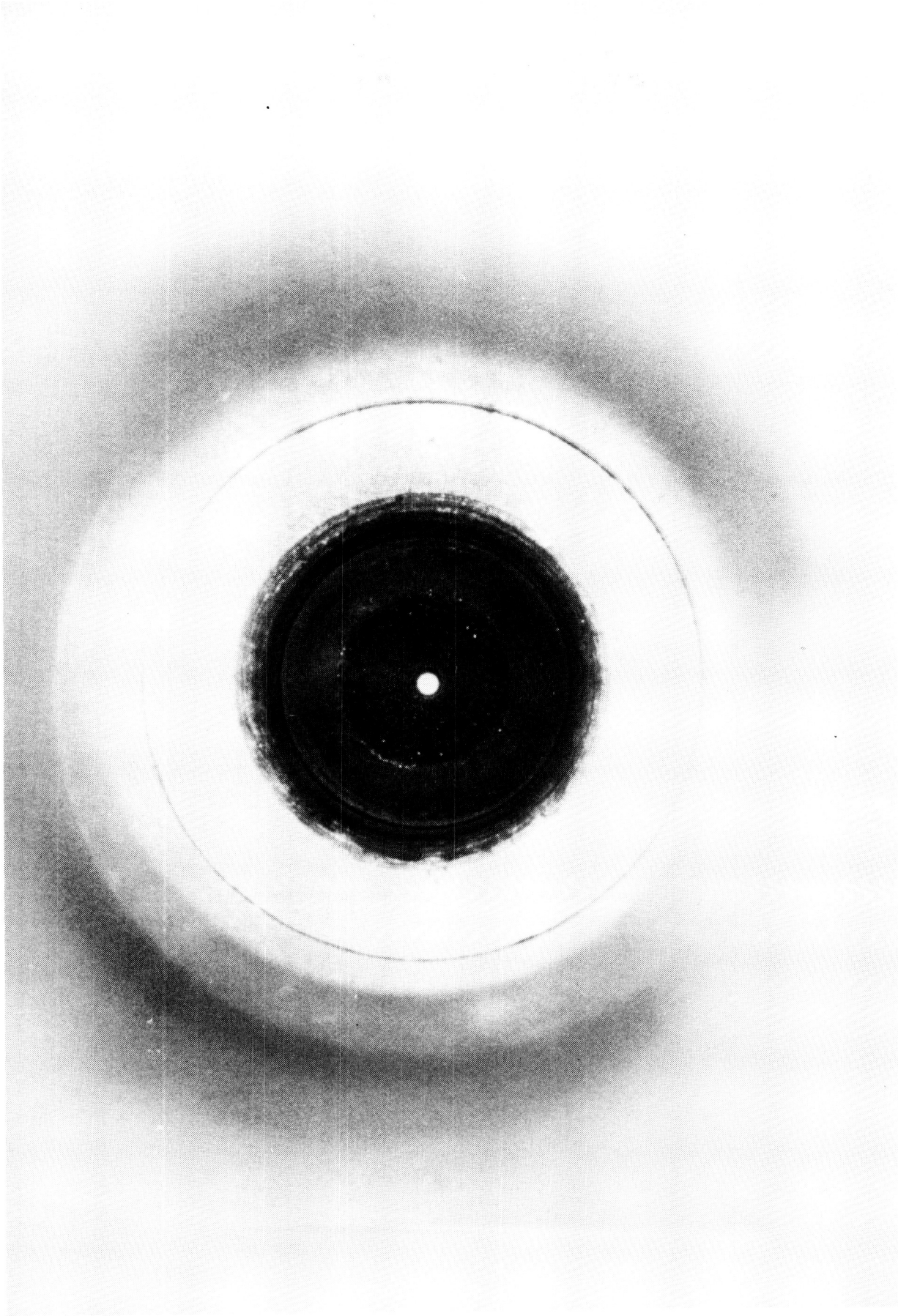

Figure 56. View of the Anode Face After Test No. 181 (≈ 50 Hrs.) (Approx. 5X)

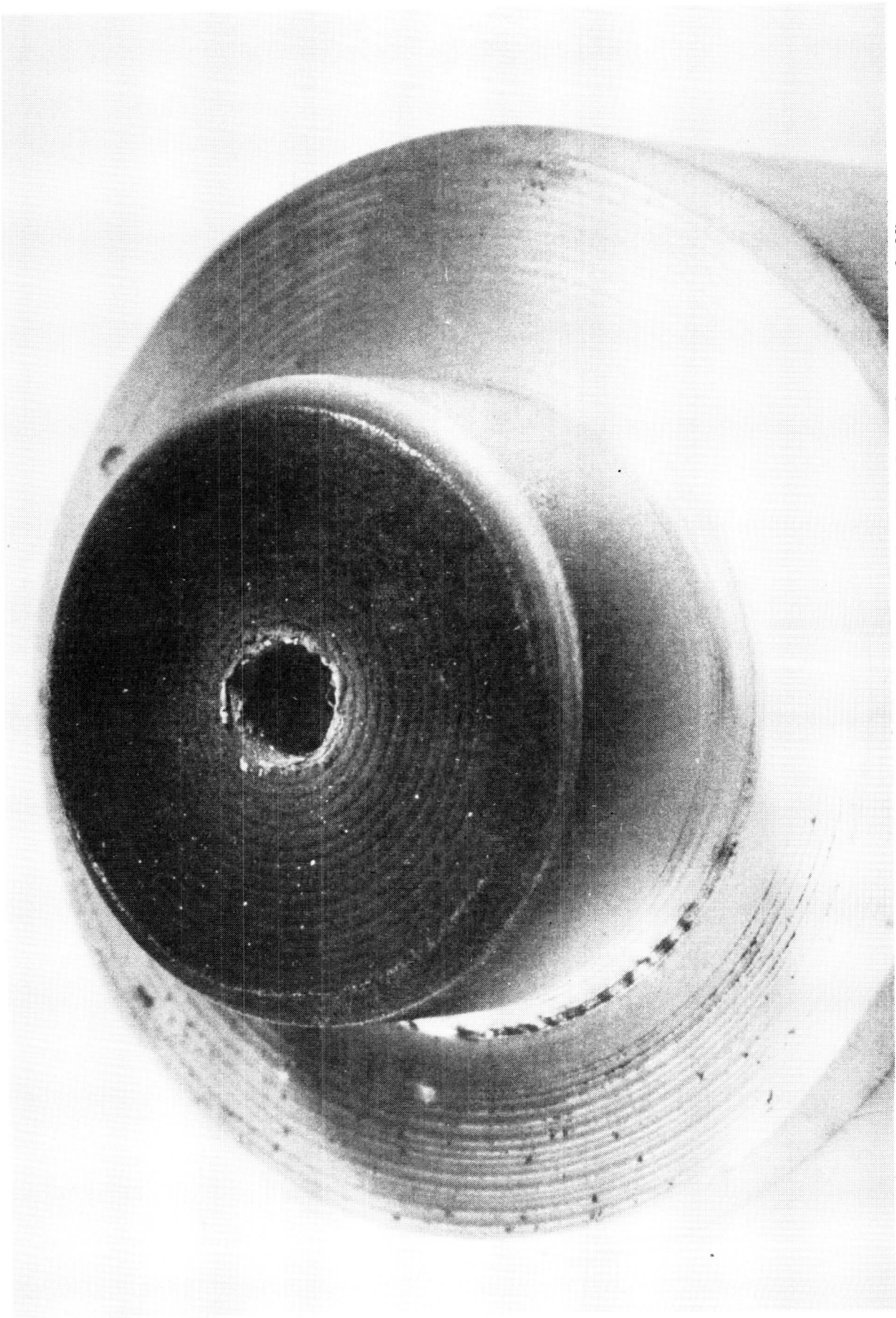

Figure 57. View of Insulator Face After Test No. 124 (Approx. 24X)

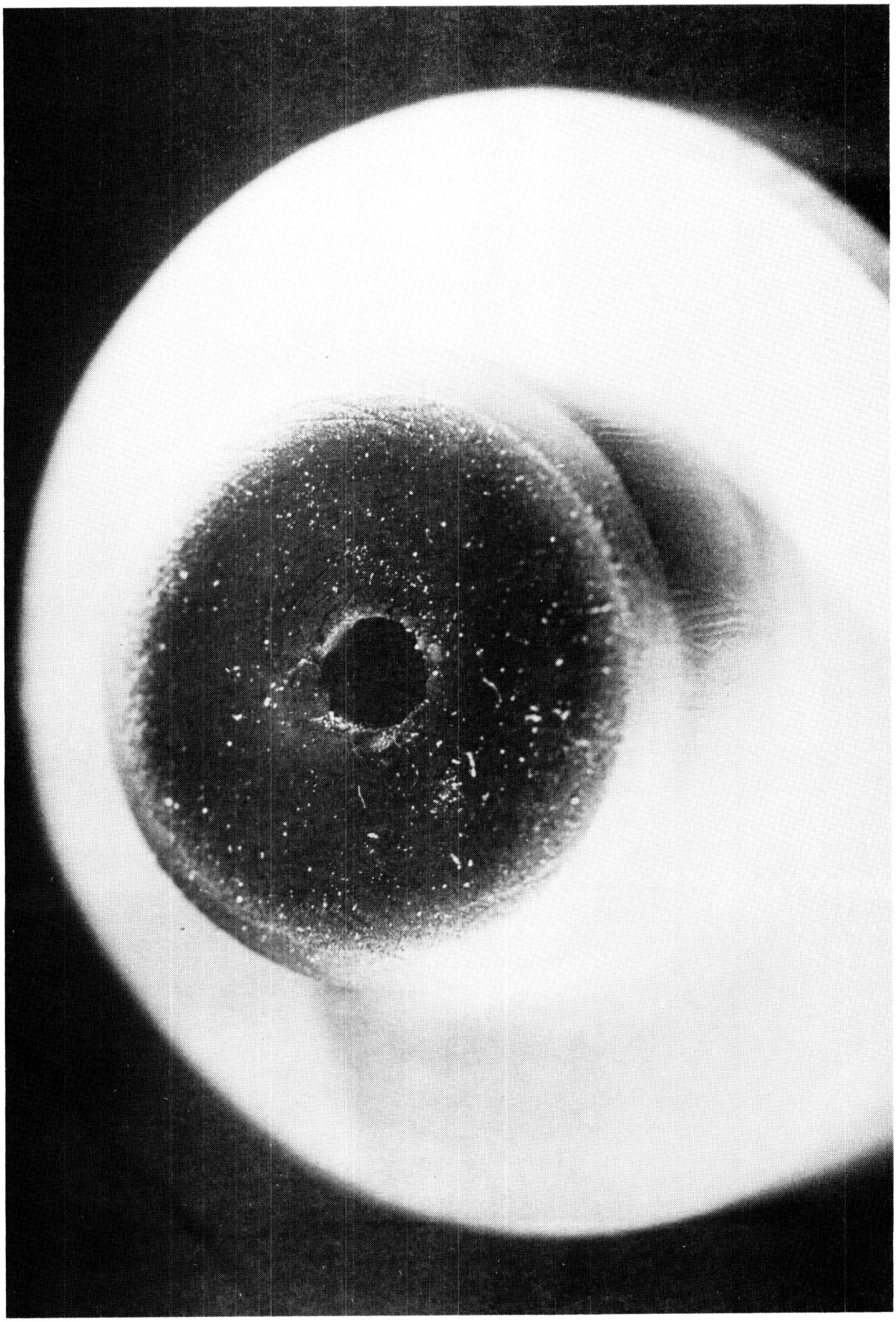

Figure 58. View of Insulator Face After Test No. 172 (Approx. 22X)

Figure 59. View of the Insulator Face After Test No. 181 (≈ 50 Hrs.) (Approx. 42X)

TABLE IX

TEST SUMMARY

	TEST No.	VIDEO CAMERA	MAGNETIC FIELD CURRENT (amps)	PURPOSE P=Parametric, E=Endurance	ARC POWER SUPPLY T=Technion E=Eratron	CAPACITANCE (uf)	RESISTANCE (Ohms)	STARTING GAS	START	TRANSITION TO PROPELLANT GAS	GAP (inches)	OFF	OUT	MODE	TEST DURATION (Minutes)	COMMENTS	ARC VOLTAGE (VOLTS)	ARC CURRENT (AMPS)
11 SEPT '85	182	Y	60	E	E	9000	37	A	Y	Y	.135	Y	-	L.V.	-	Changed H_2-N_2 flowmeter ..... Tubes from #4 to #3 New Facility Problem		
	183	"	"	"	"	" "	"	"	"	"	"	"	"	"	360	NH_3 flowmeter, #3 tube Facility Problem	135	8.00
	184	"	"	"	"	" "	"	"	"	"	"	"	"	"	- -			
	185	"	"	"	"	"	"	"	"	"	"	"	"	"	- -	" "		
	186	"	"	"	"	"	"	"	"	"	"	"	"	"	300		136	8.08
	187	"	"	"	"	"	"	"	"	"	"	-	Y	"	34		147	8.08
	188	"	"	"	"	"	49	"	N	-	"	-	Y	L.V.	1	Gas turned on too soon 2nd Try OK		
	189	"	"	"	"	"	42	"	Y	Y	"	-	Y	"	133		147	8.02
	190	"	"	"	"	18000	42	"	Y	Y	"	-	Y	"	98		146	8.02
	191	"	"	"	"	"	37	"	"	"	"	-	Y	"	11.5			
	192	"	64	"	"	"	"	"	"	"	"	-	Y	"	3			
	193	"	"	"	"	"	"	"	"	"	"	-	"	"	6.5			
	194	"	60	"	"	9000	37	"	"	"	"	-	"	"	9.5		132	8.04
	195	"	"	"	"	"	"	"	"	"	"	-	"	"	9		133	8.12
	196	"	"	"	"	"	"	"	"	"	"	-	"	"	7	Put small inductor in line		
	197	"	"	"	"	"	"	"	"	"	"	-	"	"	-			
	198	"	"	"	Y	"	"	"	"	"	"	-	"	"	30		148	8.02
	199	"	"	"	"	18000	"	"	"	"	"	-	"	"	15		150	8.00
	200	"	"	"	"	9000	37	"	"	"	.125	-	"	"	26		139	8.00

TABLE IX

TEST SUMMARY

TEST No.	VIDEO CAMERA	MAGNETIC FIELD CURRENT (amps)	PURPOSE P=Parametric, F=Endurance	ARC POWER SUPPLY T=Technion E=Eratron	CAPACITANCE (uf)	RESISTANCE (Ohms)	STARTING GAS	START	TRANSITION TO PROPELLANT GAS	GAP (inches)	OFF	OUT	MODE	TEST DURATION (Minutes)	COMMENTS	ARC VOLTAGE (VOLTS)	ARC CURRENT (AMPS)
201	Y	60	E	E	9000	37	A	Y	Y	.125	-	Y	L.V.	1.5		158	8.00
202	-	-	-	-	-	-	-	-	-	-	-	-	-	-			
203	-	70	E	T	9000	37	A	Y	Y	.125	Y	-	L.V.	30		156	8.02
204	-	"	"	"	"	"	"	"	"	"	-	Y	"	89		159	8.00
205	-	"	"	"	"	"	"	"	"	"	-	"	"	66		161	8.00
206	-	76	"	"	"	"	"	"	"	"	-	"	"	44			
207	-	"	"	"	"	"	"	"	"	"	-	"	"	15			
208	-	64	"	"	"	"	"	"	N	.115	-	"	"	-			
209	Y	"	E	T	9000	37	A	Y	Y	.115	-	Y	L.V.	.5			
210	"	"	"	"	"	49	"	"	N	"	-	"	"	2			
211	"	"	"	"	"	"	"	"	"	"	-	"	"	2.5	Operator Error		
212	"	55	"	"	"	"	"	"	"	.140	-	"	"	1	Operator Error		
213	"	"	"	"	"	"	"	"	"	"	-	"	"	3		166	7.82
214	"	"	"	"	"	"	"	"	Y	.140	-	"	"	103		166	8.00
215	"	"	"	"	"	"	"	"	"	"	"	"	"	210			
216	"	"	"	"	"	"	"	"	N	"	"	"	"	1.5	Installed transformer for primaries as industor		
217	"	"	"	"	"	"	"	"	"	"	"	"	"	1.5			

TABLE IX

TEST SUMMARY

	TEST No.	VIDEO CAMERA	MAGNETIC FIELD CURRENT (amps)	PURPOSE P=Parametric, E=Endurance	ARC POWER SUPPLY T=Technion E=Ertron	CAPACITANCE (uf)	RESISTANCE (Ohms)	STARTING GAS	START	TRANSITION TO PROPELLANT GAS	GAP (inches)	OFF	OUT	MODE	TEST DURATION (Minutes)	COMMENTS	ARC VOLTAGE (VOLTS)	ARC CURRENT (AMPS)
	217	Y	55	E	T	9000	37	A	Y	N	.140	-	Y	L.V.	1.5			
	218	"	"	"	"	"	"	"	"	Y	"	"	"	"	70		165	8.04
	219	"	56	"	"	"	"	"	"	"	"	Y	-	"	2			
	220	"	60	"	"	"	"	"	"	"	"	"	-	"	11			
	221	"	56	"	"	"	"	"	"	"	"	-	Y	"	32		161	8.00
	222	"	"	"	"	18000	"	"	"	"	"	"	"	"	9			
	223	"	"	"	"	9000	"	"	"	"	"	"	"	"	"	Remove large transformer		
	224	"	62	"	"	"	"	"	"	"	"	"	"	"	8			
	225	"	"	"	"	"	37	"	"	N	"	"	"	"	.5			
	226	"	60	"	"	"	49	"	"	Y	.130	"	"	"	39		161	7.56
	227	"	56	"	"	"	"	"	"	"	"	"	"	"	87		157	7.56
	228	"	50	"	"	"	"	"	"	"	"	"	"	"	344		148	8.00
28 SEPT '86	229	"	"	"	"	"	"	"	"	"	"	"	"	"	2			
	230	"	"	"	"	"	"	"	"	"	"	Y	-	"	463	Use H.P. P.S. for magnet 240 hz noise gone	157	8.00
29 SEPT '86	231	"	"	"	"	"	"	"	"	"	"	-	Y	"	204		161	8.06
	232	"	"	"	"	"	"	"	"	"	"	Y	-	"	44		169	8.02

TABLE IX

TEST SUMMARY

	TEST No.	VIDEO CAMERA	MAGNETIC FIELD CURRENT (amps)	PURPOSE P=Parametric, E=Endurance	ARC POWER SUPPLY T=Technion E=Eratron	CAPACITANCE (uf)	RESISTANCE (Ohms)	STARTING GAS	START	TRANSITION TO PROPELLANT GAS	GAP (inches)	OFF	OUT	MODE	TEST DURATION (Minutes)	COMMENTS
	233	Y	50	S*	T	9000	49	A	Y	N	.130	Y	-	L.V.	.5	Primaries of 2 small tansformers in for inductions
	234	"	"	"	"	"	"	"	"	"	"	"	"	"	.5	
	235	"	"	"	"	"	"	"	"	"	"	"	"	"	"	
	236	"	"	"	"	"	"	"	"	"	"	"	"	"	"	
	237	"	"	"	"	"	"	"	"	"	"	"	"	"	"	
	238	"	"	"	"	"	"	"	"	"	"	"	"	"	"	
	239	"	"	"	"	"	"	"	"	"	"	"	"	"	"	
	240	"	"	"	"	"	"	"	"	"	"	"	"	"	"	
	241	"	"	"	"	"	"	"	"	"	"	"	"	"	"	
	242	"	"	"	"	"	"	"	"	"	"	"	"	"	"	
	243	"	"	"	"	"	"	"	"	"	"	"	"	"	"	
	244	Y	50	S*	T	9000	49	H_2N_2	Y	N/A	.130	Y	-	L.V.	.5	Propellant Start
30 SEPT '86	245	"	"	"	"	"	"	"	"	"	"	"	"	"	"	
	246	"	"	"	"	"	"	"	"	"	"	"	"	"	"	
	247	"	"	"	"	"	"	"	"	"	"	"	"	"	"	

* Start Tests; Magnet energized prior to start, 2 in^3 plenum added upstream of start valve.

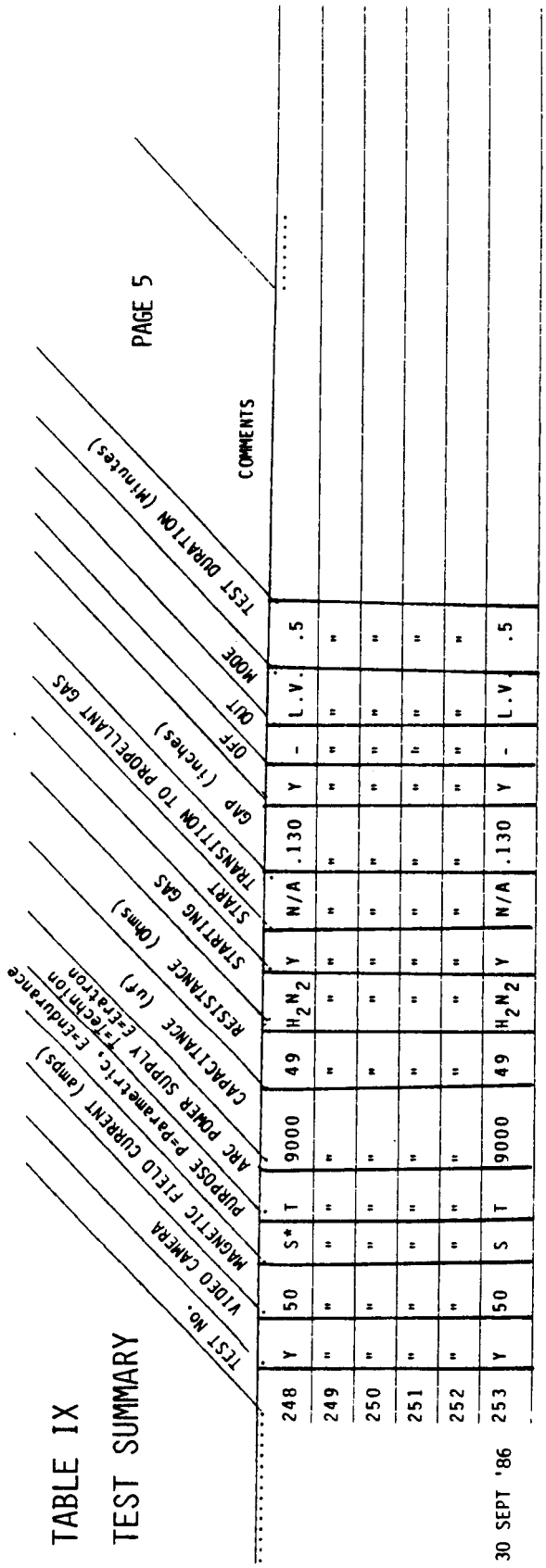

TABLE IX
TEST SUMMARY

TEST No.	VIDEO CAMERA	MAGNETIC FIELD CURRENT (amps)	PURPOSE P=parametric, E=endurance E=electron E=ebeam	ARC POWER SUPPLY	CAPACITANCE (uf)	RESISTANCE (Ohms)	STARTING GAS	START	TRANSITION TO PROPELLANT GAS	GAP (inches)	OFF	OUT	MODE	TEST DURATION (Minutes)	COMMENTS
248	Y	50	S*	T	9000	49	H_2N_2	Y	N/A	.130	Y	-	L.V.	.5	.....
249	"	"	"	"	"	"	"	"	"	"	"	"	"	"	
250	"	"	"	"	"	"	"	"	"	"	"	"	"	"	
251	"	"	"	"	"	"	"	"	"	"	"	"	"	"	
252	"	"	"	"	"	"	"	"	"	"	"	"	"	"	
253	Y	50	S	T	9000	49	H_2N_2	Y	N/A	.130	Y	-	L.V.	.5	

PAGE 5

30 SEPT '86

* Start Tests; Magnet energized prior to start, 2 in^3 plenum added upstream of start valve.

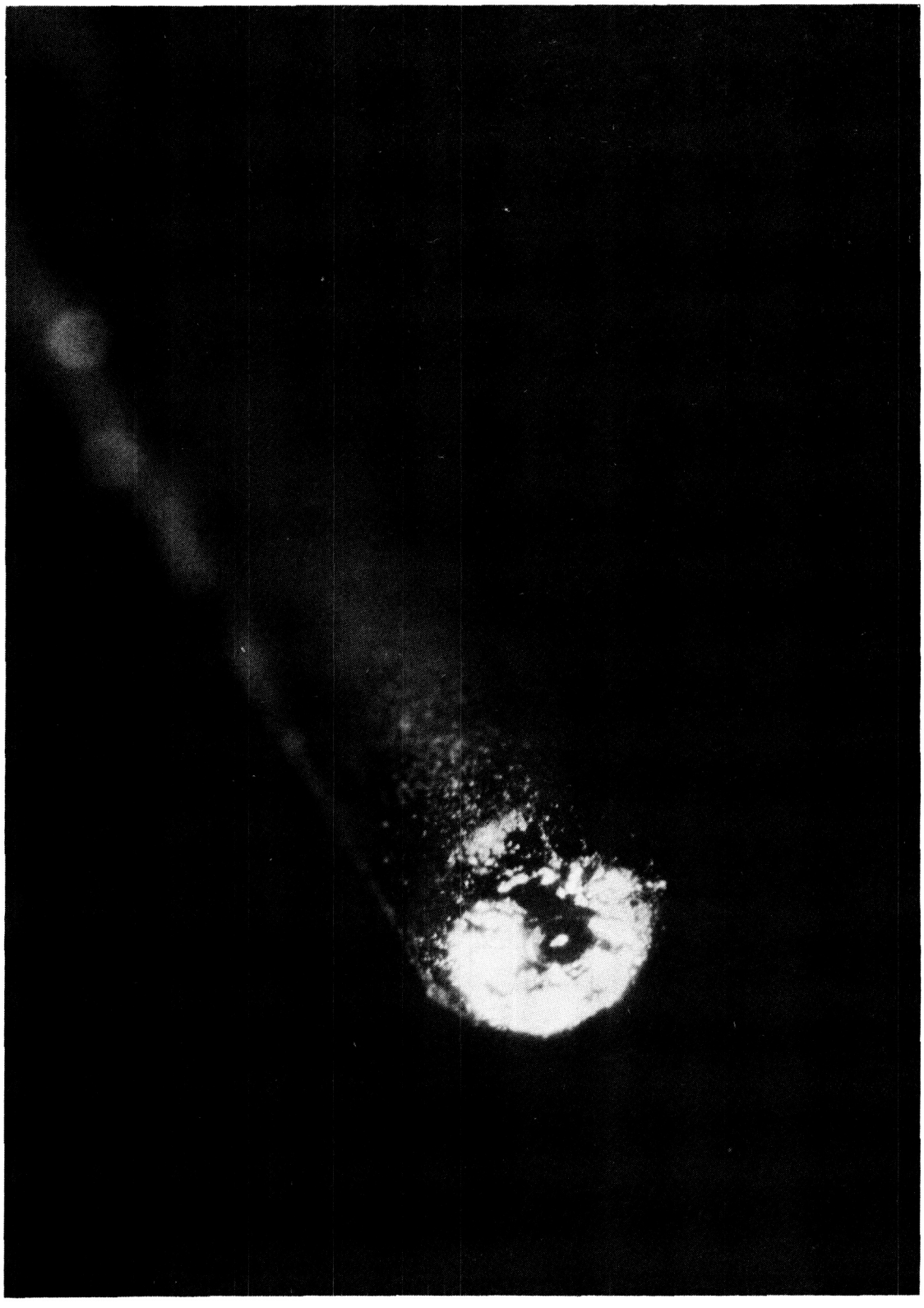

Figure 60. Cathode Tip after Run #218 (Approx. 25X)

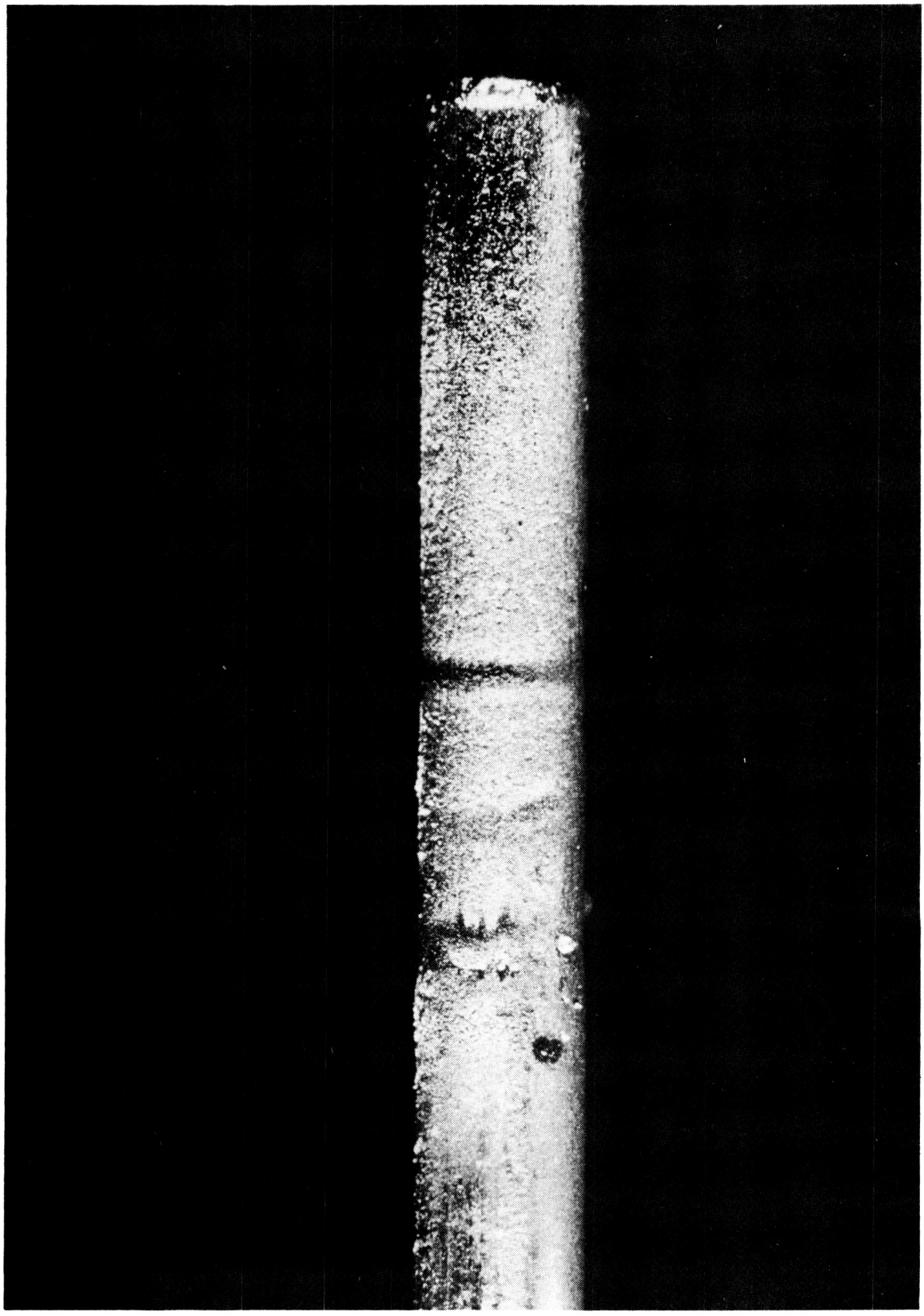

Figure 61. Cathode after Run #218 (Approx. 17X)

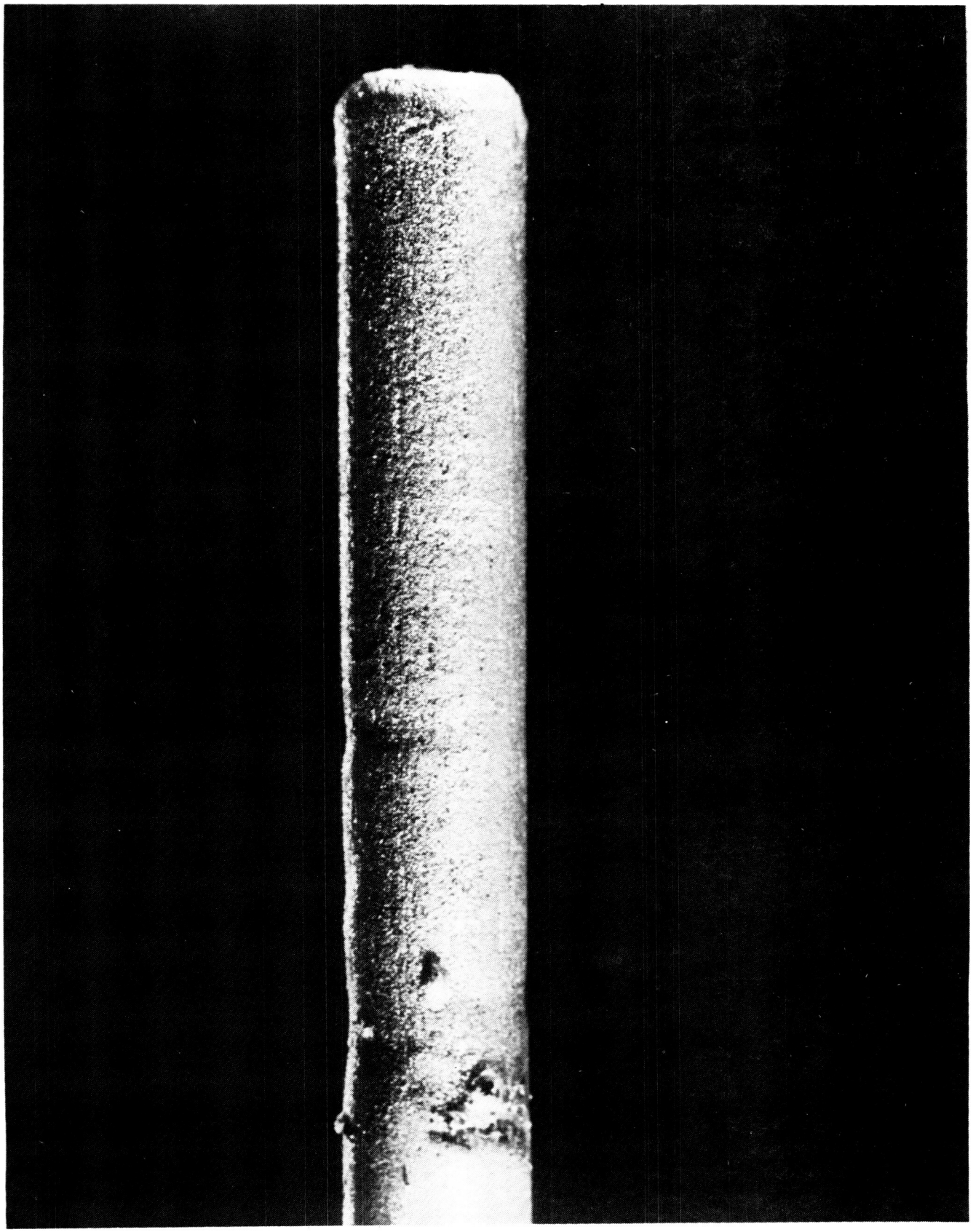

Figure 62. Cathode after Run #253 (Approx 24X)

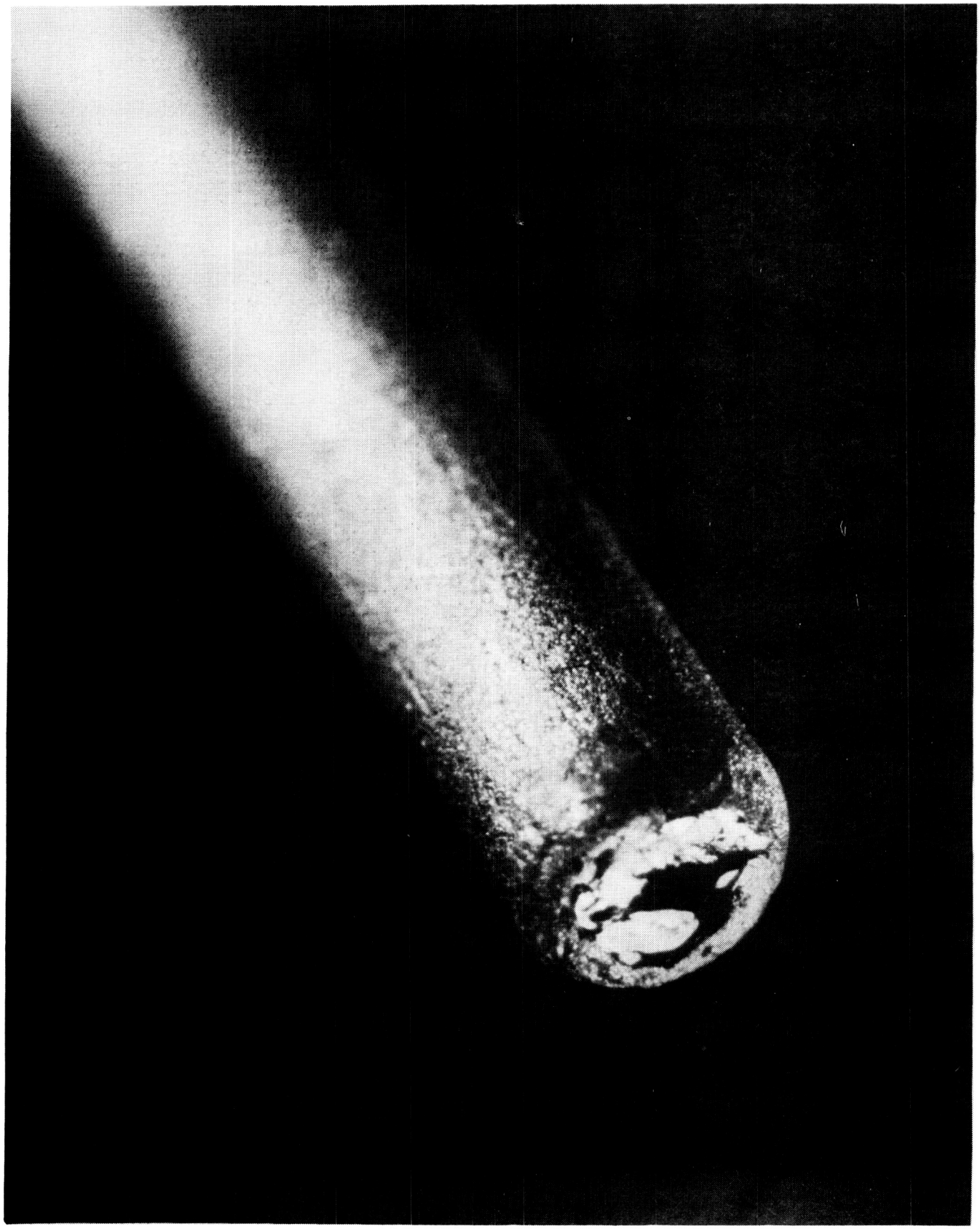

Figure 63. Cathode Tip after Run #253 (Approx 38X)

Figure 64. Anode after Run #218 (Approx. 5X)

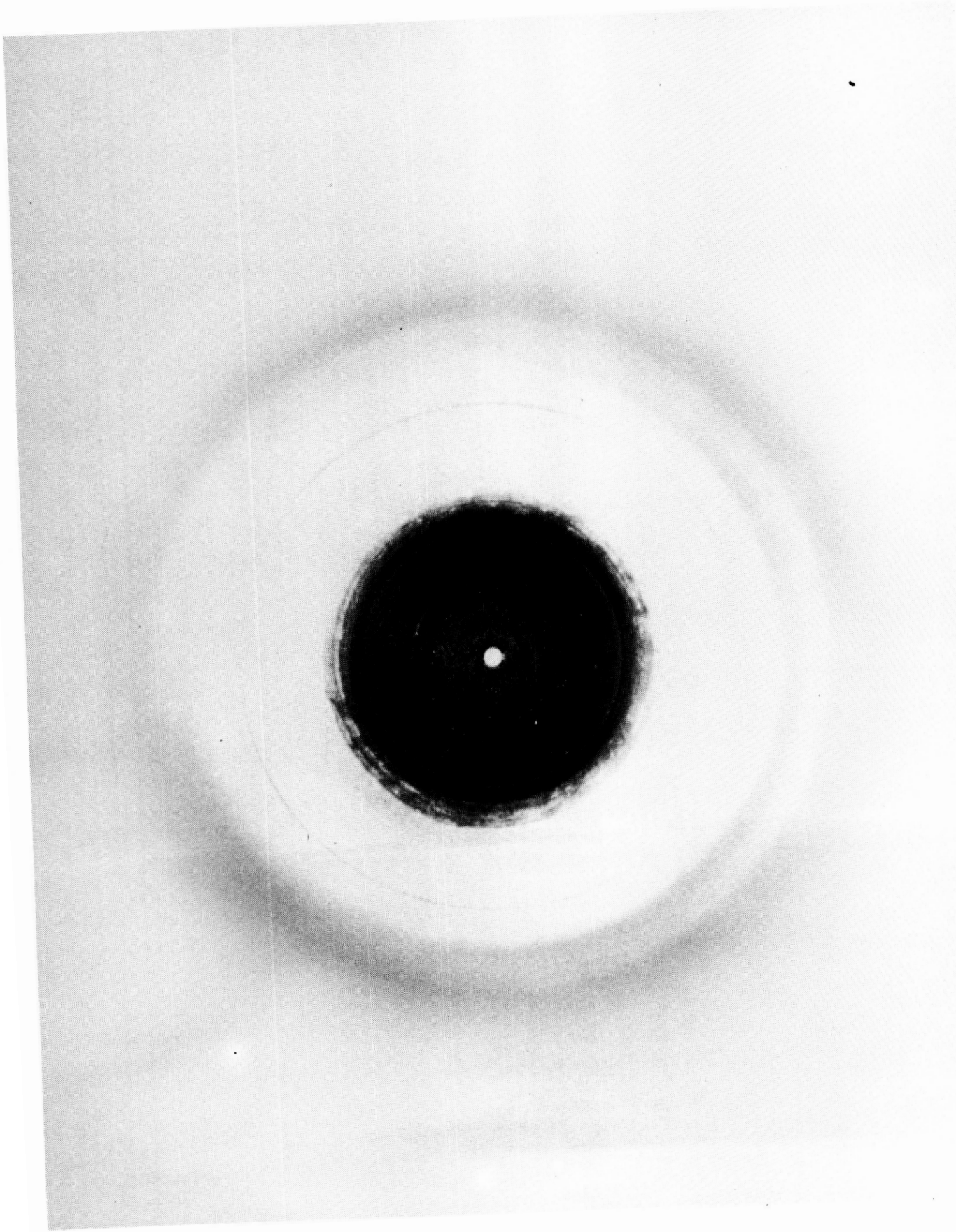

Figure 65. Anode after Run #253 (Approx. 3X)

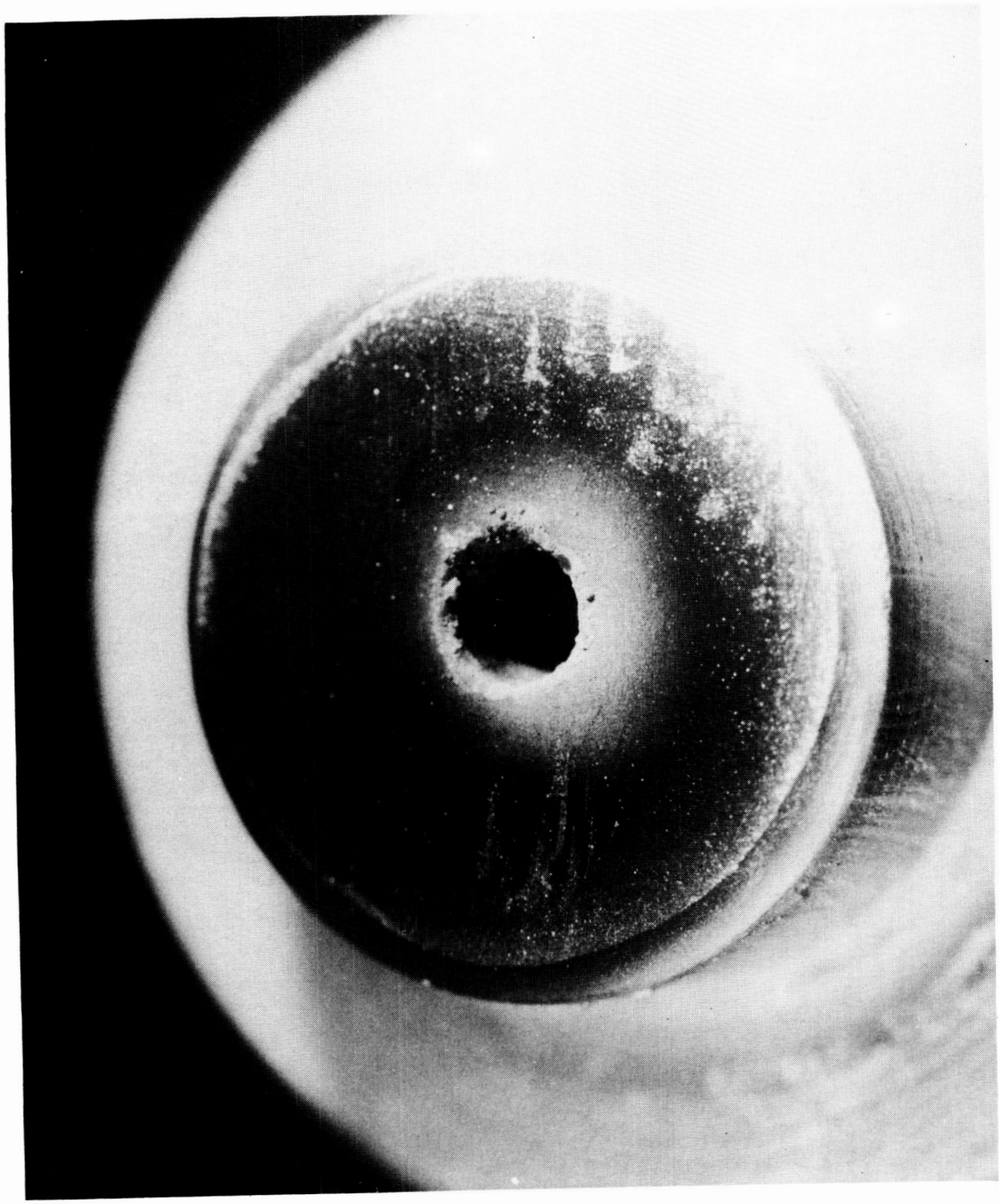

Figure 66. Insulator Face After Run #218 (Approx. 26X)

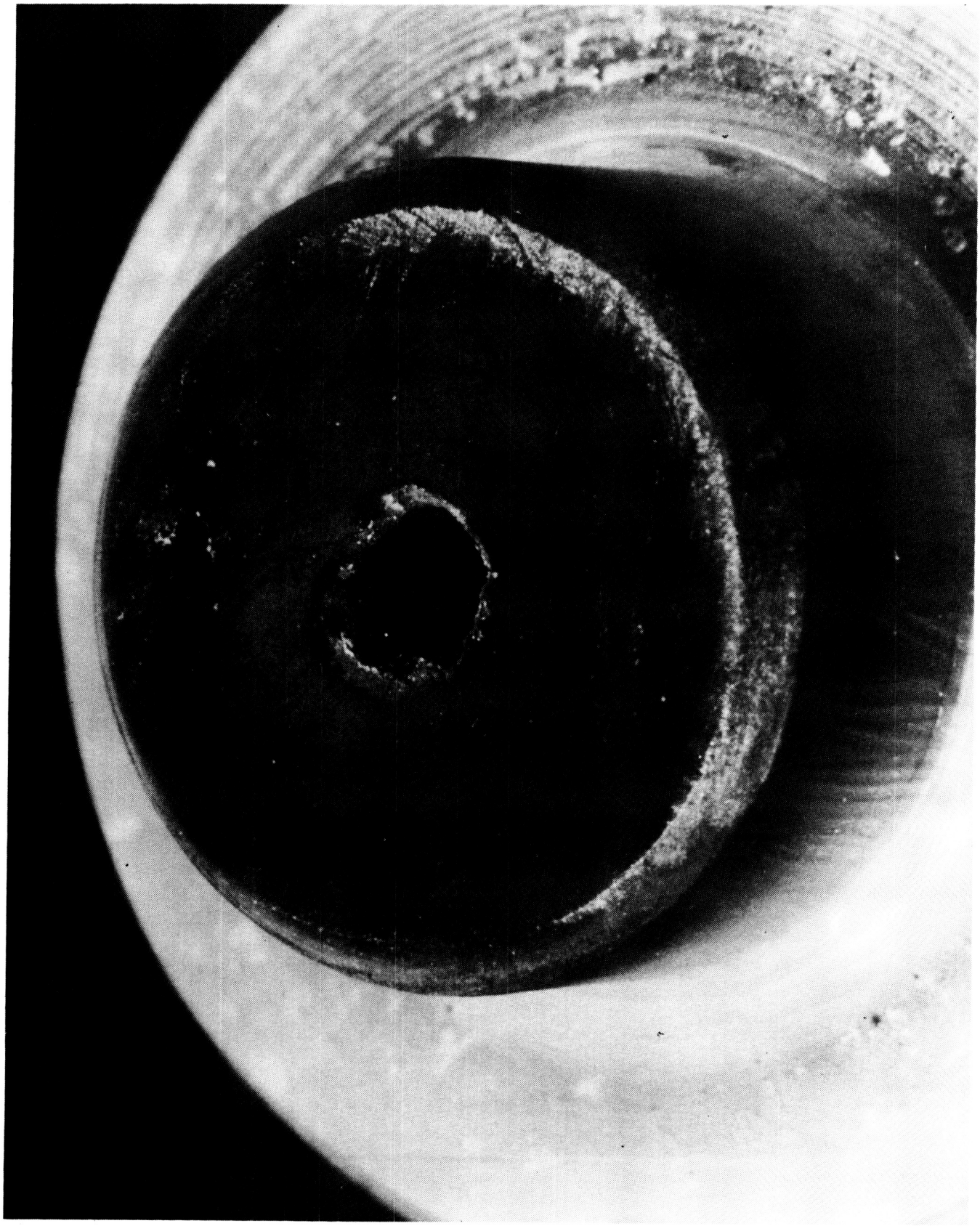

Figure 67. Insulator Face after Run #253 (Approx 18X)

3.5, Test Series 1 Testing (cont.)

The Cathode History

The cathode shape and length has been monitored 10 times during the 3 test series conducted at Technion. A summary of the recession rate of the attachment surface is given in Table X. The tip geometry is shown in Figure 68. A jig was made for measuring the length of the cathode rod. Also, the length of the conical section was measured from the photographs. As time progressed, the edge marking the beginning of the cone became less distinct, reducing the accuracy of the second set of measurements.

The first set of measurements indicate uneven recession rates over the last 50 hours of testing. This is probably due to the molten tungsten on the attachment face solidifying in different configurations.

Attempts to view the cathode attachment using telescopic lenses were only partially successful. An intense attachment spot was, however, observed to move erratically over the surface from one location to another.

The Anode History

The anode orifice diameter is nominally 0.119 cm. Some changes have occurred on the cathode (upstream) face of the anode and to the anode orifice. Measurements of the maximum size rod that would pass through the anode orifice after Tests 218 and 253 are shown in Table XI. Examination of the photos of the anode indicates that some small protrusion into the anode orifice was visible after Test 172. Observing the anode orifice through optics while under test confirmed that some material was deposited, probably in droplet form, at one location around the periphery. Watching this anomaly for extended periods of time indicated that it could be a flake which could extend out into the orifice and then instantaneously move back to the wall, leaving a barely observable protrusion.

TABLE X

CATHODE HISTORY

RUN NO.	TOTAL OPERATING TIME (HOURS)	JIG MEASUREMENT (INCH)	JIG CATHODE REGRESSION (MIL)	PHOTO CATHODE REGRESSION (MIL)
- -	0	1.036	0	- -
124	8.22	- -	- -	- .4
172	36.76	1.050	-14	-14.5
181	51.28	1.056	-20	-15
183	57.28	1.058	-22	- -
186	62.28	1.059	-23	- -
199	68.24	1.057	-21	- -
207	72.17	1.61	-25	- -
218	79.37	1.0605	-24.5	-21.7
232	100	1.066	-30	- -
253	100	1.055	-19	-23.7

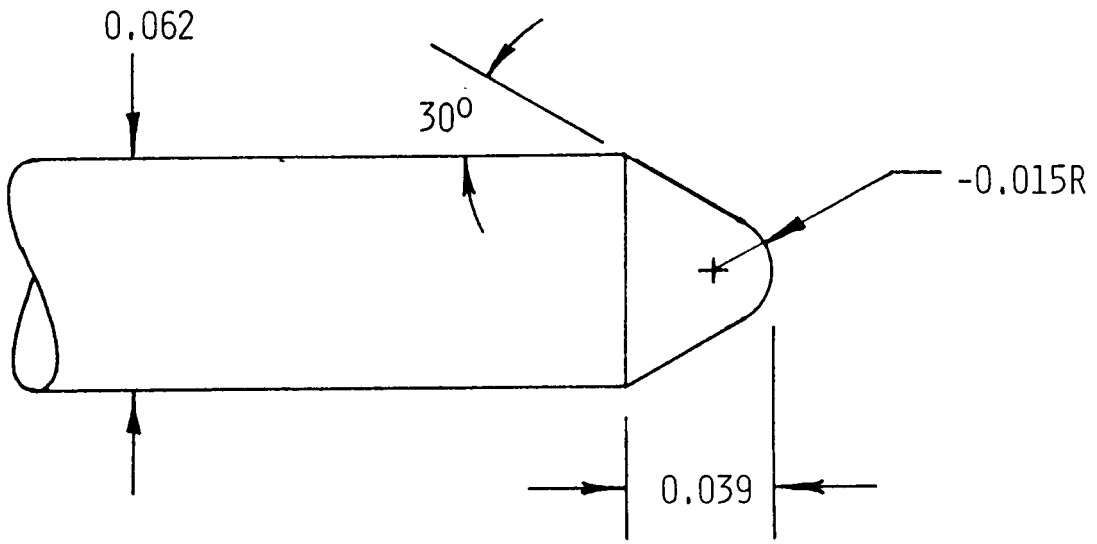

Figure 68. Cathode Tip Configuration

TABLE XI

ANODE ORIFICE AND THROAT ORIFICE HISTORY

TEST #	HOURS	ANODE ORIFICE	NOZZLE THROAT
0		.047	.0225
124	8.22	NO MEASUREMENT	.0215 - .0225
172	35.76	NO MEASUREMENT	.0215 - .0225
181	51.28	NO MEASUREMENT	.0215 - .0225
218	79.37	.038 - .040	.0215 - .0225
253	100	.036 - .037	.0200 - .0215

3.5, Test Series 1 Testing (cont.)

The outer periphery of the anode face developed a mottled appearance during the tests. It is speculated that this may be droplets of tungsten spun off the molten cathode face by the swirling propellant gas.

The Nozzle Throat History

Periodically during the tests, rods were inserted into the nozzle orifice to see if any diameter change had occurred. In Table XI, the size of the rod that would pass through the hole is listed, followed by the diameter of the next size rod available that would not pass through the throat. The diameter changes noted, a maximum reduction of 0.0064 cm, could, as was the case with the anode, be due to the deposition of one or more particles at some circumferential location, rather than be a uniform reduction in diameter.

The Insulator History

Some changes occurred to both the face of the insulator and the orifice through which the cathode protrudes. The face of the insulator blackened and was cleaned with emery cloth several times during the test.

Some asymmetrical wear occurred on the orifice, but did not appear to get progressively worse. On the cathode cylinder, some azimuthal grooving occurred where the cathode emerged from the insulator. It is possible that, in some operating mode or during start, an intermittent radial arc struck across the insulator face. This may have happened when the arc was operating in the high-voltage mode.

The Electromagnet History

In order to cover a wide range of magnetic field strength, the electromagnet was powered from a welding power supply. This power supply had a fairly high ripple component. During Tests 172 through 181, the voltage drop across the magnet fell from 2.44 to 1.86 volts, while approximately 60 amperes of current was maintained. This indicated that several turns had

shorted out, probably due to overheating of the fiberglass insulation on the coil. However, the coil resistance returned to its original value of 0.403 ohms (hot) in Test 182 and remained there for the rest of the tests.

Subsequent to Test 229, it was determined that a magnet current of 50 amperes or less would be adequate and the magnet was powered by a highly regulated HP power supply. In all previous tests, a ripple of 30-40 volts peak-to-peak at a frequency of about 240 Hz had been observed. This ripple was modulated by a higher frequency noise component. When the regulated power supply was used to power the magnet, the 240 Hz ripple disappeared completely from the scope trace of the voltage across the arc, leaving only the high-frequency component.

3.6 SERIES 2 TESTING

Scope and Objectives

The objective of the Test Series 2 Testing was two-fold, first, to establish the performance of the thruster under conditions of Test Series 1, and second, to characterize the performance of the thruster in terms of measurable and controllable parameters. At the conclusion of Test Series 1, three important technical achievements had been attained.

1. Electrode life is projected to be on the order 100's of hours for cathode and anode.

2. Stable arc operation has been demonstrated over a wide range of operating conditions.

3. Arc initiation with flight-type thruster hardware has been demonstrated.

One of the goals of Test Series 2 was to determine if the performance of the baseline thruster at the conditions examined in Test Series 1 met the program goals. This objective was achieved by performance mapping the thruster. The other goal of the test program was to obtain sufficient data so the thruster can be developed into flight-like design with acceptable life characteristics and desired specific impulse and thrust efficiency.

3.6.1 Arcjet Test Facility

The Aerojet Arcjet Test Facility used for the performance testing of the 1 kW arcjet thruster is shown in Figure 69. Figure 70 is a plan view of the facility. The facility consists of a 1.3 x 1.9m (4 x 6 ft) vacuum chamber located in a covered test bay and pumped by a Kinney 6000 CFM vacuum system. Operations and data measurements are controlled through the control room console and data acquisition system. For the Series 2 testing a

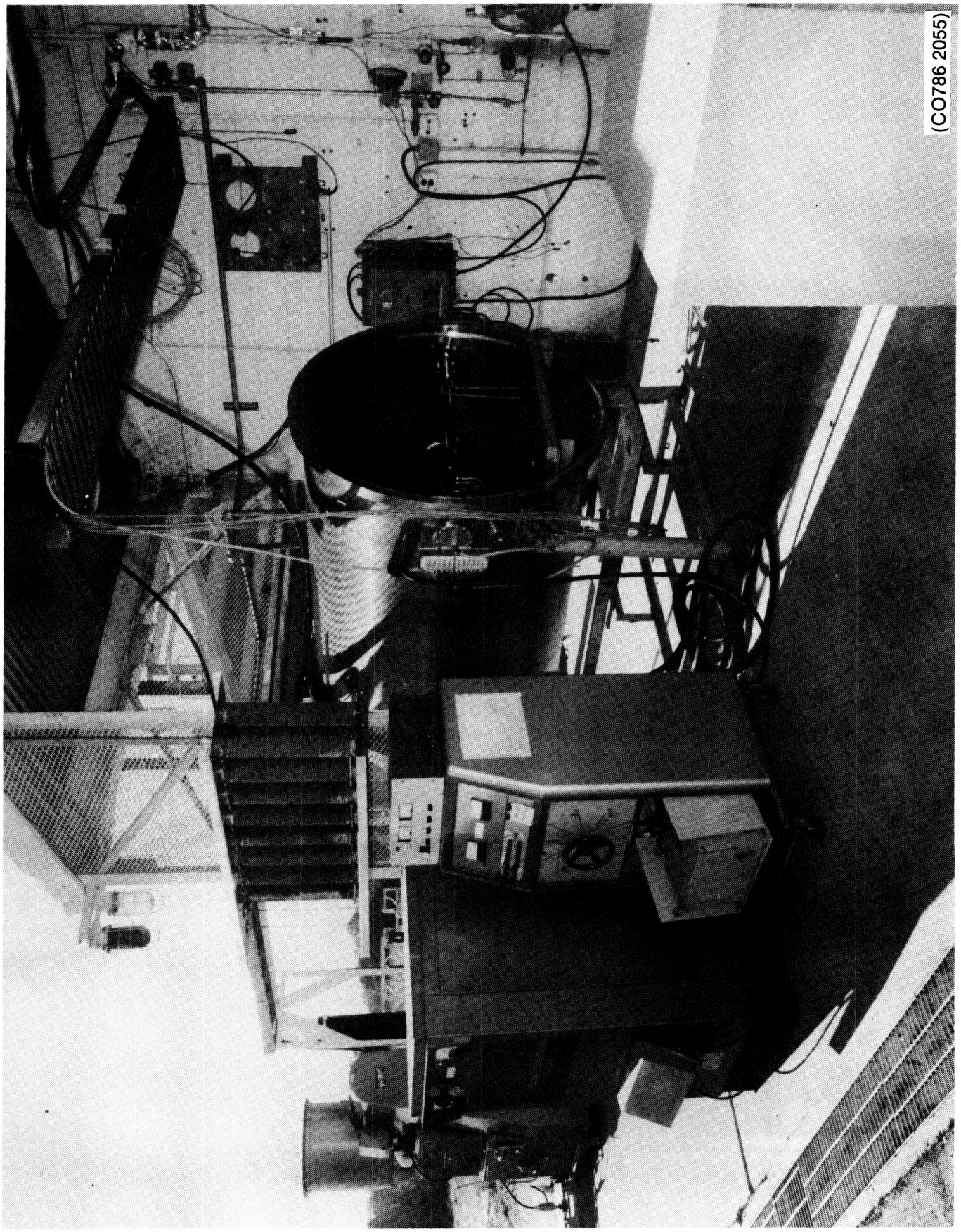

Figure 69. Aerojet Arcjet Facility

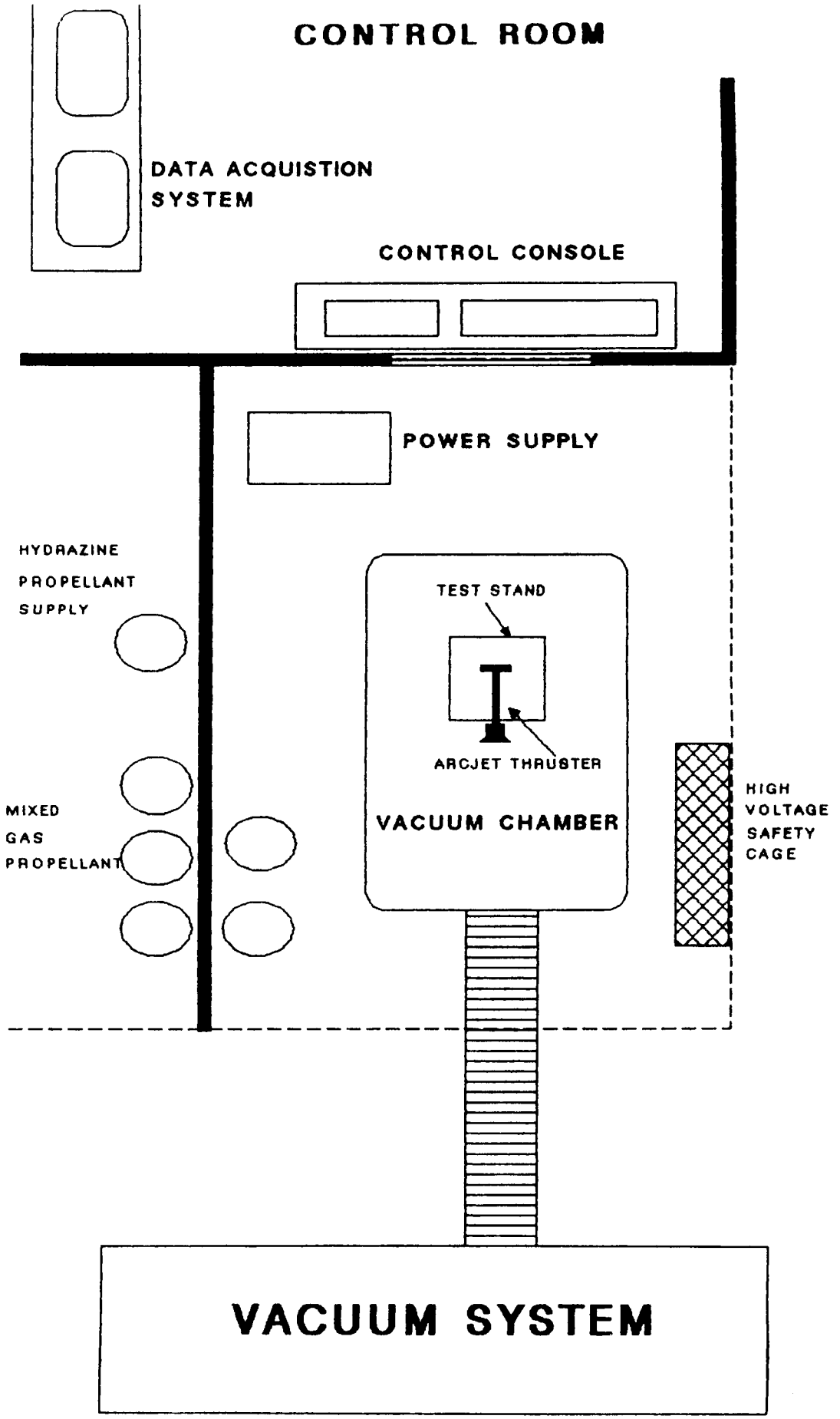

Figure 70. Plan View of Arcjet Test Facility

10 kW Eratron plasma power supply was used to provide arc power (see Figure 71). High voltage power conditioning and connections are contained in a high voltage safety cage in the test bay (see Figure 72). The thruster was mounted in the vacuum chamber on a thrust stand capable of measuring thrust levels from 0 to 250 gm. Both simulated hydrazine decomposition products (i.e., H_2, N_2, NH_3) and other storable propellants are available for testing, with supply tanks located in adjacent test bays.

Electrical Power Supplies and Conditioning Equipment

The Eratron 10 kW PPS power supply can provide up to 47 amps continuous and an open circuit voltage of 1200 volts. Operating characteristics are summarized in Figure 73. During constant current operation the voltage ripple from the power supply was measured to be less than 2% of the total voltage at a frequency of 5375 Hz. To further reduce the ripple current an inductive "T" filter was designed and installed in the arcjet power circuit.

During Test Series 1, the arcjet was operated with a 50 ohm ballast resistor in series with the arc to compensate for the slow response of the current control circuit on the Technion power supply. During checkout testing prior to test series 2 the current control response of the Eratron power supply was found to be slower than expected. A 40 ohm resistor was required to provide arc stability. The impedance of the arc during testing ranged from 10 to 20 ohms.

Propellant Delivery and Supply System

A schematic of the propellant delivery system is shown in Figure 74. The propellant consisted of a mixture of N_2, H_2, and NH_3, in the proportions shown in Table XII to simulate the decomposition products from a high performance hydrazine gas generator. The gas mixture was prepared at Aerojet and stored in 34.4 liter tanks pressurized to 4054 kPa. The maximum pressure was set at 4054 kPa to prevent condensation of the NH_3 at ambient storage temperatures. The propellant tanks were connected to a manifold as

Figure 71. Eratron 10 KW Variable Power Supply Used for Arcjet Performance Testing at Aerojet

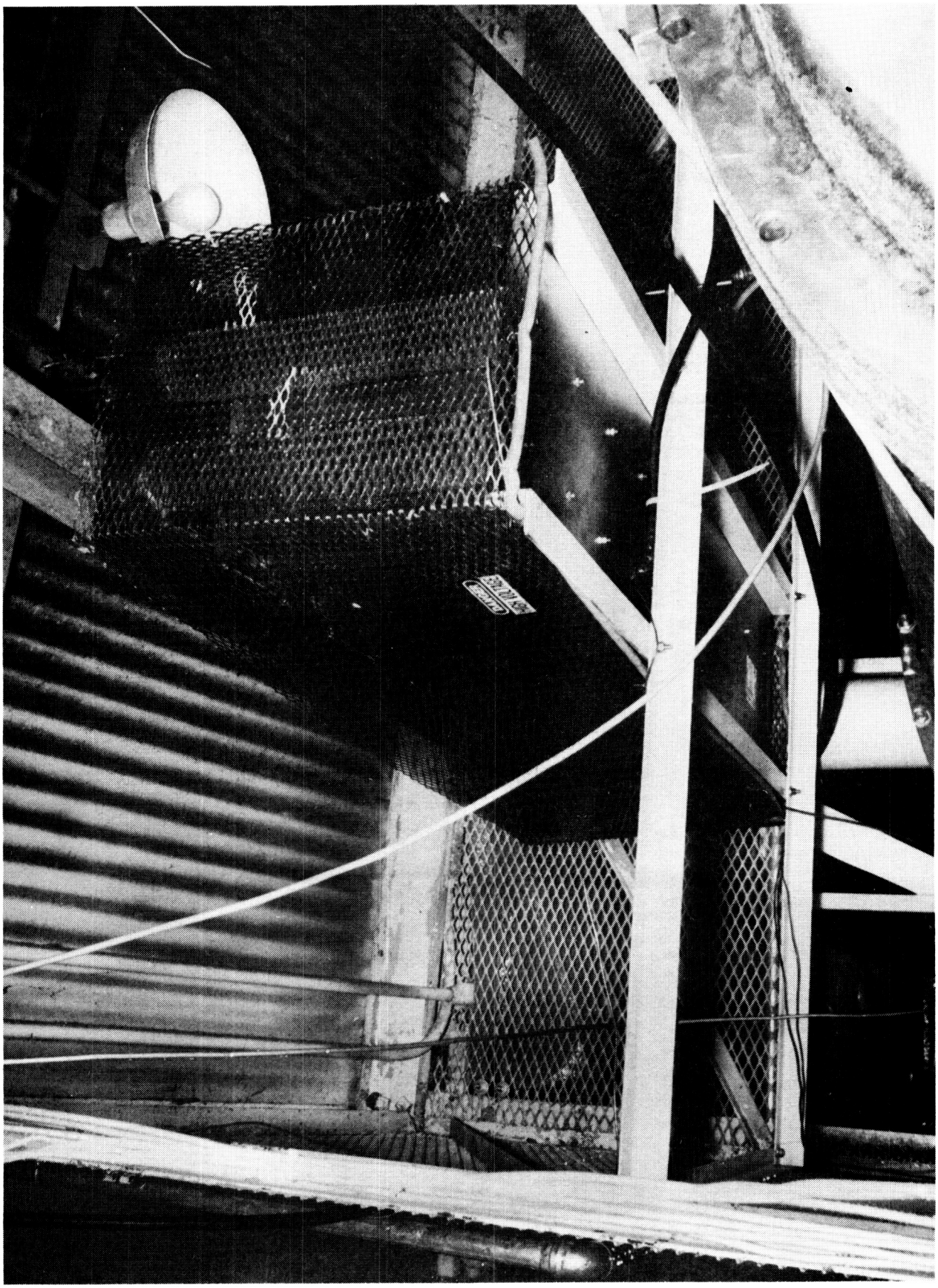

Figure 72. High Voltage Safety Cage Used to Store Ballast Resistors and Filtering Circuits

Arcjet Power Supply Characteristics

	Eratron, Model #PPS-8210
Rating	0 - 10 KW
Voltage	0 - 600/414/300
Current	0 - 16.5/24/47
Voltage Reg.	± 1%
Current Reg.	± 0.1%
Volt. Adj.	0 - 100%
Current Adj.	0 - 100%
Output Ripple	1%
Input	120 VDC

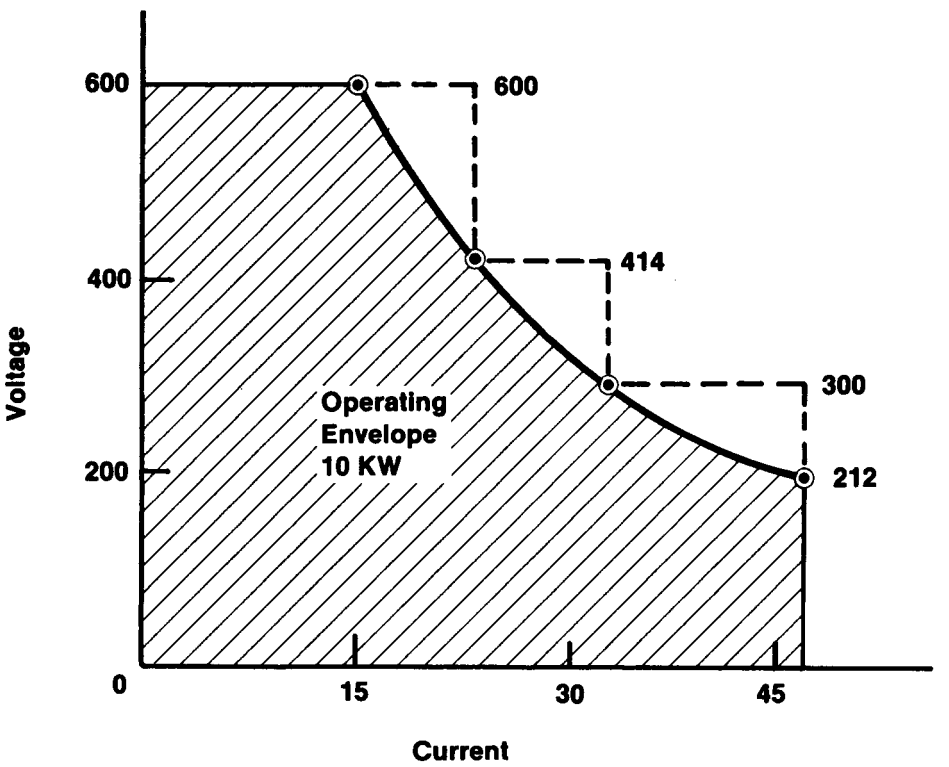

Figure 73. Operating Characteristics of Eratron Power Supply

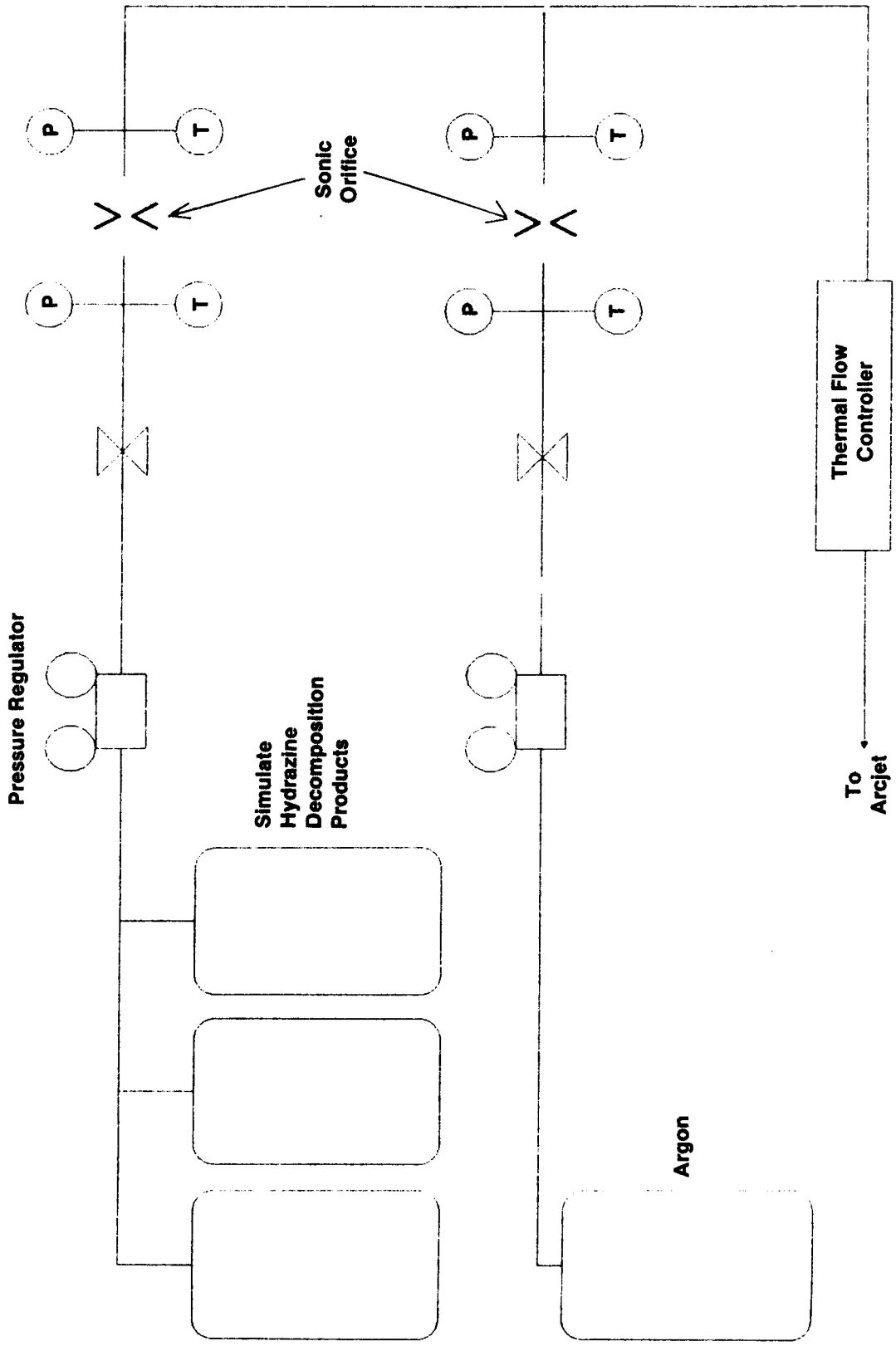

Figure 74. Propellant Delivery System

TABLE XII

COMPOSITION OF SIMULATED HYDRAZINE DECOMPOSITION PRODUCTS

Basis: 80% Decomposition of NH_3

	X_i	M_i	M_i/$\frac{kg}{kg\text{-mole mixture}}$	M_i/M $\frac{kg}{kg\text{-mixture}}$
H_2	0.585	2.0	1.17	0.100
N_2	0.317	28.0	8.88	0.758
NH_3	0.098	17.0	1.67	0.142
			11.71	1.000

shown in Figure 75 and isolated from the down stream flow metering by a pressure regulator.

The mass flow rate of propellant was measured by two methods, a sonic orifice and a Matheson 820 mass flow meter. The mass flow rate through a sonic orifice is primarily a function of orifice size and the upstream temperature and pressure. The orifice was calibrated in place by flowing propellant into a known volume which has been initially evacuated. By using a large volume and maintaining a sonic flow through the orifice, the mass flow rate could be determined with an uncertainty of ±2%. The Matheson mass flowmeter was calibrated at Aerojet's Calibration Laboratory with N_2. The propellant mass flow rate was then determined by applying a correction factor supplied by Matheson for the gas mixture.

A liquid hydrazine delivery system shown in Figure 76 is also available for use in testing but was not used. The supply tank is approximately 35 liters in capacity. The system has fast acting valves for purge and pressurization functions.

Vacuum System

A Kinney TO0850 850 CFM vacuum pump was used during the performance testing of the thruster. A high conductance heat exchanger, shown in Figure 77, was used to cool down hot gases from the arcjet, prior to entering the pump. The pumping speed curve for the pump is shown in Figure 78. Figure 79 shows the background pressure in the test cell as a function of propellant flow rate using the pump. The figure also shows the present capability of the system with a Kinney MB6500 roots blower installed (the pumps are shown in Figure 80). The vacuum chamber was pumped down to approximately 10 microns prior to testing. At this pressure, a voltage exceeding 2000 volts could be placed across the anode and cathode without an electrical breakdown. A voltage breakdown test was performed prior to every test.

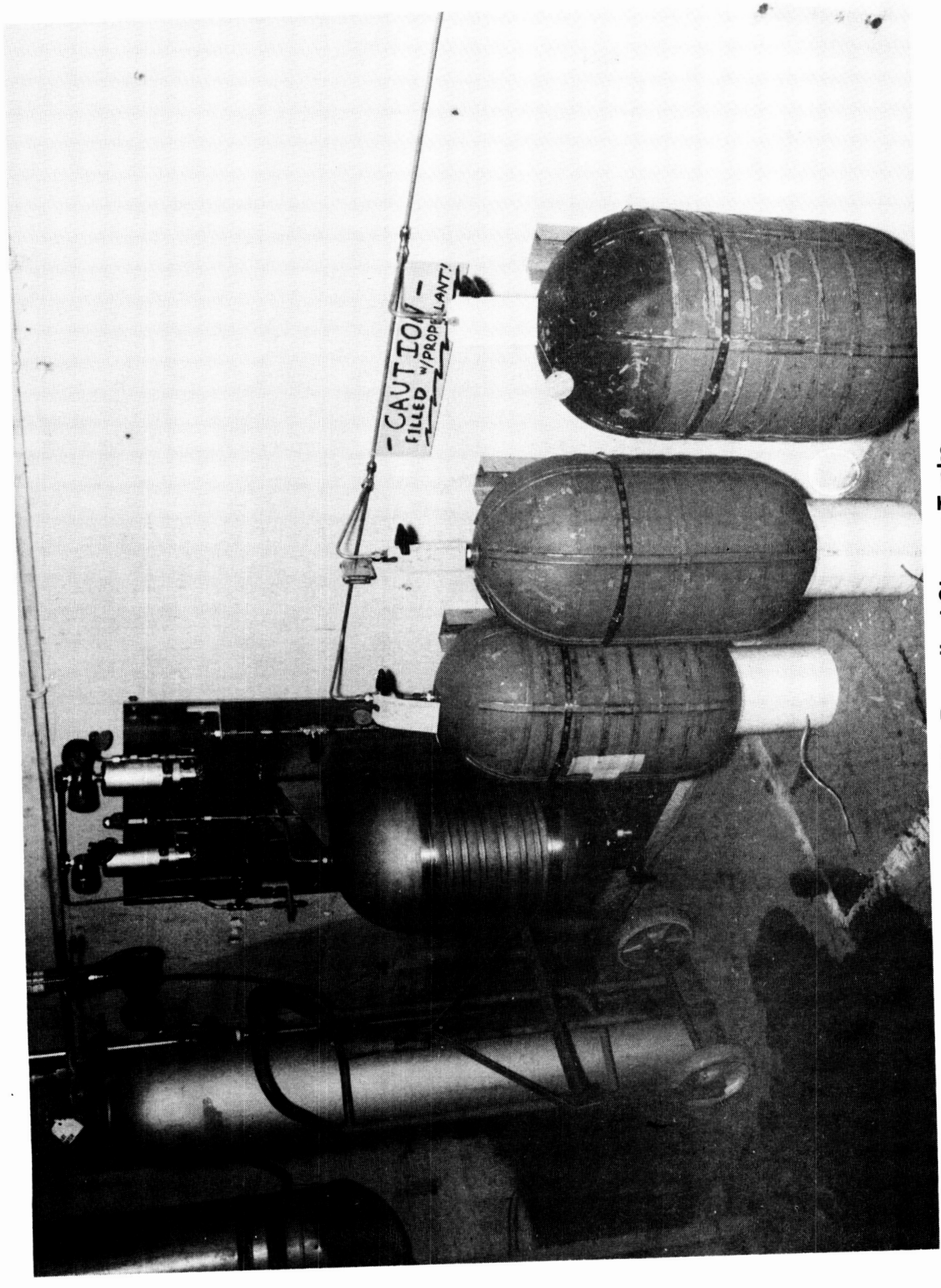

Figure 75. Propellant Storage Tanks

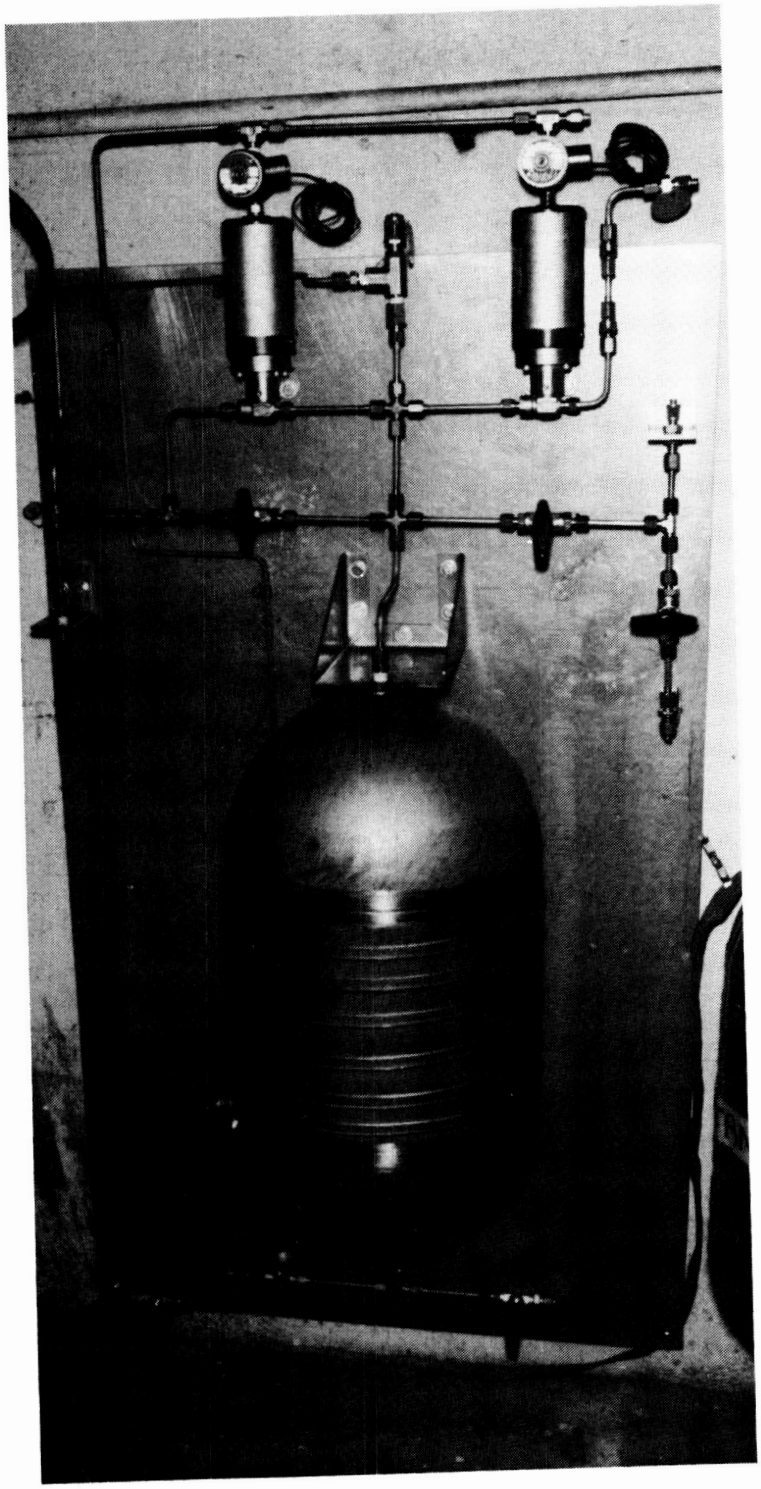

Figure 76. Hydrazine Propellant Delivery System

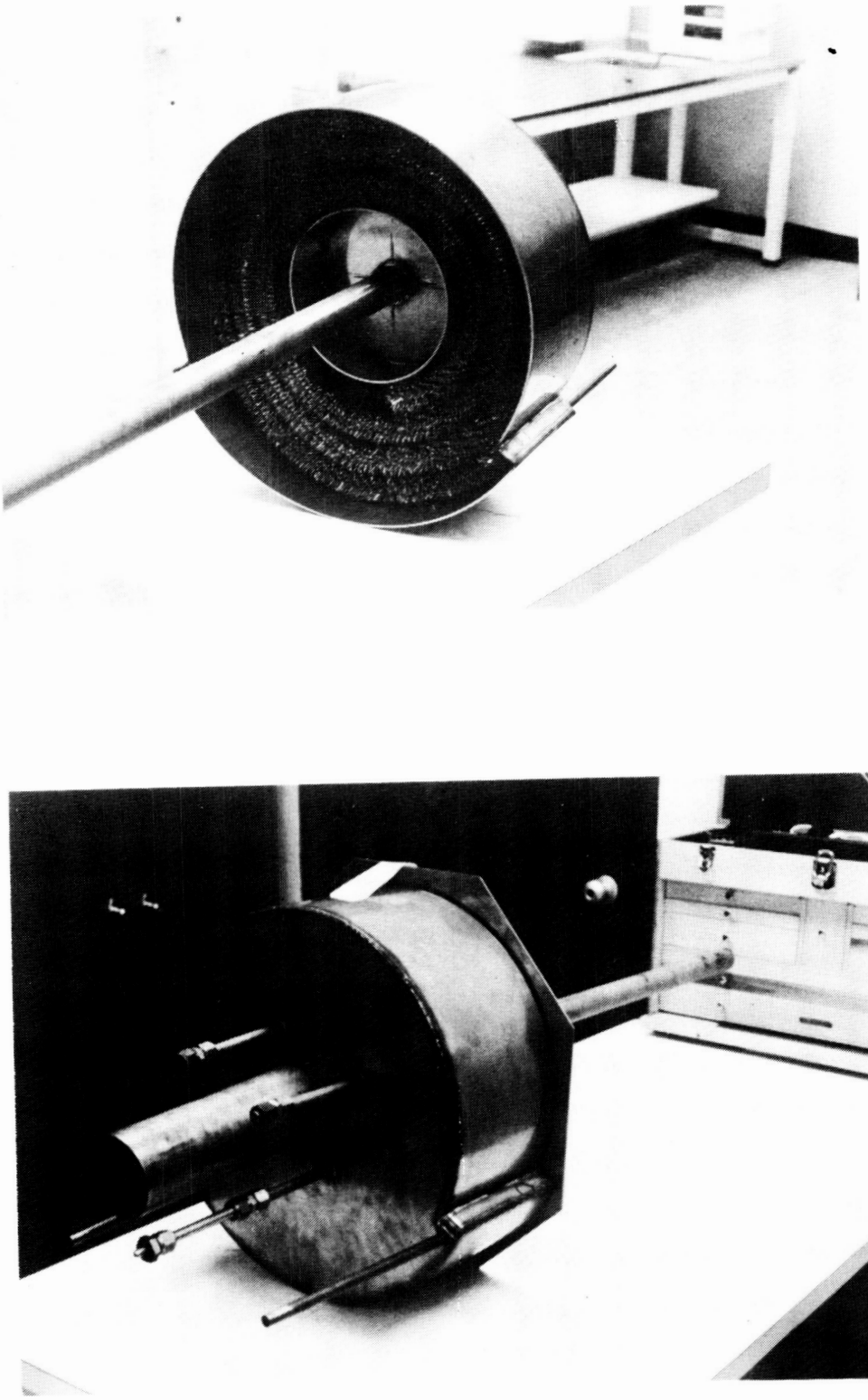

Figure 77. Vacuum Chamber Heat Exchanger

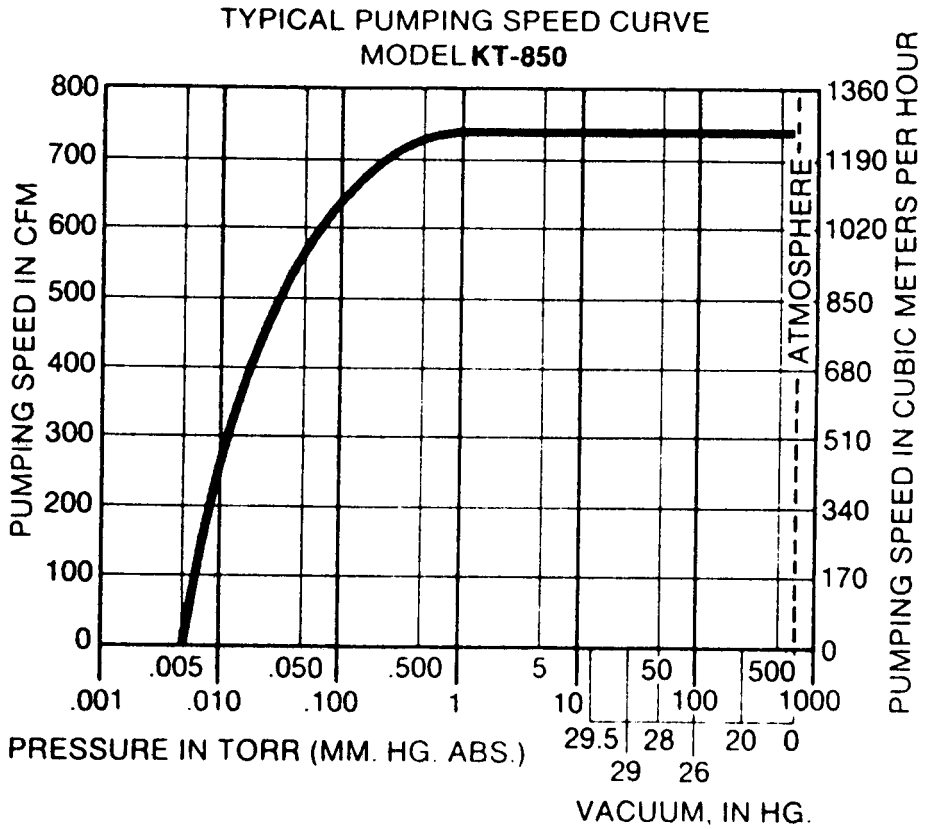

Figure 78. Pumping Curve for 850 CFM Kinney Pump

Figure 79. Vacuum Cell Pressure During Testing

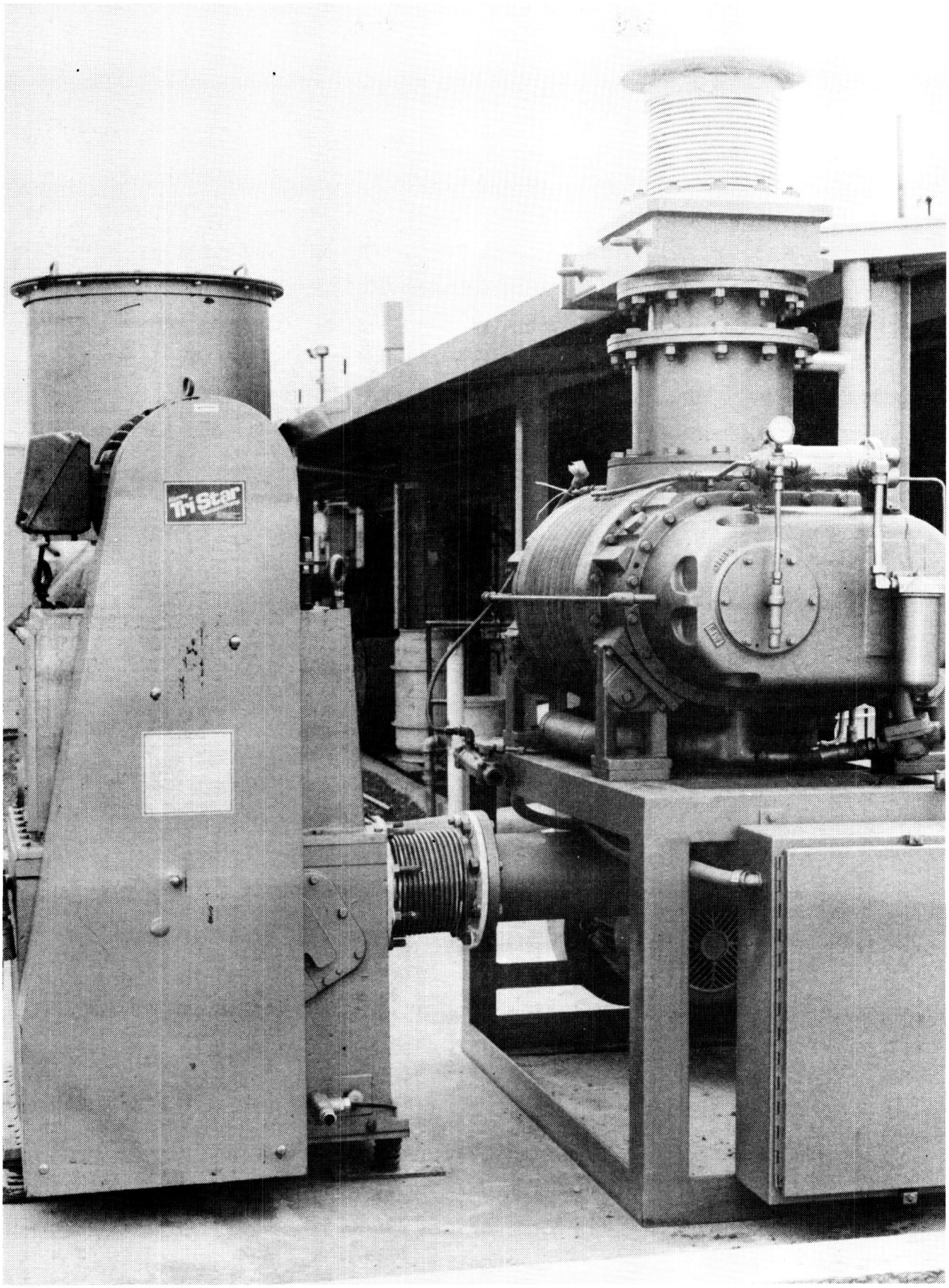

Figure 80. 6000 CFM Vacuum Pumps

3.6, Test Series 2 Testing (cont.)

Data Acquisition System and Measurements

A diagram of the data acquisition and control system is shown in Figure 81. An Apple IIe computer is used as the controller for the system, commanding the Daytronics data logger for data acquisition. Two other computers are used for data storage (one for high speed data and one for low speed). The control system is operated from the main control console by the test engineer. The computer controller is programmed with interlocks to shutdown the power to the arcjet if propellant flow is low, thruster body temperatures are out of limits, or if anomalies in the voltage/current behavior of the thruster are detected.

The following measurements were made during the testing:

1. Arc voltage and current
2. Thrust
3. Propellant mass flow rate
4. Magnet current
5. Vacuum system pressure and temperature
6. Magnet water flow rate
7. System conditions

Figure 82 lists the types of transducers and the approximate uncertainty of the measurements. All transducers have been calibrated prior to use, either in Aerojet's Calibration Laboratory or in place, against calibrated standards. Records of the calibrations have been maintained to assure traceability of the measurements.

Figure 83 shows the signal conditioning and processing of the transducer outputs. The system provides a means of in-place calibration of the data channels and checks the data system operation. The Daytronics System 10 shown in Figure 84 is the main analog-to-digital converter used to scan data channels. Outputs from the transducers can be amplified and filtered if needed to provide a signal compatible with the Daytronics.

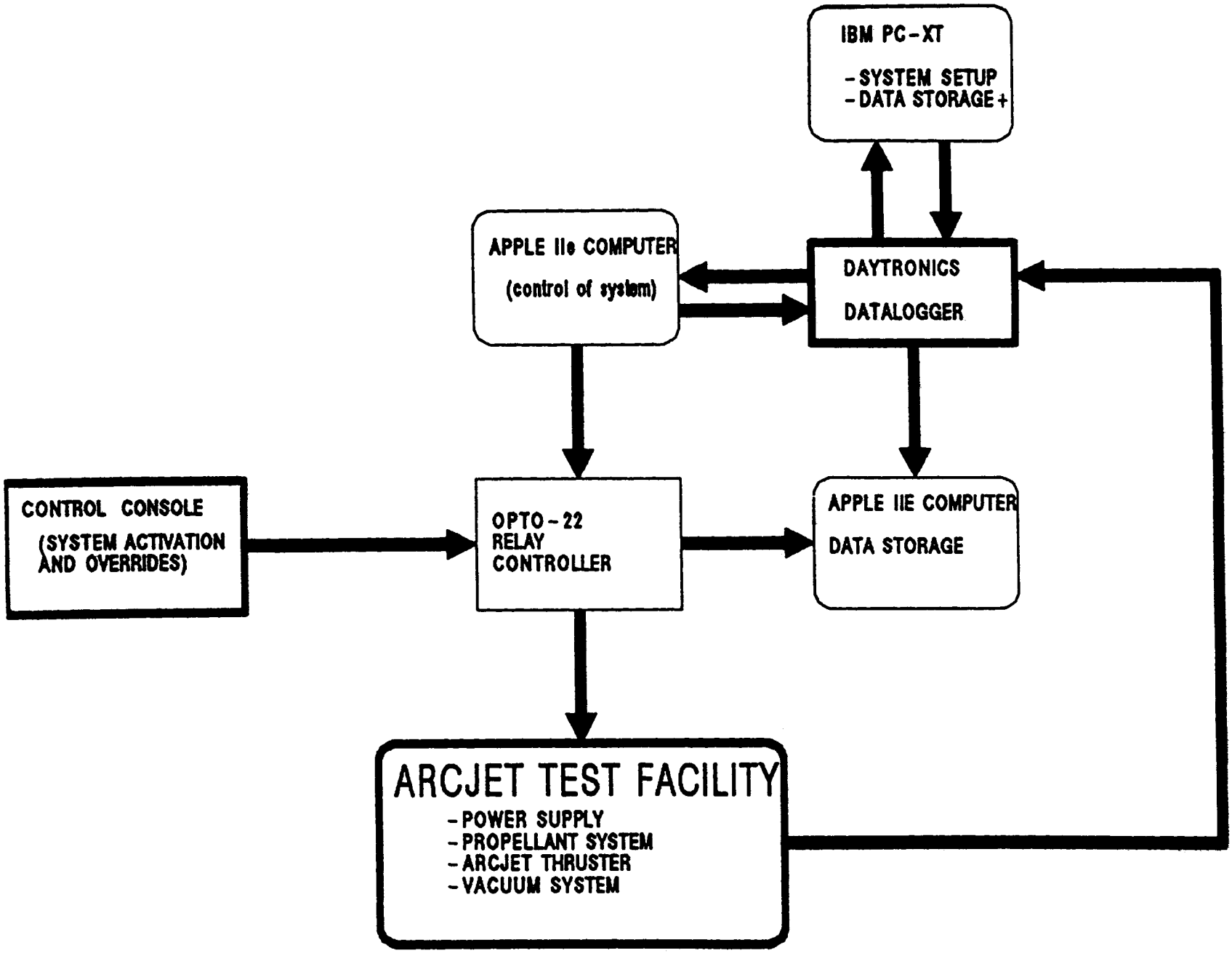

Figure 81. Arcjet Test Facility Data Acquisition Control Logic

Parameter	Range	Units	Accuracy	Inst. Type/Ident
Thrust 0-0.1000	lbf ± 0.00002		Bob Load Beam	
Propellant Flow	0-10.00	SLPM	± 3.0%	Matheson Flow Controller
Propellant Inlet Pressure	0-100	psig	± 0.5%	Pressure Transducer
Vacuum Chamber Pressure	1-1000	micron	± 2 micron	Baraton
Arc Current 0-50	Amp ± 1%	Shunt		
Arc Voltage 0-500	volts	± 1%	10,000: 1 voltage divider	
Arcjet Body Temperature	0-2000	°F	± 2°F	Type k
Propellant Inlet Temperature	0-150	°F	± 1°F	Type k
Propellant Supply Temperature	0-150	°F	± 1°F	Type k
Propellant Supply Pressure	0-200	psig	± 0.5%	

Figure 82. List of Transducers and Associated Uncertainties

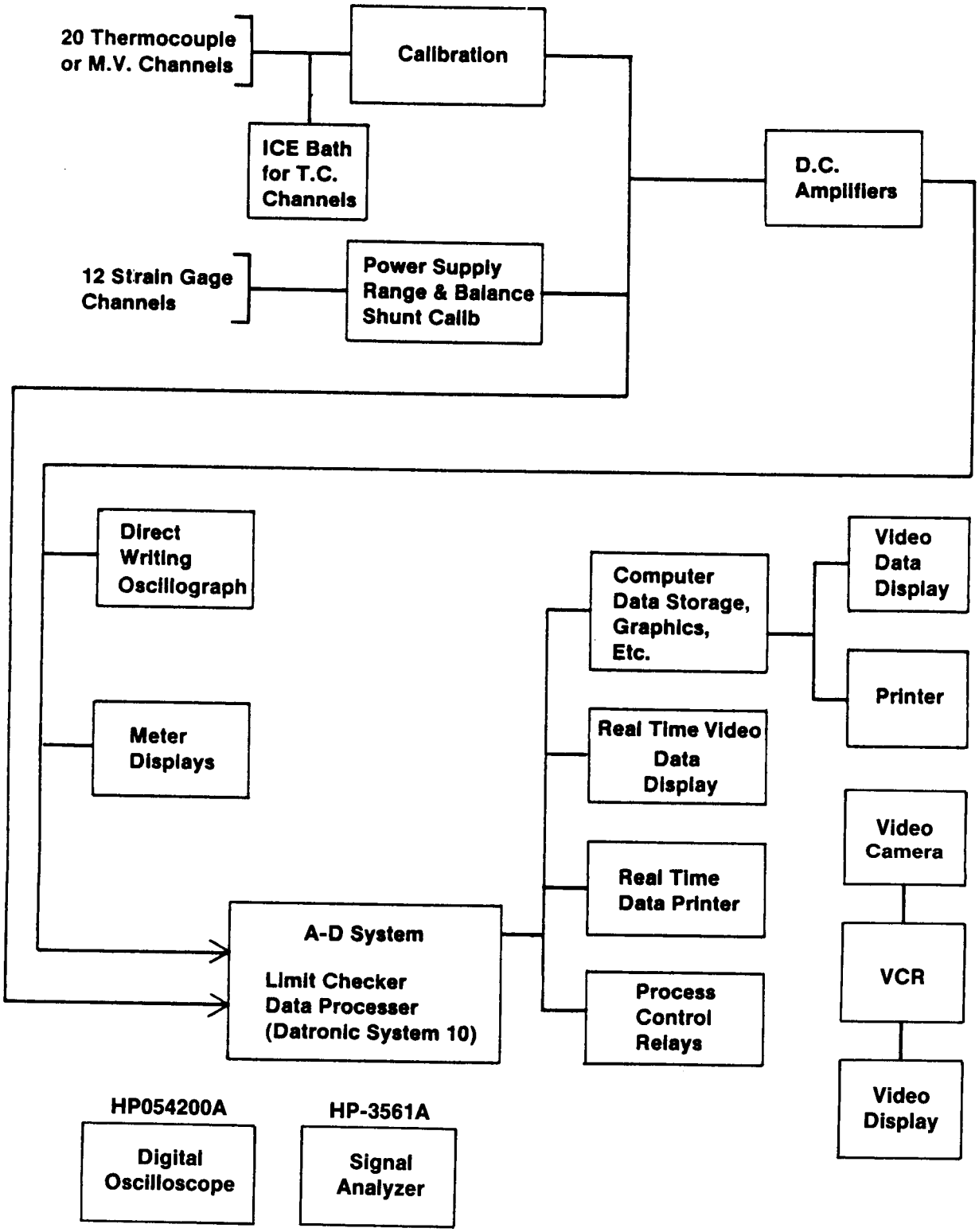

Figure 83. Instrumentation Block Diagram

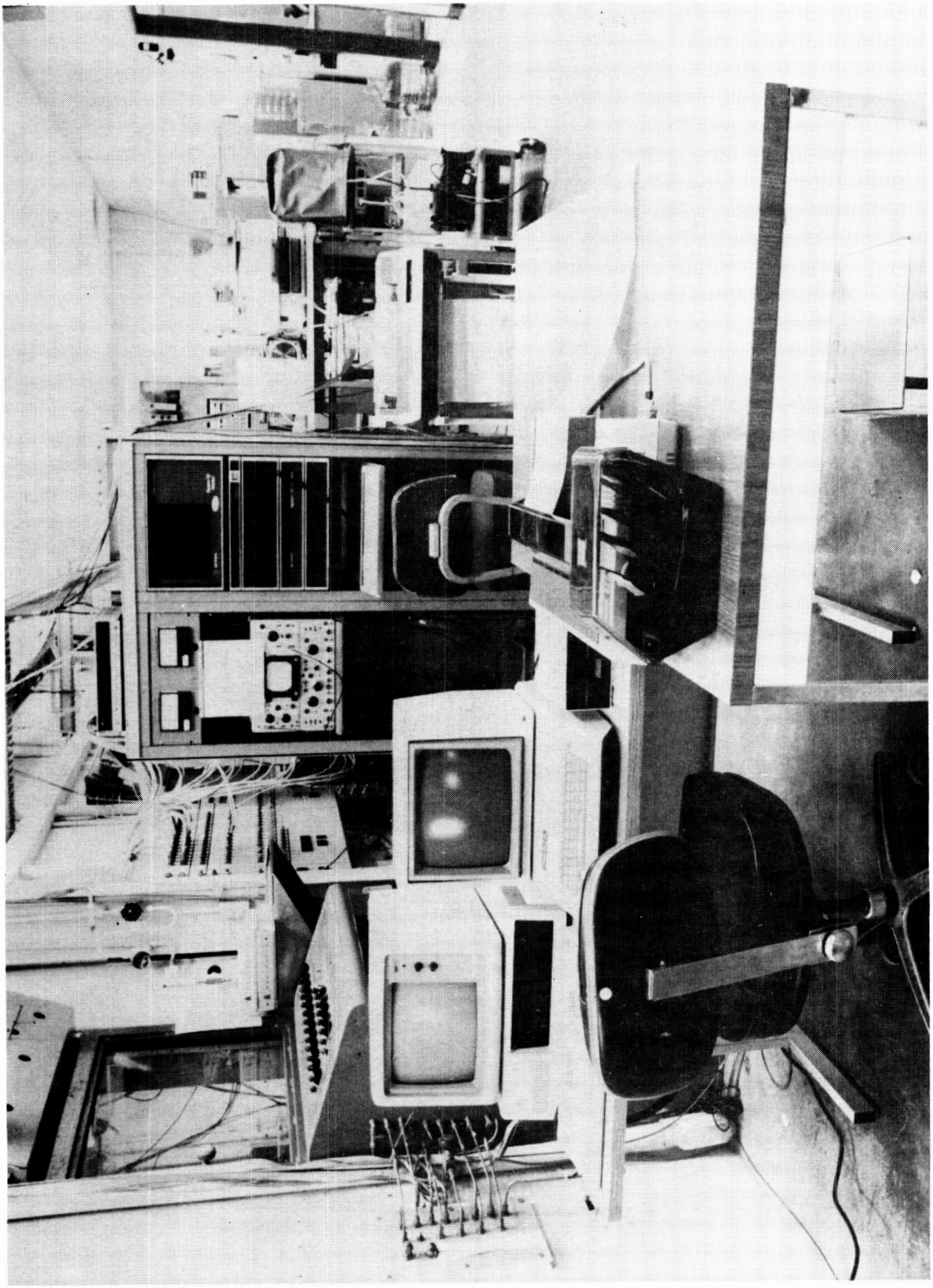

Figure 84. Data Aquisition and Control System

3.6, Test Series 2 Testing (cont.)

The most difficult measurement made during the testing was the thrust from the arcjet. A 250 gm full scale thrust stand shown in Figure 85 was used during the program. The thrust stand is a parallelogram design, with four flexures. The design greatly reduces bias in the thrust measurement due to rotation during displacement. A load beam transducer was used to measure the thrust, a second load beam was used as a calibration load cell. For in place calibration of the stand, a force is applied to the thrust measurement load cell by the external pressurization of bellows which cause the calibration load cell to push on the thrust stand. The reading from the two load cells can then be compared to determine the bias in the stand. The calibration of the load beams and the stand tare was also periodically checked with calibrated weights suspended from a pulley as shown in Figure 86. The thrust stand calibration and tare calculations details are contained in Appendix E.

Test Setup

For the Series 2 testing the thruster was mounted on the 250 gm thrust stand described previously, and installed in the vacuum test cell. Figure 87 shows the arcjet mounted in the tank prior to testing. Water cooled flexures, mounted perpendicular to the thrust direction provide arc power and magnet power. A tubular flexure provides propellant to the thruster (on the right side of Figure 87).

The arcjet power circuit is shown in Figure 88. Arc power is supplied by the Eratron power supply described previously. The current from the power supply is passed through a "T" filter consisting of two 100 micro-henry inductors, and a 110 micro-Farad capacitor, with a bleed resistor. A ballast resistor of 40 ohms was used in series with the arc. Two voltage dividers were connected across the arcjet electrodes to measure arc voltage. Arc current was measured with a precision 50 amp current shunt.

Test operations were controlled from the control console shown in Figure 89. The video monitor shown displayed an image of the arc

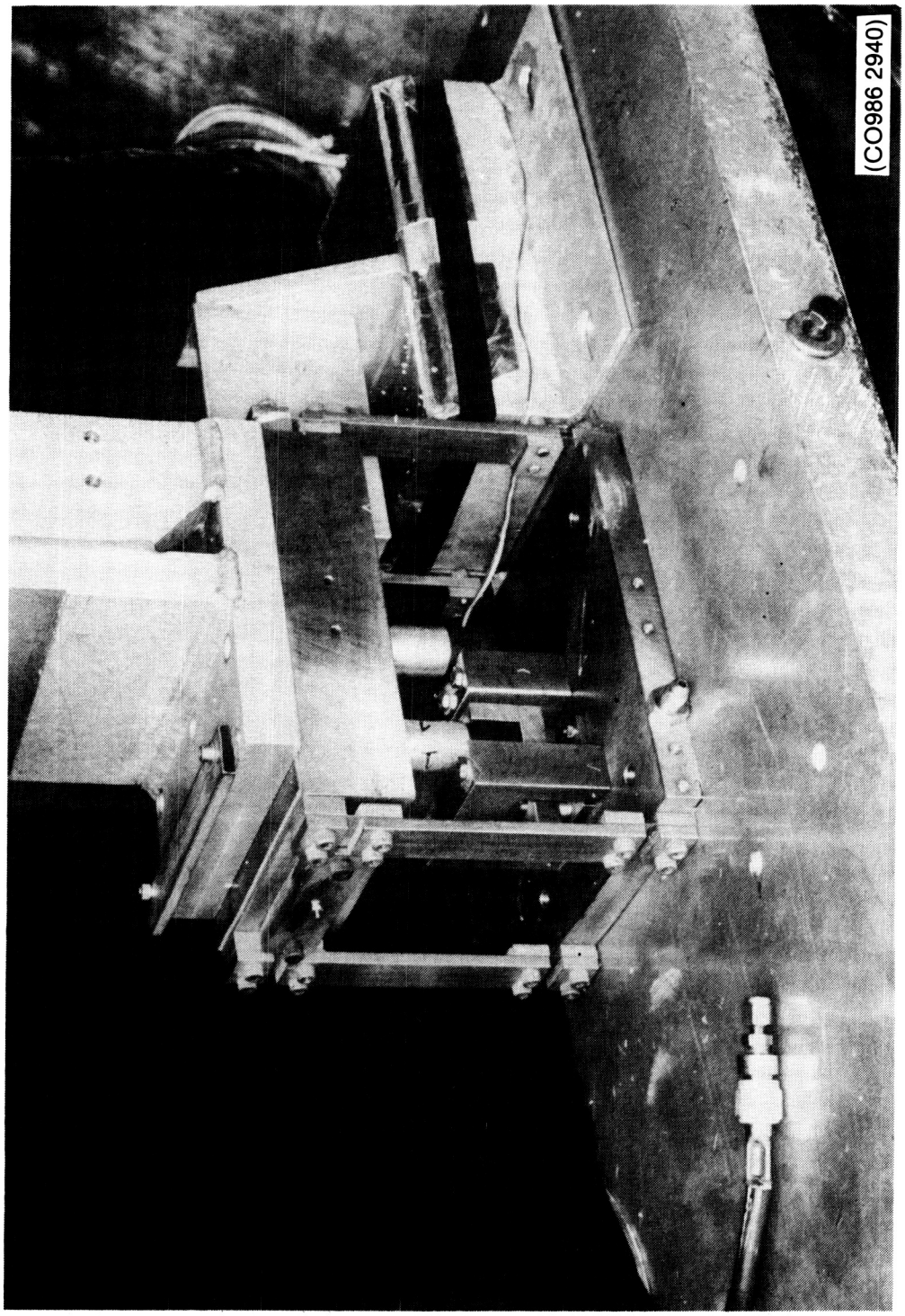

Figure 85. Aerojet Thrust Stand

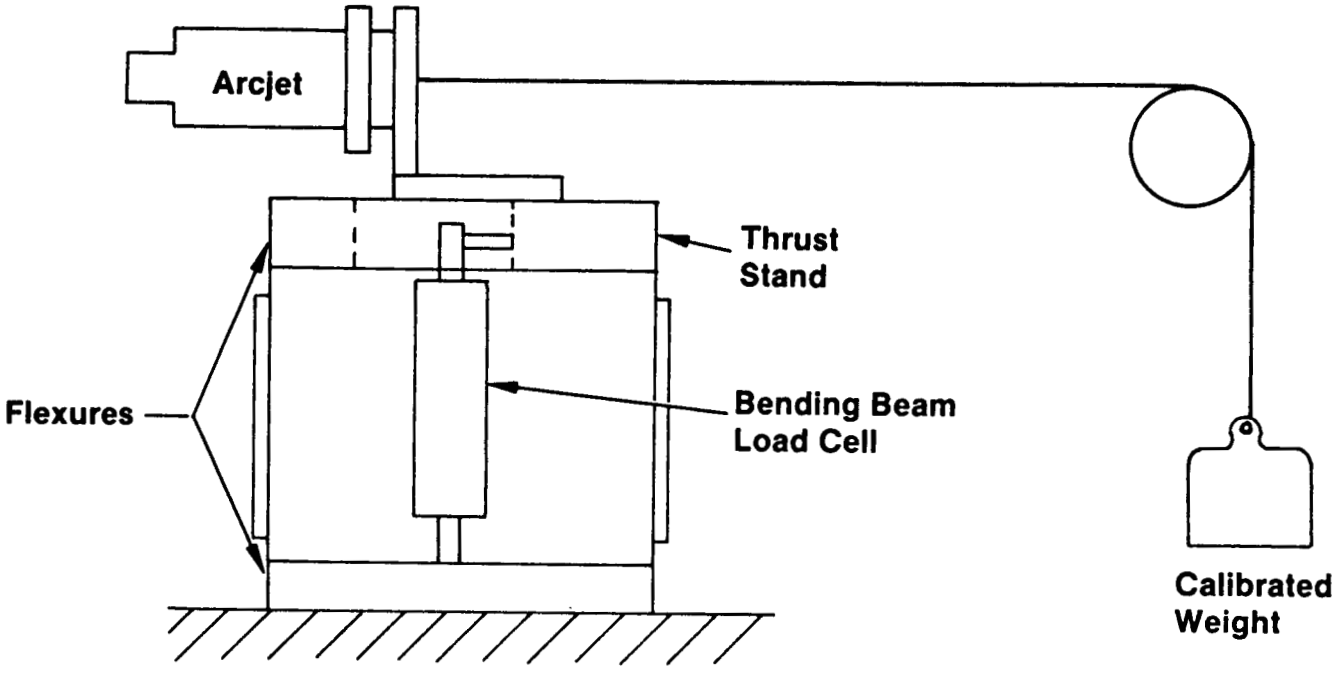

Figure 86. Calibration of Thrust Stand with Weights

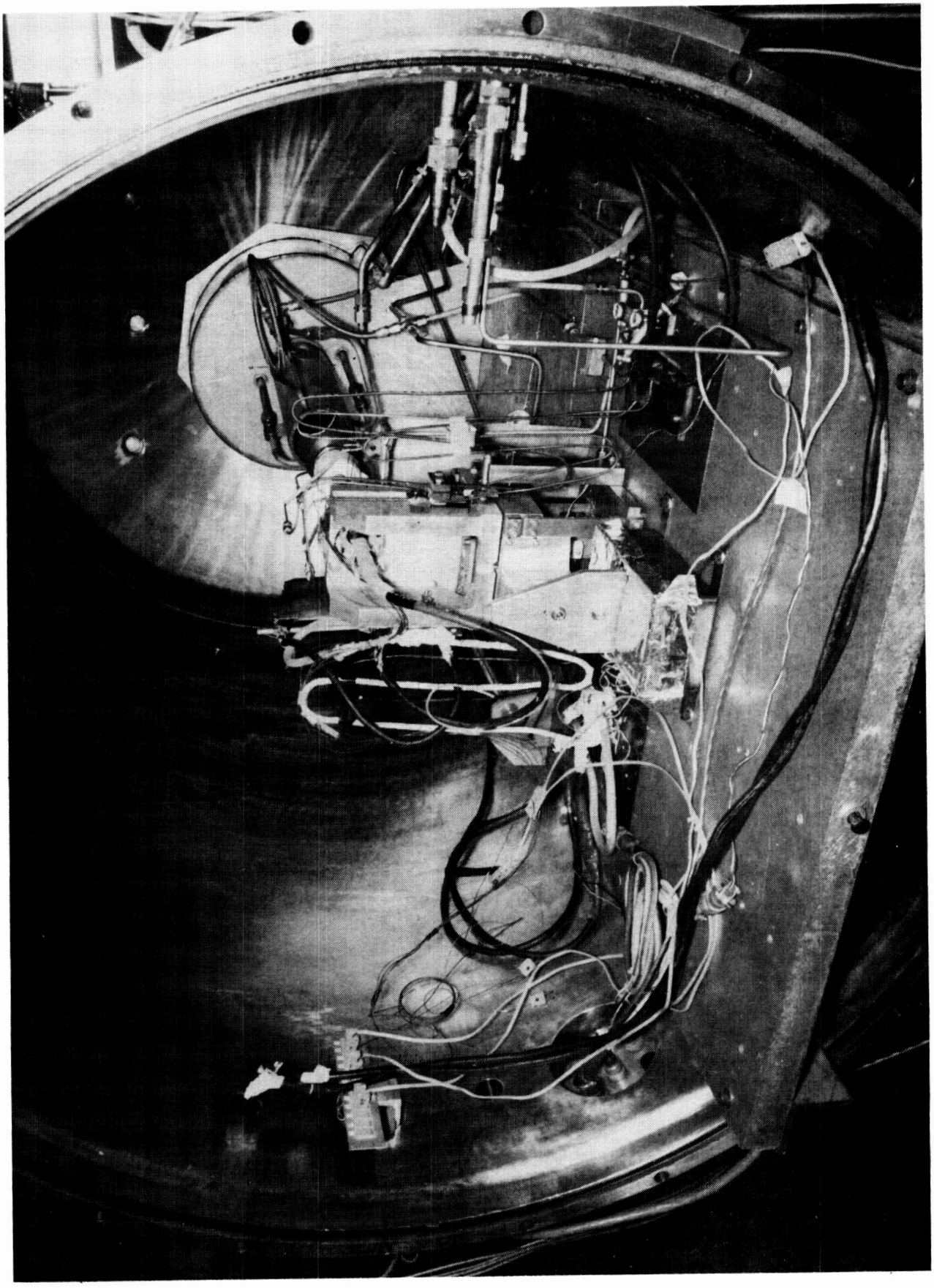

Figure 87. Overall View of Arcjet Thruster in Vacuum Tank

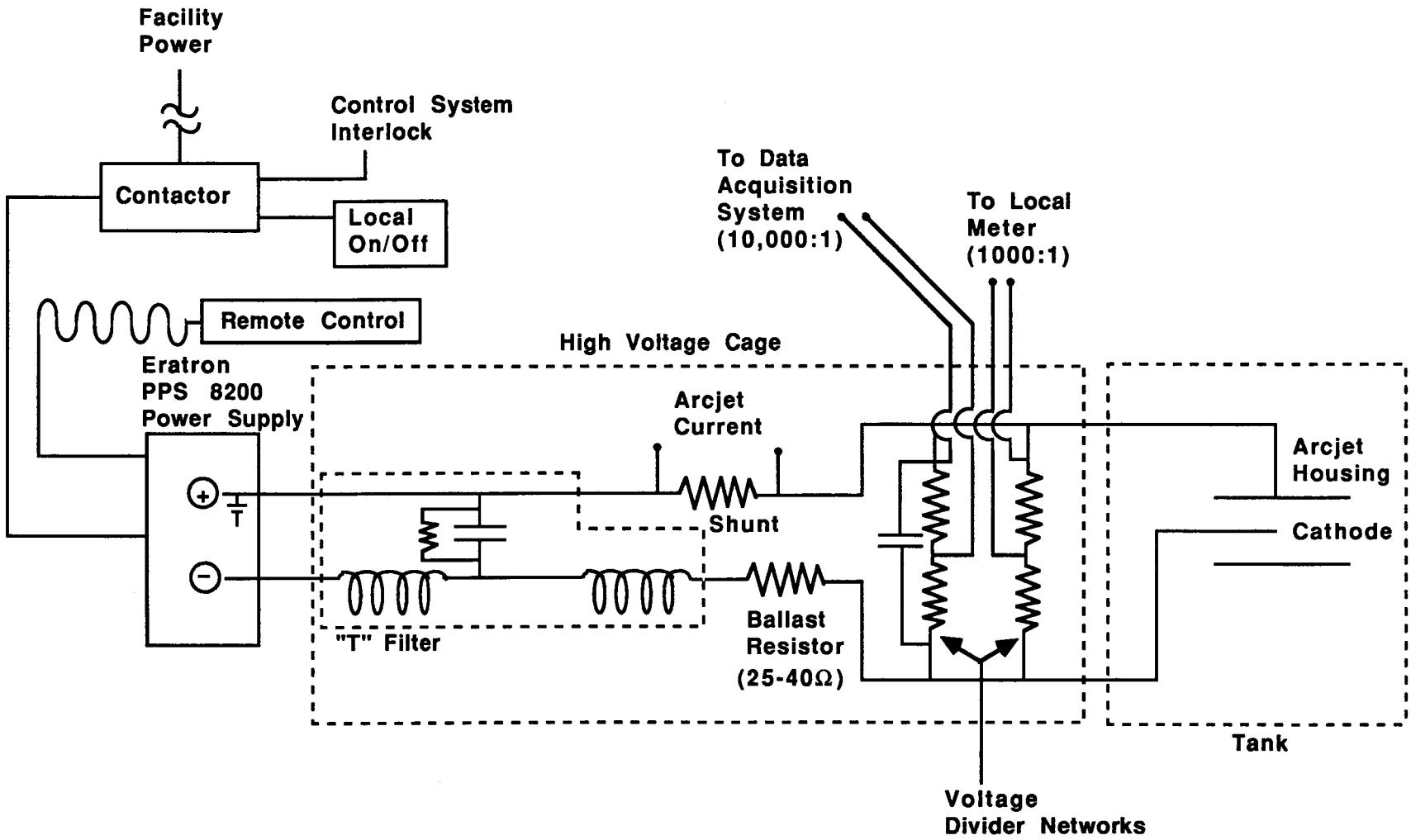

Figure 88. Schematic Drawing of 1Kw Arcjet Electrical Circuit

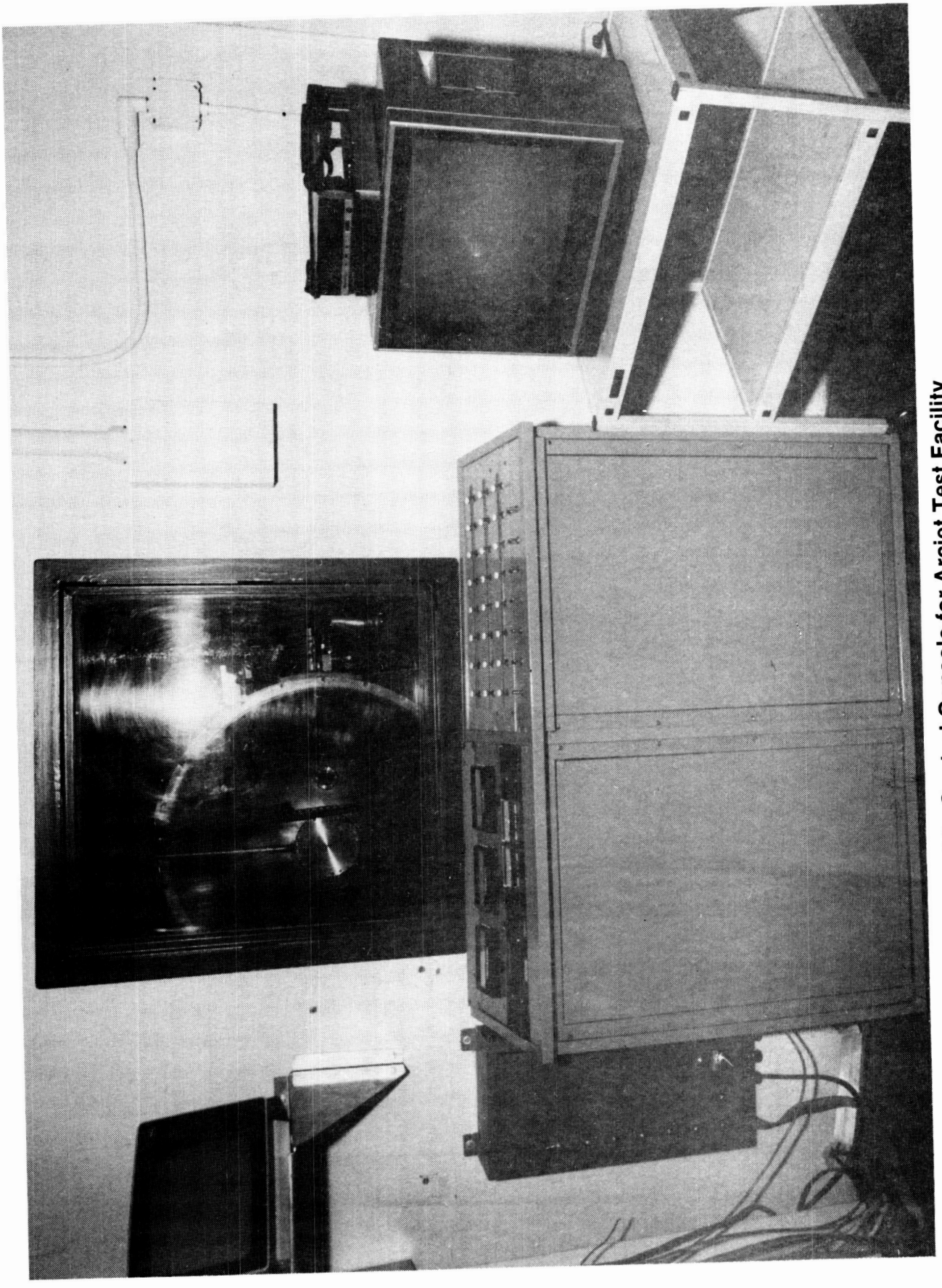

Figure 89. Control Console for Arcjet Test Facility

viewed looking up the nozzle. The video tape of each test has been maintained as a permanent record. During the tests, the video served a diagnostic tool for monitoring starts and arc operation. The operator can control the power supply current, data acquisition system and propellant supply system from the console. To ensure proper test conditions at the beginning and end of the tests, a check list of critical procedures was maintained. Figure 90 is a long form of the test record used to note exact conditions of the tests. A summary test sheet shown in Figure 91 was used by the test engineer to check all critical items.

The start procedure used during Test Series 2 is similar to that described in Section 3.5. After the vacuum chamber had been pumped down to a pressure of approximately 10 microns with no flow, a voltage breakdown test was performed. If a potential of 2000 volts could be maintained, the electrical leads and cathode were considered sufficiently isolated. An automatic thrust stand calibration was then performed to determine thrust stand offset and bias. The calibration was controlled by a computer program which activates a valve to a pressurized nitrogen supply. The gas then pressurized a set of bellows on the stand, which in turn applied load to the stand through a calibrated load cell. A summary of the thrust stand calibration data for the tests is included in Appendix E.

When the calibration was complete, the current control circuit of the power supply was then preset to a desired operating current, typically 8.0 amps. The power supply was then activated and an open circuit voltage of 700 volts was placed across the electrodes. The data acquisition system and video camera system were then turned on and a solenoid valve in the propellant line was opened. The arc would initiate as the chamber pressure in the arcjet increased. An initial flow of approximately 40 mg/sec was used for most starts, the flow rate control set point was then changed manually during the parametric tests.

The interlocks of the data acquisition system which command shut down of the power supply if propellant flow is lost or if unusual electrical operation (i.e., high current or voltage) were manually suppressed for

Run Number:_____ Date:_____ By:_____

Test Objective:

1.0 Configuration Identification Summary

1.1 Arcjet

Cathode:

Insulator:

Anode/Nozzle:

Magnet:

Other:

1.2 Facility

Vacuum System:

Propellant System:

Test Stand:

Power Supplies:

Instrumentation:

Controls:

Other:

2.0 Planned Test Conditions

Start Procedure:

Propellant:

Power Level:

Propellant Flow Rate:

Duration:

Magnetic Field:

Figure 90. 1-KW Arcjet Set-Up Sheet (Page 1 of 4)

3.0 Operation Sequence

3.1 Pretest Check

3.1.1 Instrumentation

Pretest: Functional, Zero, and Calibration_____

Data Record: Hard Copy _____; Disc _____

Data Rate: _____ Seconds/Scan

Video System Ready _____

3.1.2 Test Cell and Thruster

Cathode Gap Set to _____ inches

Cooling Water on _____

Voltage Breakdown Test to _____ volts

Stand Secured _____

Thrust Calibration Check _____

Door Installed _____

3.1.3 Vacuum System

Oil Level OK _____

Cooling Water on _____

Vacuum Pump on _____

Pump Down for _____ Minutes to Less Than _____ torr

3.1.4 Propellant System

Argon Storage Pressure _____ psig

Propellant Storage Pressure _____ psig

Argon Regulator Setting _____ psia

Propellant Regulator Setting _____ psia

Figure 90. 1-KW Arcjet Set-up Sheet (Page 2 of 4)

3.1.5 Power Supplies

Arc Power Supply Set to _____

Magnet Power Supply Set to _____

Ballast Resistor Set to _____ ohms

Capacitor _____ microfarad

Inductor _____ millihenry

3.1.6 Special Requirements

3.2 Operation

3.2.1 Start

Data System on _____

Video System on _____

Magnet Power Supply on _____

Pretest Force Calibration _____

Arc Power Supply on _____

Argon on _____

Propellant on _____

Argon off _____

Control Arc Current to _____ amps

Adjust Propellant Pressure to _____ psia

Run Duration: _____ Minutes

Figure 90. 1-KW Arcjet Set-up Sheet (Page 3 of 4)

3.2.2 Shutdown

Arc Power Supply off _____

Propellant off _____

Posttest Force Calibration _____

Magnet Power Supply off _____

Secure Video and Data Systems _____

Secure Propellant Systems _____

Prepare for Tank Entry _____

or

Prepare for Retest _____

4.0 Initial Test Results/Comments

Figure 90. 1-KW Arcjet Set-up Sheet (Page 4 of 4)

(Mod. 1)

SUMMARY

Run No.:_____ Date:_____ By:_____

Startup

1. Test stand unlocked _____
2. Tank pumped down to _____ micron _____
3. Voltage breakdown: _____ volt at ma _____
4. Test chamber cooling water ON _____
5. Argon gas system set to _____ psia and ready _____
6. Propellant gas system set to _____ psia and ready _____
7. Magnet power supply ON and set to _____ amp _____
8. Arc power supply ready/volt set to 0; current set to _____ _____
9. Instrumentation system ready _____
10. Thrust stand calibrated _____
11. Video recorder ON _____
12. Instrumentation ON _____
13. Power supplies ON _____
14. Gas supply ON _____
15. Set test conditions, conduct test _____

Shutdown

1. Power supplies OFF and secured _____
2. Switch gas supply to argon _____
3. VCR OFF and titled for next test _____
4. Argon OFF _____
5. Calibrate thrust stand _____
6. Argon ON (if hardware hot) _____
7. Instrumentation off _____
8. Record test comments _____

Figure 91. 1-KW Arcjet Checklist

30 seconds at the beginning of each test. After that start period, the Daytronics data acquisition system would perform shut down to the test in the case of abnormal operation. The test engineer also can end a test by shutting down the power supply with a master control switch. At the conclusion of a test, a post test thrust stand calibration was performed. A comparison to pre and post test calibrations was analyzed to determine the tare factor (actual thrust/measured thrust) and the zero offset for each run.

3.6.2 Arcjet Performance Testing

Table XIII is a summary of the data from the tests conducted, AJ1K001 through AJ1K026, during Test Series 2. The data values shown are just prior to the end of each test. The test set up was configured as shown in Figure 88. The tests were conducted for mass flow rates of 38 to 68 mg/sec, electric current levels of 7.5 to 8.6 amps, and voltages from 85 to 167 volts, with corresponding power levels from 700 to 1400 watts.

The tests were started using simulated hydrazine as the propellant and the start procedure described in Section 3.6. The electromagnet was turned on before each test. A test number has been assigned to each experiment when current was drawn from the power supply. The testing consisted of four subseries, 2.0 through 2.4:

Test Series	Test Number	Purpose
2.0	AJ1K001 - AJ1K005	System check out
2.1	AJ1K006 - AJ1K011	Modification of arc power circuit
2.2	AJ1K012 - AJ1K019	Baseline Performance
2.3	AJ1K020 - AJ1K026	Parametric Testing

Performance Calculations

The method for calculation of data items included in 3.6, Table XIII are described below.

TABLE XIII

ARCJET TEST SUMMARY

1 kW Arcjet Test Summary Log

RUN #	DATE	PROPELLANT	DURATION (min)	POWER (watts)	VOLTAGE (volts)	CURRENT (amps)	MASS FLOW (mg/sec)	THRUST (N)	Is (sec)	EFFICIENCY (%)	Pc (kPa)	C* (m/sec)	Tbody (K)	Cf	TEST PURPOSE	COMMENTS
AJ1K001	11-4-86	SIMULATED HYDRAZINE	1.0	684.0	129.0	5.3	42.1	0.098	236.9	16.6	331.0	1925.3	430.0	1.207	SYSTEM CHECKOUT	BASELINE CONFIGURATION
AJ1K002	11-4-86	" "	1.0	880.0	110.0	8.0	46.2	0.098	216.2	11.8	454.4	2409.7	448.0	0.880	" "	
AJ1K003	11-5-86	" "	0.1	510.0	60.3	8.5	42.0	---	0.0	0.0	---	---	---	---	" "	
AJ1K004	11-5-86	" "	10.0	981.0	122.4	8.0	42.2	0.114	275.4	15.7	426.8	2477.9	1194.0	1.090	" "	
AJ1K005	11-5-86	" "	20.0	999.0	124.3	8.0	41.9	0.114	277.3	15.5	445.4	2604.4	1231.0	1.045	" "	THRUST CORRECTED FOR THERMAL OFFSET
AJ1K006	11-12-86	" "	0.0	0.0	0.0	0.0	41.9	---	0.0	0.0	---	---	---	---	SIMPLIFY POWER CIRCUIT	
AJ1K007	11-12-86	" "	0.0	0.0	0.0	0.0	41.9	---	0.0	0.0	---	---	---	---	" "	ATTEMPT TO REDUCE EXTERNAL POWER CIRCUIT BY REMOVING BALLAST AND INCREASING INDUCTANCE IN NETWORK. THE ARC INITIATED MOMENTARILY AND THEN EXTINGUISHED.
AJ1K008	11-12-86	" "	0.0	0.0	0.0	0.0	41.9	---	0.0	0.0	---	---	---	---	" "	
AJ1K009	11-12-86	" "	0.0	0.0	0.0	0.0	41.9	---	0.0	0.0	---	---	---	---	" "	
AJ1K010	11-12-86	" "	0.0	0.0	0.0	0.0	41.9	---	0.0	0.0	---	---	---	---	" "	
AJ1K011	11-12-86	" "	0.5	0.0	0.0	0.0	41.9	---	0.0	0.0	---	---	---	---	SYSTEM CHECK OUT	RETURN TO BASELINE CONFIGURATION
AJ1K012	11-21-86	" "	0.3	0.0	0.0	0.0	41.9	---	0.0	0.0	---	---	---	---	" "	CONTROL COMMANDED SHUTDOWN
AJ1K013	11-24-86	" "	0.5	1270.0	118.6	10.7	40.1	0.078	197.3	5.9	298.6	1824.4	365.0	1.061	" "	ARC EXTINGUISHED WHILE CURRENT WAS
AJ1K014	11-24-86	" "	0.5	1080.0	138.6	7.9	39.6	0.070	180.2	5.7	289.9	1793.6	352.0	0.986	" "	CONTROL COMMANDED SHUTDOWN

TABLE XIII (cont.)

1 kW Arcjet Test Summary Log

RUN #	DATE	PROPELLANT	DURATION (min)	POWER (watts)	VOLTAGE (volts)	CURRENT (amps)	MASS FLOW (mg/sec)	THRUST (N)	Is (sec)	EFFICIENCY (%)	Pc (kPa)	C* (m/sec)	Tbody (K)	Cf	TEST PURPOSE	COMMENTS
AJ1K015	11-24-86	• •	1.2	1130.0	143.4	7.9	40.3	0.073	184.6	5.9	356.5	2167.3	495.0	0.836	• •	ARC EXTINGUISHED
AJ1K016	11-24-86	• •	13.0	1214.0	153.1	7.9	40.4	0.077	194.3	6.0	384.1	2329.3	1142.0	0.818	BASELINE PERFORMANCE	ARC EXTINGUISHED
AJ1K017	11-25-86	• •	8.5	1220.0	157.3	7.8	39.2	0.080	207.0	6.6	377.8	2361.3	1093.0	0.860	• •	ARC EXTINGUISHED
AJ1K018	11-26-86	• •	18.4	710.0	85.7	8.2	38.2	0.068	182.7	8.6	377.2	2419.2	1030.0	0.741	• •	ARC EXTINGUISHED
AJ1K019	11-26-86	• •	19.2	730.0	90.0	8.2	38.2	0.064	170.8	7.3	379.2	2432.0	1031.0	0.689	• •	TEST ENDED BY OPERATOR
AJ1K020	12-3-86	• •	0.0	0.0	110.0	8.2	0.0	0.000	0.0	0.0	0.0	0.0	0.0	0.000	• •	VOLTAGE BREAKDOWN THROUGH AFT INSULATOR
AJ1K021	12-11-86	• •	2.3	0.0	0.0	0.0	0.0	0.000	0.0	0.0	0.0	0.0	0.0	0.000	PARAMETRIC TESTING	ARC EXTINGUISHED
AJ1K022	12-11-86	• •	0.7	0.0	0.0	0.0	0.0	0.000	0.0	0.0	0.0	0.0	0.0	0.000	• •	ARC EXTINGUISHED
AJ1K023	12-11-86	• •	80.0	1300.6	156.7	8.3	65.5	0.185	287.4	20.0	793.0	2966.2	1213.0	0.951	• •	
AJ1K024	12-11-86	• •	0.5	0.0	0.0	0.0	0.0	0.000	0.0	0.0	0.0	0.0	0.0	0.000	• •	LIMIT ERROR
AJ1K025	12-11-86	• •	0.5	0.0	0.0	0.0	0.0	0.000	0.0	0.0	0.0	0.0	0.0	0.000	• •	LIMIT ERROR
AJ1K026	12-11-86	• •	37.0	1388.8	160.6	8.7	64.2	0.172	273.1	16.6	784.0	2991.9	1242.0	0.895	• •	ARC EXTINGUISHED

3.6, Test Series 2 Testing (cont.)

Vacuum Corrected Thrust:

$$T = T_{meas} + A_t \, \epsilon \, P_V$$

A_t = Nozzle throat area
T_{meas} = Measured thrust
ϵ = Effective area ratio of nozzle
P_V = Vacuum chamber pressure

Specific Impulse:

$$I_s = \frac{T}{\dot{m} \, g}$$

T = Vacuum corrected thrust
$\dot{m}$ = Mass flowrate
g = acceleration of gravity

Thrust Efficiency:

$$E = \frac{(.5\dot{m}v^2)_{HOT}}{P_{elec} + (.5\dot{m}v^2)_{COLD}}$$

No direct measurement of the chamber pressure was possible with the design of the research thruster. Calculation of the thrust coefficient and characteristic velocity have been made using the inlet pressure to the arcjet. This pressure was measured from a tap external from the tank and downstream of the flow control. The pressure in the mixing chamber is the pressure which should be used for the calculation. The flows to the arc chamber and mixing chamber are branched parallel from the supply. Most of the arc power is absorbed by the flow through the arc chamber, causing an increase in the arc chamber pressure relative to the mixing chamber pressure. Since the inlet pressure is always greater than the arc chamber pressure a significant difference may exist between the inlet pressure and the mixing chamber pressure.

Thrust Coefficient:

$$C_F = \frac{T}{A_t \, P_c}$$

A_t = Nozzle Throat Area
P_c = Chamber pressure
$\simeq P_{inlet}$

Characteristic Velocity:

$$C^{*\prime} = \frac{P_c \, A_t \, g}{\dot{m}}$$

Arc Power:

$$P = I \, V$$

I = Arc Current
V = Arc Voltage

Arc Resistance:

$$R = \frac{V}{I}$$

3.6, Test Series 2 Testing (cont.)

Test summary sheets containing measured and calculated data values for the tests are included in Appendix F.

System Checkout

The system checkout test series was conducted to debug the test setup and data acquisition system. The testing also familiarized the test personnel with the operating characteristics of the thruster. Limited data were taken during tests AJ1K001 and 002 while the start procedure was reviewed. During tests 004 and 005 the thruster was operated for 10 and 20 minutes respectively. During these tests a drift in the thrust measurement due to radiation heating of the stand flexures and load cell was detected. The thermal effects on the stand became apparent after approximately 12 minutes of operation. Figures 92 and 93 show the chamber inlet pressure and thruster body temperature for tests 004 and 005, thermal equilibrium of the thruster is achieved reached 10 to 13 minutes into a test.

The arc voltage and current during tests 004 and 005 are shown in Figures 94 and 95. The arc resistance has been calculated from the arc current and voltage as has the power; these are plotted on Figures 96 and 97 for the tests. Using the thrust stand tare correction calculated from the pre and post test calibrations and zero shift offsets (procedure and values are given in Appendix E) the measured thrust was corrected and the specific impulse and thrust efficiency was calculated. Figures 98 and 99 show these performance values for tests 004 and 005.

In addition to obtaining the initial performance data, measurements were made on the voltage and current signal to characterize the operation of the arc with the Eratron power supply. Figure 100 shows the arcjet voltage and current trace during test 002. The measurements were taken with an HP 54200A digital oscilloscope. A spectrum analysis of the arc voltage has been obtained during testing, as shown in Figure 101. These measurements were made with an HP 3561A dynamic signal analyzer. The FFT of the signal, shown in Figure 102, shows a high frequency component of the voltage signal at 5375 Hz which is the power supply ripple frequency. Figure 103 3.6,

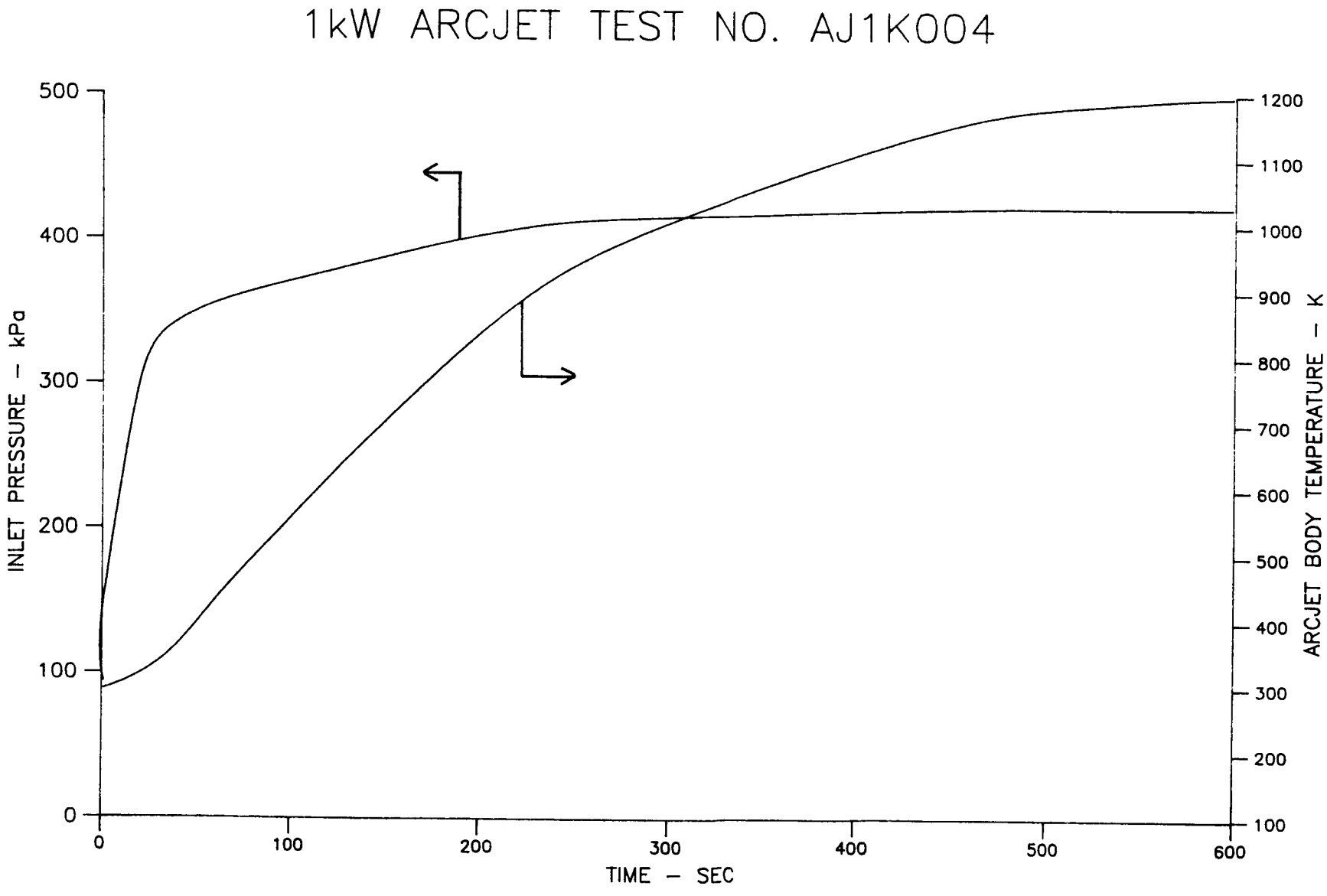

Figure 92. Inlet Pressure and Arcjet Body Temperatures for AJ1K004

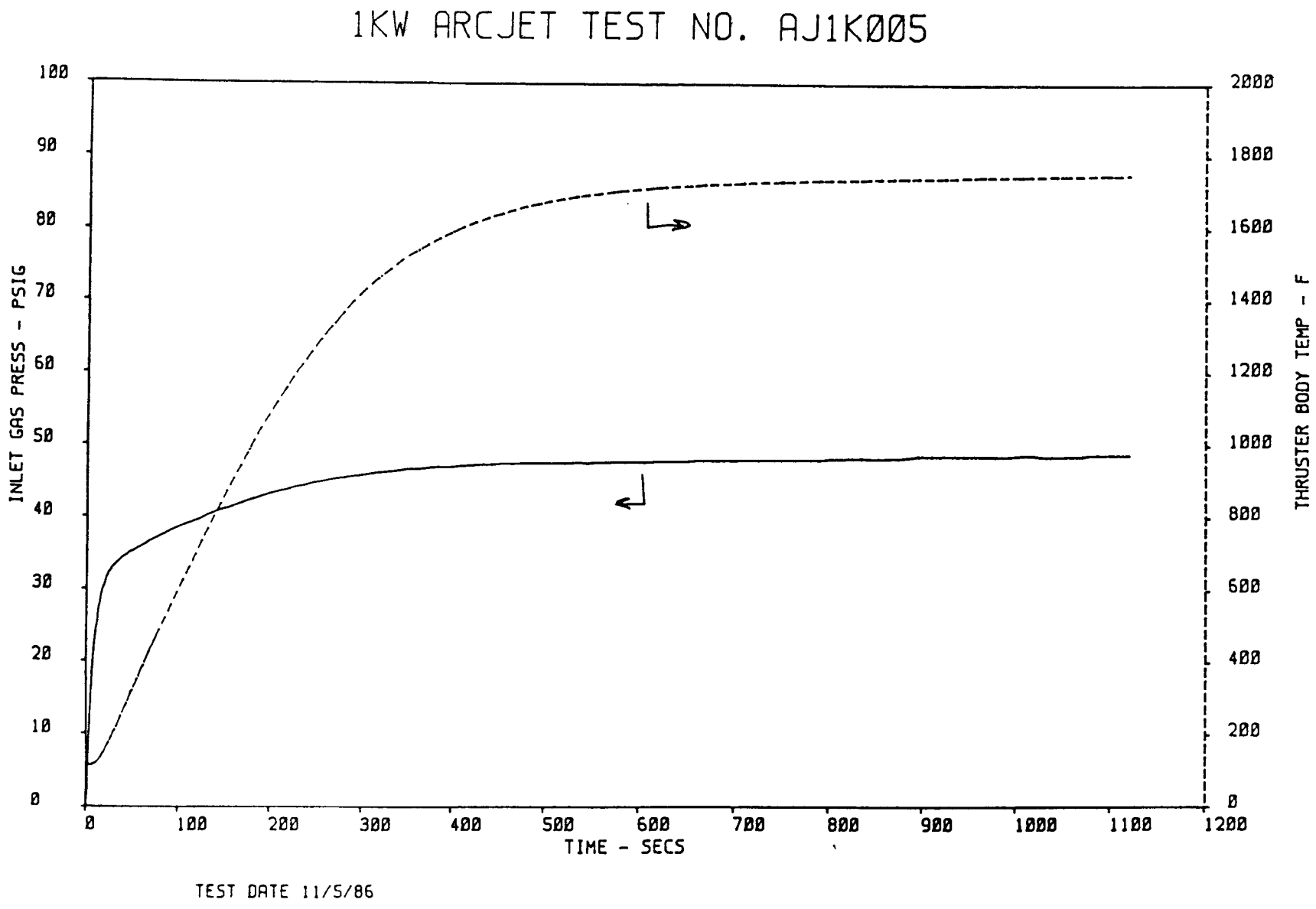

Figure 93. Inlet Pressure and Body Temperature AJ1K005

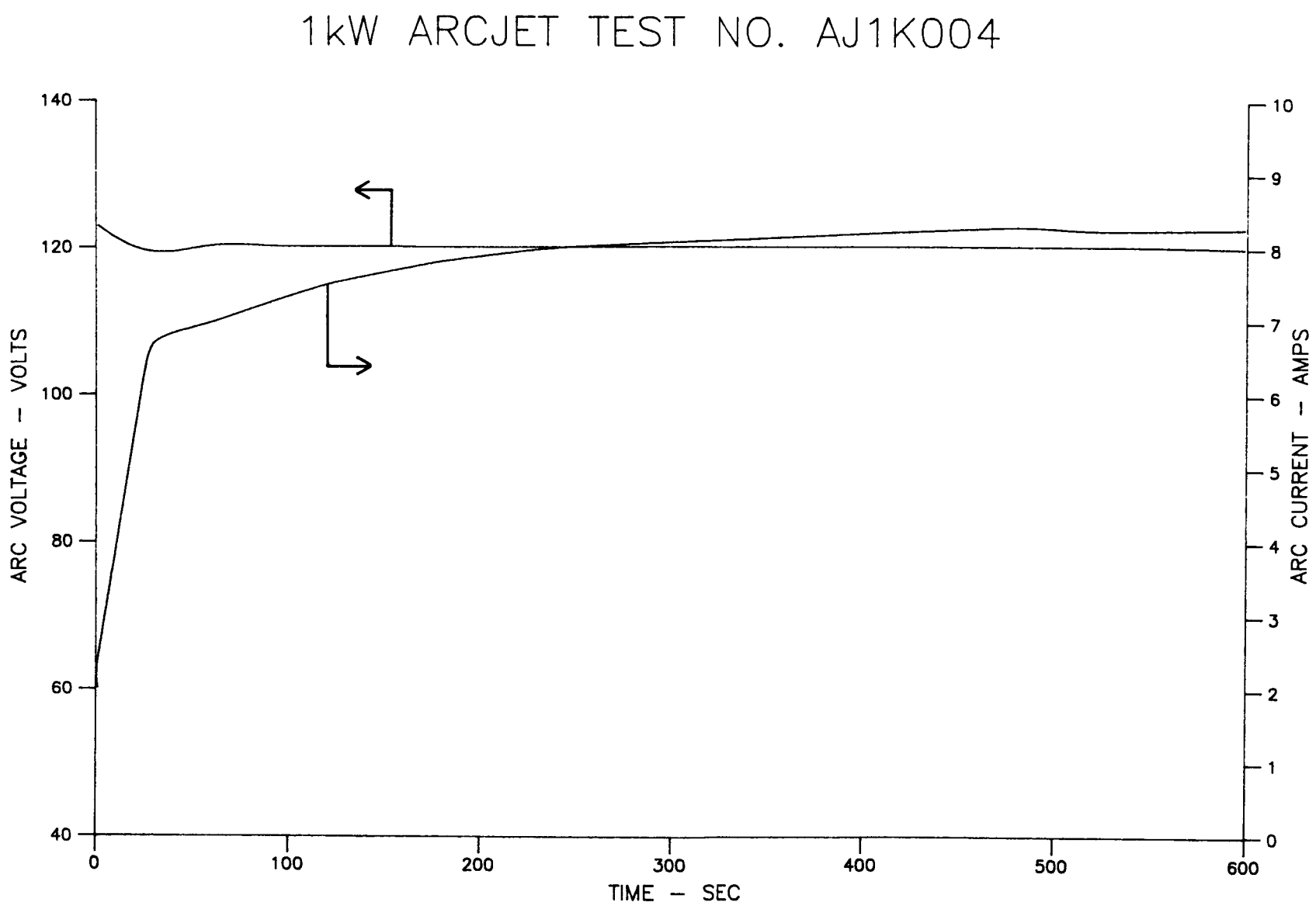

Figure 94. Voltage and Current for AJ1K004

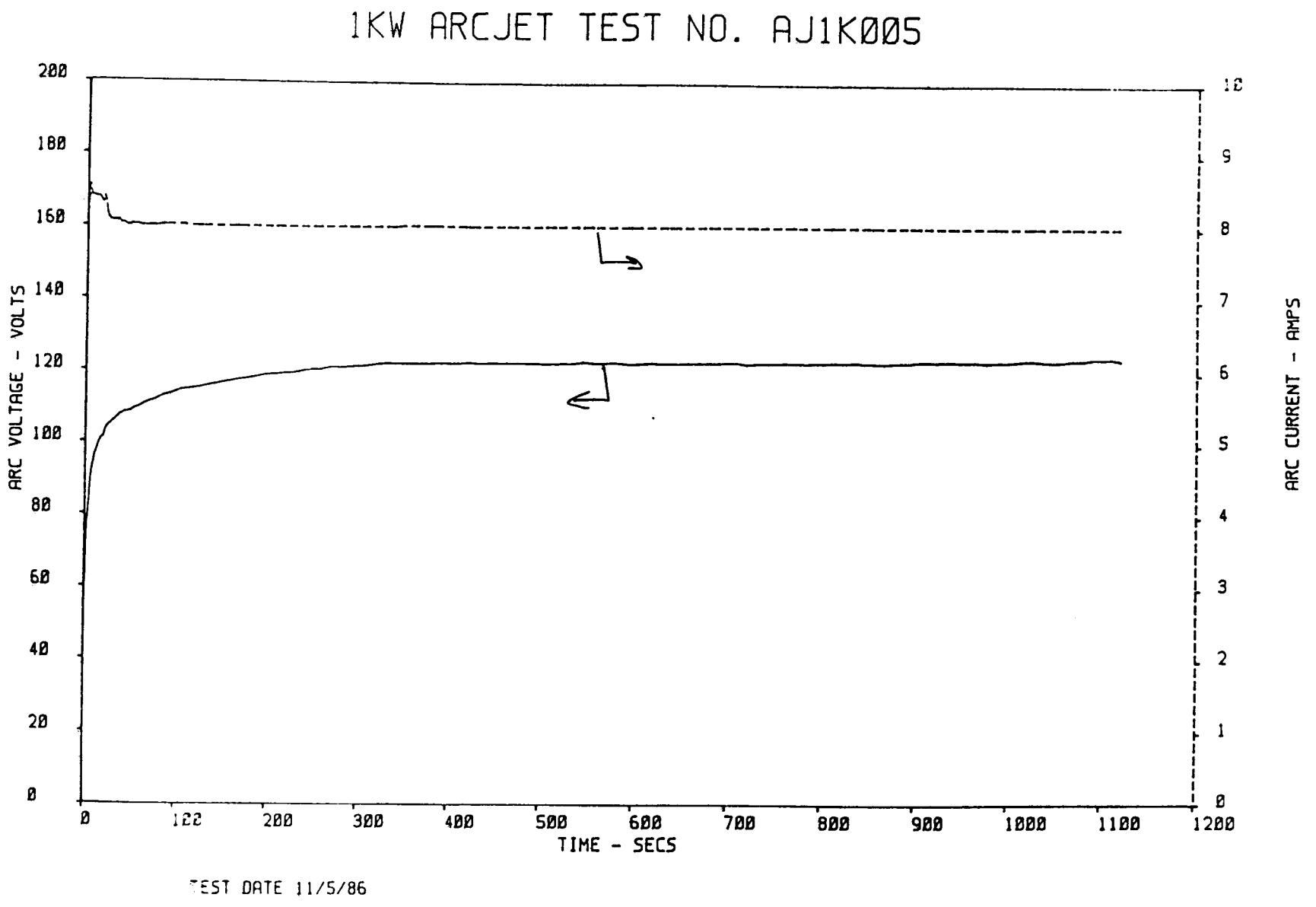

Figure 95. Voltage and Current for AJ1K005

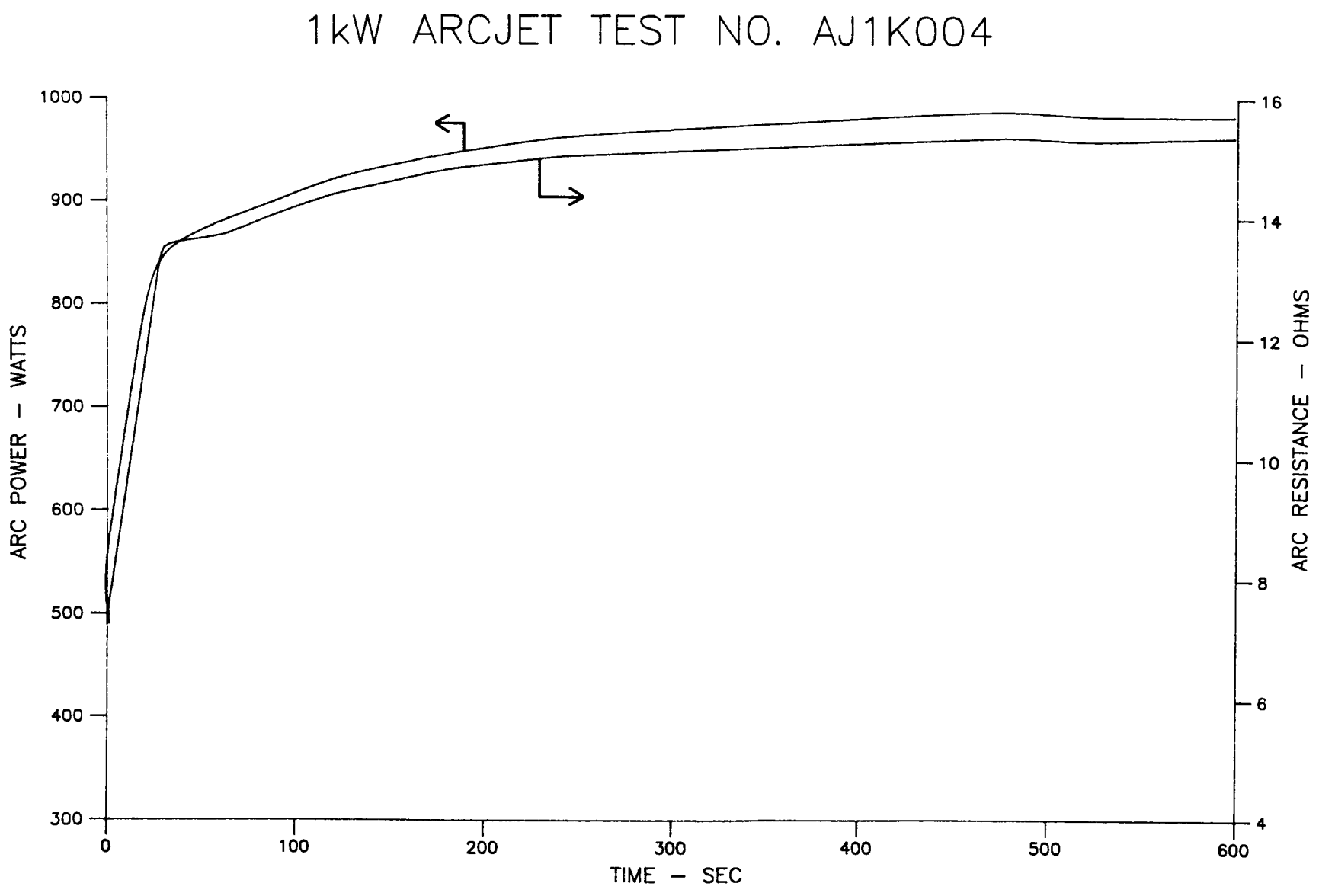

Figure 96. Power and Resistance for AJ1K004

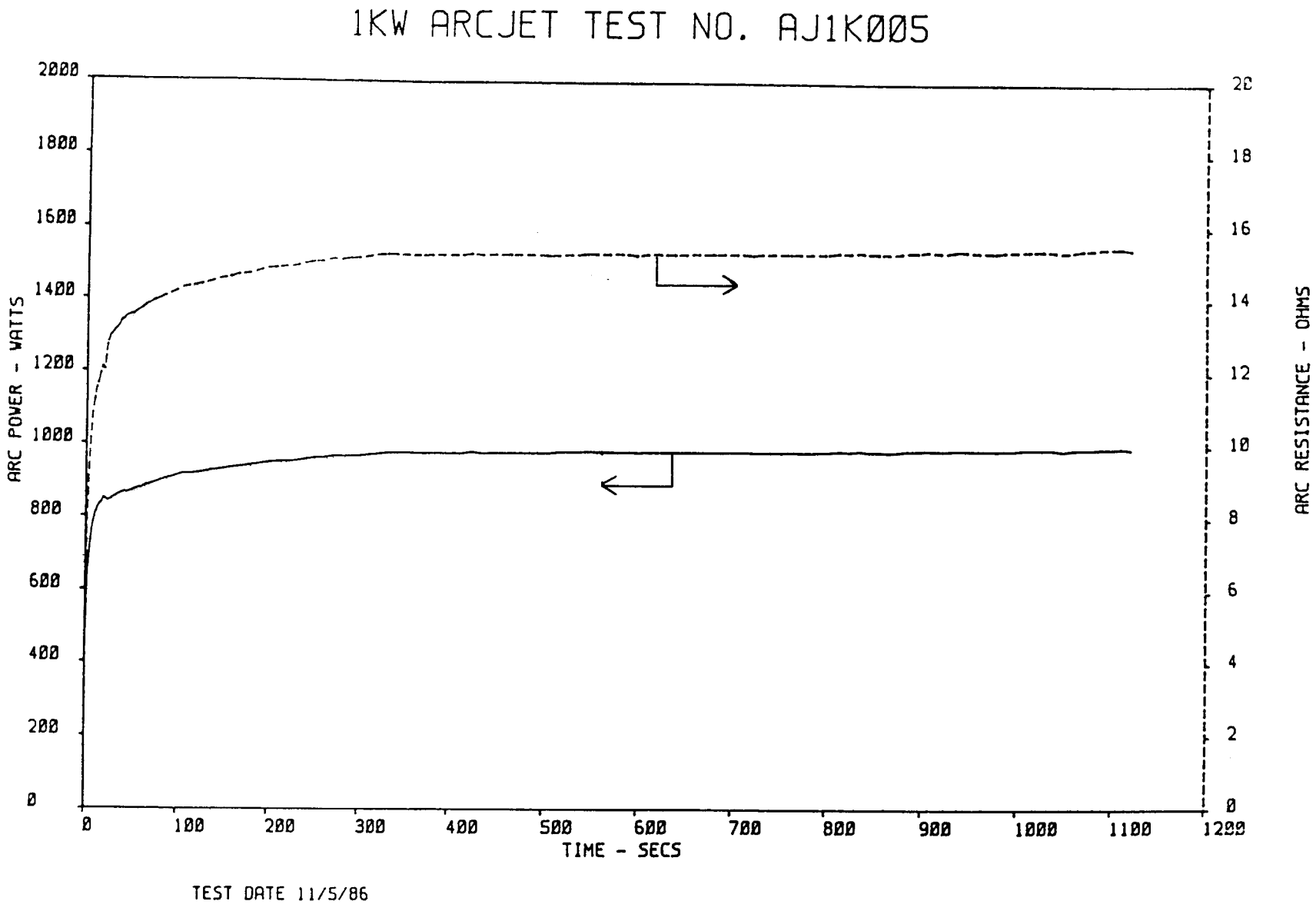

Figure 97. Arc Power and Resistance for 005

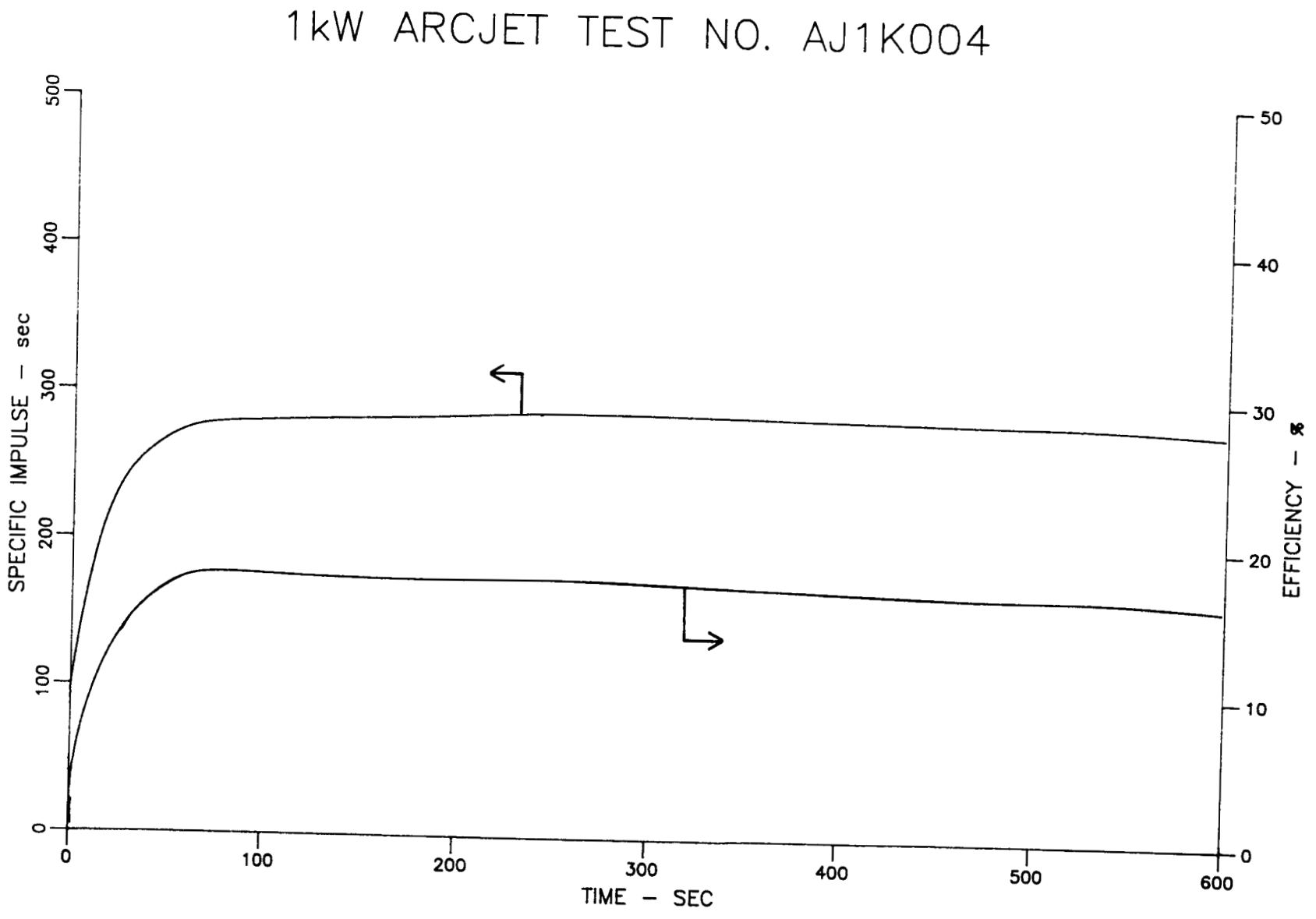

Figure 98. Performance Measurements for AJ1K004

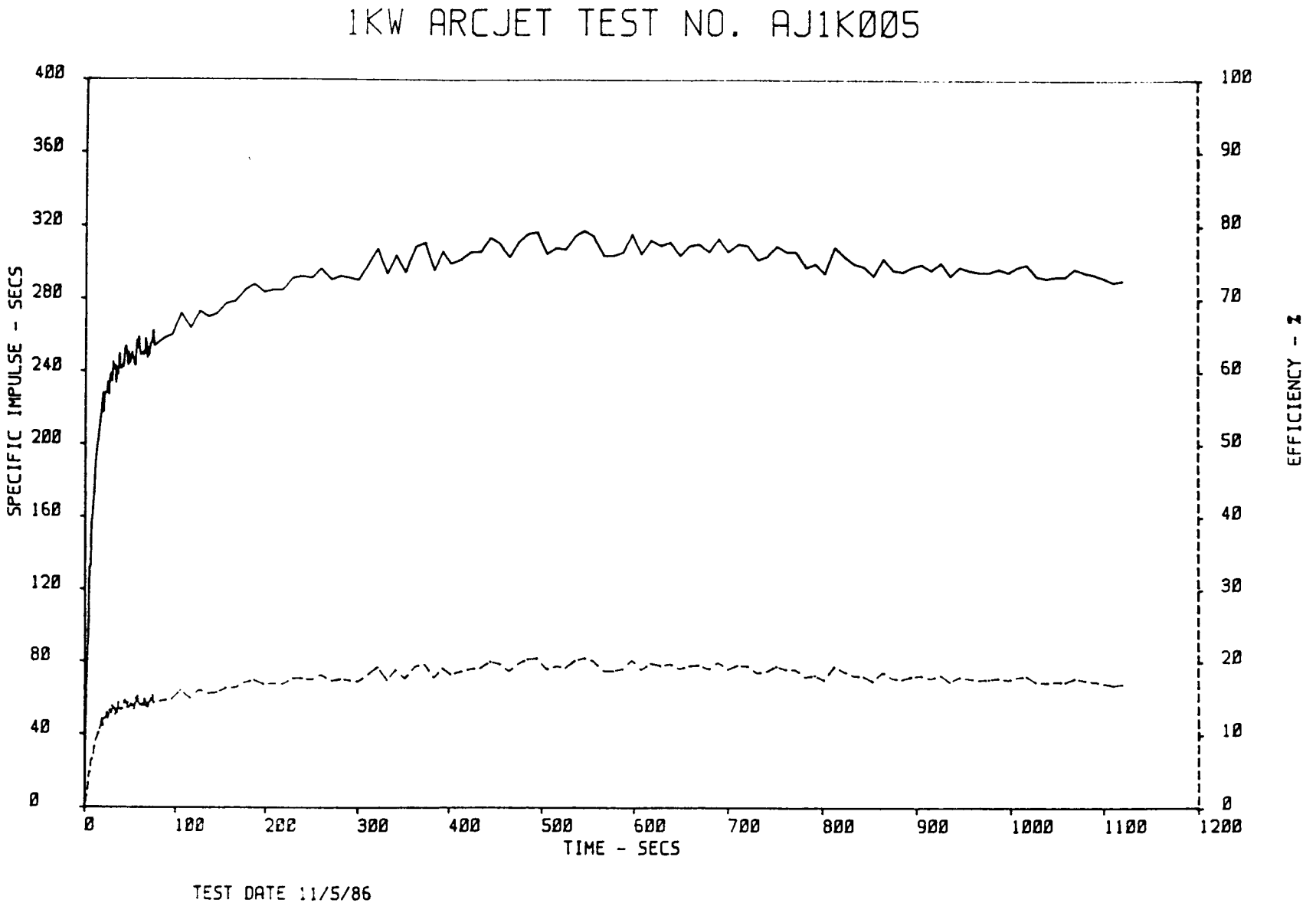

Figure 99. Performance Measurements for AJ1K005

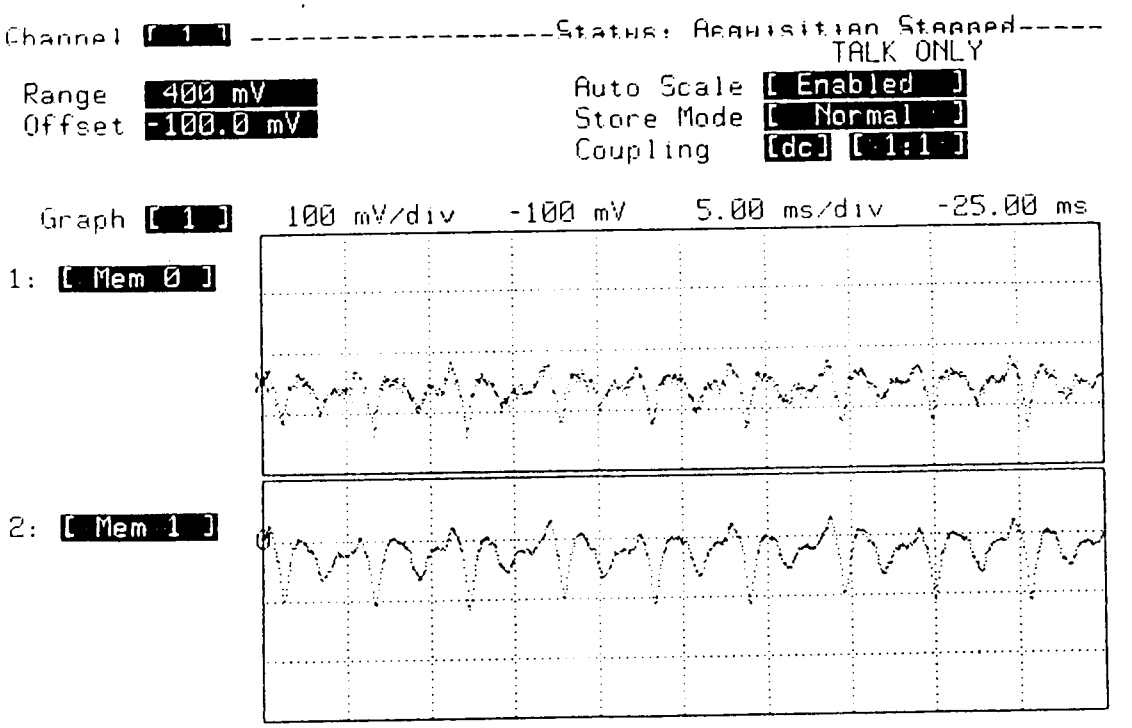

Figure 100. Arcjet Current Trace (Top) and Voltage Trace (Bottom) During AJ1K002

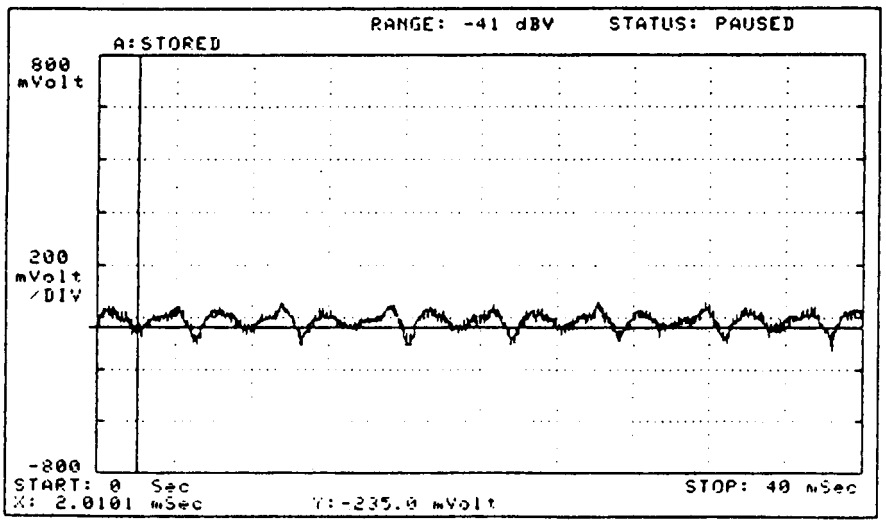

Figure 101. Spectrum Analysis for Arcjet Voltage

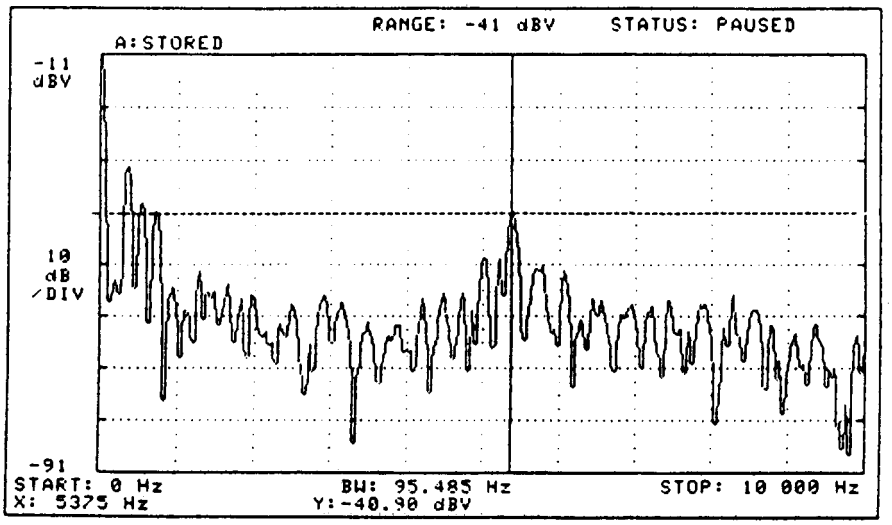

Figure 102. FFT of Voltage Signal

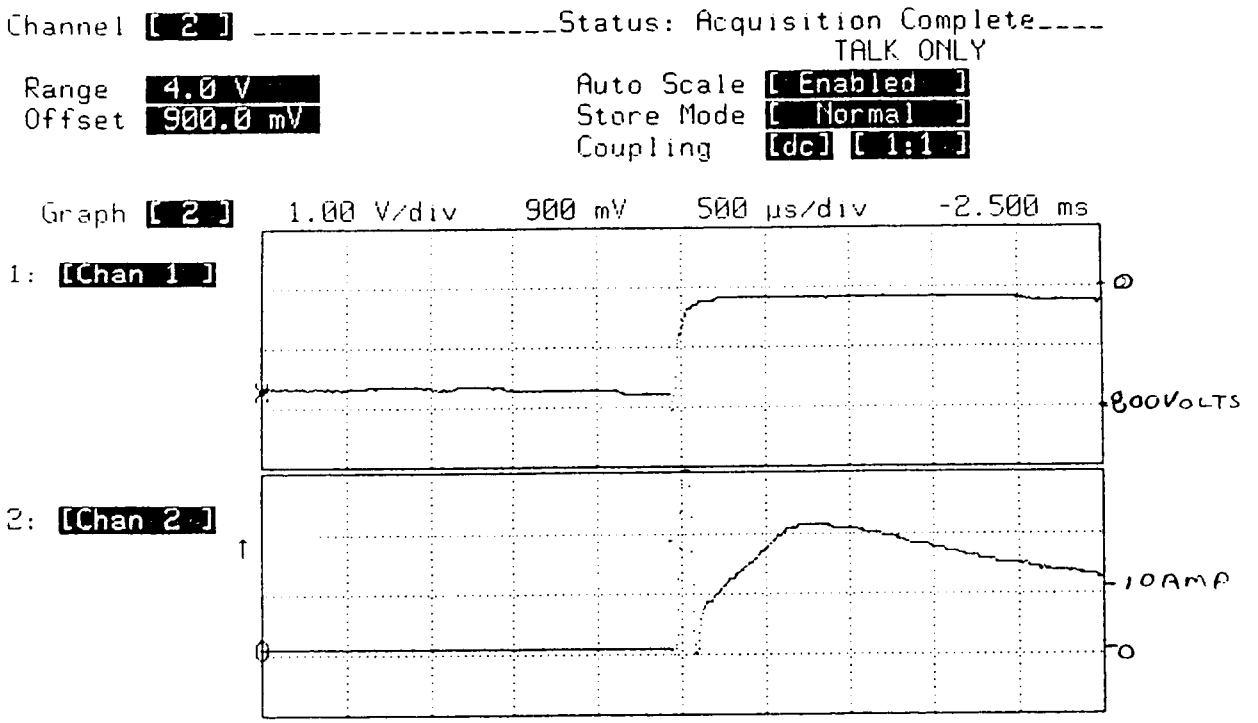

Figure 103. Typical Arcjet Start Transient

shows a typical start transient of the voltage and current measured during test 004. Differences in the arc voltage/current characteristics (both transient and steady-state) were used throughout the test program as means of detecting changes in the thruster's operation from test to test and as parameters during an individual test were varied.

Modification of Arc Power Circuit

A series of six tests were conducted with inductive "T" filters to investigate reducing or eliminating the ballast resistor in the arcjet power circuit. For flight applications a ballast resistor is not feasible and eventually all filtering and arc impedance compensation must be performed with minimal power dissipation. During tests 006 through 010, no data values are reported; the arc extinguished immediately after initiation. During these tests, the external ballast resistor was completely removed from the circuit. An electrical breakdown occurred at the beginning of test 011 from the cathode to the aft insulator. The external power circuit was returned to the pre-006 configuration prior to the test.

Baseline Performance of Thruster

The lower performance measured during tests 004 and 005 prompted a reevaluation of the data acquisition system and thrust stand operation. No problems were discovered, except for an incorrect constant used to calculate the propellant mass flow rate in the data reduction program. The correction of this constant represented an increase in the actual mass flow rate and reduced the specific impulse by approximately 10 percent. Figures 98 and 99 were calculated using the corrected values.

Tests 012 through 019 were conducted to document the performance of the thruster at design conditions. The arc was extinguished during the start of tests 012 and 014 by computer control due to an interlock limit incorrectly programmed into the control logic. During tests 013 and 015 the arc extinguished early in the test while the current was being reduced at the power supply.

3.6, Test Series 2 Testing (cont.)

Tests 016 through 019 were operated at design flow rate over a range of power levels. Tests 016 and 017 were at high power and the arc operated in a high voltage mode. During tests 018 and 019 the arcjet operated in a low power, low voltage mode. The current in tests 016 and 017 was 7.9 and 7.8 amps respectively, while the current in tests 018 and 019 was 8.2 amps. At present there is no explanation for the low arc impedance of tests 018 and 019.

Plots of the digital data from tests 016 through 019 are shown in Figures 104 through 119. Figures 104, 105, 106, and 107 show the arc voltage and current during the tests. During the start procedure, a 700 volt potential is set between the anode and cathode. The voltage spike on 017, 018, and 019 is the drop of the start voltage to operating conditions. The power and arc resistance calculated for the voltage and current measurements are shown in Figures 108, 109, 110, and 111. The arcjet body temperature and chamber inlet pressure are shown in Figures 112, 113, 114, and 115. The performance measured during these tests is shown on Figures 116, 117, 118 and 119.

Parametric Testing

The purpose of tests 020 through 026 was to obtain parametric data on the thruster performance and operating conditions with the intent of identifying an operating regime of improved performance. A voltage breakdown on the aft insulator of the apparatus occurred during test 020. The ceramic tube surrounding the cathode required replacement and the design was improved by cementing the tube into the aft insulator. During tests 021 and 022 the arc extinguished after 135 sec. and 45 sec. respectively. The cause of the arc going out has been attributed to overshoot of the Matheson thermal flow controller. Test AJ1K023 lasted 80 minutes with the mass flow rate increased in increments during the test. Figures 120, 121, 122, and 123 show the voltage, current, specific impulse, thrust efficiency, injection pressure, thruster body temperature, input power, and arc resistance during the test.

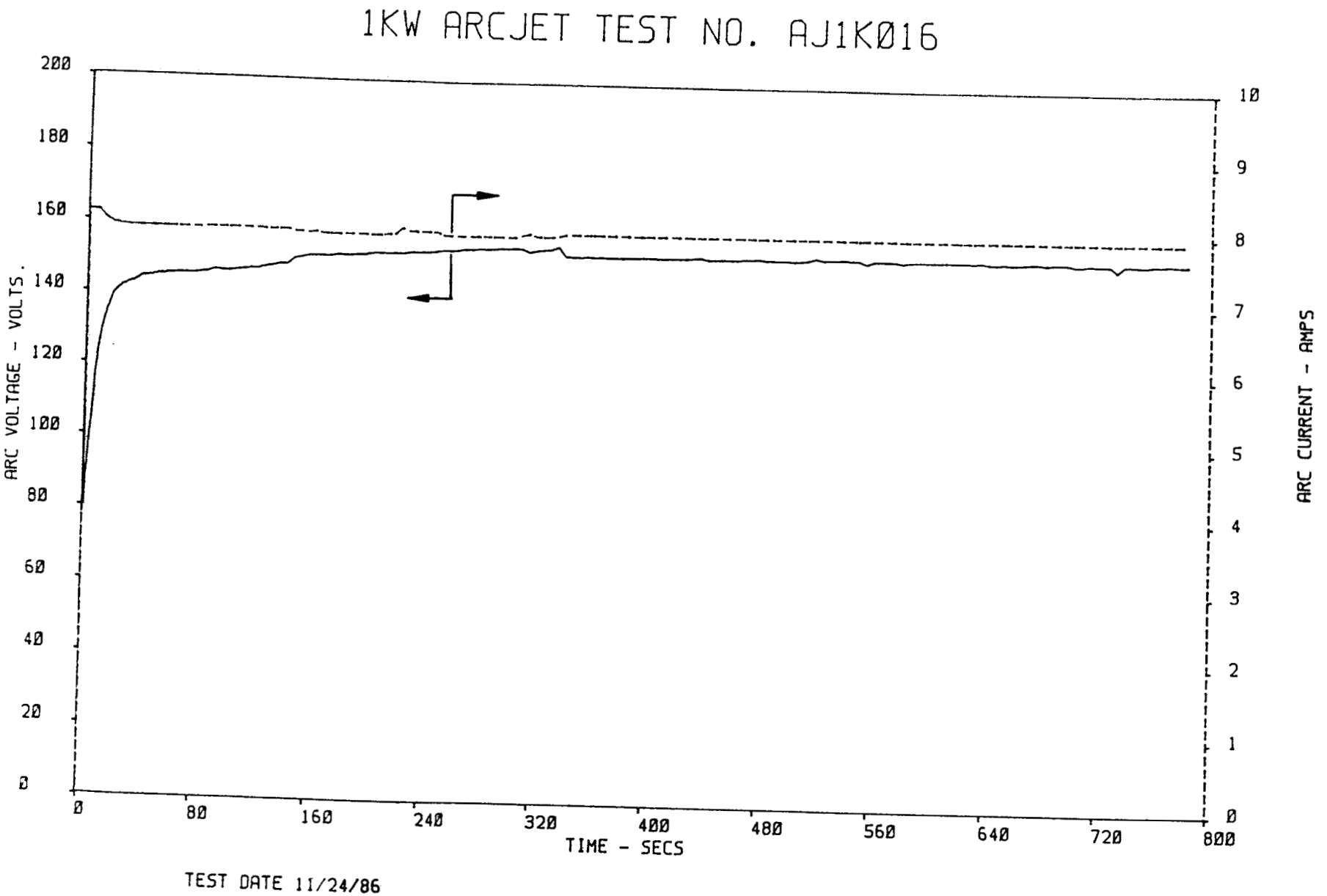

Figure 104. Voltage and Current for AJ1K016

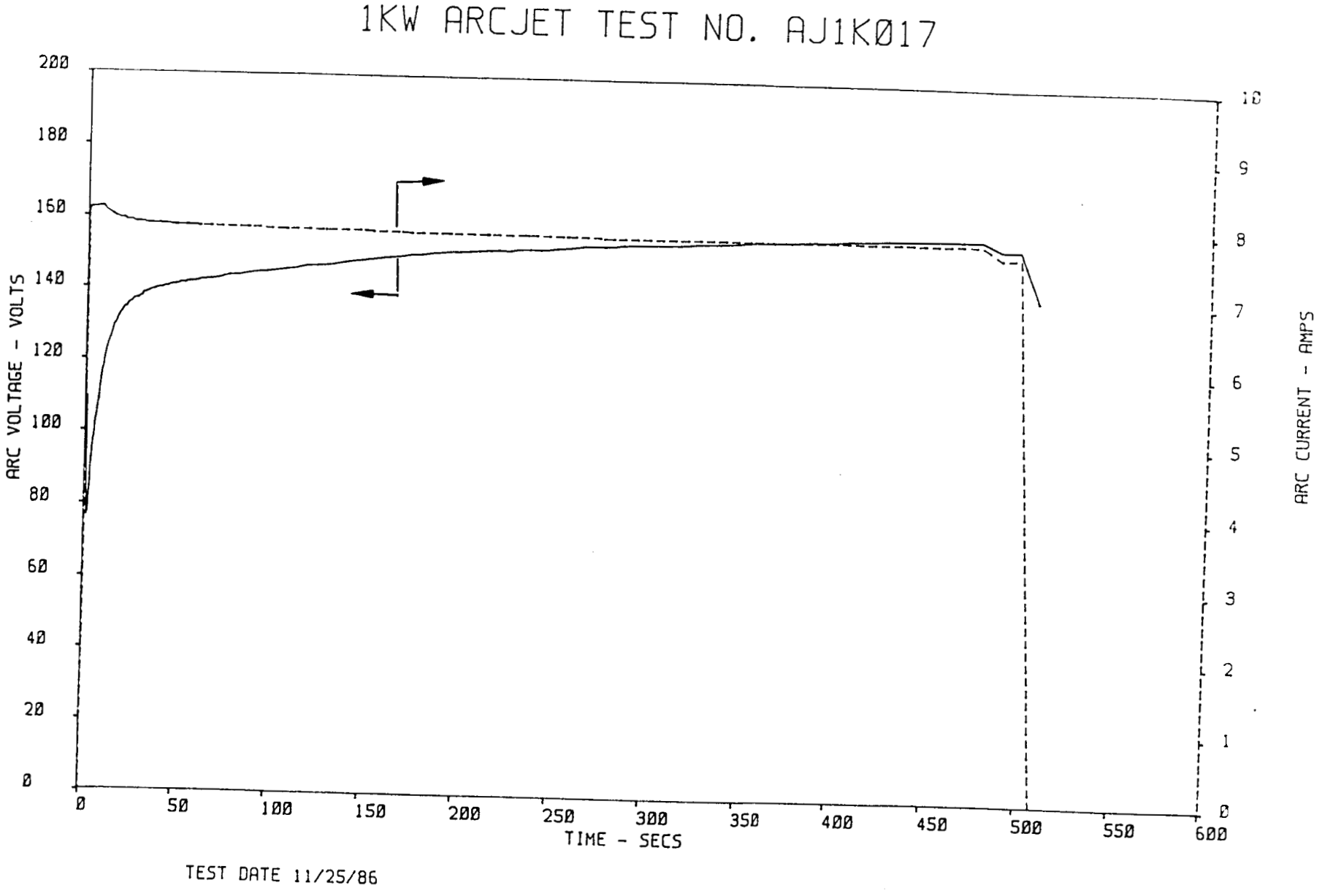

Figure 105. Voltage and Current for AJ1K017

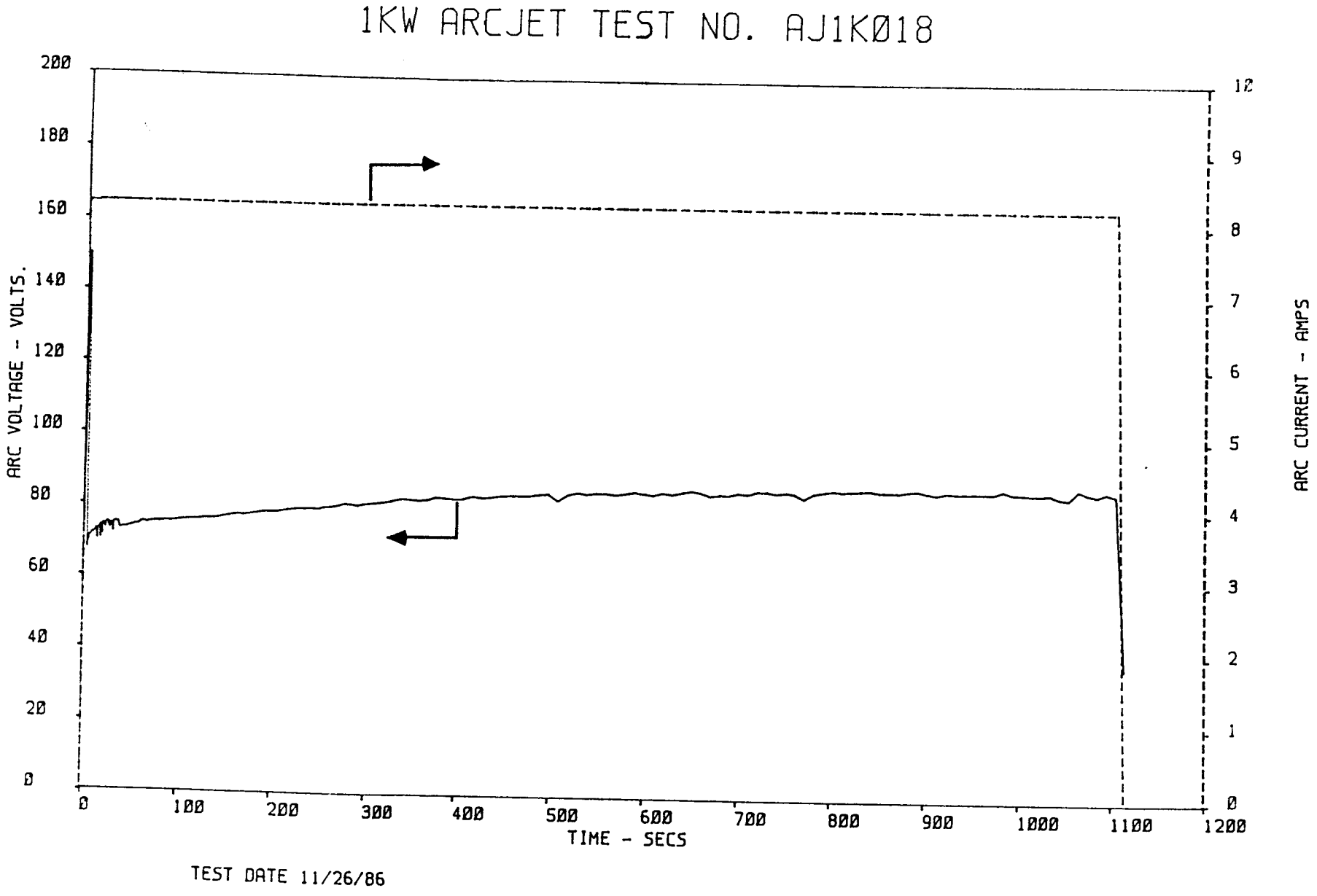

Figure 106. Voltage and Current for AJ1K018

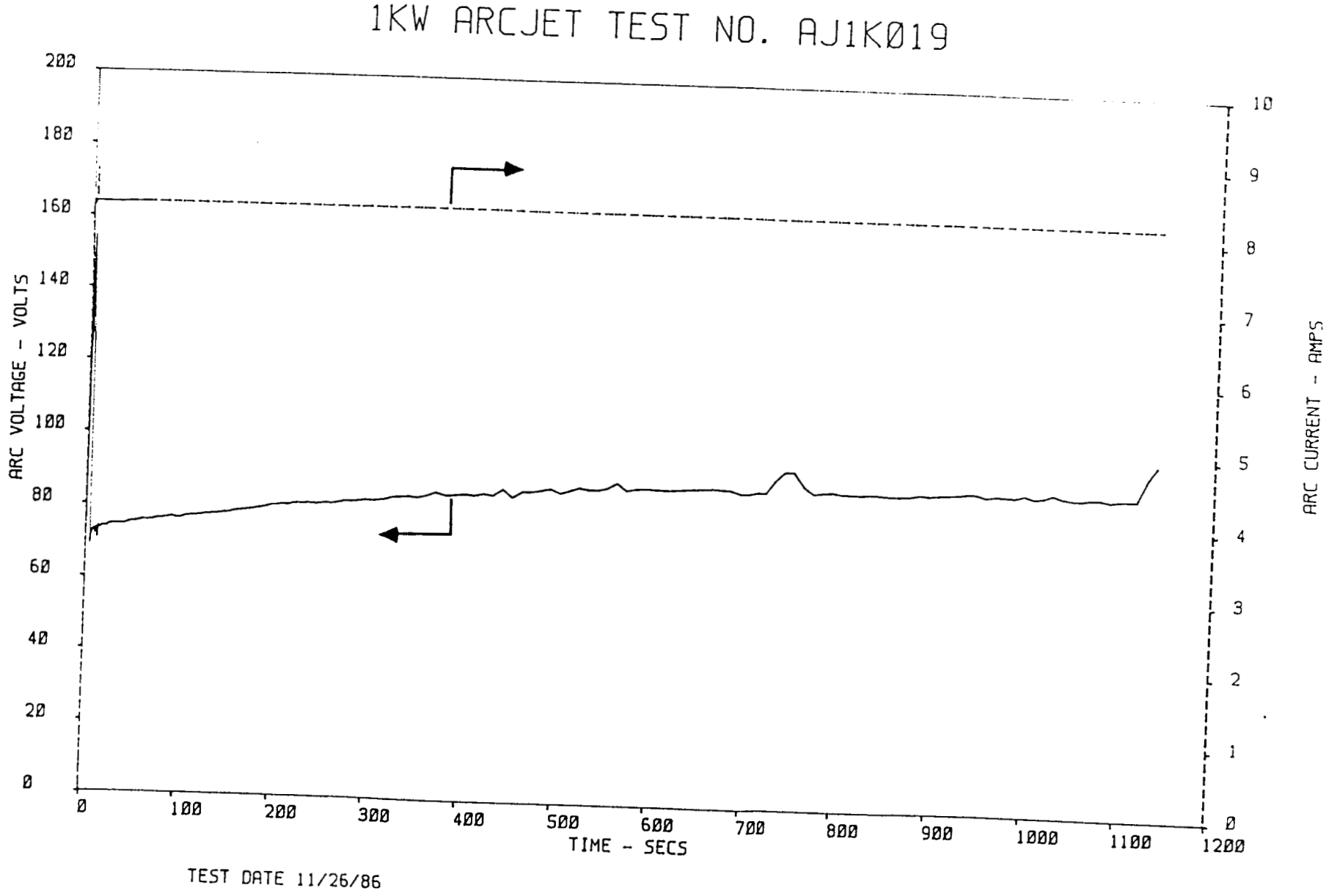

Figure 107. Voltage and Current for AJ1K019

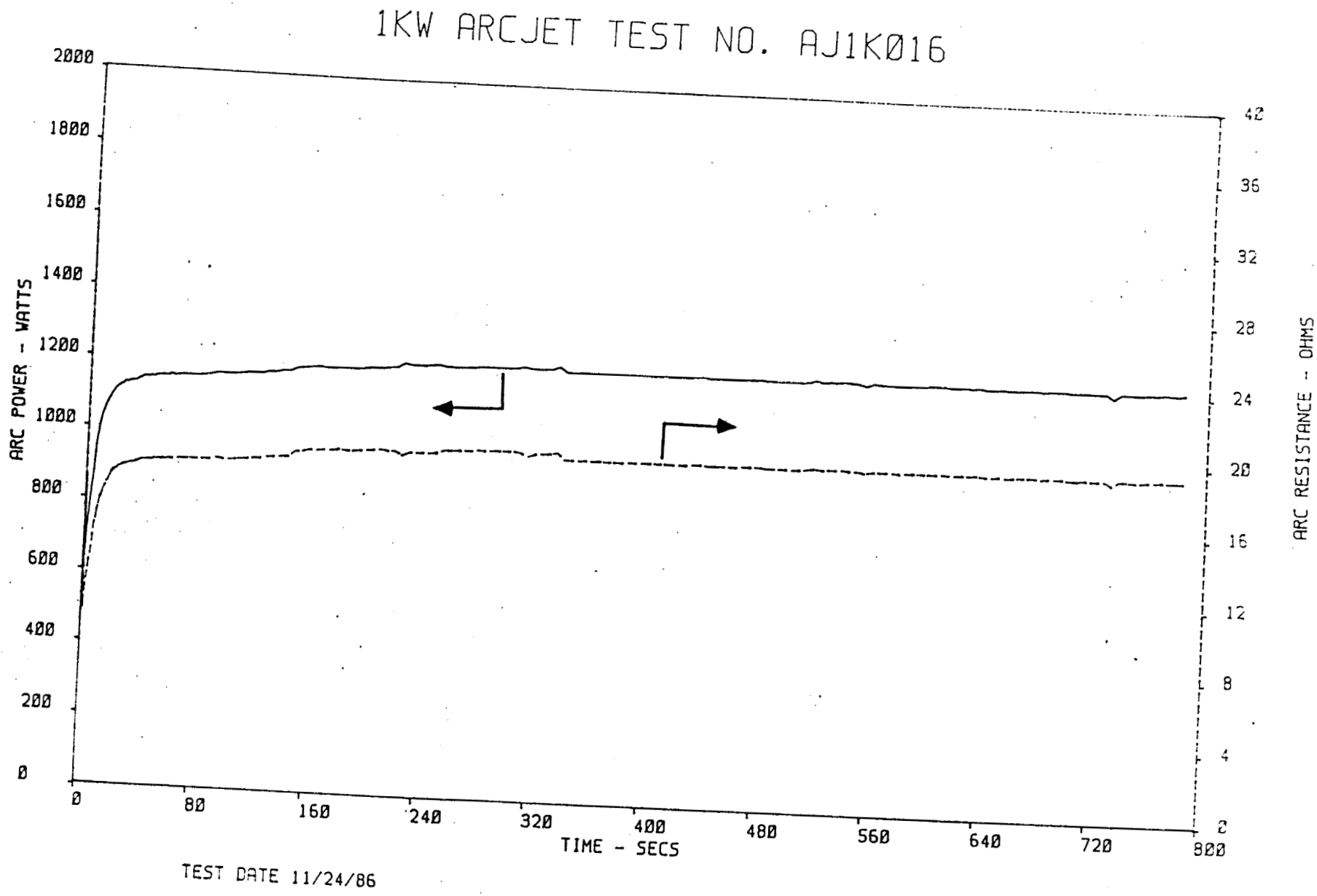

Figure 108. Power and Resistance for AJ1K016

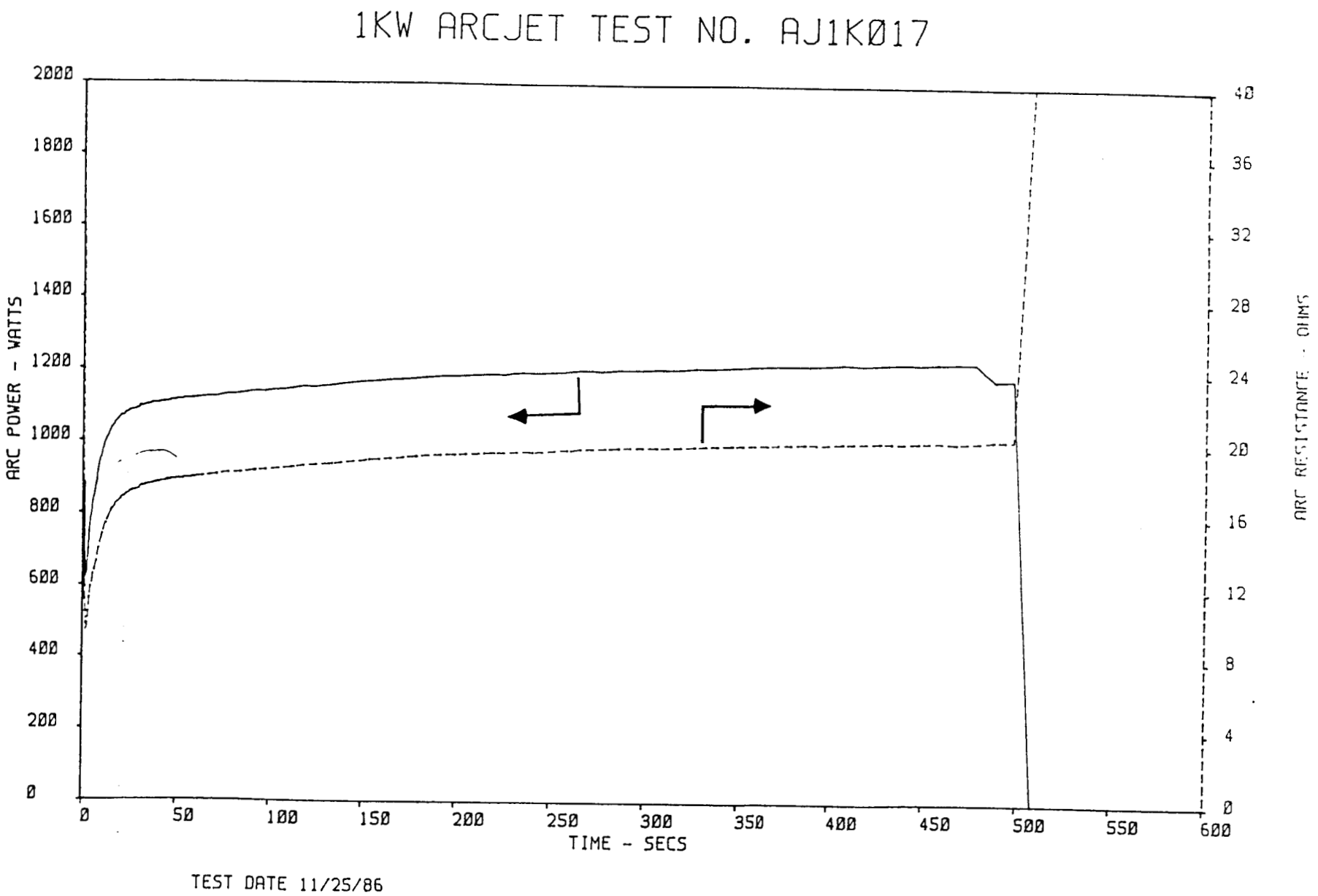

Figure 109. Power and Resistance for AJ1K017

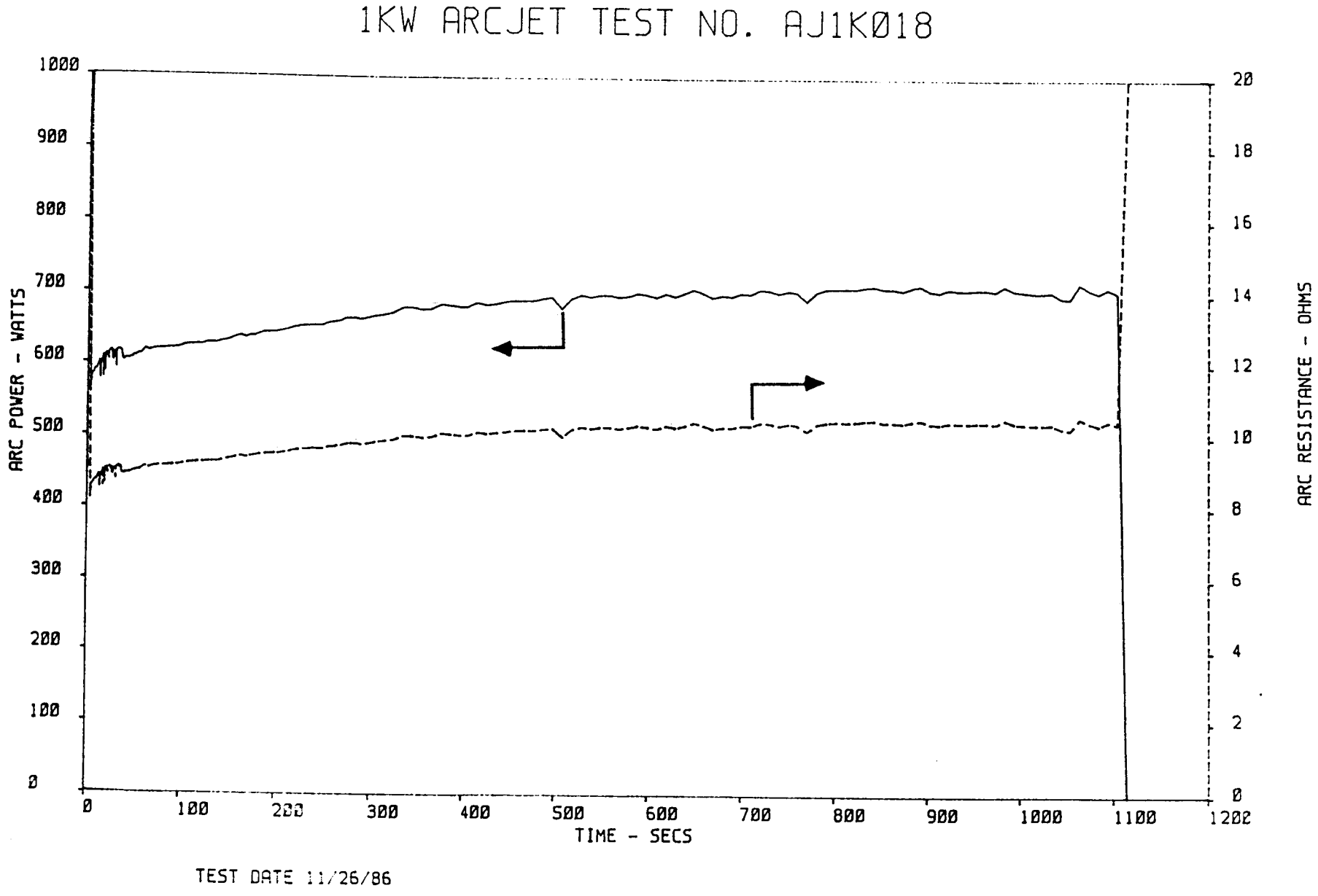

Figure 110. Power and Resistance for AJ1K018

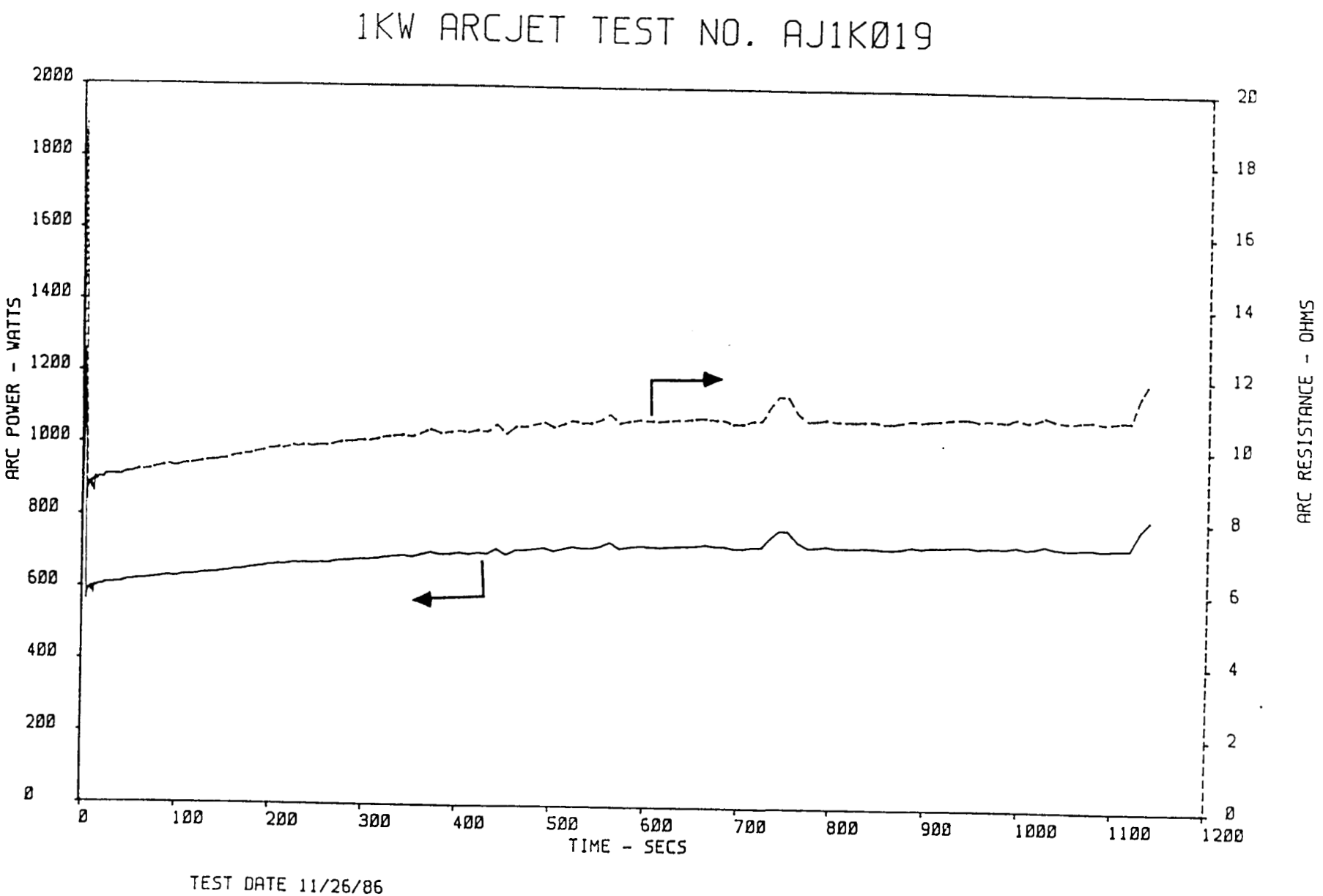

Figure 111. Power and Resistance for AJ1K019

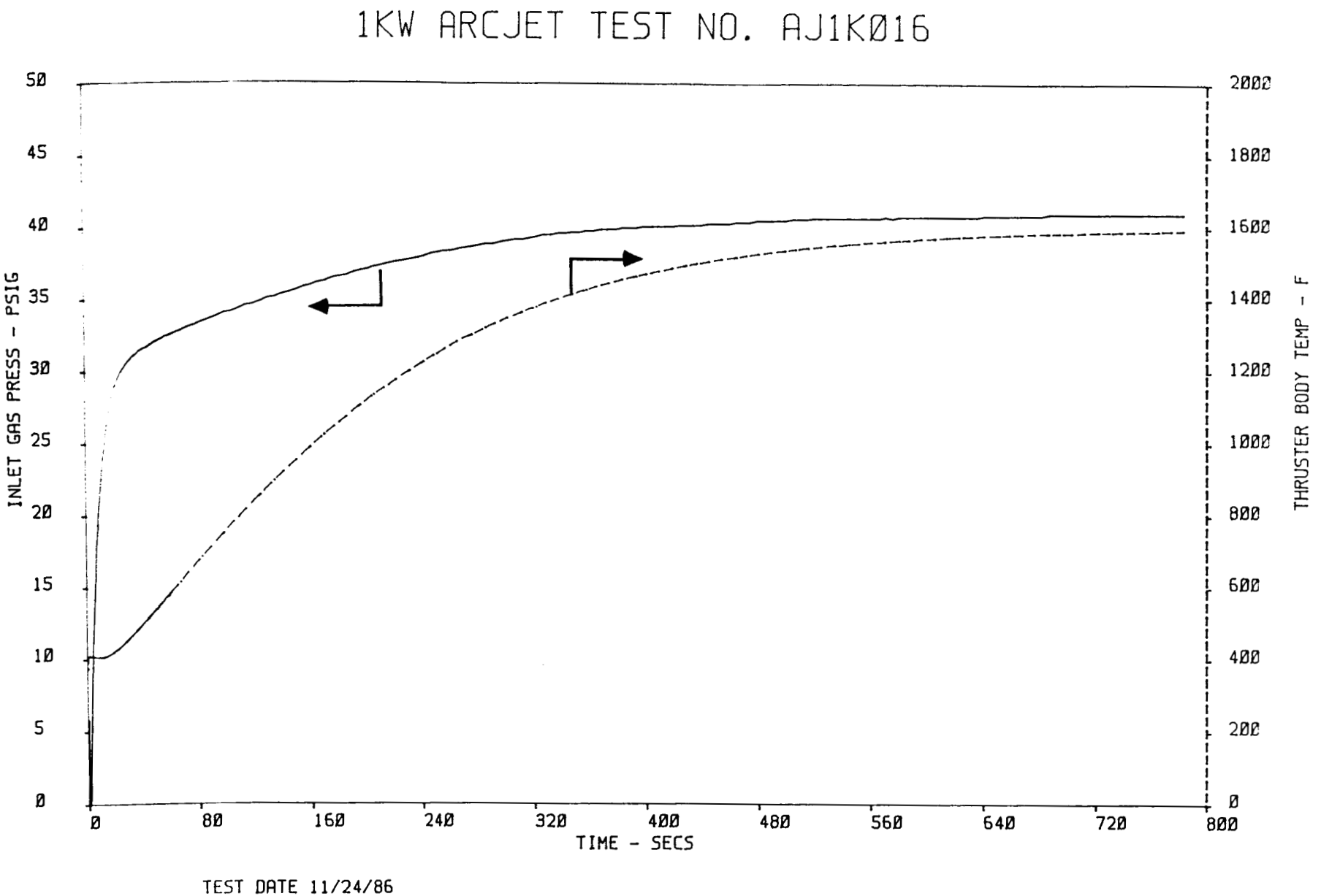

Figure 112. Inlet Pressure and body Temperature for AJ1K016

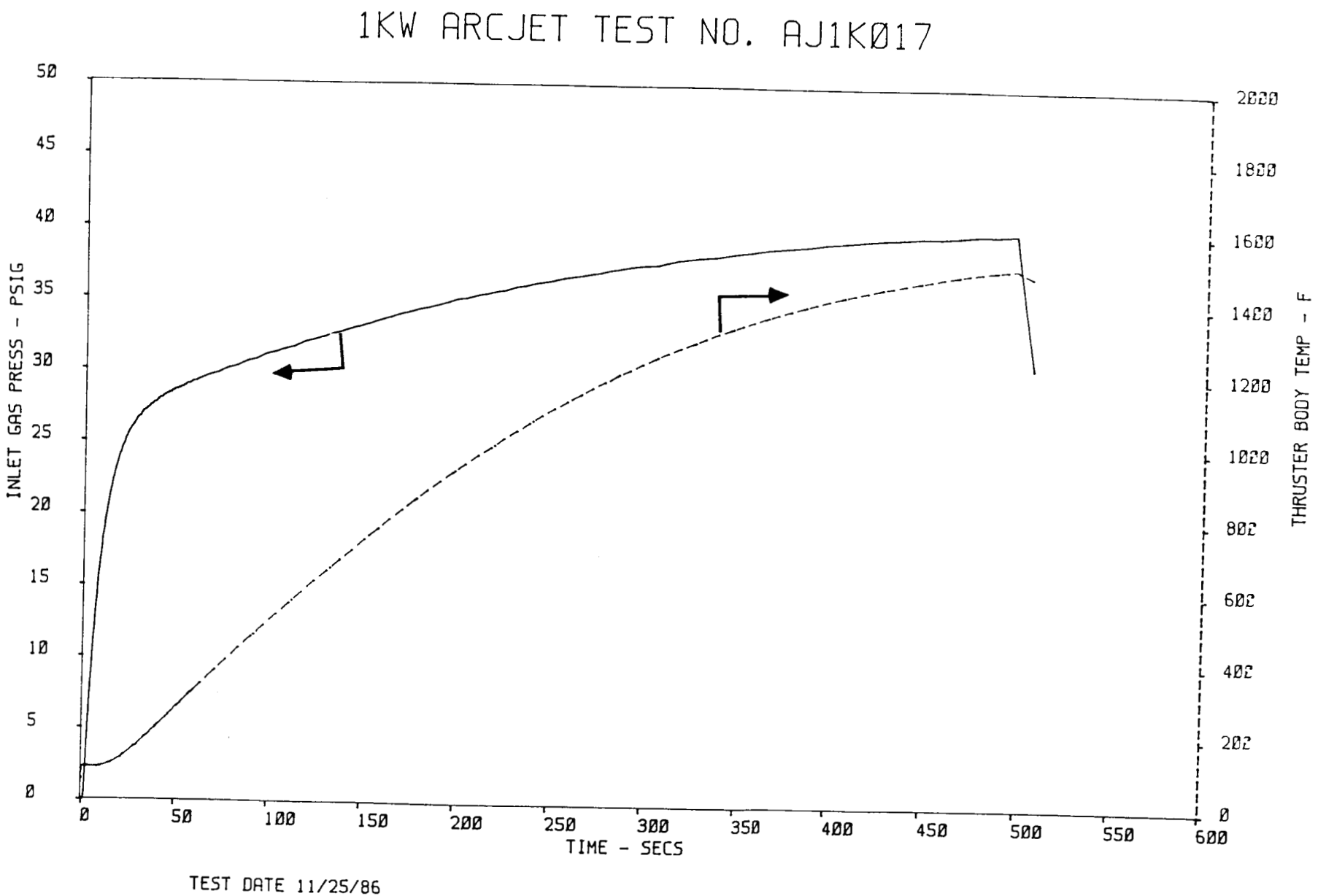

Figure 113. Inlet Pressure and Body Temperature for AJ1K017

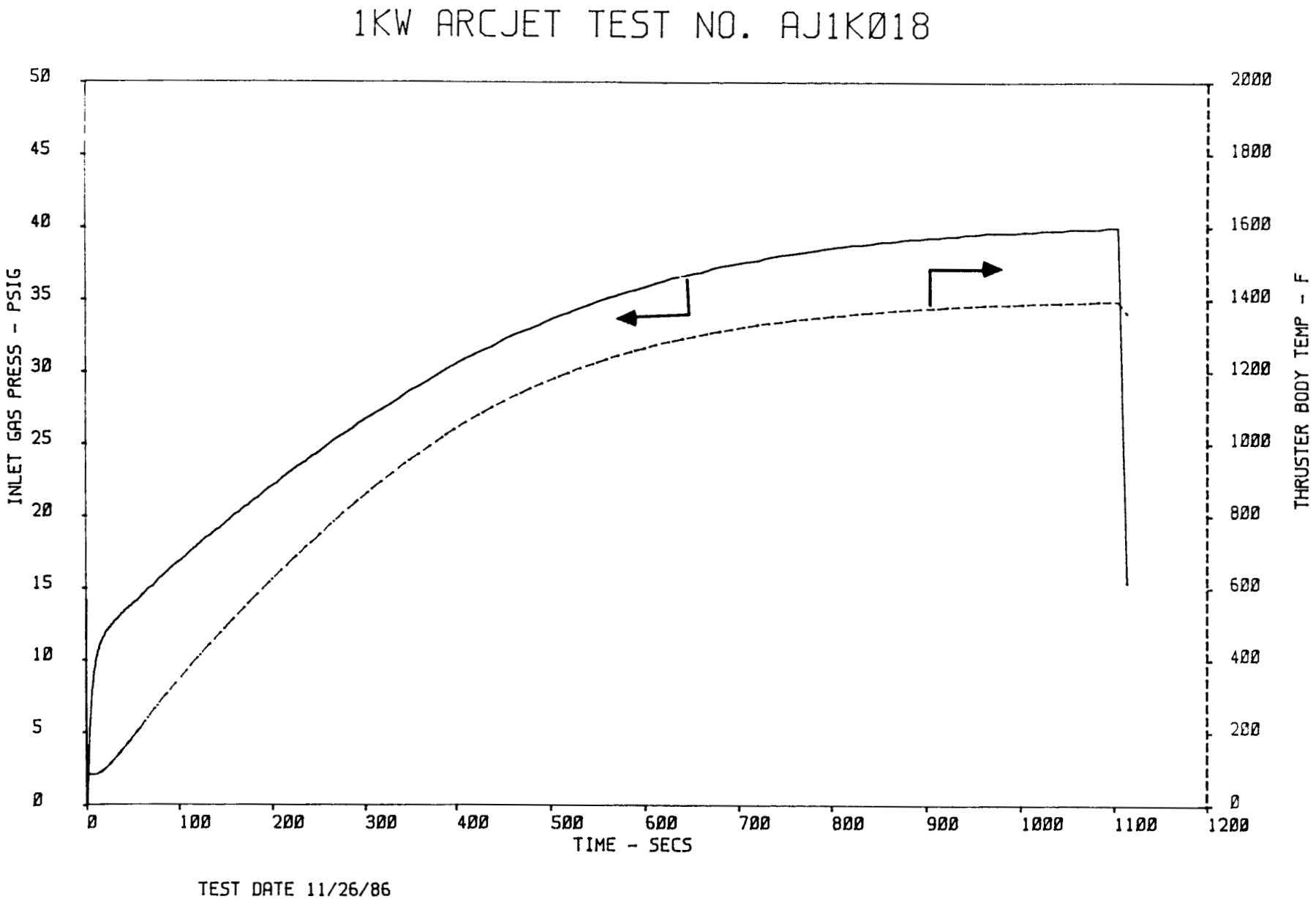

Figure 114. Inlet Pressure and Body Temperature for AJ1K018

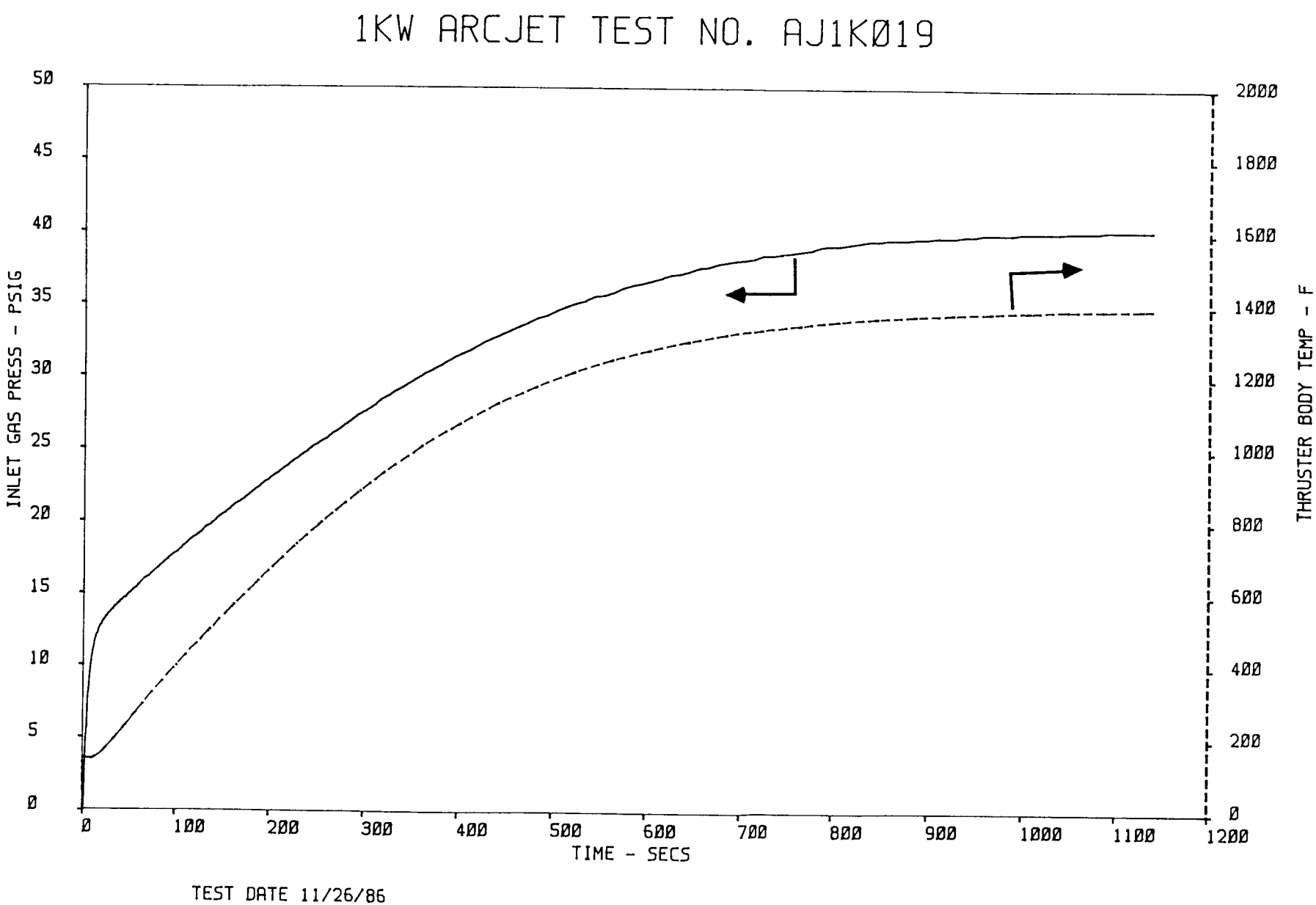

Figure 115. Inlet Pressure and Body Temperature For AJ1K019

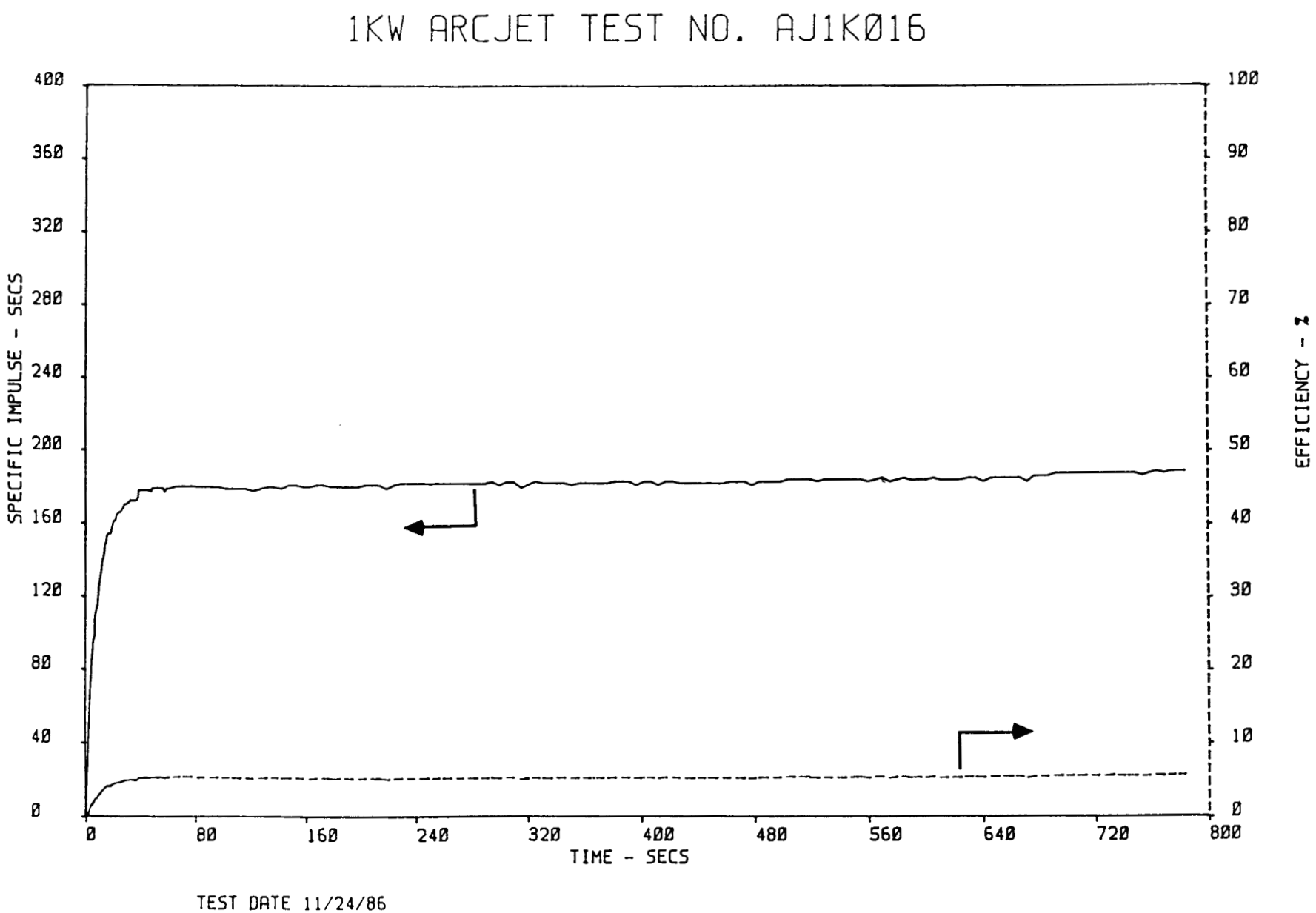

Figure 116. Performance Measurement for 016

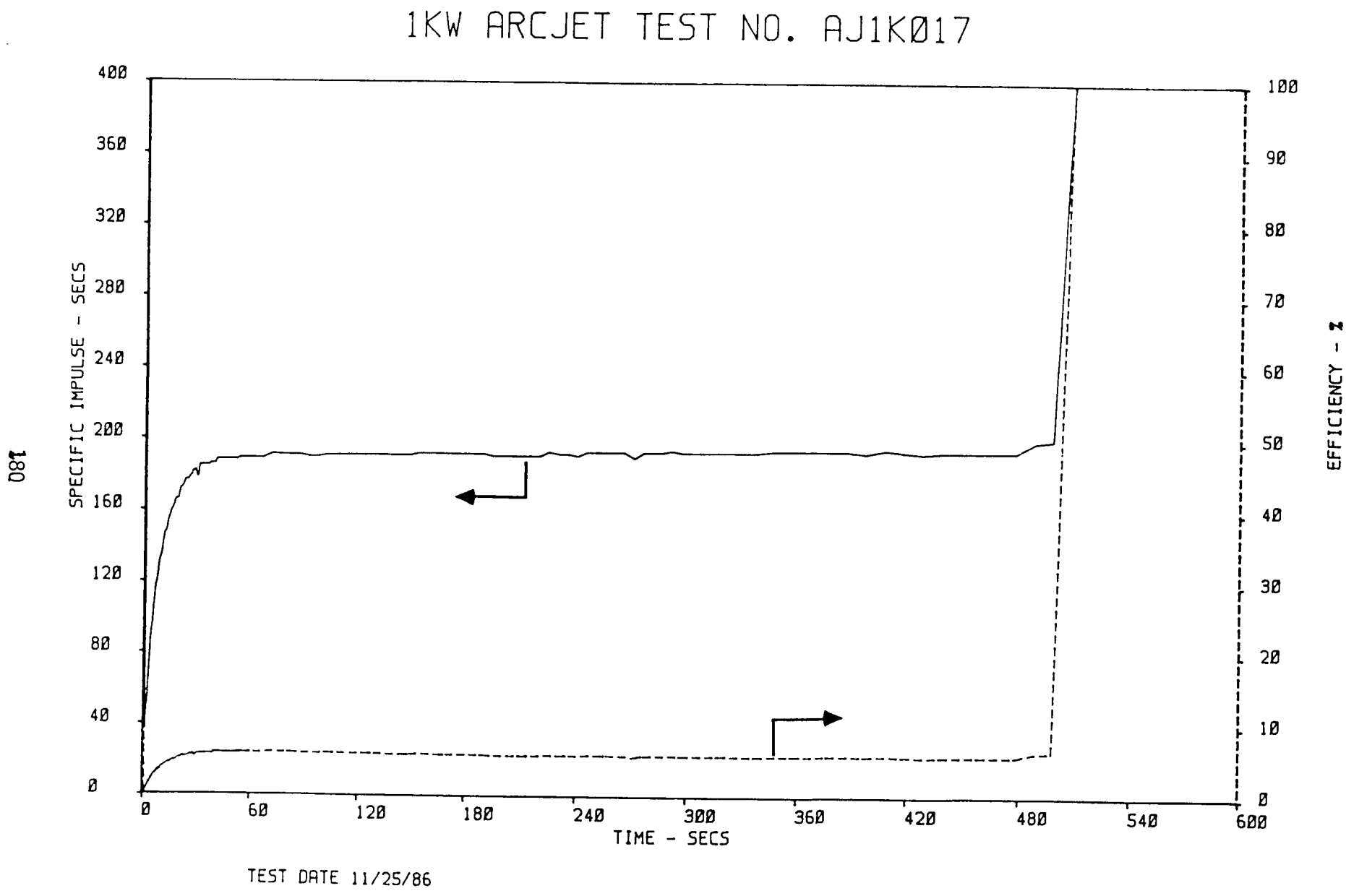

Figure 117. Performance Measurement for 017

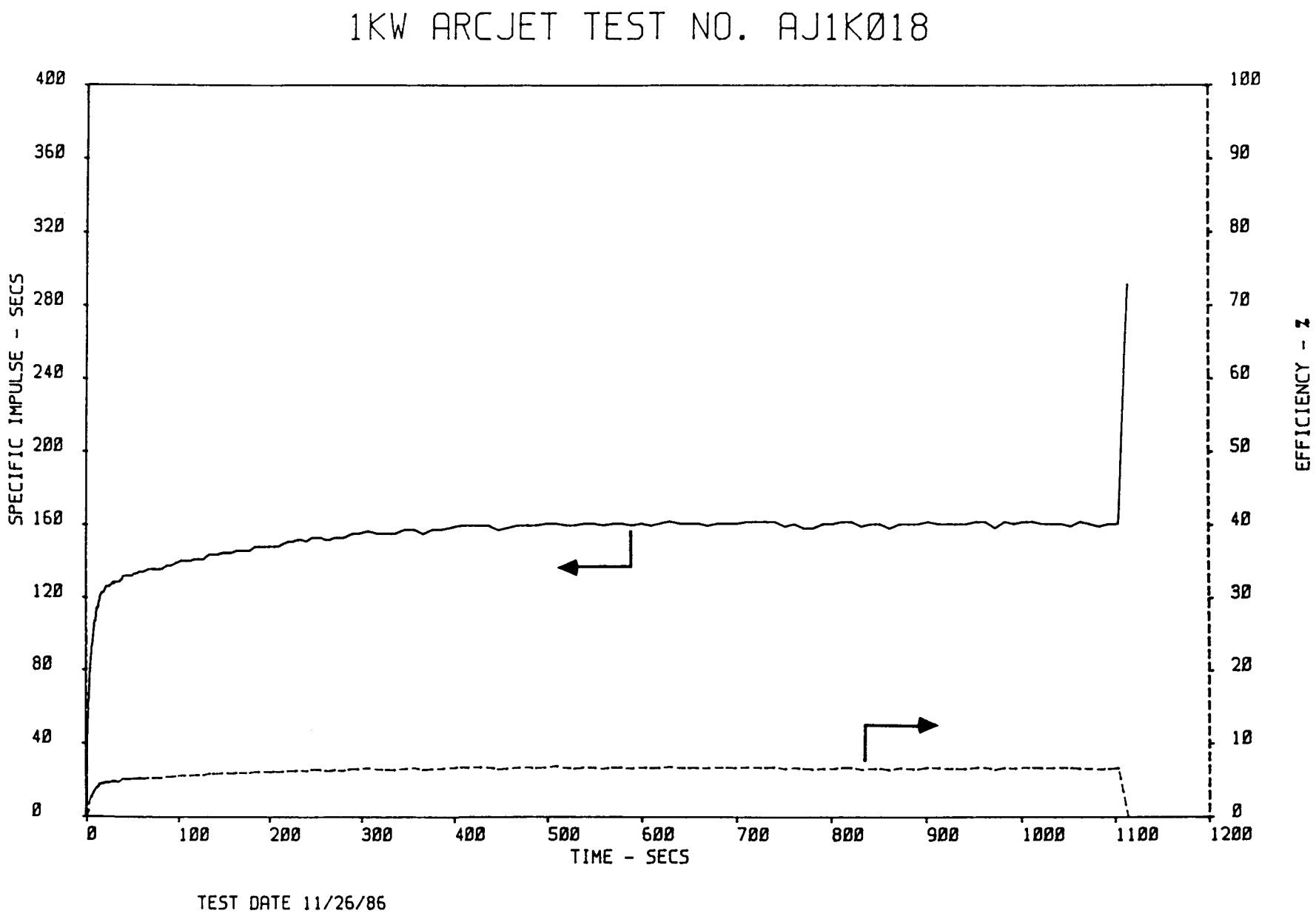

Figure 118. Performance Measurement for 018

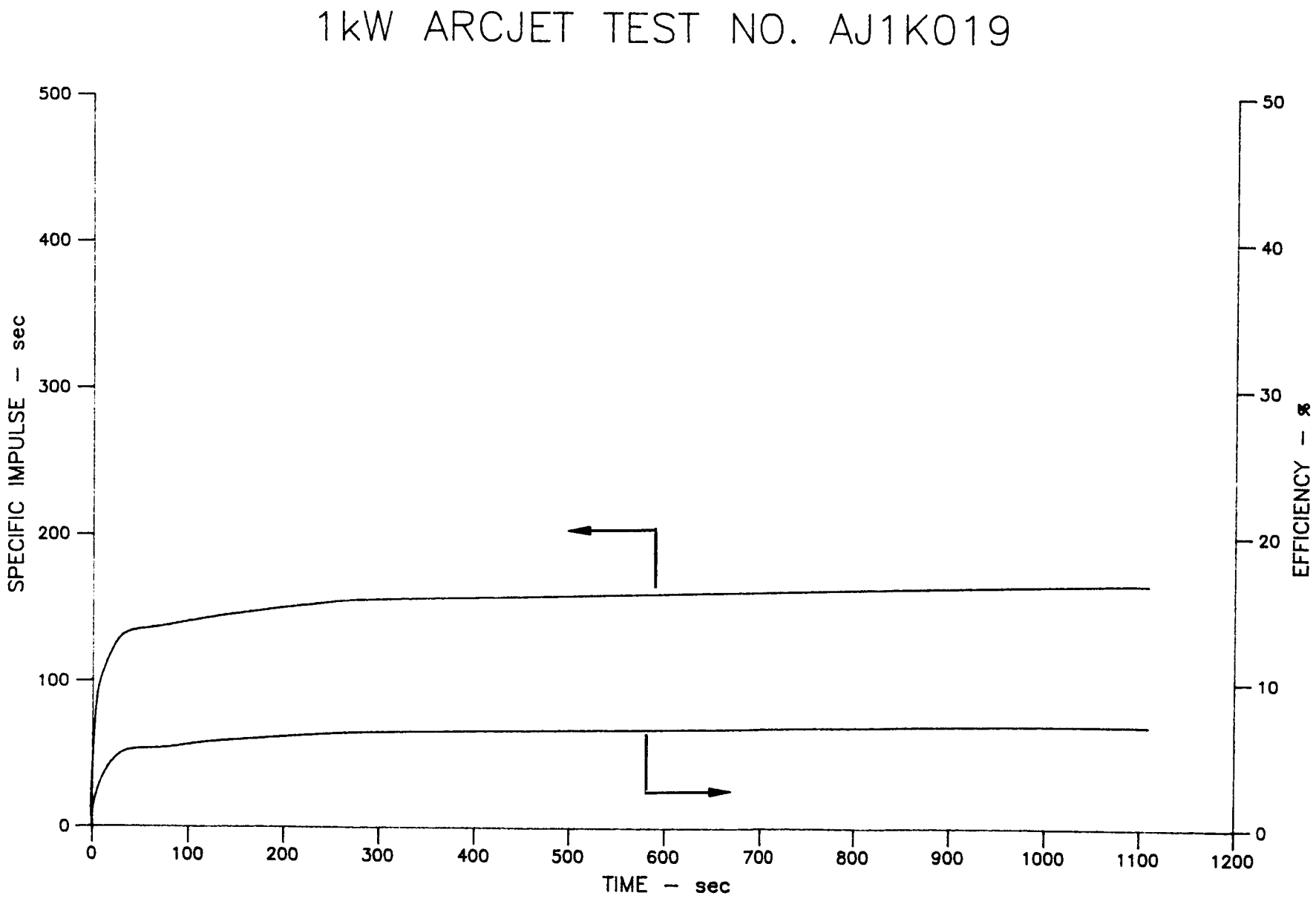

Figure 119. Performance Measurement for 019

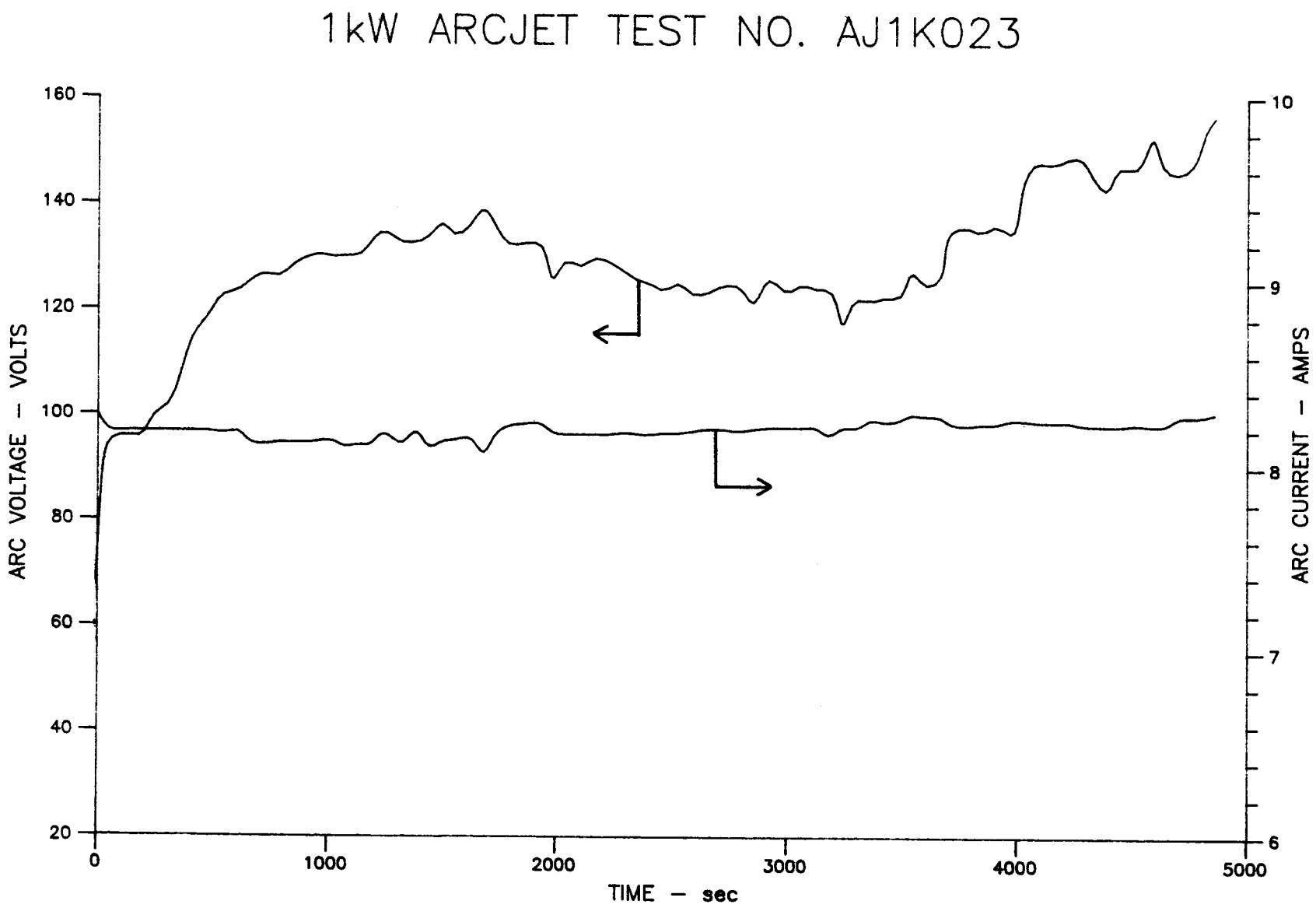

Figure 120. Voltage and Current for AJ1K023

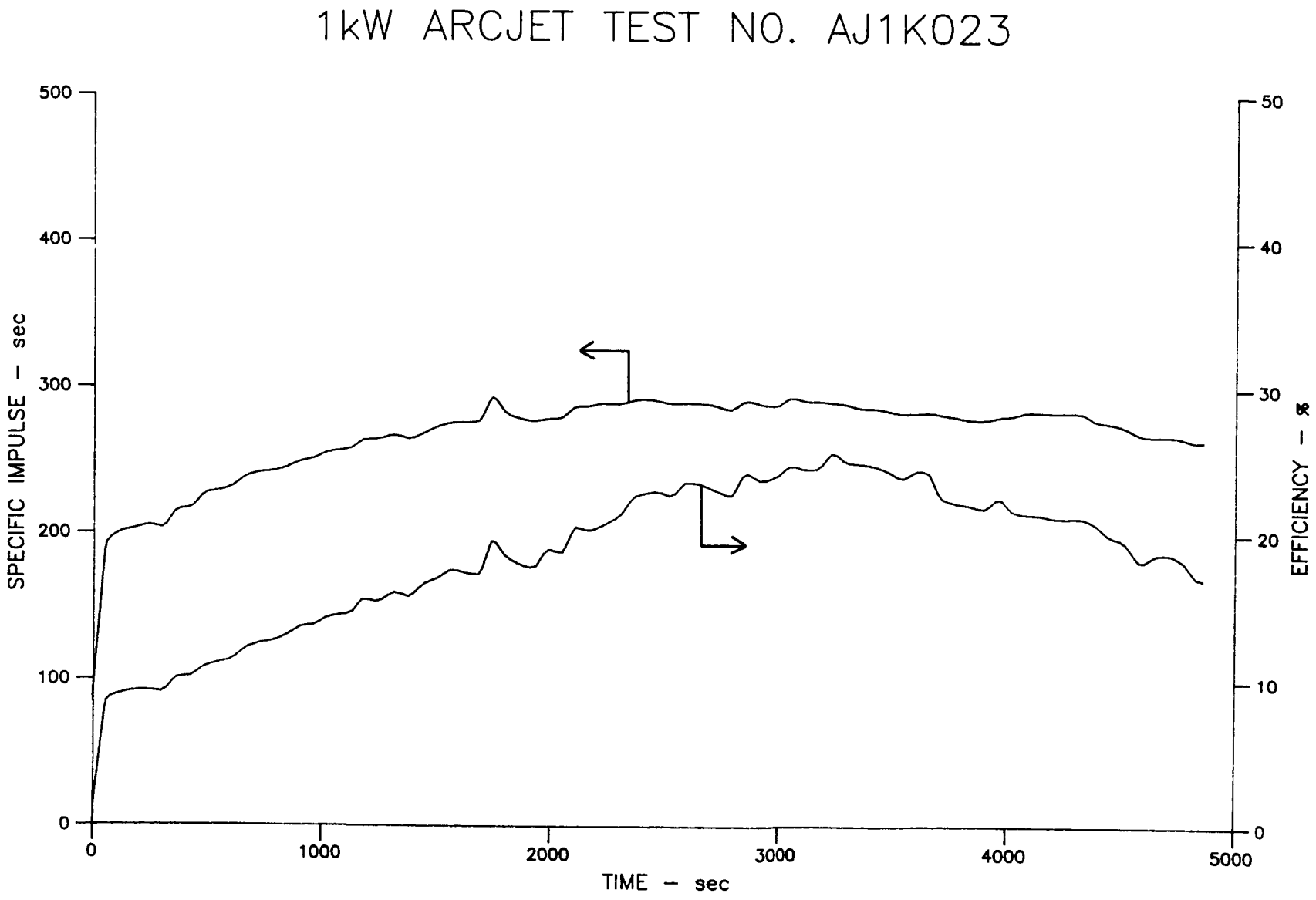

Figure 121. Specific Impulse and Thrust Efficiency for AJ1K023

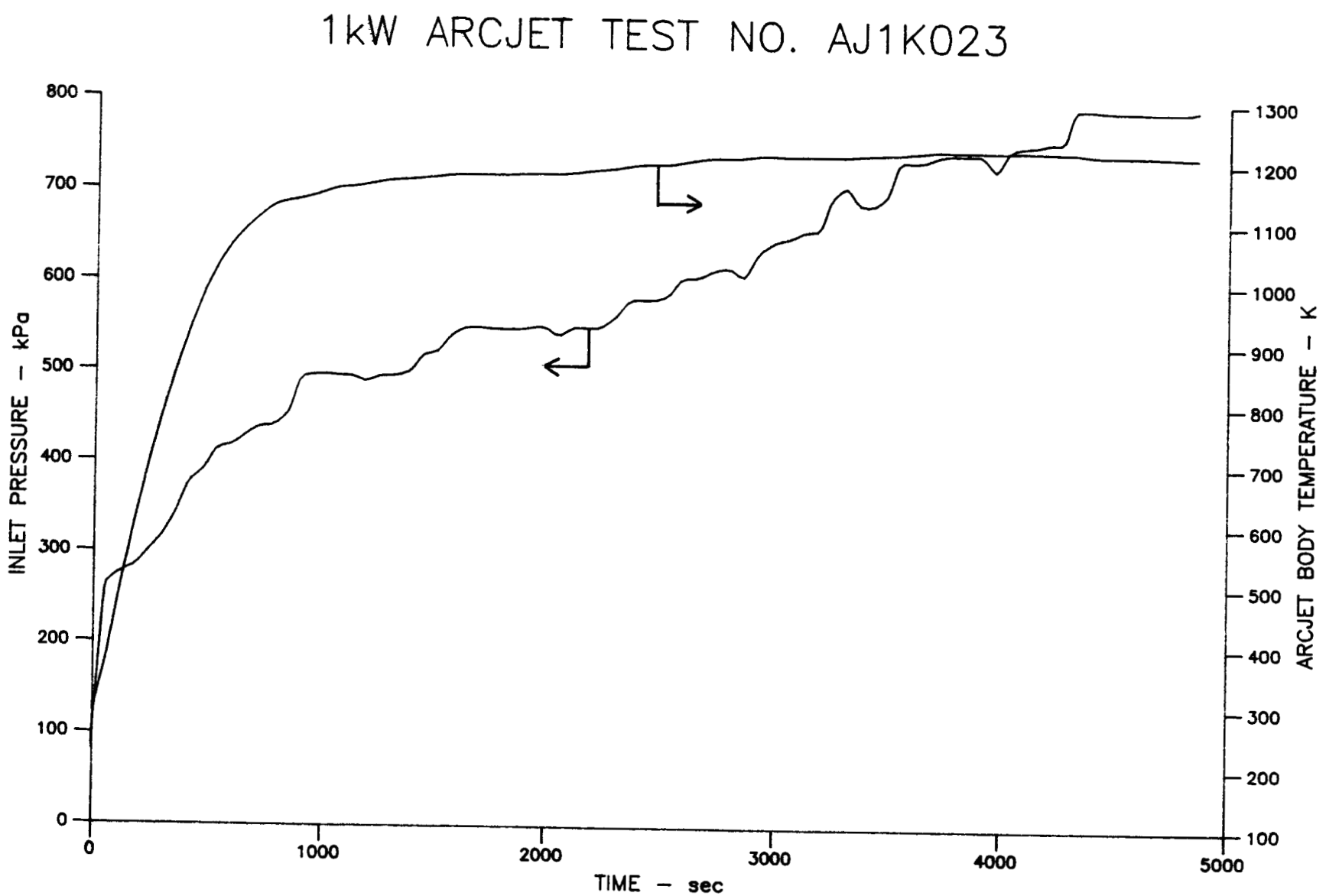

Figure 122. Inlet Pressure and Body Temperature for AJ1K023

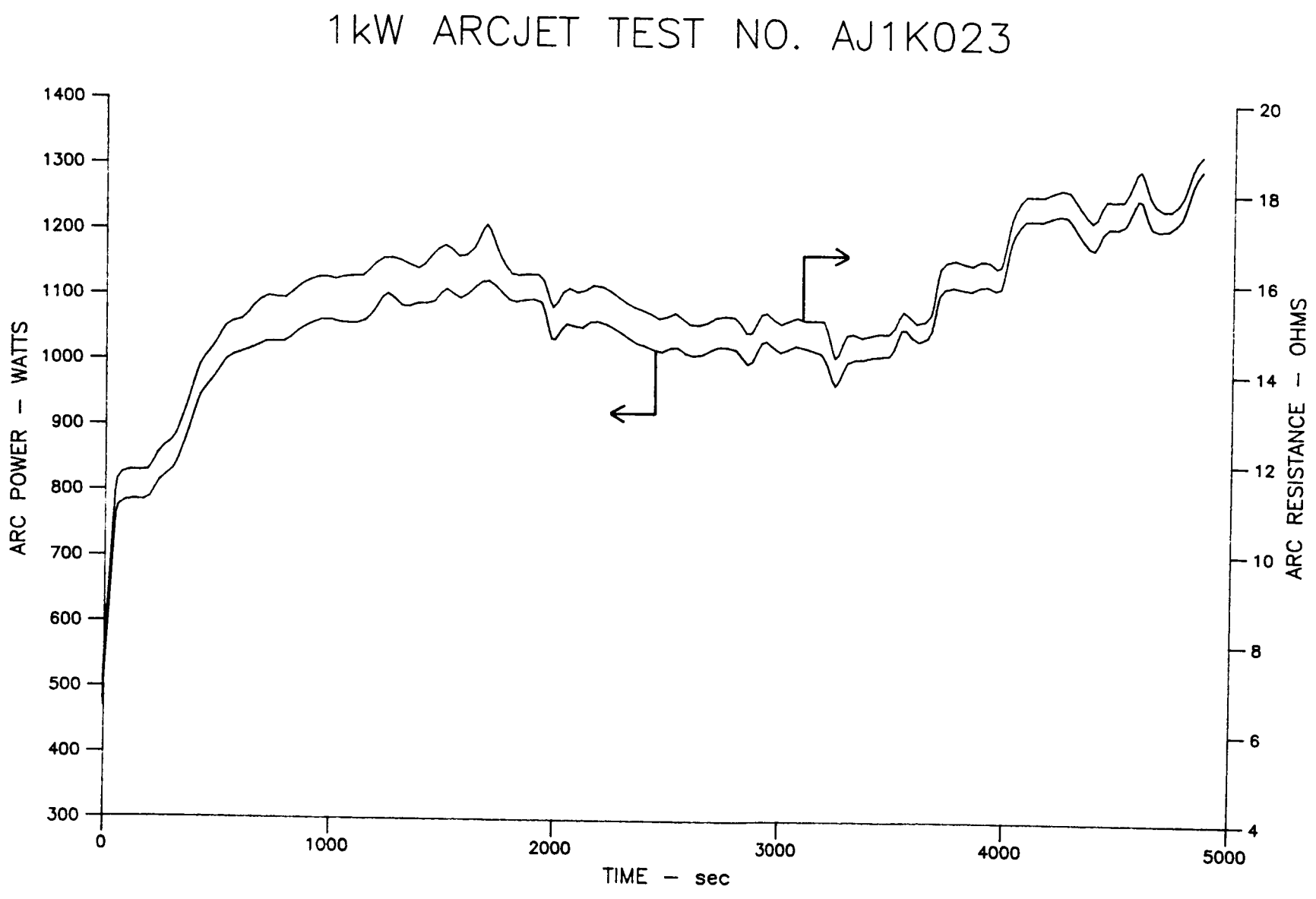

Figure 123. Power and Resistance for AJ1K023

3.6, Test Series 2 Testing (cont.)

Tests 024 and 025 were shut down after 30 seconds by the computer because limits were out of range on the flow. The cause of the limit problem was that an orifice was removed from the propellant line in order to allow higher flow rates and the limits were not changed accordingly.

Test 026 lasted 37 minutes, the arc extinguished while the current was being increased up to 8.7 amps and the flow rate was 64.5 mg/sec. Several combinations of current and flow rate were tested during the run. The data obtained from test 026 is valuable in mapping the performance of the thrust. Figures 124, 125, 126 and 127 show the variation of data during the test.

Data Analysis

The parametric performance data obtain from tests 023 and 026 has been cross plotted along with previous data (test conditions were kept constant in tests prior to 023) in order to determine conditions yielding improved performance. The data obtained to date has been with the nominal "best" arc gap (gap = 0.348 ± 0.005 cm) determined in the test series 1.0 testing. Figure 128 shows the relationship of specific impulse and electrical power input. Figure 129 shows the variation of electrical power with propellant mass flow. Figure 130 shows the variation of specific impulse and thrust efficiency with mass flow. The data points were obtained during tests where the power level varied from 700 to 1400 watts with most points at 1000 watts.

Figure 131 shows the specific impulse of the thruster as a function of specific power. A band is shown which represents the envelope of operation typical of constricted type arcjets. At a given specific power, an increase in specific impulse requires a corresponding increase in thrust efficiency of the device. Lines of constant thrust efficiency are included on the Figure 131 for reference. Two observations are apparent from the figure, the first is that the measured specific power was only two thirds of the design value of 30 mw*sec/kg. The second, most striking observation is the trend of decreasing specific impulse with increasing specific power.

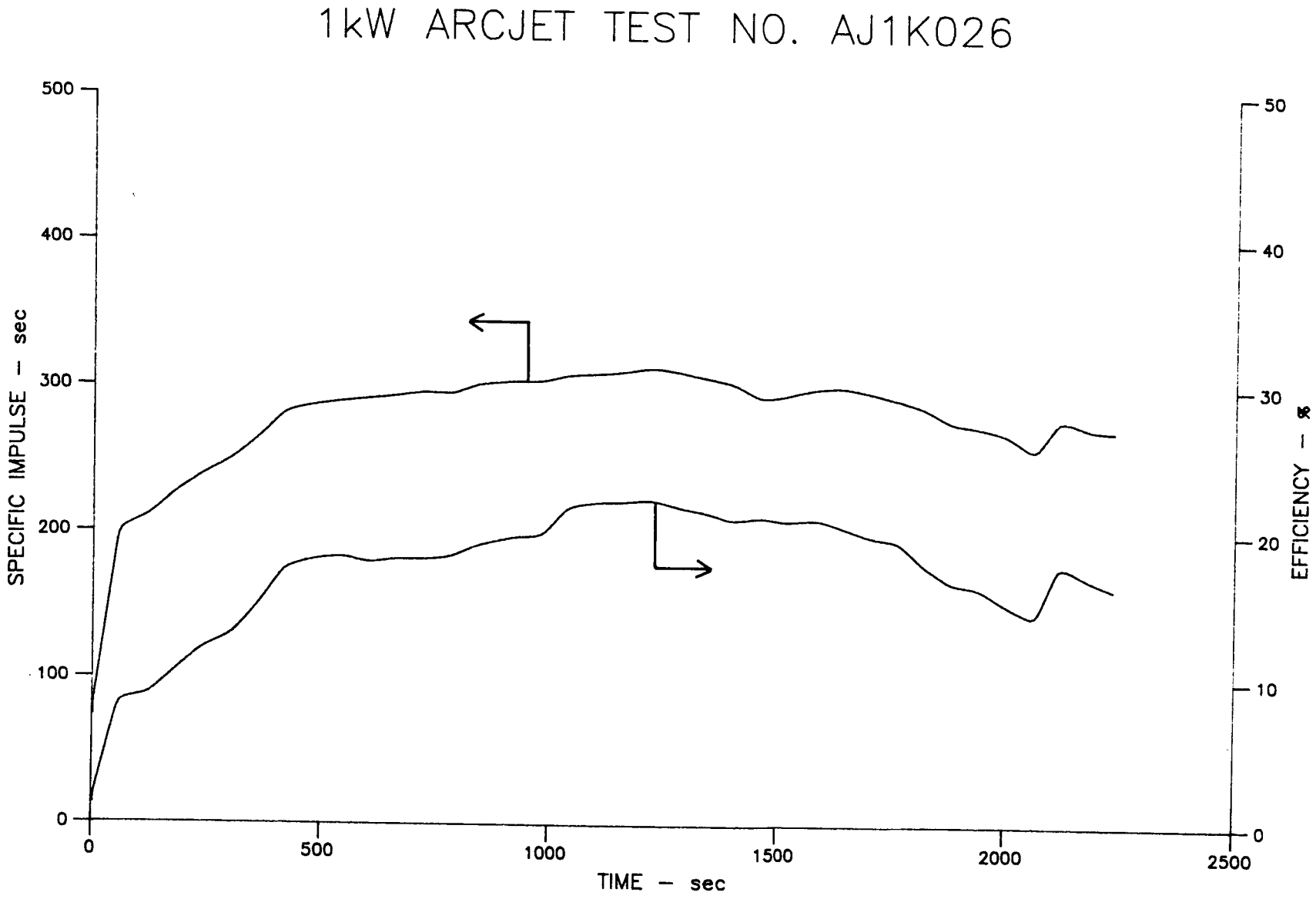

Figure 124. Specific Impulse and Thrust Efficiency for AJ1K026

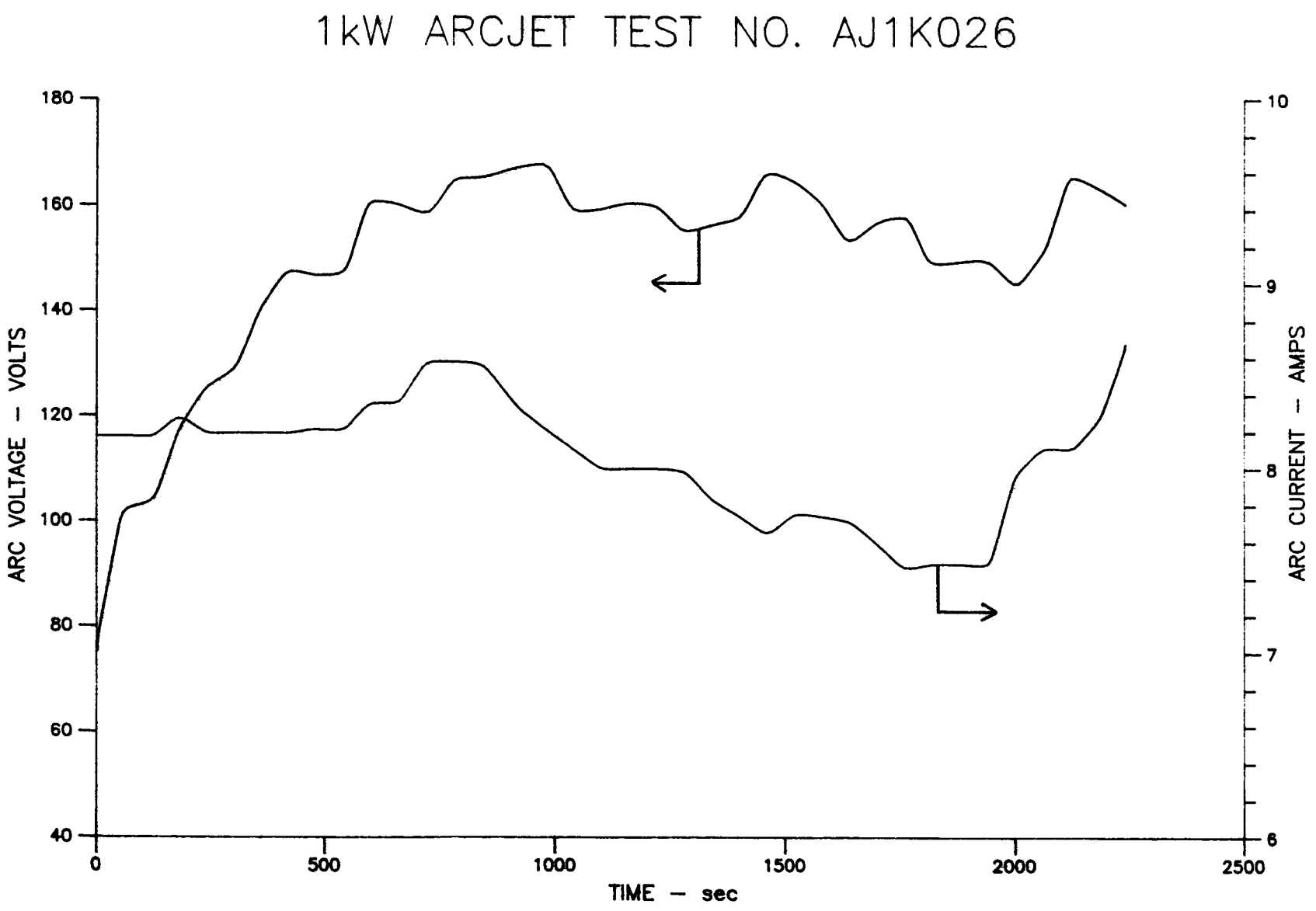

Figure 125. Current and Voltage for AJ1K026

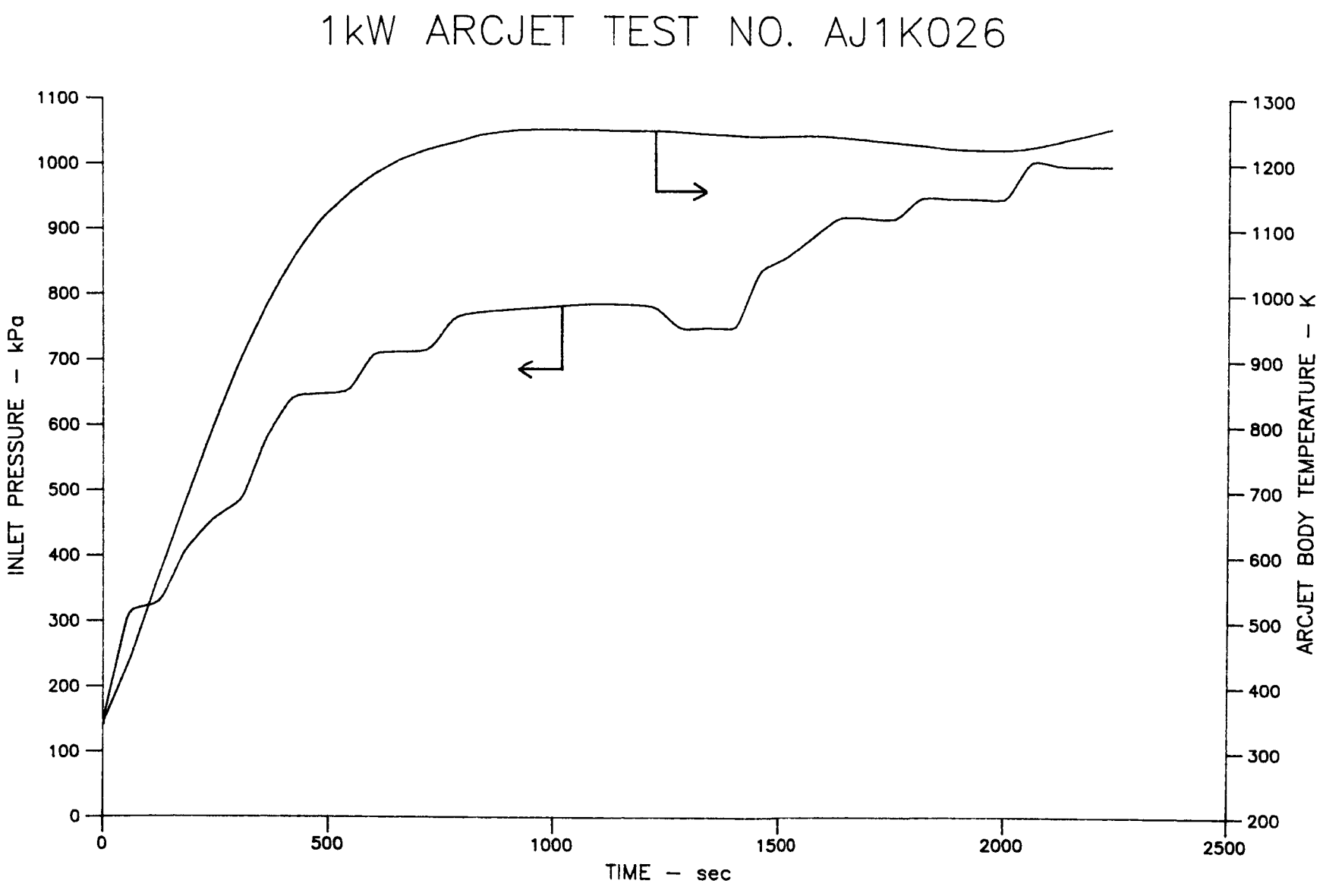

Figure 126. Inlet Pressure and Body Temperature for AJ1K026

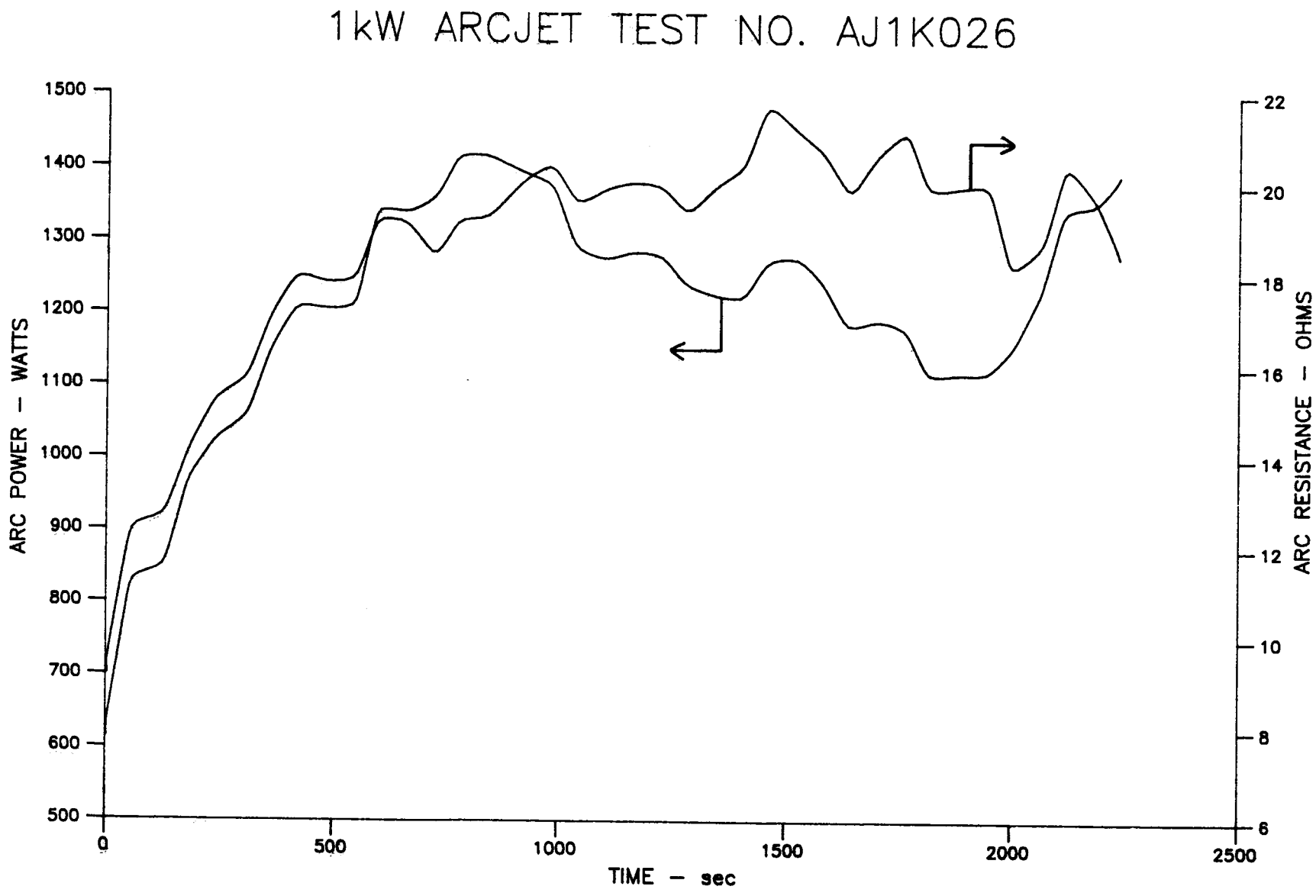

Figure 127. Power and Arc Resistance for AJ1K026

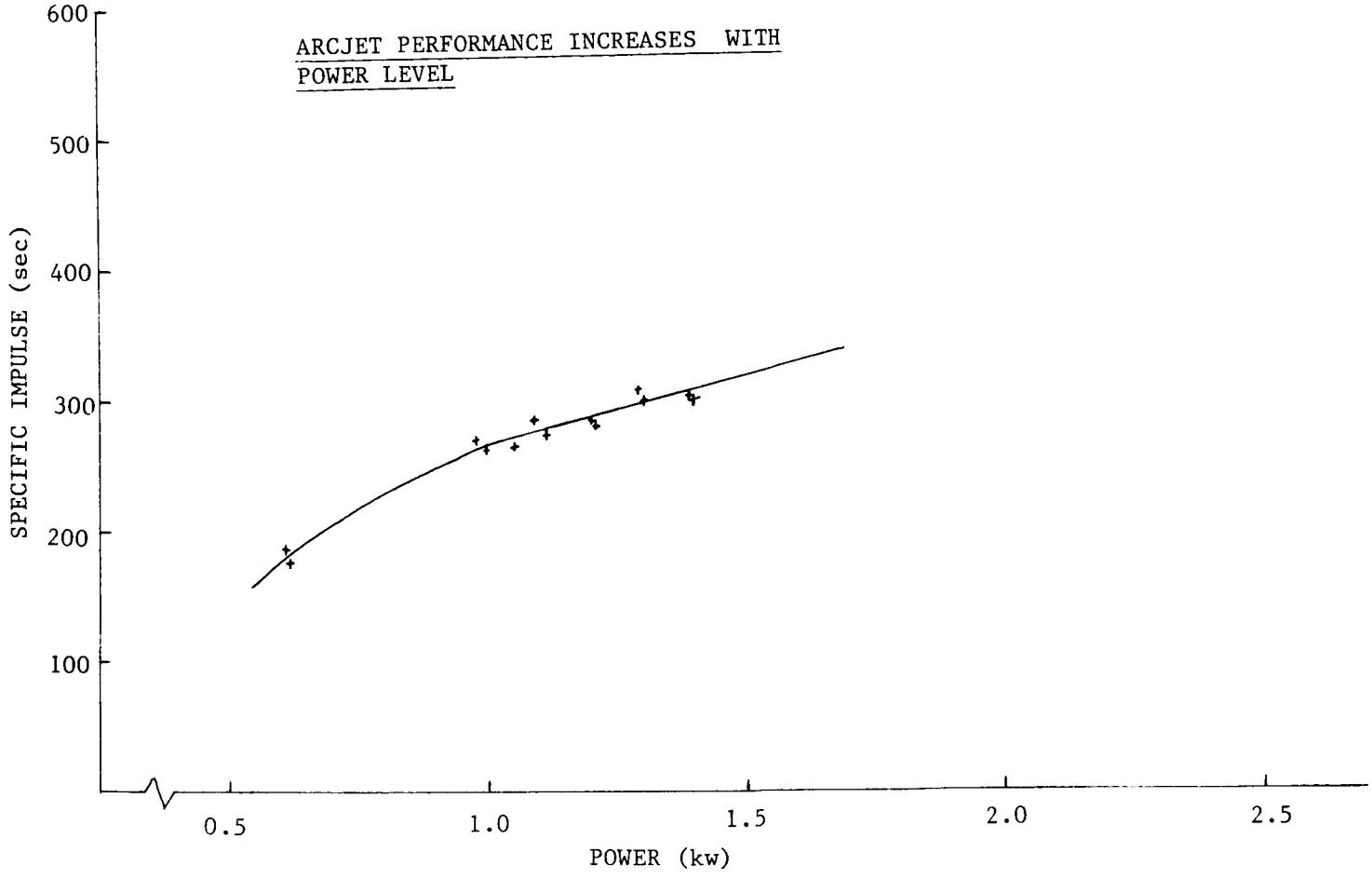

Figure 128. Specific Impulse vs. Power

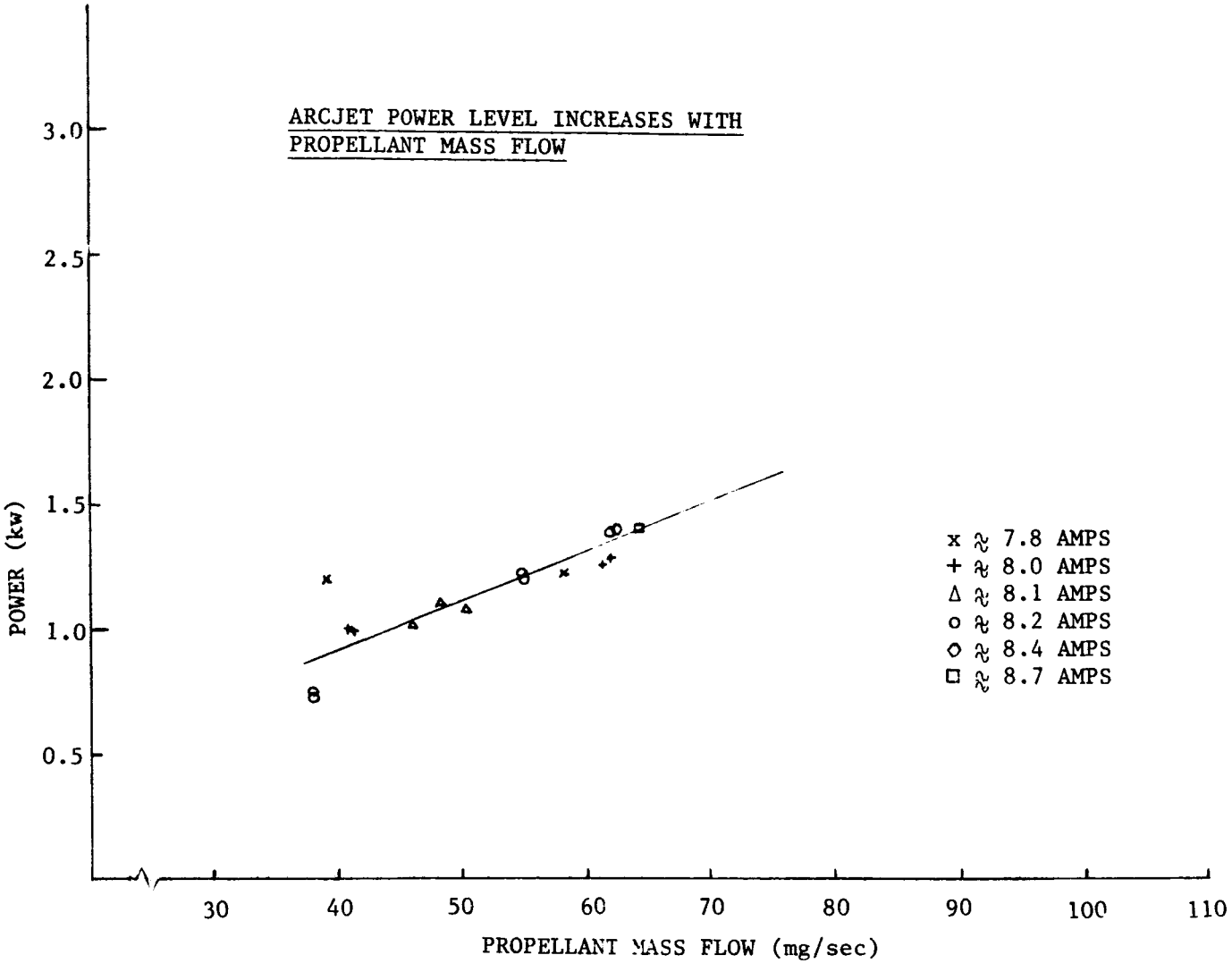

Figure 129. Power vs. Mass Flowrate

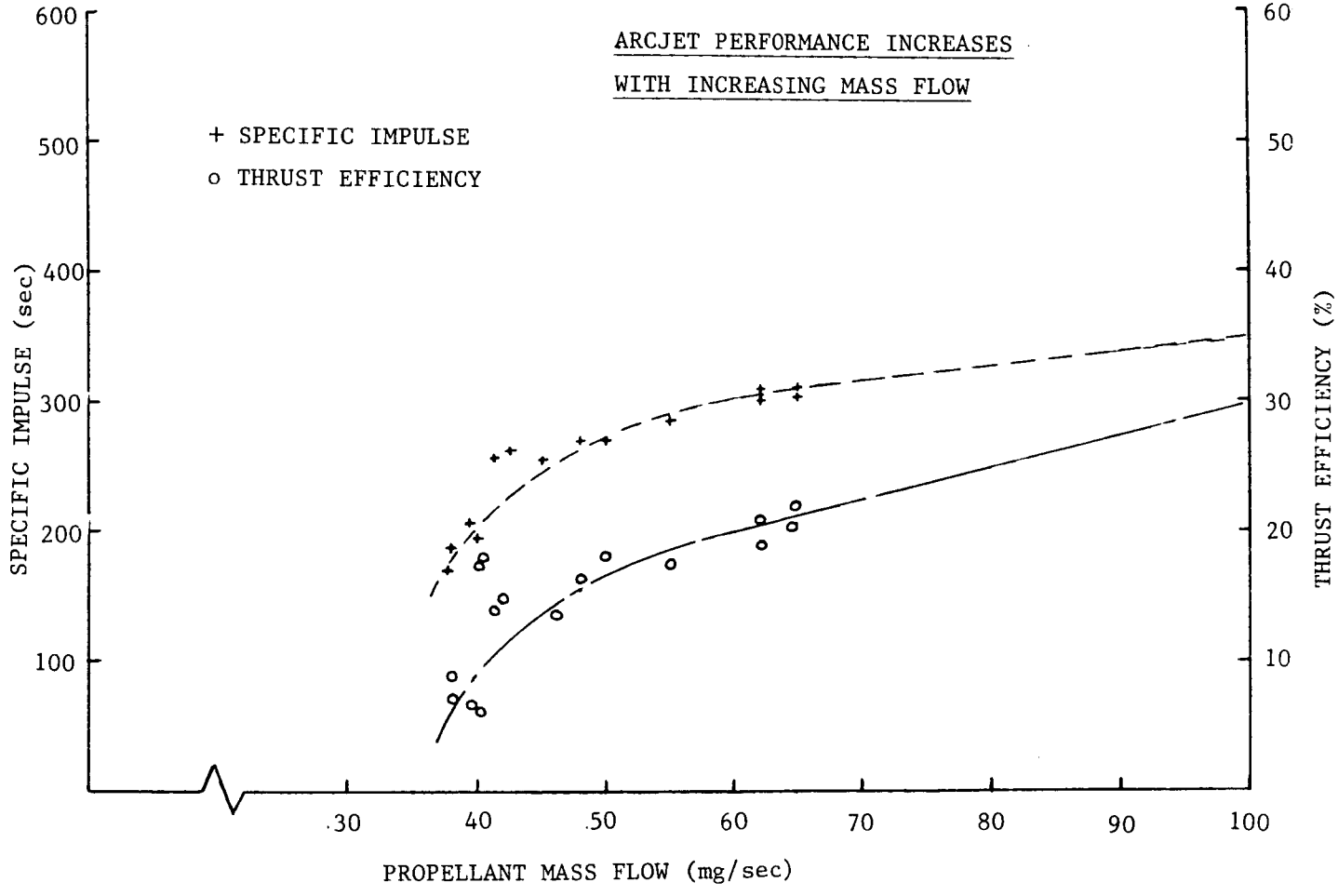

Figure 130. Specific Impulse and Thrust Efficiency vs. Mass Flow

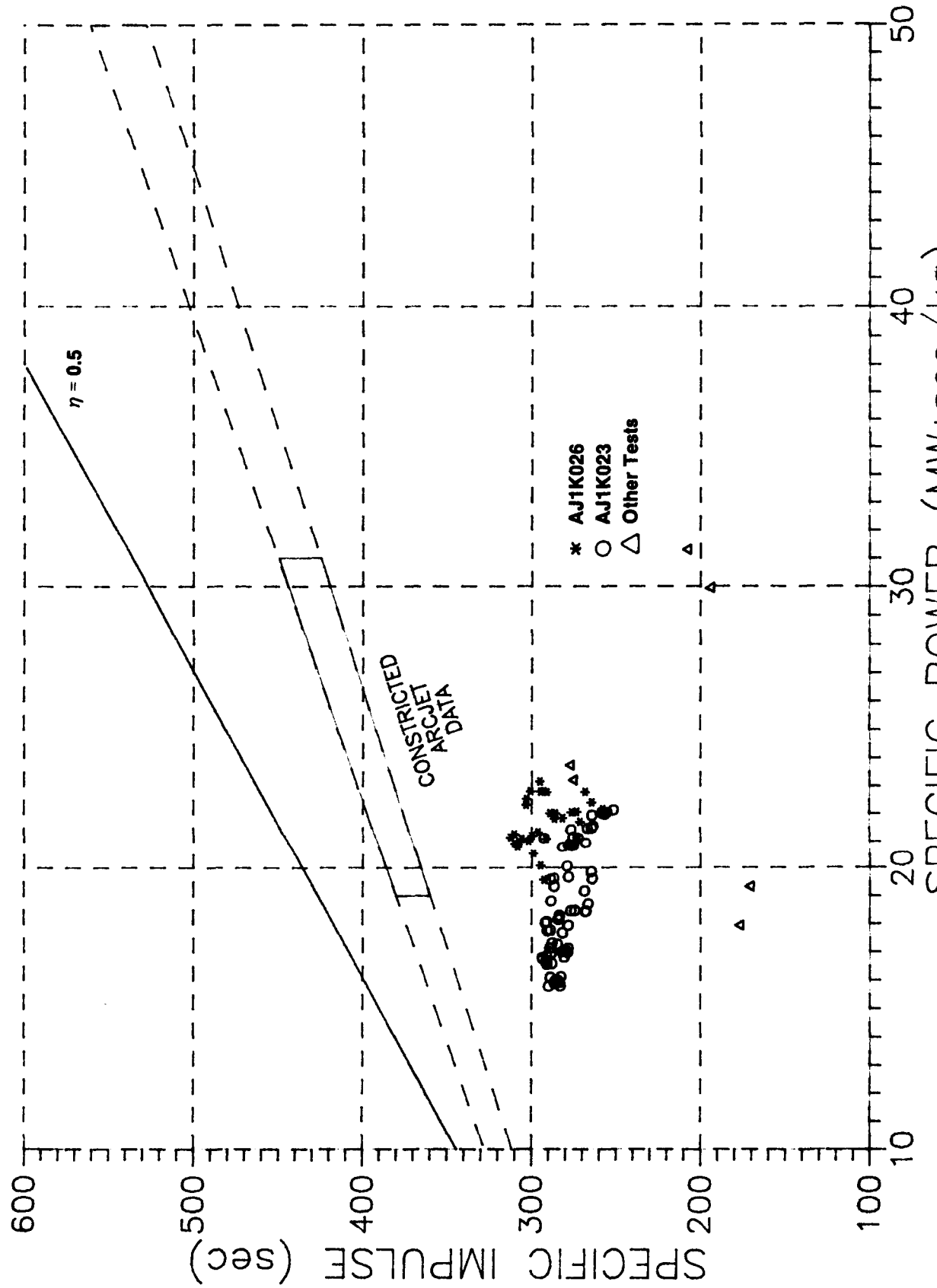

Figure 131. Comparison of Arcjet Performance

Figure 132 shows the thrust to power ratio plotted against the specific impulse. The data shows an unexpected trend in that thrust to power ratio increases with increasing specific impulse. Typically, the thrust to power ratio is inversely proportional to the specific impulse. Since the higher specific impulses were measured at high mass flow rates and high power, the trend may indicate that the device performs better at a 3 or 4 kw power level. The reason for this may be a change in the internal flow at the elevated flowrates, including an increase in the average Reynolds number in the thruster, which may reduce flow losses.

The thrust efficiency of the device as a function of specific impulse is shown in Figure 133. Again an atypical trend can be seen in the data. The thrust efficiency of the thruster increased with increasing specific impulse. This data also indicates that the thruster design was more suitable for operation at higher mass flow and power than the design point.

Mixing and Heat Transfer Losses

The operating conditions of 2.25 kw and 107 mg/sec, projected from Figures 128, 129, and 130, assume that no modifications are performed on the thruster. The measured arcjet body temperatures of between (900 to 1000 C) indicate that there is more heat transfer from the arc and gas to the thruster internal surfaces than designed. One explanation for this heat transfer is that excessive mixing is occurring in the mix chamber between the hot core gases and the injected film cooling. This results in an increase in the gas temperature near the wall and a reduction of average temperature of the core flow and a corresponding increase in the gas temperature in the boundary layer near the wall. A reduction in the amount of mixing could be achieved by reducing or eliminating the expansion ratio between the anode and mix chamber. A modification the relative aspect ratios of the anode and mix chamber may enable the thruster to achieve 400 sec specific impulse at the 1.0 kw power level.

In addition to eliminating the expansion ratio into the mixing chamber, recent studies at Technion[15] under contract to Aerojet and

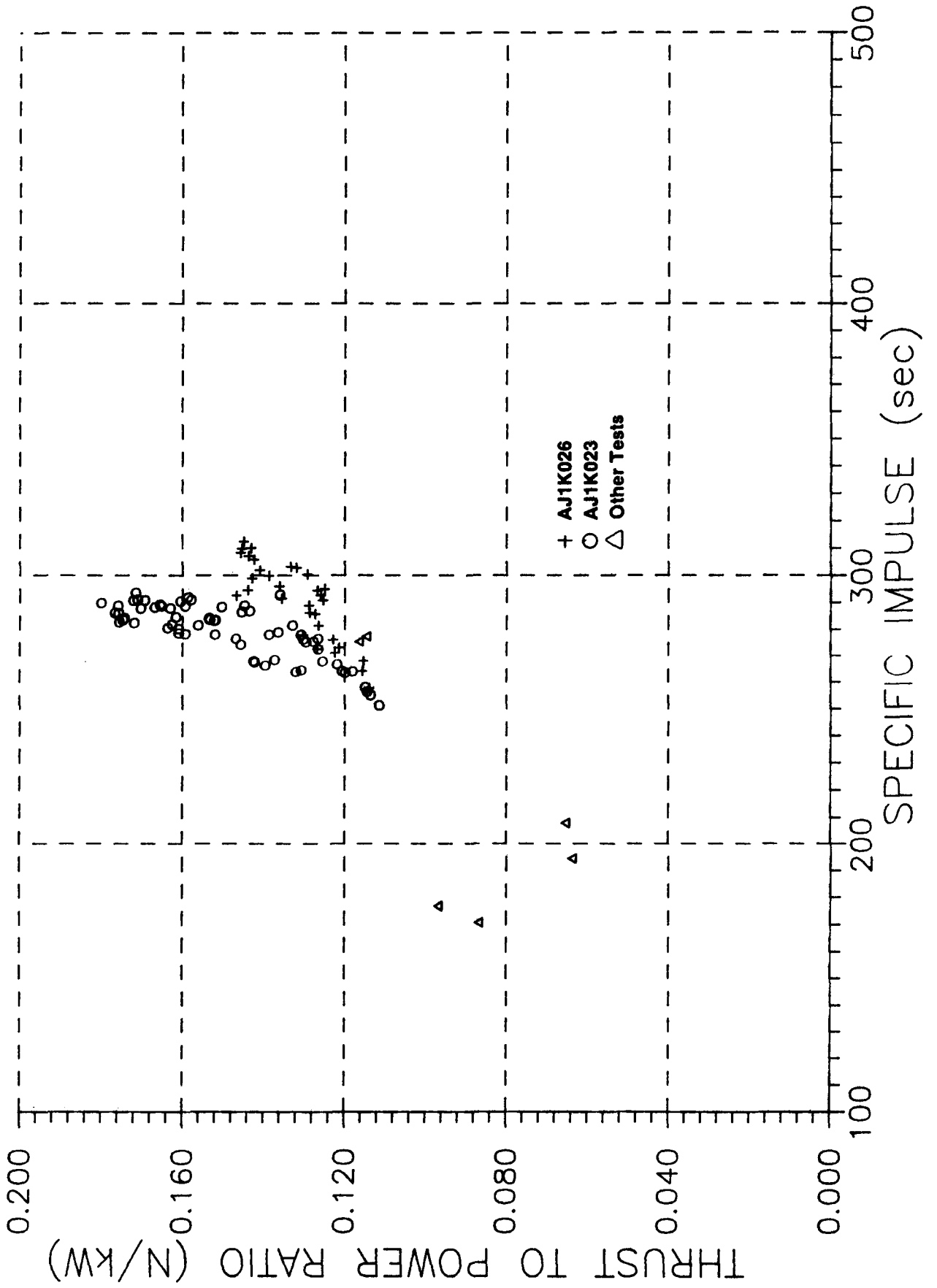

Figure 132. Thrust to Power Ratio vs. Specific Impulse

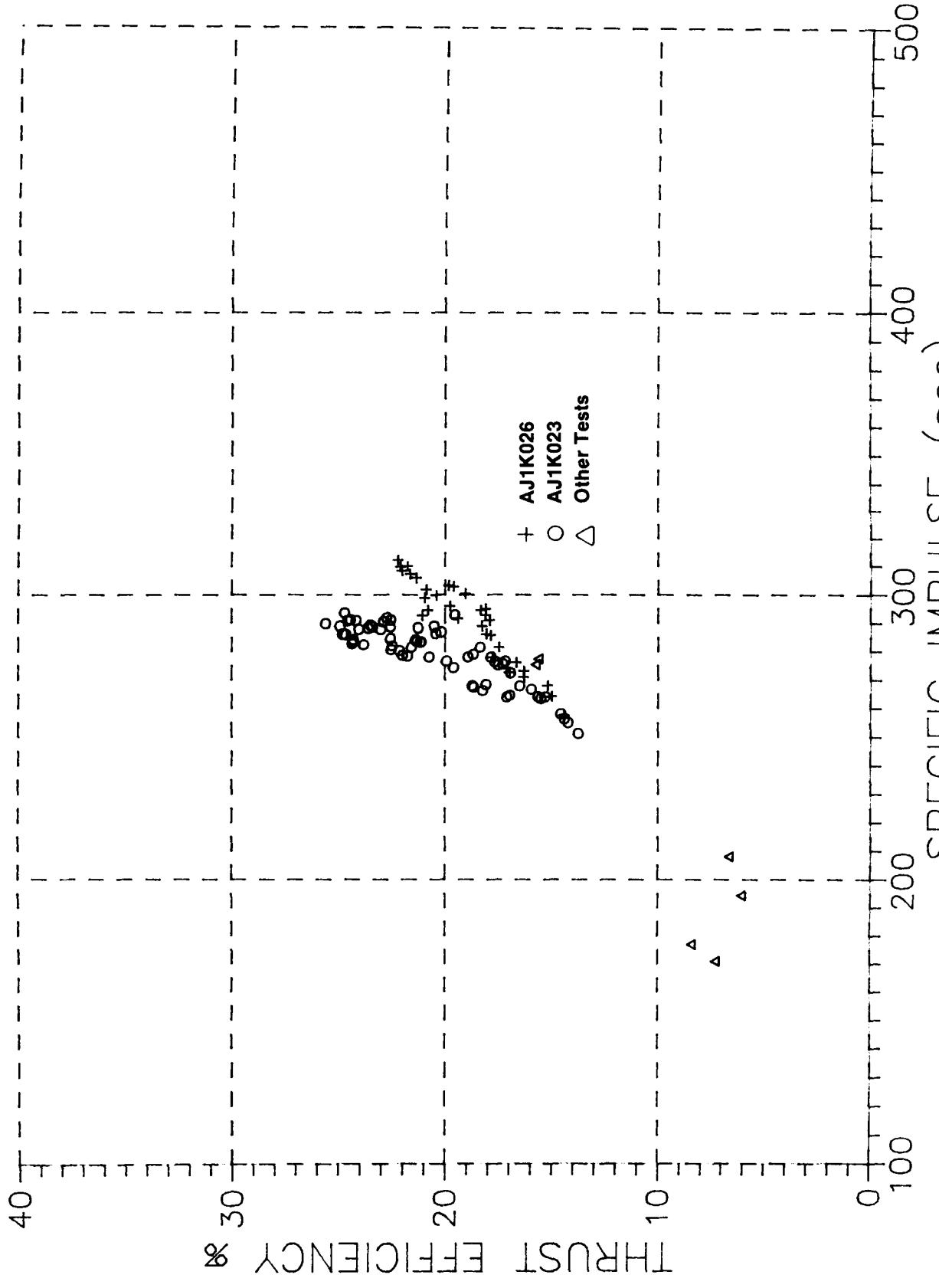

Figure 133. Thrust Efficiency vs. Specific Impulse

AFAL on 25 kW class arcjets, indicate that for certain propellants, including hydrazine and ammonia, the amount of energy that can be recovered in the mixing chamber is negligible and can be detrimental because convective heat transfer and momentum losses in the region are high.

Flow Split Between Arc Chamber and Mixing Chamber

The injection ports in the arc chamber and the mixing chamber were sized so 75% of the total propellant mass flow rate would flow through arc chamber and be heated by the arc. This was a conservative design to ensure that the components of the baseline thruster would be overcooled and have long enough life that the thruster would survive the test program. The remaining 25% of the flow is injected in the mixing chamber to provide film cooling in the nozzle. At the conclusion of Test Series 2, cold flow measurements were performed to check the flow split. The flow split was measured to be 40% of the total mass flow through the mixing chamber. A reason for the difference could be either the arc chamber injection ports having diameters larger than design due to machining variation or a port(s) might be clogged with metal shavings. Another possibility is that leaking is occurring through the internal weld connecting the anode (part #T508002) and the nozzle (part #T508003).

Since the flow split is fixed for the thruster as it is presently designed, less flow than expected was coupled to the arc during testing. The additional gas injection in the mixing chamber lowered the performance of the thruster in two ways. The major effect was a built-in upper limit on achieveable specific impulse. A fixed plasma arc configuration heats the gas flowing through the discharge to essentially a fixed enthalpy. Therefore, reducing the percentage of gas available for arc heating has a profound effect on delivered specific impulse. Not only is a smaller quantity of hot gas available for mixing with a larger quantity of cold gas, but also, to a first approximation, as the flow rate through the arc is reduced, the achieveable power input is also reduced.

3.6, Test Series 2 Testing (cont.)

In addition, excessive mixing of the hot centerline flow and the injected mix chamber flow caused further I_s reduction because of enhanced convection losses to the mix chamber and nozzle. The excessive mixing was the result of the anode-to-mix chamber transition geometry, which was too abrupt, and the larger than design amount of injected cold gas.

Figure 134 shows a possible projection of the improvement in performance of the arcjet with the design flow split of 25%. The projection assumes that the arc power absorbed per unit mass flow and the fixed losses are the same as measured data values. The first assumption is only valid over a limited range of flow splits. The second assumption is conservative since convective losses to the thruster would be less. As seen from the figure, a projected flow split of 10% of the flow through the mixing chamber, which may represent an optimum flow split, leads to dramatically improved performance. Future work on the thruster must contain a provision for varying the flow split in order for the performance to reach desired levels. Figure 135 shows our estimate of the improvement in specific impulse as the flow split of the thruster is changed.

Figure 134 and 135 may be conservative since it is assumed that the flow split during operation is equal to that measured at cold flow conditions. Since the flow to the arc chamber and mixing chambers are parallel branches from the inlet propellant line, the flow through the arc chamber actually decreased due to an evaluation in arc chamber pressure as the gas was heated. Since no arc power is absorbed in the mixing chamber and cold gas is mixed with the hot arc heated gas, the mixing chamber pressure is less than the arc chamber pressure. Figure 136 illustrates the reduction in the percentage of propellant mass flowrate through the arc chamber as power level increases. The specific enthalpy of the mass flow through the arc chamber increases as the mass flow through the arc chamber decreases, in order to maintain a constant exit enthalpy.

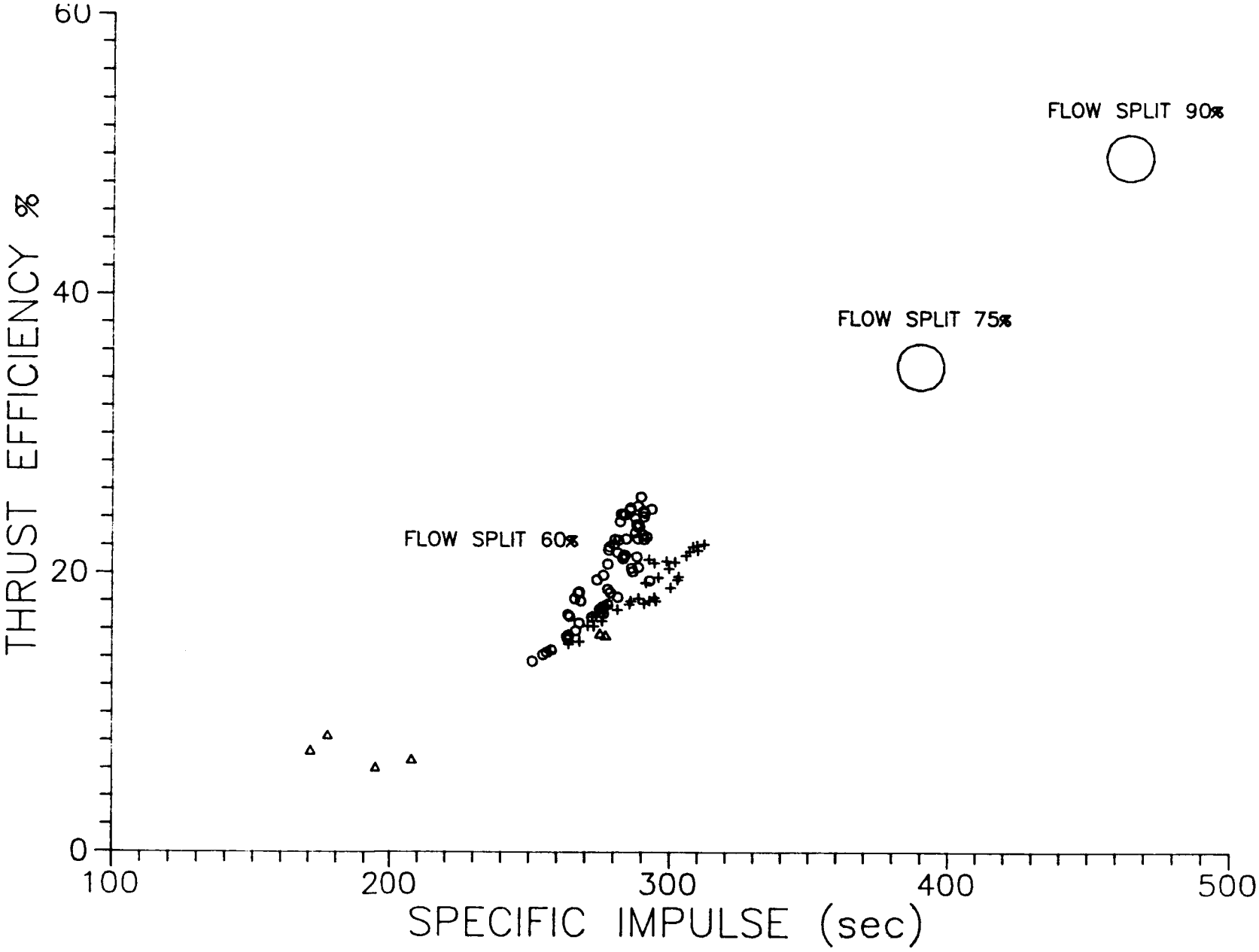

Figure 134. Performance Improvement of Increasing Flow through Arc Chamber

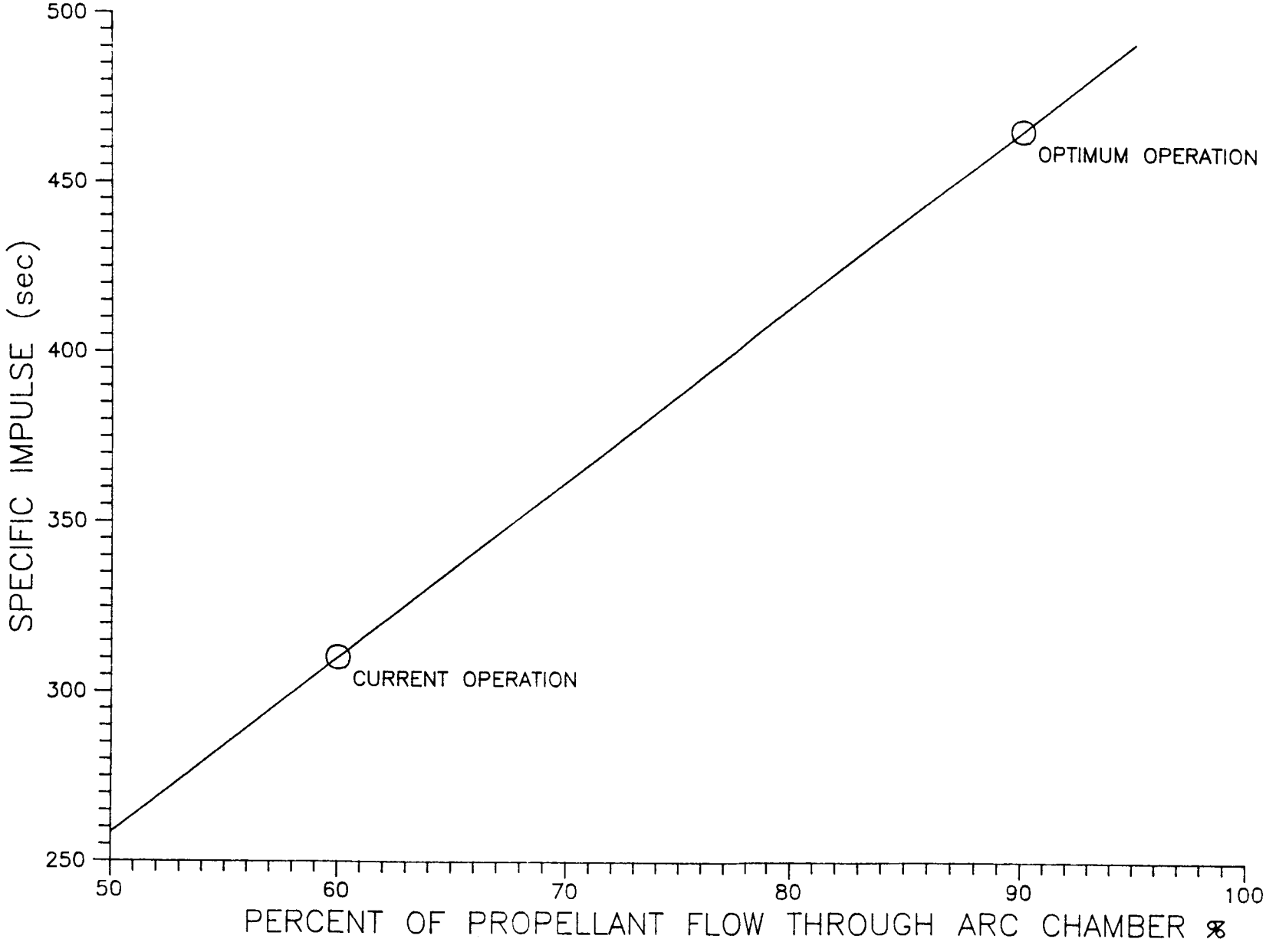

Figure 135. Relationship of Isp to Flow Split

Figure 136. Decrease in Arc Chamber Flow with Increasing Power

3.6, Test Series 2 Testing (cont.)

Nozzle Losses

Thrust coefficients calculated from the data have ranged from 0.9 to 1.1 during hot operation. These values are below the C_f/C_d of 1.6 assumed in the design and is well below what is expected for orifice flow. Part of the discrepancy is due to the use of the inlet pressure rather than the true chamber pressure in the calculation and the effects of the vortex flow. Improper machining of the nozzle could result in viscous losses causing a significant reduction in the thrust coefficient. The actual thrust coefficient of a nozzle can be expressed as the product of a discharge coefficient C_d, a cosine loss term λ, and the theoretical thrust coefficient $C_{f_{theo}}$ as:

$$C_{f_{act}} = C_{f_{theo}} * \lambda * C_d$$

Typically the value of C_d is a approximately 0.96 to 0.99. Roughness and a long cylindrical section (3 to 6 L/D) in place of the intended throat could reduce the discharge coefficient by 30% to 40%. The length of the throat and roughness on the inlet section cannot be determined due to the re-entrant geometry of the thruster. However, measurements have been made on the nozzles used for the nozzle test program, which were machined in a similar manner to the thruster nozzle, and the existence of a long cylindrical section was verified. A 30% improvement in the actual thrust coefficient would increase the best performance measured, 310 sec Isp and 22% thrust efficiency, to 400 sec Isp and 37% thrust efficiency. A combination of improved nozzle design, reduced mixing and heat transfer from the hot core gases with the film cooling layer, and optimization of the flow split should result in an even greater improvement in performance of the thruster.

Summary of Thruster Condition at Conclusion of Testing

Figure 137 shows and overall view of the thruster and its components after test 026. In order to prevent the electrical breakdown from the cathode to the rear flange of the arcjet which occurred during the start

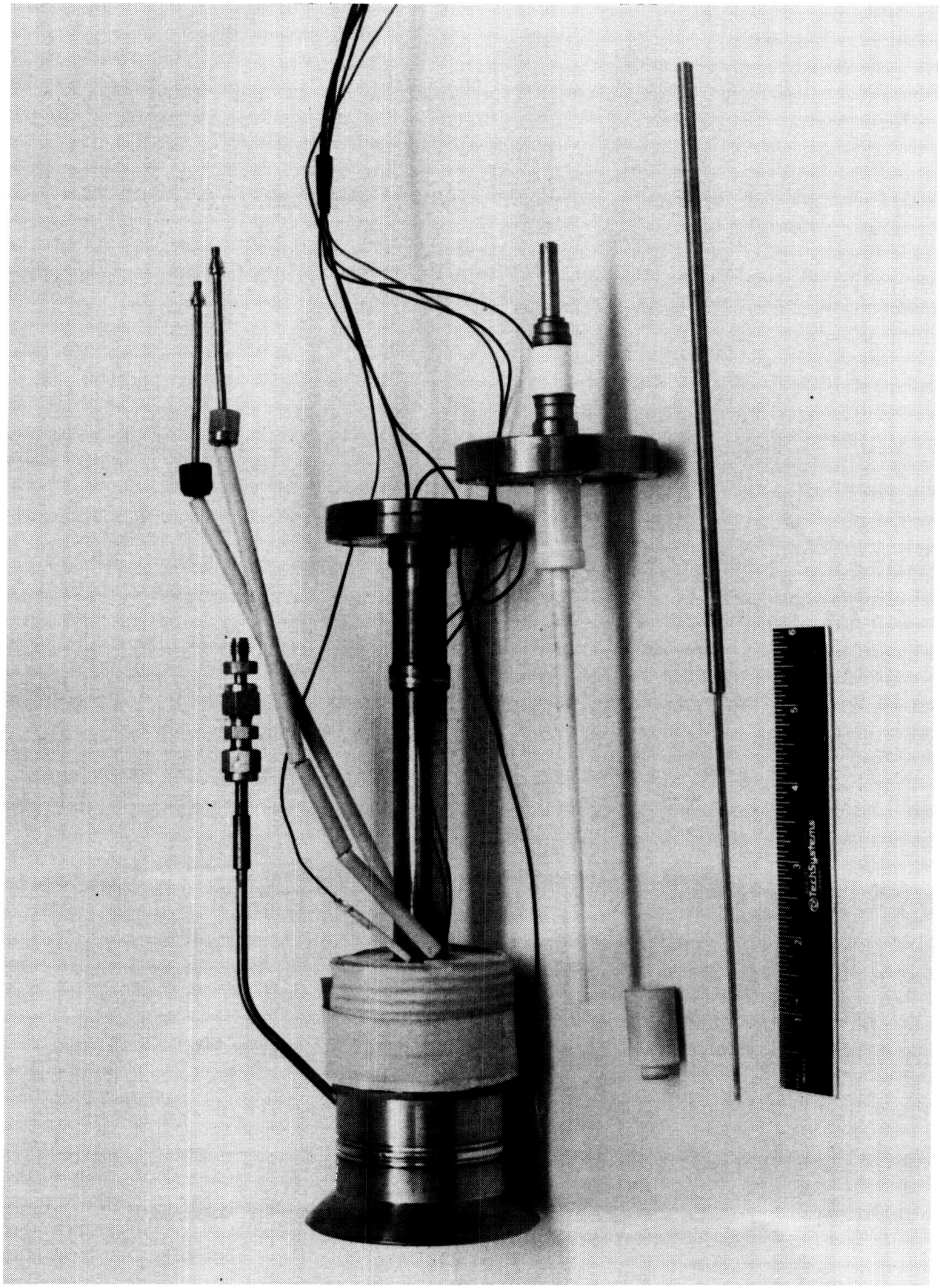

Figure 137. Arcjet Components at the Completion of Test Series 2.0

of 020, the aft insulator, ceramic tube, and rear flange were permanently sealed together with ceramic cement as shown.

Figure 138 shows the cathode after test 026. No significant change in appearance or dimensions of the cathode was detected from the conclusion of Test Series 1 to the finish of Test Series 2. The arc chamber insulator is shown in Figure 139. Slight wear at the lip of the cathode feed-through can be seen. This wear may be attributable to removal and replacement of the cathode for inspection and during assembly during the test program. The arcjet anode is shown in Figure 140 (viewed from rear flange). By scaling the photograph the anode diameter appears to be approximately 0.107 cm ± 0.008 cm. Earlier estimates of the anode reducing to 0.094 cm (determined by passing a rod through the anode) may have been due to deposition of cathode material in one location rather than a uniform reduction in diameter.

Figure 141 shows a view of the nozzle. The darkened appearance on the inner diameter appears to be oxidation. A crack in the nozzle can be seen from the photograph. This crack has been examined under a microscope and can be seen only with certain lighting angles. It cannot be determined if the crack is newly formed or has been present during the entire test program. During the inspection of the crack, arc tracking in the nozzle slightly down stream of throat was detected.

Detail photographs of the arc tracking are shown in Figure 142. The photographs are oriented so the view is looking towards the nozzle with the top the photo corresponding to the top of the thruster. It can not be determined when the arc tracking occurred during the testing.

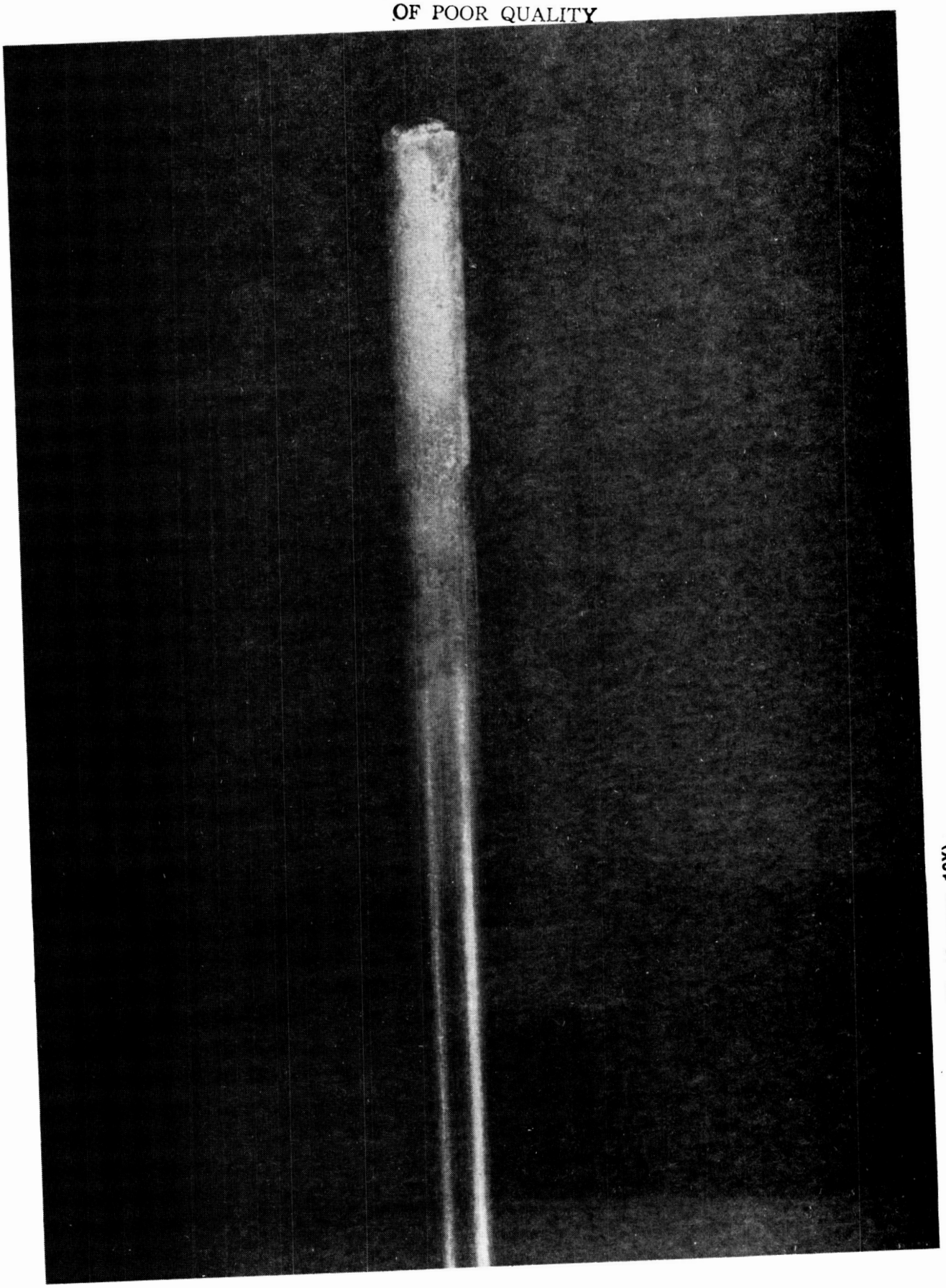

(a) Side View of Cathode Tip (Approx. 10X)

Figure 138. Cathode after Completion of Test Series 2

(b) Cathode Tip (Approx. 19X)

Figure 138. Cathode after Completion of Test Series 2 (cont)

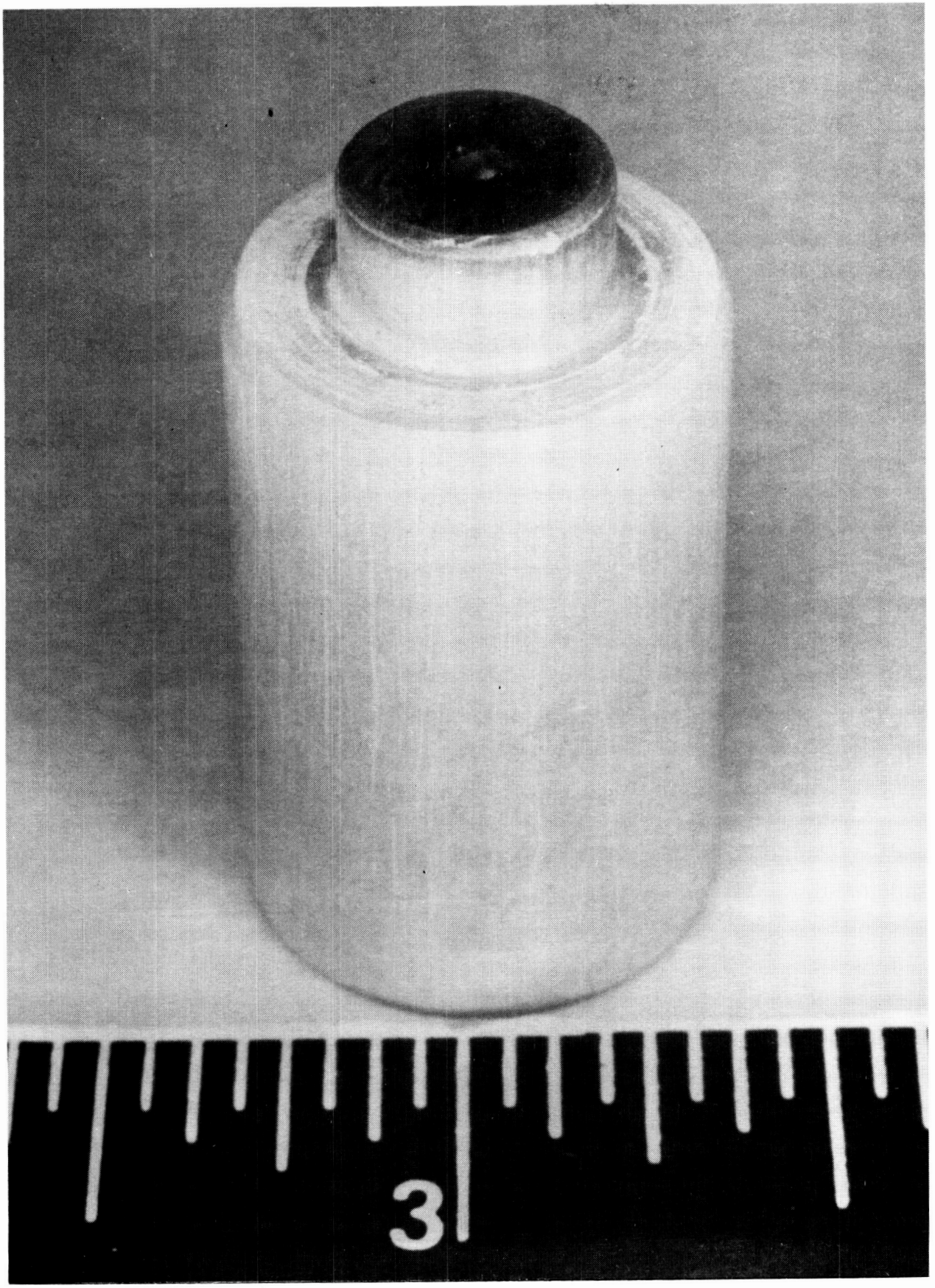

(a) Overall View (Approx. 11X)

Figure 139. Arc Chamber Insulator after Test Series 2

(b) Face of Insulator (Approx 18X)

Figure 139. Arc Chamber Insulator after Test Series 2 (cont.)

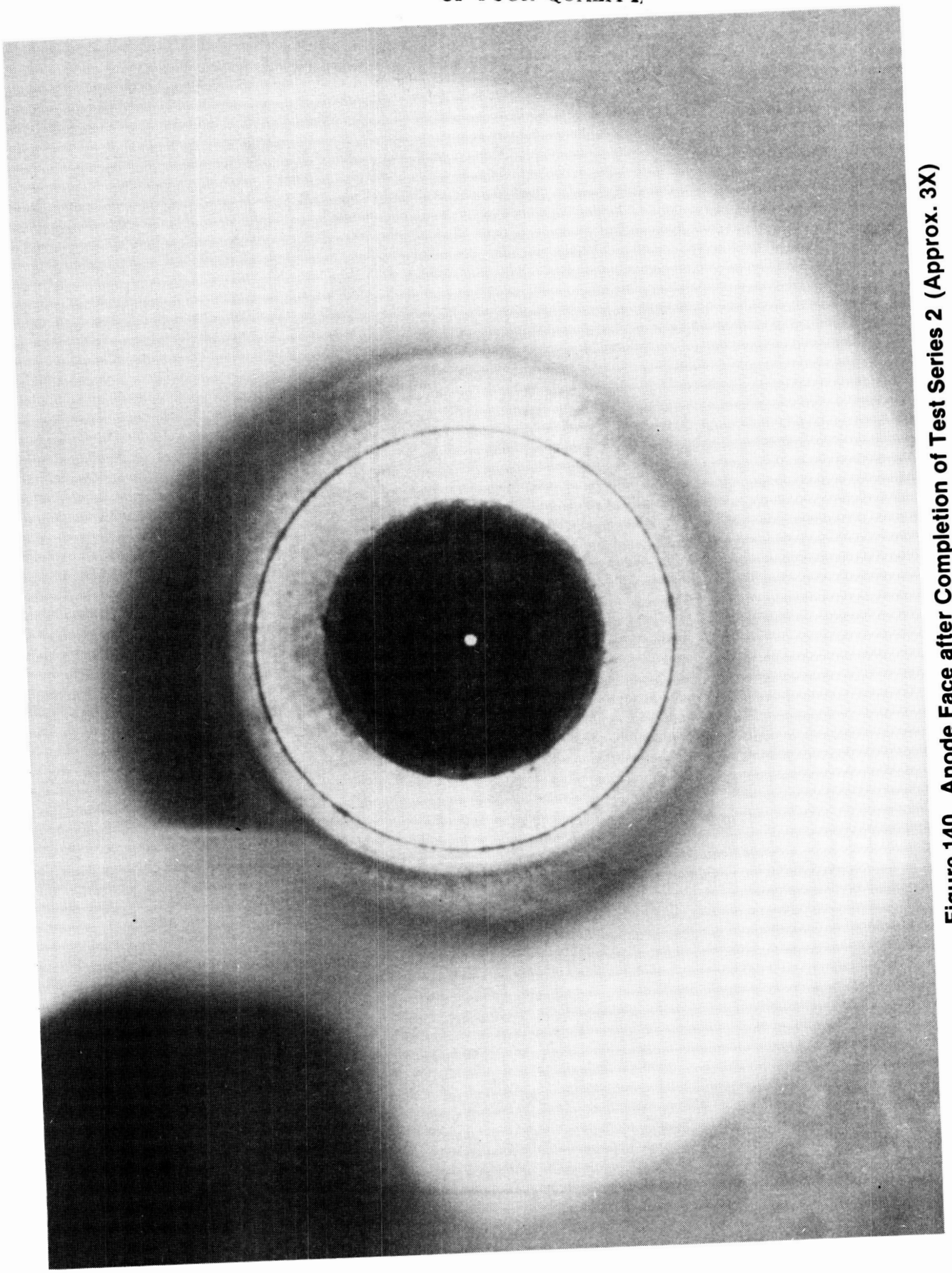

Figure 140. Anode Face after Completion of Test Series 2 (Approx. 3X)

Figure 141. View of Arcjet Nozzle, Shows Crack in Side Wall (Approx. 5X)

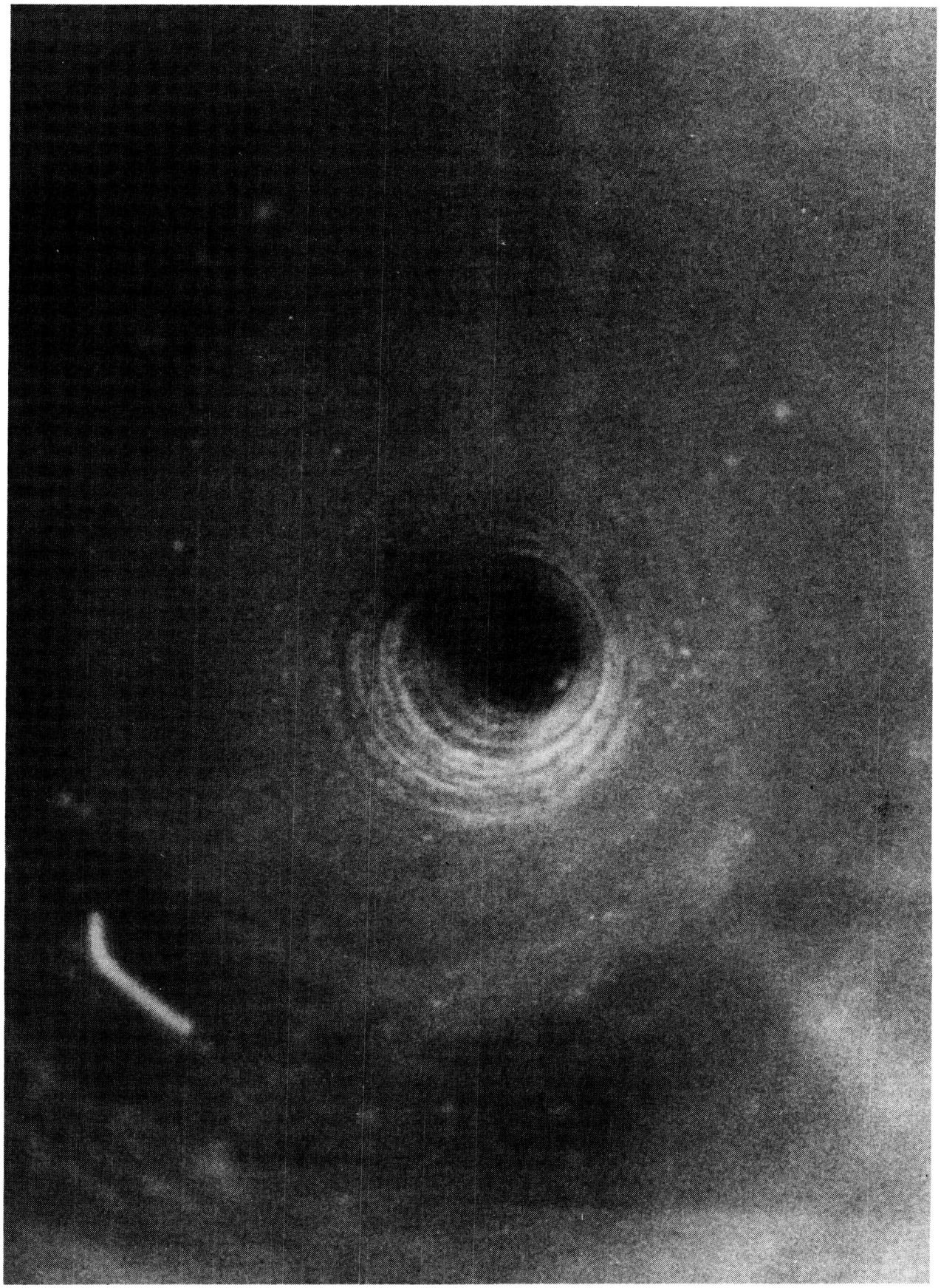

(a) First View in Nozzle Throat (Approx. 25X)

Figure 142. Arc Tracking

(b) Second View in Nozzle Throat (Approx. 25X)

Figure 142. Arc Tracking (cont.)

4.0 CONCLUSIONS AND RECOMMENDATIONS

The following sections present the specific conclusions and recommendations of the program based on the Phase I results. The program performance goals of a specific impulse greater than 400 seconds, a thrust efficiency of greater than 40%, with a storable propellant and components with 3000 hours of life were not achieved during of the program. In spite of this disappointment, we feel the program successfully demonstrated the feasibility of an advanced arcjet concept, which when optimized may provide the high performance and long life needed to the program goals.

Three critical issues were addressed during Phase I of the program concerning the development of the thruster. The first is the demonstration of stable arc operation with projected electrode life long enough to make the device a viable propulsion system. The second issue is that the arcjet can provide the minimum performance required to perform anticipated missions and justify the cost of development. The final issue is that the arcjet can be developed into a flight-weight, reliable, and cost effective propulsion unit. The work performed during Phase I of the program has addressed each of these issues and the potential benefits of the advanced arcjet concept. While the results during Phase I were less than hoped for, we believe that the approach the advanced arcjet shows merit and with continued development can meet NASA's needs.

ASSESSMENT OF ARCJET OPERATION AND LIFE

The high impedance, vortex stabilized, arcjet has been tested over a wide range of operating conditions.

Power:	500 - 2000 watts
Propellant Mass Flow:	23 -70 mg/sec
Current:	5 - 12 amps
Voltage:	80 - 220 volts
Arc Gap:	0.25 - 0.87 cm
Magnetic Field:	0 - 800 gauss

4.0, Conclusions and Recommendations (cont.)

The most stable arc operation was found at the following Conditions.

Power:	700 - 1400 watts
Propellant Mass Flow:	40 < mass flow < 70 mg/sec
Current:	7.5 - 8.5 amps
Voltage:	120 - 160 volts
Arc Gap:	0.34 cm
Magnetic Field:	400 gauss

During the test no failure of the thruster in the arc region and nozzle occurred. Electrode erosion of the baseline design extrapolates to 1000's of hours of life for the cathode and anode. the cathode erosion slowed as the conical portion of the tip recessed to the flat tip. Once the cathode attained a nearly flat shape, no significant erosion was measurable. Figure 143 shows the cathode tip erosion rate calculated from cathode tip regression measurements. The erosion rate measured between 80 and 104 hours of operation was 0.23 μ m/hr. the rapid decrease in the erosion rate indicates that the cathode was approaching a "stable" (i.e., minimal erosion) geometry. Further testing with a baseline flat cathode tip should be undertaken to confirm this conclusion. Minimal erosion of the anode was measured during the testing. A reduction in the anode diameter was detected, but it could not be determined if it was due to redistribution of anode material or deposition of cathode material.

ASSESSMENT OF ARCJET PERFORMANCE AND SUGGESTED DESIGN IMPROVEMENTS

Several causes for the low performance measured form the baseline research thruster have been identified.

1. Convective heat loss from the arc heated propellant gas to the internal surfaces of the thruster prior to expansion through the nozzle.

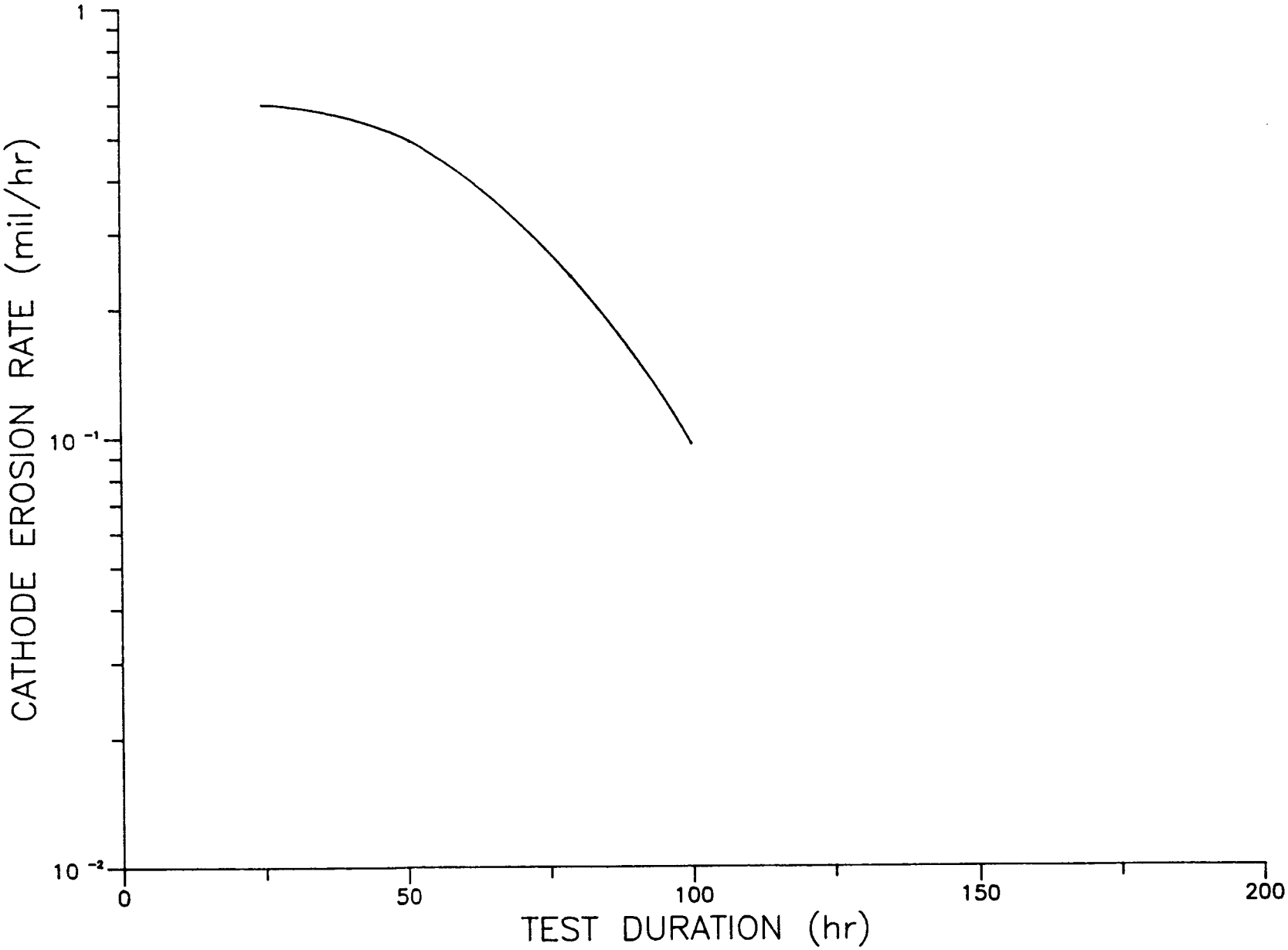

Figure 143. 1KW Arcjet Cathode Erosion Rate

4.0, Conclusions and Recommendations (cont.)

2. Fixed flow split limiting the amount of propellant mass flow which could be heated by the arc.

3. Viscous losses and inefficient expansion of propellant through nozzle.

Each of these causes is the result of thruster design and not a deficiency in the physics of the approach.

One of the goals of the high impedance, vortex stabilized arcjet is to achieve high efficiency by reducing energy loss from the arc and hot core gas to the thruster body. Since the centerline temperature of the arc and gas are estimated to be less for the advanced arcjet than the constricted arcjets of the 1960's (12,000 to 16000 K compared to 30000 to 40000 K), radial temperature gradients in the gas and resultant heat loss should be less for the advanced arcjet. However, for a given specific impulse, the mass averaged temperature of the exhaust gas must be the same for both the constricted arcjet and the advanced arcjet. This implies that more gas must flow through the arc for the advanced arcjet, and that less gas is available for film cooling.

Mixing of the film coolant gas and of the hot core gas in the present thruster design has actually increased the amount of heat transfer to the thruster in the mixing chamber region. In addition, temperature stratification of the flow due to its vortex action was reduced by the abrupt expansionof the gas from the anode to the mixing chamber. To correct these problems, we recommend that the expansion from the anode to the mixing chamber be reduced as shown in Figure 144. Also, the amount of flow used for film cooling should be reduced. This is not possible in the present thruster, but could be included in a future design.

Not only was the absolute amount of film cooling more than required, the ratio of the flow through the arc chamber to the flow injected for film cooling (mass flow_{arc}/mass $\text{flow}_{film\ cooling}$ = 1.5) was too low. To achieve optimum performance from the thruster only 10 to 15 percent of the total

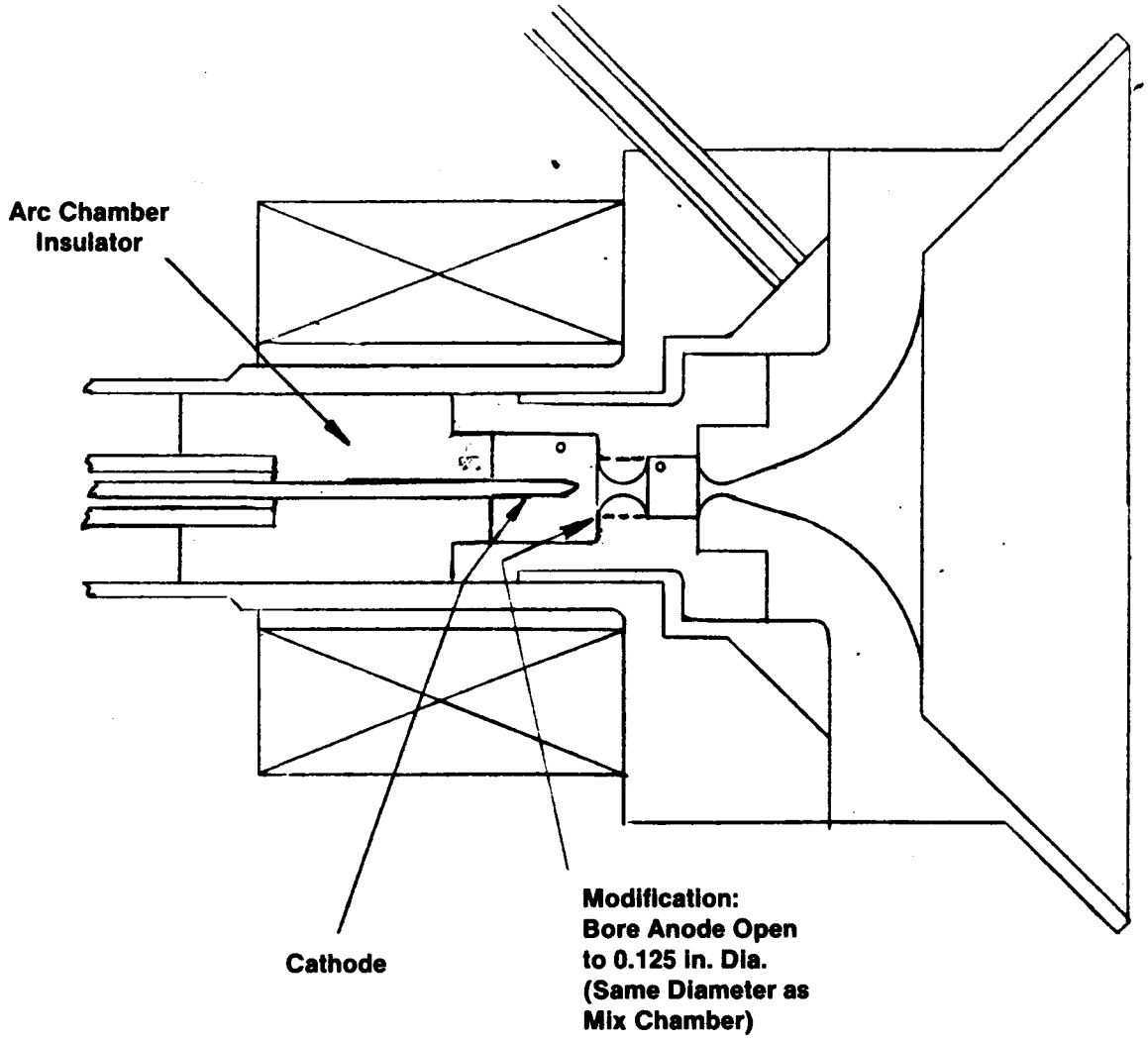

Figure 144. Proposed Modification of Baseline Thruster to Improve Performance

propellant flow should be injected as film coolant. A new thruster with separate flow control is required to determine the optimum amount of film cooling. At the time of the design of the baseline thruster, the sensitivity of the thruster's performance to the amount of film cooling and mixing was not expected. Now in light of the Phase I test results, it is clear that this issue is of primary importance.

The loss mechanisms described above were responsible for the low performance measured from the advanced arcjet thruster. In addition, we feel that through changes to the existing thruster and (or) the design of a new thruster each of these loss mechanisms can be reduced and the performance of the thruster improved.

ASSESSMENT OF FEASIBILITY OF DEVELOPING ARCJET INTO A FLIGHT UNIT

In order for an arcjet to be useful as a thruster, all enabling technologies and components must be suitable for space application. For the advanced arcjet developed during this program, the major areas of concern were:

1. The use of high temperature materials to allow for radiation cooling of dissipated power.

2. The use of a permanent magnet to provide rotation of anode attachment spot.

3. Adapting the arcjet to the characteristics of a flight-weight power conditioning unit (PCU) with adequate current control to provide stable arc operation.

4. The integration of tankage (a flight qualified gas generator for H_2N_4 propellant), valves, and a control system into a propulsion package suitable for commercial and military satellite station keeping.

4.0, Conclusions and Recommendations (cont.)

Since the size of a flight-type arcjet will be small compared to other components of the propulsion unit, the weight penalty for using refractory materials is negligible. The baseline thruster was built using thoriated tungsten and TZM moly. No problems are foreseen using these materials on a flight-type thruster.

The permanent magnet described in section 3.2 was designed to withstand the thermal conditions of the arcjet, while providing the required magnetic field for life of the thruster. The development of rare earth cobalt materials has increased the maximum operating temperature of permanent magnets to approximately 350 C. Testing of the permanent magnet on the thruster planned during Phase I was postponed when the Series 2 testing was restructured to emphasize parametric testing of the thruster. To verify the thermal analysis and life prediction, future testing of the baseline thruster or a modified thruster should be done with the magnet in place.

Development of a flight-weight PCU and the integration of tankage and controls for an arcjet propulsion unit will require only the use of state of the art technology. Flight weight power supplies are currently being developed for high power arcjets by the Air Force; including working being done by Aerojet and Technion under contract to AFAL (F04611-86-C-0118) for a 25 kW arcjet propulsion unit. Storable propellant tankage and high performance hydrazine gas generators (some even flight qualified) are available for integration into an arcjet propulsion unit suitable for a flight experiment.

ASSESSMENT OF BENEFITS OF PURSUING ADVANCED ARCJET CONCEPT

The advanced vortex stabilized arcjet concept was developed to meet NASA's mission requirements for high performance, low power, long life electric propulsion. The requirements include operating for 3000 hours and hundreds of firings. The previous 25 years of research on constricted arc type arcjets has not yielded a device which could meet life time requirements. Therefore, Aerojet and Technion have pursued a completely new approach for arcjets, by scaling down the demonstrated technology developed for high power arc heaters in the 1970's.

4.0, Conclusions and Recommendations (cont.)

The arc heater studies in the 1970's [16,17] showed that a higher average gas enthalpy could be achieved with arc heaters operating with low (12,000 to 16,000K) arc centerline temperatures. Heat losses from arc heaters using high (30,000 to 40,000K) centerline temperature arc reduced their efficiency. A high centerline temperature arc is typical of constricted arc type arcjets and is considered by the authors as a fundamental short coming of the conventional approach to arcjet thrusters.

The development of the advanced arcjet concept is based on creating and maintaining a stable low temperature arc. Operationally, the low temperature arc is achieved by keeping the current density of the arc low and the impedance of the arc high, so at a given power level the current is less than a conventional constricted arc type arcjet. The advantages and disadvantages of operating either a high or low temperature are summarized as follows:

Advantages of Operating in the Lower Temperature Regime are:

a) Profile losses are kept low, i.e., the peak velocity is not higher than about 1.4 times the average gas velocity.

b) The axial heat conduction from the arc channel into each electrode will be lower since there will be smaller temperature differences.

Disadvantages of this Low Temperature Approach are:

a) A higher percentage of the gas flow must flow through the arc, leaving less for film cooling the anode - mixing chamber - nozzle structure. This may require more sophistication in the design of the gas flow system and in the radiation cooling of the anode.

b) There has not been an intensive, long term development of this approach for radiation cooled arc thrusters. Technology transfer from arc heater technology must be used.

c) More interaction between analysis and experiment is needed in order to optimize this type of engine.

4.0, Conclusions and Recommendations (cont.)

Advantages of the High Centerline Temperature Approach are:

a) There is a significant data base of thruster development from the 1960's for this type of engine.

b) There is a thick layer of cool gas between the arc and the constrictor wall, keeping the heat transfer to the wall low.

c) The arc attachment at the anode is self adjusting.

Disadvantages of the High Centerline Temperature Approach are:

a) The high ratio of centerline to wall temperature results in high profile losses, reducing both Isp and efficiency.

Since the most efficient arcjet will be the one with the best coupling of arc power to the gas and the lowest losses, the low centerline temperature arc approach appears best suited for arcjet propulsion. The greatest risk of pursuing this approach is that the technology is far less mature than that for constricted type arcjets, therefore several fundamental issues already addressed for constricted arc type arcjets must be studied for the low centerline temperature advanced arcjet.

PROPOSED APPROACH FOR CONTINUED DEVELOPMENT OF THE ADVANCED ARCJET CONCEPT

In view of the results of Phase I of the program, the advanced, high impedance, vortex stabilized arcjet requires further fundamental research before being advanced to a flight- type hardware development stage. We propose a four step program to advance the technology of the advanced arcjet to that of the conventional constricted arc type arcjet. The steps are as follows:

1. Baseline performance testing of the thruster as currently configured in a low pressure test facility at NASA LeRC.

2. Modification and reevaluation of the existing thruster to improve performance.

3. Design and test a bread-board research thruster based on the data obtained from (2) and Phase I.

4. If test results from (3) are favorable, then the continuation of a limited scope Phase II activity. This program should be oriented towards producing an integrated arcjet propulsion unit.

In order to compare the baseline research thruster to a conventional constricted arc type arcjet, testing in a common facility is recommended. We feel that the thruster should be tested by NASA LeRC in their electric propulsion test facility. The analysis of the Series 2 test data indicates that the thruster should be tested at a higher power and higher mass flow rate than the design point in order to achieve a specific impulse of 400 seconds. In addition, we recommend that a cold flow test of the nozzle be performed to determine its cold thrust coefficient and that the thruster be X-rayed to determine if any welds have been cracked or obstructions in the nozzle exist.

Once the above testing has been completed, we recommend that the design improvements discussed in detail previously be performed, namely:

1. Eliminate anode expansion into the mixing chamber.

2. Increase the nozzle throat diameter and modify the nozzle contour to a conventional shape (i.e. bell or cone).

The thruster should be retested after these modifications. If it is not possible to modify the hardware, we recommend that the thruster be sectioned and material analysis be performed on the internal surfaces.

The above activities (1 and 2) describe a low cost approach for NASA to evaluate most of the conclusions of this report. In order to continue development beyond this, we recommend that a bread-board thruster be supplied for

testing at NASA with Aerojet and Technion personnel assisting in a consultant role. The bread-board unit would have as a minimum, the following design features:

1. Adjustable flow split between the arc chamber and film cooling injection ports.

2. Completely "inspectable" hardware.

3. Arc chamber pressure tap.

4. Allow for nozzle inserts and electrical isolation of the nozzle from the anode.

5. Permanent magnet.

This bread-board thruster could be performance tested at NASA LeRC with consulting provided by Aerojet and Technion at NASA's discretion. At the conclusion of this activity, and assessment could clearly be made by NASA whether further development of the advanced arcjet thruster is warranted.

If further development is approved, we recommend the initiation of a limited scope Phase II of the Arcjet Thruster Research and Technology program. The program would be structured towards producing an integrated arcjet propulsion unit suitable for a 1kW arcjet flight experiment. The program would emphasize design and test activities, with limited check out tests at Aerojet and Technion and the majority of the testing at NASA LeRC.

The above program is a low cost and technically sound approach to continue work on the advanced arcjet. We feel such work is required before a through evaluation of the advanced arcjet concept can be made. The above plan allows for maximum use of NASA facilities and experience.

REFERENCES

1. Duncan, D.B., Makel, D.B., "Arcjet Thruster Research and Technology: State-of-the-Art Assessment," Contract No. NASA 3-24842, February 1986.

2. Wallner, L.E., Czika, J., "Arcjet Thruster for Space Propulsion," NASA Lewis Research Center, NASA-TN-D-2868, June 1965.

3. Cann, Gordon L., Moore, Robert A., Harder, Robert L., and Jacobs, Paul F., "High Specific Impulse Thermal Arcjet Thruster Technology, Part II: Performance of Hall Arcjets with Lithium Propellant," rep. EOS-5090-Final, Electro-Optical Systems, Inc. (AFAPL-TR-65-48, Pt. 2, DDC No. AD-805309), January 1967.

4. Cann, G.L., et al., "Basic Performance Limits of Coaxial Arc Gas Heaters," Paper Presented at IEEE Symposium on Plasma Phenoma and Measurements at San Diego, California, October 30, 1963.

5. John R.R., Bennett, S., Chen, M., and Connors, J.F., Arcjet Engine Performance - Experiment and Theory V." Presented at ARS 17th Annual Meeting, Los Angeles, November 1962, ARS Preprint #62-2667.

6. John, R.R., Bennett, S., Connors, J.F., and Enos, G., "Thermal Arcjet Research," Avco Corp., Report No. ASD-TDR-63-717, June 1963.

7. Bruber, G.G., et al., "Experimental Study of a Transpiration-Cooled, Constricted Arc," Minnesota University Minneapolis Heat Transfer Lab, ARL-68-0023, February 1968, p. 114.

8. Bryson, D.A., et al., "Characteristics of High Voltage Vortex-Stabilized Arc Heaters," IEEE Trans. on Nuclear Science, Volume NS-11, January 1964, p. 41-46.

9. Bunting, K.A., "The Development and Characteristics of an Arc Heater with Hydrogen as the Plasma Working Fluid," 2nd International Conference on Gas Discharges 138-40, 11-15 September 1972, London, England.

10. Rothe, D. W., "Experimental Study of Viscous Low-Density Nozzle Flows: Final Report," Cornell Aeronautical Lab, Report No. NASA-CR-116247, Contract No. NASW-1668, 1971.

11. Sovey, J.S., Penko, P.F., Grisnik, S.P., Whelan, M., "Vacuum Chamber Pressure Effects on Thrust Measurements of Low Reynolds Number Nozzles," NASA Tech Memo 86955, NASA Lewis Research Center, p. 11, 1985.

12. Murch, C.K., Broadwell, J.E., Silver, A.E., and Marcisz, T.J., "Performance Losses in Low Reynolds Number Nozzles," TRW Systems Group, Journal of Spacecraft and Rockets, Vol. 5, p. 1090-1094, 1968.

13. Spisz, E.W., Brinich, P.F., Jack, J.R., "Thrust Coefficients of Low-Thrust Nozzles," NASA Lewis Report No. NASA-TN-D-3056, October 1965.

REFERENCES (cont.)

14. Cline, Michael, C., "VNAP2: A Computer Program for Computation of Two-Dimensional, Time-Dependent, Compressible, Turbulent Flow, "Los Alamos National Laboratory, Report No. LA-8872, August 1981.

15. Duncan, D.B., Cann, G.L., "Advanced 30-kW-Class Arcjet: Monthly Technical Report," No. 0118-M-4, Contract F04611-86-C-0118, January 1987.

16. Morris, J.C., and Yos, G.M., "Radiation Studies of Arc Heated Plasmas," Aerospace Research Laboratories Report ARL 71-9317 (AD#740570).

17. Shaeffer, J.F., "Swirl Arc: A Model for Swirling, Turbulent, Radiative Arc Heater Flowfields," McDonnell Douglas Corp., AIAA J., Vol. 16, No. 10, pp. 1068-1075, October 1978.

18. Cann, G.L., "An Experimental Investigation of a Vortex-Stabilized Arc in an Axial Magnetic Field," USAF Aerospace Research Laboratories, ARL 73-0043, March 1973.

19. Stine, H.A., Watson, V.R., and Shepard, C.E., "Effect of Axial Flow on the Behavior of the Wall-Constricted Arc," AGARDograph 84, Part 1, September 1964.

20. Stine, H.A., and Watson, V.R., "The Theoretical Enthalpy Distribution of Air in Steady Flow Along the Axis of a Direct Current Electric Arc," NASA TN D-1331, August 1962.

21. Watson, V.R. and Pegot, E.B., "Numerical Calculations for the Characteristics of a Gas Flowing Axially Through a Constricted Arc," NASA TN D-4042, June 1967.

22. Graves, R.A. and Wells, W.L., "Preliminary Study of a Wall-Stabilized Constricted Arc," NASA Technical Memorandum X-2700, February 1973.

23. Shaeffer, J.F., "Swirl Arc: A Model for Swirling, Turbulent Radiative Arc Heater Flowfields," McDonnell Douglas Corp., AIAA J. Vol 16, No. 10, October 1978, p. 1068-1075.

24. Marlotte, G.L., Cann, G.L., Harder, R.L., "A Study of Interactions Between Electric Arcs and Gas Flows," ARL Report 68-0049, March 1968, Thermomechanics Research Laboratory, Aerospace Research Laboratories, Wright Patterson Air Force Base, Ohio.

25. John, R.R., Bennett, S., Cass, L.A., Chen, M.M., and Connors, J.F., "Energy Addition and Loss Mechanics in the Thermal Arcjet Engine," Presented at AIAA Electric Propulsion Conference, Colorado Springs, March 1963, AIAA Preprint #63-022.

REFERENCES (cont.)

26. Masser, T.S., and Peterson, R.E., "Axis of Metric Flow in Electric Arcjets and Nozzles," AIAA-84-1385, June 1984.

27. Breingan, W.D., "A Self Consistent Model for the Cathode Region of a High Pressure Arc, I". Inter. Conf. of Plen, in Ionized Gases, 7th Belgrade, Yogoslavia, August 22-27, 1965 Proceedings.

28. Cann, G.L., and Harder, R.L., "Study of Electrode Attachment Regions in High-Current Gaseous Discharges," AEDC Report, EOS N.3240.

29. Ecker, G., "Electrode Components of the Arc Discharge," Ergeb. Exakt. Naturwiss 33, 1-104 (191).

30. Maecker, H., "Messung and Answertung von Bogencharacteristicken (Ar, N_2)," Zeitscrift fur Physik, Vol. 58, 392-404, 1960.

31. Maecker, H., "Plasmastromungen in Lichtobogen Infolge Ergen Magnetischer Kompression," Z. Phys., 14, 198 (1955).

32. Maecker, H., "Uber die Charakteristiken Zyhlindrischer Bogen," Ziet f. Phys, 157, 1-29, 1959.

33. Smith, R.T., Falck, J.L., "Operating Characteristics of a Multimegawatt Arc Heater Used with the Air Force Flight Dynamics Laboratory 50 Mw Facility," AFFDL-TR-69-6, April 1969.

APPENDIX A

AN APPROACH TO THE ANALYTIC OR QUASI-ANALYTIC SOLUTION OF THE ARC-LAMINAR GAS FLOW INTERACTION WHERE THE ARC IS VORTEX STABILIZED

LIST OF SYMBOLS

A	flow cross-sectional area (variable)
B_r	radial component of the magnetic field
B_θ	azimuthal component of the magnetic field
B_z	axial component of the magnetic field
$\|e\|$	charge on the electron
E_z	strength of the axial electric field
h_t	total enthalpy of the gas
j_r	radial component of the current density
j_θ	azimuthal component of the current density
j_z	axial component of the current density
k	Boltzman's constant
m_a	mass of the molecule
$(MW)_a$	molecular weight of the atom
p	gas pressure
r	radial coordinate
R	gas constant
T	gas temperature
u	radial component of velocity
U	specific radiation/volume from the gas
v	azimuthal component of velocity
V_D	dissociation energy of the molecule
V_I	ionization energy of the atom
w	axial component of velocity
z	axial coordinate

LIST OF SYMBOLS (cont.)

α	ionization level
α_{eq}	equilibrium ionization level
β	dissociation level of molecule
β_{eq}	equilibrium dissociation level
γ_m	ratio of specific heats for the molecule
γ_a	ratio of specific heats for the atom
Γ	circulation level in the gas, = rv
θ	azimuthal coordinate
μ	viscosity of the gas
ζ_r	radial vorticity component
ζ_θ	azimuthal vorticity component
ζ_z	axial vorticity component
ρ	density of the gas
σ	electrical conductivity of the gas

EQUATIONS:

The full equations for axisymmetric flow will be presented first, and then the set resulting from simplifying assumptions will be written.

The equation of mass conservation is:

$$\frac{1}{r}\frac{\partial}{\partial r}(r\rho u) + \frac{\partial}{\partial z}(\rho w) = 0 \tag{A1}$$

The radial momentum equatin can be expressed as follows:

$$\rho u \frac{\partial u}{\partial r} + \rho w \frac{\partial u}{\partial z} - \rho \frac{\Gamma^2}{r^3} = -\frac{\partial p}{\partial r} + \frac{\partial}{\partial r}\left(\frac{\mu}{r}\frac{\partial}{\partial r}(ur)\right)$$

$$+ \frac{\partial}{\partial z}\left(\mu \frac{\partial u}{\partial z}\right) + j_\theta B_z - j_z B_\theta \tag{A2}$$

When expressed in terms of the circulation in the gas, Γ, the azimuthal momentum equation is:

$$\frac{\rho u}{r}\frac{\partial \Gamma}{\partial r} + \rho w \frac{\partial \Gamma}{\partial z} = \frac{\partial}{\partial r}\left\{\frac{\mu}{r}\frac{\partial \Gamma}{\partial r}\right\} + \frac{\partial}{\partial z}\left\{\frac{\mu}{r}\frac{\partial \Gamma}{\partial z}\right\} + j_z B_r - j_r B_z \tag{A3}$$

For convenience, the three components of vorticity are listed:

$$\zeta_r = -\frac{1}{r}\frac{\partial \Gamma}{\partial r} \tag{A4}$$

$$\zeta_\theta = \frac{\partial u}{\partial z} - \frac{\partial w}{\partial r} \tag{A5}$$

$$\zeta_z = \frac{1}{r}\frac{\partial \Gamma}{\partial r} \tag{A6}$$

The axial momentum equation is conventionally written as:

$$\rho u \frac{\partial w}{\partial r} + \rho w \frac{\partial w}{\partial z} = -\frac{\partial p}{\partial z} + \frac{1}{r}\frac{\partial}{\partial r}\left\{r\,\mu \frac{\partial w}{\partial r}\right\} + \frac{\partial}{\partial z}\left(\mu \frac{\partial w}{\partial z}\right) \tag{A7}$$

$$+ j_r B_\theta - j_\theta B_r$$

If the cross-sectional area of the flow field and of the arc are independent of z, equation (A7)can be partially integrated and written as:

$$\frac{\partial}{\partial z}\int_0^A (\rho w^2 + p - \mu \frac{\partial w}{\partial z})\, dA = 2\pi r\, (\mu \frac{\partial w}{\partial r} - \rho u w) \qquad (A7a)$$

To date, the most useful equation for investigating arcs has been the enthalpy conservation equation:

$$\rho w \frac{\partial h_t}{\partial r} + \rho w \frac{\partial h_t}{\partial z} = j_z E_z - U + \frac{1}{r}\frac{\partial}{\partial r}(r \chi \frac{\partial T}{\partial r}) + \frac{\partial}{\partial z}(\chi \frac{\partial T}{\partial z}) \qquad (A8)$$

Again, if the cross-sectional area of the flow field and of the arc are independent of z, then a partial integration over $A > A_A$ yields:

$$\frac{\partial}{\partial z}\int_0^A (\rho w\, h_t - \chi \frac{\partial T}{\partial z})\, dA = IE - 2\pi r \{\rho u\, h_t - \chi \frac{\partial T}{\partial r}\} - \int_0^A U dA \qquad (A8a)$$

In the above, if the gas is molecular,

$$h_t = \{\frac{\gamma_m}{\gamma_m - 1}\frac{1-\beta}{2} + \frac{\gamma_a}{\gamma_a - 1}\beta\,(1+\alpha)\}\frac{kT}{m_a} + \frac{u^2 + v^2 + w^2}{2} + \frac{\beta\,|e|\,V_D}{2m_a}$$

$$+ \frac{\beta\alpha\,|e|\,V_I}{m_a} \qquad (A9)$$

Frequently, the thermal energy (1^{st} line of Equation (A9)) and the potential energy at equilibrium, e.g., $B = B_{eq}$ and $\alpha = \alpha_{eq}$ (3^{rd} and 4 terms on right of Equation (A9)) are combined into a single term, called the thermodynamic enthalpy, if the specific heat is integrated over the temperature range from ≈ 300°K to the temperature T. For a number of important reasons, this will not be done here.

Since the pressure is sufficiently high to make Hall effects and thermo-electric effects negligible, Ohm's law can be written as

$$j = \sigma\,(E + uxB) \qquad (A10)$$

The equation of state, for a dissociating, ionizing diatomic gas can be written as

$$\rho = \frac{2\,(M.W.)_a}{1 + \beta + 2\alpha\beta}\frac{p}{RT} \qquad (A11)$$

MODEL AND SIMPLIFYING ASSUMPTIONS

On the basis of observations (Ref [18]) and some physical reasoning, the arc column will be analyzed under assumptions as follows:

1) The arc diameter is constant over its length.

2) The electric field is constant over the length of the arc column.

3) The arc centerline temperature is constant over the length of the column.

4) The radial profile of temperature is similar at each axial position.

5) Gas is injected through the constrictor with a specified constant radial velocity and circulation level over the length of the constrictor.

6) The radial profile of the radial velocity is similar at each axial position.

7) The radial profile of circulation is similar at each axial position.

Under the above assumptions and simplification the equations to be investigated reduce to:

$$\frac{1}{r}\frac{\partial}{\partial r}(r\rho u) + \frac{\partial}{\partial z}(\rho w) = 0$$

$$\rho \frac{\Gamma^2}{r^3} = \frac{\partial p}{\partial r}$$

$$\rho \frac{u}{r}\frac{\partial \Gamma}{\partial r} = \frac{\partial}{\partial r}\left\{\frac{\mu}{\gamma}\frac{2\Gamma}{\partial r}\right\}$$

$$\int_0^A (\rho w + p)\, dA = \int_0^z 2\pi r \left(\mu \frac{\partial w}{\partial r} - \rho u w\right) dz$$

$$\rho u \frac{\partial h_t}{\partial r} = j_z E_z - U + \frac{1}{r} \frac{\partial}{\partial r} \left(r \times \frac{\partial T}{\partial r}\right)$$

$$j_z = \sigma E_z$$

$$\rho = \frac{2m_a}{1 + \beta + 2\alpha\beta} \frac{p}{kT}$$

INVESTIGATION OF THE RELATION BETWEEN THE DISTRIBUTION OF CIRCULATION AND THE MASS FLUX

The equation to be investigated here is:

$$\rho \frac{u}{r} \frac{\partial \Gamma}{\partial r} = \frac{\partial}{\partial r} \left\{ \frac{\mu}{r} \frac{\partial \Gamma}{\partial r} \right\} \tag{A12}$$

There are two ways to investigate this equation:

1) Specify ρu and μ as functions of r and solve for $\Gamma(r)$.

2) Specify Γ and μ as functions of r and solve for $\rho u(r)$.

Some of the implications of the second approach are investigated below.

Typically, in an arc heater, the radial distributions of the circulation, Γ, and the viscosity, μ, will be similar to those shown in Figures A1 and A2.

For convenience these distributions are modeled as follows:

$$\Gamma = \frac{\Gamma_w (1 + \alpha) \eta^2}{1 + \alpha \eta^2} \tag{A13}$$

$$\mu = \frac{\mu_\ell}{1 + \beta \eta^2} \tag{A14}$$

where:

$\eta = r/r_w$

α = constant, greater than unity

β = constant, greater than unity

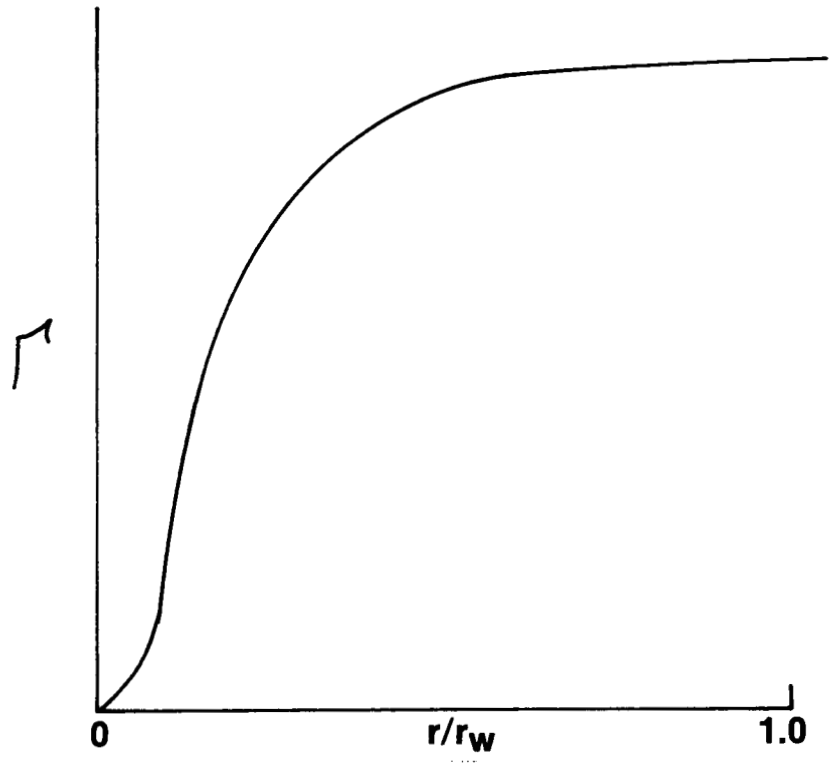

Figure A-1. Schematic of the Radial Distribution of Circulation in an Arc Vortex Chamber

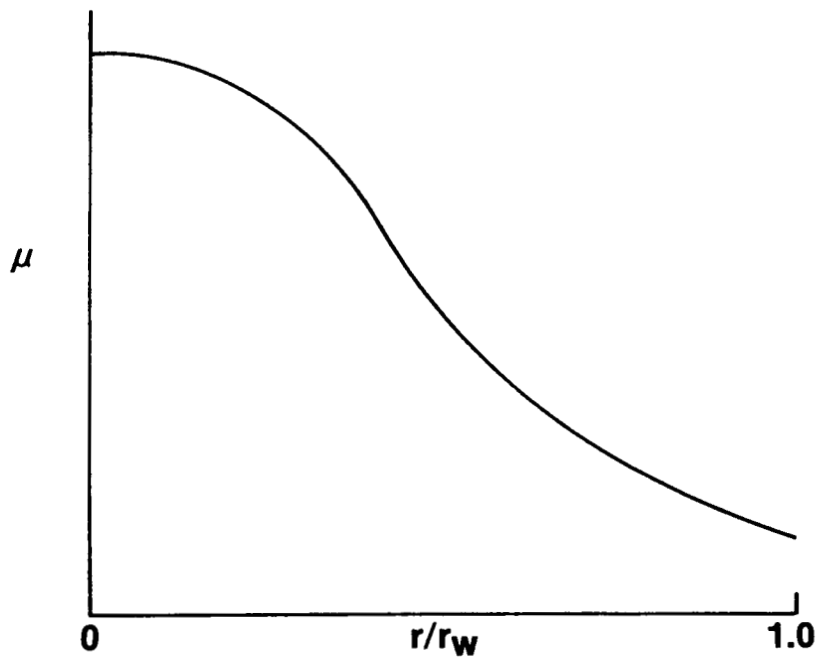

Figure A-2. Schematic of the Radial Distribution of Viscosity in an Arc Constrictor

With these models, the mass flux can be expressed as follows:

$$r\rho w = -2\mu_{\ell} \frac{\eta^2}{1+\beta\eta^2}\left[\frac{2\alpha}{1+\alpha\eta^2}+\frac{\beta}{1+\beta\eta^2}\right] \tag{A15}$$

$$\rho w = \frac{2\mu_{\ell}\, \ell a}{r_w^2}\left\{\frac{2\alpha(1-\alpha\beta\eta^4)}{[1+(\alpha+\beta)\eta^2+\alpha\beta\eta^4]^2}+\frac{\beta(1-\beta\eta^2)}{(1+\beta\eta^2)^3}\right\} \tag{A16}$$

$$\dot{m}_{core} = \frac{4\pi\mu\ \ell a}{1+\beta/\alpha}\left(1+\frac{\beta/\alpha}{1+\beta/\alpha}\right) \tag{A17}$$

$$\dot{m}_{total} = \frac{4\pi\mu\ \ell a}{1+\beta}\left[\frac{2\alpha}{1+\alpha}+\frac{\beta}{1+\beta}\right] \tag{A18}$$

On the basis of this investigation, some rather startling conclusions can be drawn.

1) There is a limit to the amount of mass flux that can be processed through a vortex. The maximum occurs with constant viscosity and a vortex core diameter much smaller than the wall diameter. In this case

$$\dot{m}_{total} = 8\pi\mu_{\ell}\ell a$$

2) The mass flux through the vortex core, for constant viscosity, is always more than 1/2 of the total mass flow.

3) Conclusions (1) and (2) are valid for all levels of circulation.

4) The distribution of viscosity decreases the mass flow rate that can be processed through the vortex.

5) The gas always flows radially inward.

6) The viscosity distribution appears to cause the axial velocity to reverse and flow backward at outer radial locations. The solutions do not indicate reverse flow for constant viscosity.

Solutions have been made using other models for the radial distribution of circulation and viscosity. These solutions lead to the same conclusions, (1) through (6) above.

Conclusions (1) through (5) would appear to be generally valid. More detailed investigations are needed to determine whether (6) is an artifact of the modeling or a manifestation of some physical phenomenon. Besides this, a number of other questions require investigation, e.g.

1) At what level of r_w, does this limiting effect of mass flux cease?

2) If more mass flow rate than the computed maximum is injected into a vortex chamber, what happens?

APPENDIX B

PLASMA FLOW EQUATIONS

Model Development

In the equations used to describe the plasma flow, the question has been raised as to the difference between the Navier-Stokes equations for compressible flow and incompressible flow. This problem has been studied.

Summarizing briefly the results:

1) In the continuity equation, the density term must stay inside of the differential.

2) In the momentum equations:

   - The convective terms are identical.

   - In Cartesian coordinates, the pressure term is modified by a term as follows:

$$p \rightarrow p + \mu \left(2 \frac{\partial w}{\partial x} - \frac{2}{3} \operatorname{div} \bar{w}\right).$$

When the pressure is about 1 atm, the additional term is negligible.

   - The viscous terms must keep the viscosity inside of the differential, e.g., in the angular momentum equation the viscous term is:

$$r \frac{\partial}{\partial r} \left(\frac{\mu}{r} \frac{\partial \Gamma}{\partial r}\right)$$

- The equation of state must be used to define the density.

- The compressible enthalpy equation must be solved for the temperature distribution. With energy input from an electrical discharge, the viscous dissipation terms can be neglected.

A model for the radial distribution of circulation has been proposed and used to investigate the implications of momentum conservation. The model has the following properties.

1) Near the origin, the gas rotates as a solid body.

2) Near the wall, but outside of the boundary layer, the product of the aximuthal velocity and the radius remains constant.

3) Near the wall, but still outside of the boundary layer, the level of circulation is a constant, independent of axial position.

As with all models, this one has limitations. When compared with the measured values of spin velocity. The following observations can be made:

1) The model matches the values of measured spin velocity fairly accurately at all radial locations greater than where the peak spin velocity occurs.

2) The measured spin velocities for smaller radii are higher by 20-30% than the values predicted from the model.

In low-power arcjets, when the gas is spinning, there can be very pronounced radial gradients in the axial velocity. There will also be significant radial gradients in the temperature. All of these effects make it difficult to define a Mach 1 location. Simultaneously, it becomes extremely difficult to establish a discharge coefficient, C_D, in the following equation:

$$\dot{m} = C_D \frac{4\, p_c\, A^*}{a_c}.$$

For instance, in some cold-flow tests conducted recently at Technion, where there was a high value of spin in the gas, values of

$$C_D \simeq 0.35 \text{ to } 0.42$$

were estimated, based on the chamber pressure measured just upstream of the vortex injection holes. Without the spin, a value,

$$C_D \simeq 0.98$$

was anticipated.

An investigation of this problem was conducted. The Mach number was not being used. Rather, using the mass and momentum conservation equations, relations were established among the following nondimensional variables:

A mass flow variable $$X = \frac{a \dot{m}}{A p_o}$$

A spin variable $$Z = \frac{\Gamma w}{r_w a}$$

A wall drag variable $$Y = \frac{6 \pi \mu \ell a}{A p_o}$$

The pressure ratio $$P = \bar{p}/p_o$$

In the above equations:

T = gas temperature = constant

a = speed of sound

A = flow cross-sectional area

p_o = wall pressure at upstream end

$\bar{p}$ = average pressure at each flow cross-section

Γ_w = peak circulation in the gas

r_w = radius of the flow channel

μ = viscosity of the gas

ℓ = length of the flow channel

Once closed-form relations have been established among X, Z, Y, and P; Z and Y are held constant and the maximum value of X as a function of P is found. This criterion is used to establish the critical flow rather than the sonic condition which is ambiguous with the pronounced radial gradients that occur throughout the whole flow field.

APPENDIX C

SCALING LAWS FOR ARC THRUSTERS

INTRODUCTION

There are three sets of variables that need to be given consideration in establishing scaling laws. These are:

1) Performance Parameters (User Interface)

- Power level
- Specific impulse
- Thrust efficiency
- Thrust level
- Lifetime
- Engine weight
- Engine size

2) Controllable Quantities (Engineering Interface)

- Type of propellant
- Mass flow rate and the distribution of its injection
- Circulation level of gas injected into the vortex chamber
- Discharge current
- Geometry of the engine and nozzle
- Stability effects of interaction between the arc and the power supply

3) Operational Parameters (Scientific Interface)

- Peak temperature in the electrical discharge
- Heat flux rates at all critical locations
- Chamber pressure
- Voltage drop across the discharge
- Reynolds number effects (laminar vs. turbulent flow)
- Arc stability effects

In practice, scaling laws for any magneto-fluid-dynamic device can consist of any one of the following:

a) Relations among controllable parameters and output performance quantities can be obtained from making analytic solutions to all of the relevant magneto-hydrodynamic equation. Simultaneously, the solutions must ensure that the values of important operational quantities, e.g., potential drop across the discharge, wall heat flux at all critical locations, etc., must fall within limits controlled by materials properties and facility limitations.

b) Same as a), only replace "analytic solutions" by "an adequate number of numerical solutions."

c) Assembly all relevant experimental data. Using cross-plots, nondimensional parameters, etc., and ingenuity, establish relations between Group 1) and Group 2) parameters. As feasible, also establish relations between Group 3) and Group 2) parameters.

DISCUSSION

If Approaches a) and b) can, in reality, be carrier out, then an optimum arc thruster can be designed and built to meet specified performance requirements, e.g., maximum Isp, maximum life, etc. Despite numerous attempts, however [19,20,21,22,23,24,25,26] practical scaling laws have not resulted from these approaches without "calibration" of "constants" or codes. This is not totally surprising since the analysis must include, at least, all of the following:

1. A solution to the arc-gas flow interaction in the region between the cathode attachment and the column. This region is dominated by what can be called current-density constrictions; this results in the highest power dissipation per unit length of the arc and usually the highest temperature seen anywhere in the arc. As gas is pumped electromagnetically through the expanding arc column, it can be heated to the highest enthalpy available from arcs. For this reason, when the driving design criterion is the attainment of maximum specific impulse, as occurred in the 1960's, many of the arc thrusters were designed to

capitalize on heating the gas in this region only and were hence short enough so that no recognizable arc column developed (References 23, 386). Because this region is dominated by nonequilibrium effects, analytic solutions to the relevant equations have only been partially successful (References 27,38,29).

2. A solution to the arc-gas flow interaction in the constrictor region. This must include the constraints on the axial and radial flow of gas imposed by introducing the gas with some circulation level. Simultaneously, the parameters of the vortex core must be solved for. In most arc heaters and thrusters, where gas flow has been mapped, gas has been found to flow upstream (away from the nozzle) in the radial positions near the constrictor wall over some fraction of the constrictor length. To date, no analytic or, for that matter, numerical code for arc heaters has been able to predict this type of flow and its influence on arc properties and gas heating.

3. Some method of accurately predicting the centerline temperature of the arc over its length, from the cathode attachment to the anode attachment. Some success has been achieved in calculating arc temperatures in the column region for wall-constricted arcs (References 30,31,32). Typically, temperatures calculate out to be close to that found for wall-confined arcs with negligible gas flow through the channel. In these cases, centerline temperatures are related to wall heat fluxes and, hence, the calculation of temperature distribution and peak centerline

temperature represents the solution to a well-defined thermal boundary value problem. This is not the case for a vortex-stabilized arc where the radial inward mass flow often precludes any conducted or convected energy from the arc from ever reaching the "constrictor" wall. In such cases, the determination of an arc centerline temperature is no longer a well-defined thermal boundary value problem, and alternate methods of evaluating the centerline temperature and radial temperature distribution must be investigated.

When a high percentage of the heating of the gas is done in a constrictor where the arc is wall-confined, then reasonably useful and accurate scaling laws have been derived and found useful in designing high-current (over 1000 amps), low-pressure (under 10 atmospheres), high-power (over 100 kW) wind tunnels. These scaling laws are only marginally useful to the 1 kW arc thruster program for the following reasons:

1. Wall confining a low-current (under 10 amps) arc leads to unacceptably high wall heat fluxes.

2. Turbulent flow occurs in almost all arc wind tunnels. The flow is likely to be totally laminar in the 0.5-3.0 kW arc thruster.

For arc heaters/thrusters that are not wall confined, data correlation techniques have been relied upon almost exclusively for establishing scaling laws (References 18,33). Such techniques can be very useful and accurate for interpolation over the range of controllable parameters where data have been acquired. Extrapolation outside of the data base must be done with great caution.

CONCLUSIONS

In view of the limitations of existing analytic and experimental arc heater and arc thruster studies, great care must be exercised in extrapolating these data to the low power level of this program (0.5 to 3.0 kW).

APPENDIX D

PREPARATION OF PERFORMANCE ESTIMATE CHARTS FOR GASEOUS PROPELLANTS

The following steps are followed in generating these charts:

1) Using the thermodynamic data from the JANAF tables, the equilibrium partial pressures for all constituents are computed.

2) The equilibrium enthalpy change, h, entropy, S, and molecular weight, MW, are computed using the partial pressures from No. 1.

3) The "frozen" specific heat, $(C_p)_f$, is computed. Using this quantity, the ratio of the specific heats, γ_f, is computed for frozen flow.

$$\gamma_f = C_o/C_p = R/MW$$

4) The speed of sound for frozen flow is computed.

$$a_c = \sqrt{\gamma_f \frac{RT}{MW}}$$

5) The flow coefficient, γ_f, is computed.

$$\gamma_f = \gamma_f \left(\frac{2}{\gamma_f + 1}\right)^{\frac{\gamma_f + 1}{2(\gamma_f - 1)}}$$

6) Assume a power transferred to the gas, P_C.

7) Assume a set of values for C_F/C_D.

8) Compute a mass flow raee.

$$\dot{m} = P_c/\Delta h$$

9) Compute an exhaust velocity, w.

$$w = \frac{C_F}{C_D} \frac{a_c}{\gamma}$$

10) Compute a thrust.

$$F = \dot{m}w$$

11) Compute a specific impulse.

$$Isp = \frac{C_F \; a_c}{C_D \; \gamma_f g}$$

12) Plot Isp vs. F over desired temperature range and desired range of C_F/C_D.

APPENDIX E

THRUST STAND CALIBRATION DATA

A calibration of the thrust stand was performed before and after each performance test during Test Series 2. The calibration was done by applying a known force to the thrust stand (measured with a calibrated load beam) and recording the force measured by the load beam used for the thrust measurement. The accuracy of the load beams was checked periodically by loading them with precision weights. The effect on the thrust measurement caused by pressurization of propellant and the cooled power leads was also measured and found to be insignificant.

The pre- and post-test calibration was computer controlled. The computer controller commands two fast acting solenoid valves, one which pressurizes the system and one which vents the system. Pressurized nitrogen was used to expand a bellows which pushed a calibrated load cell up against the thrust stand. The thrust stand was loaded in increments of approximately 10 gm from 0 to 50 gm and then the load was reduced in 10 gm increments back to 0 gm. At each step in the calibration, the computer controller would wait a sufficient time (30 to 90 sec) to allow the stand to reach a steady reading, and then would collect data for that step. A sample output for test AJ1K023 is shown in Figure 1F. The output data was reduced to determine the average tare at each load step, the initial and final zero offsets. Test were only conducted if the pre-test calibration indicated that the stand was reading properly (i.e., $Tare_{ave} < 10\%$, and no significant difference in zero at beginning and end of calibration).

From the thrust stand calibration the tare and offset corrections for the thrust measurement were determined as follows:

$$\text{Tare} = \text{Force}_{actual}/\text{Force}_{measured}$$

Initial Offset = load beam measurement with no propellant flow immediately prior to test

Final Offset = load beam measurement with no propellant flow immediately after test

$$\text{Thrust}_{cor} = \text{Tare}*(\text{Force}_{meas} - \text{initial offset})$$

When the final stand offset differed from the initial stand offset due to thermal drift of the stand and load cell the offset was determined by linear interpolation during the test. Table 1F summarizes the corrections to the measured thrust for the performance data included in this report.

TEST NO. THRUST CAL PRE AJ1K023
DATE 12/11/86
DISK VOLUME NO. 45

(SECS)	(LBS)	(LBS)	(LBS/LBS)
DATE: 12/11/86	TIME:	09:21:57	THRUST STAND CALIBRATION - CAL STEP 1
0.2	0.0001	-0.0001	****
0.8	0.0001	-0.0001	****
1.4	0.0001	-0.0001	****
2.2	0.0001	0.0000	****
2.8	0.0001	0.0000	****
3.4	0.0001	0.0000	****
4.3	0.0001	0.0000	****
4.8	0.0001	-0.0003	****
5.7	0.0001	-0.0002	****
6.3	0.0001	-0.0002	****
6.8	0.0001	-0.0001	****
7.7	0.0001	-0.0001	****
8.3	0.0001	0.0000	****
9.1	0.0001	0.0000	****
DATE: 12/11/86	TIME:	09:24:10	THRUST STAND CALIBRATION - CAL STEP 2
0.5	0.0061	0.0059	1.0338
1.3	0.0061	0.0059	1.0338
1.9	0.0061	0.0059	1.0338
2.5	0.0061	0.0061	1
3.3	0.0063	0.0061	1.0327
3.9	0.0063	0.0062	1.0161
4.5	0.0065	0.0063	1.0317
5.3	0.0065	0.0063	1.0317
5.9	0.0065	0.0063	1.0317
6.9	0.0065	0.0063	1.0317
7.5	0.0065	0.0063	1.0317
8.3	0.0067	0.0063	1.0634
8.9	0.0067	0.0063	1.0634
DATE: 12/11/86	TIME:	09:25:01	THRUST STAND CALIBRATION - CAL STEP 3
0.6	0.0137	0.0131	1.0458
1.4	0.0137	0.0131	1.0458
2.0	0.0137	0.0131	1.0458
2.8	0.0138	0.0132	1.0454
3.4	0.0138	0.0132	1.0454
4.3	0.0138	0.0132	1.0454
4.9	0.0139	0.0132	1.053
5.7	0.0139	0.0133	1.0451
6.3	0.0140	0.0133	1.0526
7.1	0.0140	0.0134	1.0447
7.7	0.0141	0.0134	1.0522
8.6	0.0142	0.0134	1.0597
9.2	0.0142	0.0135	1.0518
DATE: 12/11/86	TIME:	09:25:52	THRUST STAND CALIBRATION - CAL STEP 4
0.4	0.0197	0.0189	1.0423

TEST NO. THRUST CAL PRE AJ1K023
DATE 12/11/86
DISK VOLUME NO. 45

(SECS)	(LBS)	(LBS)	(LBS/LBS)
1.2	0.0197	0.0189	1.0423
2.0	0.0197	0.0190	1.0368
2.6	0.0198	0.0190	1.0421
3.5	0.0198	0.0190	1.0421
4.1	0.0199	0.0190	1.0473
4.6	0.0199	0.0190	1.0473
5.5	0.0199	0.0190	1.0473
6.1	0.0200	0.0191	1.0471
6.6	0.0200	0.0192	1.0416
7.2	0.0201	0.0192	1.0468
8.0	0.0201	0.0193	1.0414
8.6	0.0202	0.0193	1.0466
9.2	0.0202	0.0193	1.0466
DATE: 12/11/86	TIME:	09:26:40 THRUST STAND CALIBRATION - CAL STEP 5	
0.1	0.0242	0.0235	1.0297
1.0	0.0242	0.0235	1.0297
1.5	0.0242	0.0235	1.0297
2.4	0.0244	0.0235	1.0382
3.0	0.0244	0.0235	1.0382
3.5	0.0244	0.0236	1.0338
4.4	0.0245	0.0237	1.0337
5.0	0.0245	0.0237	1.0337
5.8	0.0246	0.0237	1.0379
6.4	0.0249	0.0237	1.0506
7.2	0.0249	0.0238	1.0462
7.9	0.0249	0.0238	1.0462
8.7	0.0249	0.0239	1.0418
DATE: 12/11/86	TIME:	09:27:29 THRUST STAND CALIBRATION - CAL STEP 6	
0.5	0.0287	0.0279	1.0286
1.3	0.0287	0.0279	1.0286
1.9	0.0288	0.0279	1.0322
2.7	0.0288	0.0279	1.0322
3.3	0.0288	0.0280	1.0285
3.9	0.0289	0.0280	1.0321
4.7	0.0291	0.0280	1.0392
5.3	0.0291	0.0280	1.0392
6.2	0.0291	0.0281	1.0355
6.8	0.0291	0.0281	1.0355
7.6	0.0291	0.0281	1.0355
8.2	0.0291	0.0282	1.0319
8.8	0.0291	0.0282	1.0319
DATE: 12/11/86	TIME:	09:28:17 THRUST STAND CALIBRATION - CAL STEP 7	
0.3	0.0333	0.0325	1.0246
1.1	0.0334	0.0326	1.0245
1.7	0.0335	0.0326	1.0276

TEST NO. THRUST CAL PRE AJ1K023
DATE 12/11/86
DISK VOLUME NO. 45

(SECS)	(LBS)	(LBS)	(LBS/LBS)
2.6	0.0335	0.0326	1.0276
3.2	0.0335	0.0328	1.0213
3.7	0.0335	0.0328	1.0213
4.3	0.0336	0.0328	1.0243
5.1	0.0338	0.0328	1.0304
5.8	0.0338	0.0328	1.0304
6.6	0.0338	0.0329	1.0273
7.2	0.0339	0.0330	1.0272
8.0	0.0339	0.0330	1.0272
8.6	0.0339	0.0330	1.0272
DATE: 12/11/86	TIME:	09:29:08 THRUST STAND CALIBRATION - CAL STEP 8	
0.2	0.0394	0.0389	1.0128
1.0	0.0394	0.0389	1.0128
1.8	0.0394	0.0389	1.0128
2.4	0.0394	0.0389	1.0128
2.9	0.0394	0.0390	1.0102
3.6	0.0394	0.0390	1.0102
4.1	0.0395	0.0390	1.0128
5.0	0.0395	0.0391	1.0102
5.6	0.0396	0.0391	1.0127
6.4	0.0396	0.0391	1.0127
7.0	0.0397	0.0391	1.0153
7.8	0.0397	0.0392	1.0127
8.4	0.0399	0.0392	1.0178
9.0	0.0399	0.0393	1.0152
DATE: 12/11/86	TIME:	09:29:56 THRUST STAND CALIBRATION - CAL STEP 9	
0.3	0.0437	0.0433	1.0092
1.1	0.0437	0.0433	1.0092
1.7	0.0437	0.0433	1.0092
2.3	0.0437	0.0433	1.0092
3.1	0.0437	0.0434	1.0069
3.7	0.0439	0.0434	1.0115
4.5	0.0439	0.0435	1.0091
5.1	0.0439	0.0435	1.0091
5.7	0.0439	0.0436	1.0068
6.3	0.0439	0.0436	1.0068
7.1	0.0439	0.0436	1.0068
7.7	0.0439	0.0436	1.0068
8.3	0.0440	0.0438	1.0045
8.9	0.0443	0.0438	1.0114
DATE: 12/11/86	TIME:	09:30:48 THRUST STAND CALIBRATION - CAL STEP 10	
0.6	0.0358	0.0366	.9781
1.1	0.0358	0.0367	.9754
2.0	0.0360	0.0367	.9809
2.6	0.0360	0.0367	.9809

TEST NO. THRUST CAL PRE AJ1K023
DATE 12/11/86
DISK VOLUME NO. 45

(SECS)	(LBS)	(LBS)	(LBS/LBS)
3.4	0.0360	0.0367	.9809
4.0	0.0361	0.0367	.9836
4.8	0.0361	0.0369	.9783
5.4	0.0361	0.0369	.9783
6.3	0.0362	0.0370	.9783
6.9	0.0362	0.0370	.9783
7.7	0.0363	0.0370	.981
8.3	0.0363	0.0370	.981
9.1	0.0365	0.0370	.9864
DATE: 12/11/86	TIME:	09:31:56 THRUST STAND CALIBRATION - CAL STEP 11	
0.5	0.0304	0.0313	.9712
1.3	0.0304	0.0313	.9712
1.9	0.0304	0.0313	.9712
2.8	0.0304	0.0314	.9681
3.4	0.0304	0.0312	.9743
4.2	0.0307	0.0312	.9839
4.8	0.0307	0.0315	.9746
5.6	0.0307	0.0315	.9746
6.2	0.0308	0.0316	.9746
7.1	0.0308	0.0316	.9746
7.7	0.0308	0.0317	.9716
8.5	0.0309	0.0317	.9747
9.1	0.0310	0.0318	.9748
DATE: 12/11/86	TIME:	09:33:04 THRUST STAND CALIBRATION - CAL STEP 12	
0.2	0.0256	0.0265	.966
1.0	0.0256	0.0268	.9552
1.6	0.0257	0.0268	.9589
2.2	0.0257	0.0269	.9553
3.0	0.0257	0.0269	.9553
3.6	0.0258	0.0269	.9591
4.2	0.0258	0.0269	.9591
5.0	0.0258	0.0269	.9591
5.6	0.0258	0.0270	.9555
6.5	0.0260	0.0270	.9629
7.1	0.0260	0.0271	.9594
7.9	0.0260	0.0271	.9594
8.5	0.0261	0.0271	.963
9.1	0.0261	0.0273	.956
DATE: 12/11/86	TIME:	09:34:13 THRUST STAND CALIBRATION - CAL STEP 13	
0.2	0.0211	0.0222	.9504
1.0	0.0211	0.0222	.9504
1.6	0.0213	0.0222	.9594
2.4	0.0213	0.0223	.9551
3.0	0.0214	0.0223	.9596
3.6	0.0214	0.0224	.9553

TEST NO. THRUST CAL PRE AJ1K023
DATE 12/11/86
DISK VOLUME NO. 45

(SECS)	(LBS)	(LBS)	(LBS/LBS)
4.2	0.0215	0.0224	.9598
4.8	0.0215	0.0225	.9555
5.6	0.0215	0.0225	.9555
6.2	0.0216	0.0225	.9599
7.0	0.0218	0.0225	.9688
7.6	0.0218	0.0226	.9646
8.5	0.0218	0.0226	.9646
9.1	0.0219	0.0226	.969
DATE: 12/11/86	TIME:	09:35:20 THRUST STAND CALIBRATION - CAL STEP 14	
0.5	0.0159	0.0164	.9695
1.1	0.0159	0.0164	.9695
1.7	0.0160	0.0164	.9756
2.2	0.0160	0.0164	.9756
3.1	0.0161	0.0165	.9757
3.7	0.0161	0.0165	.9757
4.2	0.0163	0.0165	.9878
5.1	0.0163	0.0165	.9878
5.7	0.0164	0.0166	.9879
6.2	0.0164	0.0166	.9879
6.8	0.0164	0.0166	.9879
7.4	0.0164	0.0166	.9879
8.2	0.0164	0.0167	.982
8.8	0.0164	0.0167	.982
DATE: 12/11/86	TIME:	09:36:28 THRUST STAND CALIBRATION - CAL STEP 15	
0.2	0.0112	0.0115	.9739
0.9	0.0113	0.0116	.9741
1.7	0.0113	0.0117	.9658
2.3	0.0115	0.0117	.9829
3.2	0.0115	0.0118	.9745
3.8	0.0115	0.0118	.9745
4.6	0.0116	0.0119	.9747
5.2	0.0116	0.0120	.9666
6.0	0.0117	0.0120	.9749
6.6	0.0117	0.0120	.9749
7.5	0.0118	0.0121	.9752
8.1	0.0118	0.0121	.9752
8.9	0.0119	0.0121	.9834
DATE: 12/11/86	TIME:	09:37:35 THRUST STAND CALIBRATION - CAL STEP 16	
0.2	0.0063	0.0063	1
0.9	0.0063	0.0063	1
1.4	0.0063	0.0063	1
2.3	0.0063	0.0064	.9843
2.9	0.0063	0.0064	.9843
3.4	0.0065	0.0064	1.0156
4.3	0.0065	0.0064	1.0156

TEST NO. THRUST CAL PRE AJ1K023
DATE 12/11/86
DISK VOLUME NO. 45

(SECS)	(LBS)	(LBS)	(LBS/LBS)
4.9	0.0065	0.0067	.9701
5.4	0.0066	0.0067	.985
6.3	0.0066	0.0067	.985
6.9	0.0067	0.0068	.9852
7.4	0.0067	0.0069	.971
8.0	0.0067	0.0069	.971
8.9	0.0068	0.0070	.9714
DATE: 12/11/86	TIME:	09:38:37	THRUST STAND CALIBRATION - CAL STEP 17
0.2	-0.0001	-0.0002	****
0.9	-0.0001	-0.0002	****
1.8	-0.0001	-0.0002	****
2.4	-0.0001	-0.0002	****
3.2	-0.0001	-0.0002	****
3.8	0.0000	-0.0002	****
4.7	0.0000	-0.0005	****
5.2	0.0000	-0.0005	****
6.1	0.0000	-0.0004	****
6.7	0.0000	-0.0002	****
7.2	0.0000	-0.0002	****
8.1	0.0000	-0.0002	****
8.7	0.0000	-0.0002	****
9.2	0.0000	-0.0002	****

TEST NO. THRUST CAL PRE AJ1K023
DATE 12/11/86
DISK VOLUME NO. 45

CAL STEP NO.	FCAL AVG (LBS)	FLC AVG (LBS)	TARE AVG (LBS/LBS)
1	1E-04	-1E-04	****
2	6.3E-03	6.1E-03	1.0335
3	.0139	.0132	1.0487
4	.0199	.019	1.0441
5	.0245	.0236	1.0377
6	.0289	.028	1.0332
7	.0336	.0327	1.0262
8	.0395	.039	1.0129
9	.0438	.0435	1.0083
10	.0361	.0368	.9801
11	.0306	.0314	.9738
12	.0258	.0269	.9589
13	.0215	.0224	.9591
14	.0162	.0165	.9809
15	.0115	.0118	.9747
16	6.5E-03	6.5E-03	.9885
17	0	0	****

DATA SUMMARY

FORMULA: TARE = A + B * FLC
A = .982373257
B = .688918795
SIGMA^2 = 6.11185371E-05
AVG TARE = .998765791

TABLE 1E

SUMMARY THRUST STAND TARE CORRECTIONS

Run No.	Calculated Tare	Initial Offset (lbf)	Final Offset (lbf)
AJ1K004	1.00	0.0007	0.0068
AJ1K005	1.00	-0.0007	0.0112
AJ1K016	0.90	0.0002	0.0006
AJ1K017	0.903	0.0004	0.0008
AJ1K018	0.904	0.0009	0.0023
AJ1K019	0.903	0.0000	0.0008
AJ1K023	0.993	-0.0002	0.0081
AJ1K026	1.02	0.0001	0.0062

APPENDIX F

SERIES 2 TEST DATA

```
]LIST

10  REM  PROGRAM REDUCES 1KW ARCJET DATALOGGER OUTPUT
20  REM  "ARCREDL10"
30  REM  C.M.GRACEY  12/11/86
35  HIMEM: 40000
40  DIM CD$(50),CD(50),A$(10)
42  HOME
44  INPUT "VOLUME NO. ";VN
45  FOR N = 1 TO 3:A$(N) = "": NEXT N
46  PRINT  CHR$ (4)"BLOAD READWRIT.OBJ,S7,V2"
48  POKE 769,VN: POKE 773,2
49  CALL 768
50 NC = 8:K = 1:KK = 1
52 W$ = "TIME    " + "TAS1    " + "TAS2    " + "TAS3    " + "TAS4    " +
     "TAS5    " + "TAS6    " + "TAS7    " + "THCI    "
53 W$ = W$ + "THCE    " + "TCO     " + "TFI     " + "TFO     " + "TPS
      " + "TMG     " + "TF2     " + "TGG     "
54 W$ = W$ + "TMCI    " + "TMCO    " + "TARS    " + "PPS     "
55 X$ = "(SECS)  " + "(F)     " + "(F)     " + "(F)     " + "(F)     " +
     "(F)     " + "(F)     " + "(F)     " + "(F)     "
56 X$ = X$ + "(F)     " + "(F)     " + "(F)     " + "(F)     " + "(F)
      " + "(F)     " + "(F)     " + "(F)     " + "(F)     "
57 X$ = X$ + "(F)     " + "(F)     " + "(PSIG)  "
58 Y$ = "PUF1    " + "PDF1    " + "PUF2    " + "PDF2    " + "PVCB    " +
     "PVCT    " + "PAO     " + "PARS    " + "IAM     " + "IA      "
59 Y$ = Y$ + "VA      " + "VAM     " + "FCAL    " + "FLC     " + "AL1
      " + "PWR     " + "FVAC    " + "WPG     " + "ISV     " + "EFF     "
60 Z$ = "(PSIG)  " + "(PSIG)  " + "(PSIG)  " + "(PSIG)  " + "(MICRS) " +
     "(MV)    " + "(PSIG)  " + "(PSIG)  " + "(AMPS)  " + "(AMPS)  "
61 Z$ = Z$ + "(VOLTS) " + "(VOLTS) " + "(LBS)   " + "(LBS)   " + "(MV)
      " + "(WATTS) " + "(LBS)   " + "(MGS/S) " + "(SEC)   " + "(%)     "
64  INPUT "TEST NO. ";TN$
65  INPUT "DATE ";DA$
68  PRINT  CHR$ (4)"PR#2"
70  PRINT  CHR$ (9)"1D"
72  PRINT  CHR$ (9)"7P"
74  PRINT  CHR$ (9)"1T"
76  PRINT  CHR$ (9)"Z"
78  PRINT  CHR$ (27)"E"
80  PRINT  CHR$ (27)"&l1O"
82  PRINT  CHR$ (27)"(s16.66H"
84  PRINT  CHR$ (27)"&s0C"
88  PRINT  CHR$ (12)
90  CALL 768:I = 511
95  IF J = 192 THEN  PRINT  CHR$ (4)"PR#0": END
96  PRINT  SPC( 80)"PAGE NO. "KK: PRINT : PRINT "TEST NO. "TN$: PRINT "DA
     TE "DA$: PRINT "DISK VOLUME NO. "VN
97  PRINT
98  PRINT  SPC( 3)W$: PRINT  SPC( 3)X$: PRINT  SPC( 7)Y$: PRINT  SPC( 7)Z
     $
100  PRINT
105  FOR N = 1 TO 3
110 A$(N) = ""
115  IF I = 767 THEN I = 511: CALL 786
120 J =  PEEK (I + 1): IF J = 192 THEN  PRINT  CHR$ (12): PRINT  CHR$ (4)
     "PR#0": END
122  IF J = 135 THEN  PRINT D$:I = I + 1: GOTO 255
```

```
125  IF J = 141 THEN I = I • 1: GOTO 200
130 A$(N) = A$(N) +  CHR$ (J - 128):I = I + 1: GOTO 115
200  IF  LEN (A$(N)) = 72 THEN 220
201  IF  LEN (A$(N)) <  > 128 THEN D$ = A$(N): GOTO 105
206  IF  LEN (A$(N)) <  > 128 THEN 105
210  NEXT N
220  IF N < 3 THEN 105
230 A$ = A$(1) +  LEFT$ (A$(2),40)
235  GOSUB 1000
237 A$(3) =  LEFT$ (A$(3),32)
240 B$ = "   " +  RIGHT$ (A$(2),88) + A$(3) + C$
250  PRINT A$: PRINT B$
255  IF K =  > 30 THEN K = 1:KK = KK + 1: PRINT  CHR$ (12): GOTO 95
258 K = K + 2
260 X =  FRE (0)
300  GOTO 105
1000  FOR N = 1 TO 16:M = (N - 1) • 8 + 1
1010 CD$(N) =  MID$ (A$(1),M,8):CD(N) =  VAL (CD$(N))
1020  NEXT N
1030  FOR N = 17 TO 32:M = (N - 17) * 8 + 1
1040 CD$(N) =  MID$ (A$(2),M,8):CD(N) =  VAL (CD$(N))
1050  NEXT N
1060  FOR N = 33 TO 41:M = (N - 33) * 8 + 1
1070 CD$(N) =  MID$ (A$(3),M,8):CD(N) =  VAL (CD$(N))
1080  NEXT N
1090 PW =  INT ((CD(31) • CD(32))):PW$ = "        " +  STR$ (PW):PW$ =  RIGHT$
     (PW$,8)
1100 FV =  INT ((1.000 • CD(35) + 0.04155 * 200.0 • 0.00001933) • 10000) /
     10000:FV$ = "        " +  STR$ (FV):FV$ =  RIGHT$ (FV$,8)
1105  IF CD(21) <  = 0 THEN WG$ = "       0": GOTO 1120
1110 WG =  INT (CD(40) * 1000) / 1000:WG$ = "        " +  STR$ (WG):WG$ =
      RIGHT$ (WG$,8)
1120  IF  VAL (WG$) <  = 0 THEN IV$ = "    ****":EF$ = "    ****":WG$ = "
           0": GOTO 1200
1130 IV =  INT (FV / WG / 0.0000022 * 10) / 10:IV$ = "        " +  STR$ (
     IV):IV$ =  RIGHT$ (IV$,8)
1135  IF  VAL (PW$) <  = 0 THEN EF$ = "    ****": GOTO 1200
1140 EF =  INT (21.810 • FV • IV / PW • 10000) / 100:EF$ = "        " +  STR$
     (EF):EF$ =  RIGHT$ (EF$,8)
1200 C$ = PW$ + FV$ + WG$ + IV$ + EF$
1210  RETURN

]
```

TEST NO. AJ1K004
DATE 11/5/86

TIME	ARC VOLTAGE (VOLTS)	ARC CURRENT (AMPS)	ARC POWER (WATTS)	GAS FLOW (mgm/S)	THRUST (N)	ISP (SEC)	EFF (%)	C* (M/S)	Cf	P in (kPA)	T body (K)	P tank (MICRS)	MAG CURRENT (AMPS)
1.2	60.1	8.28	498	42.3	0.0134	32.2	0.42	594	0.532	93.8	295	33	50
30.3	107.0	7.92	847	42.3	0.1021	246.1	14.54	2106	1.146	332.3	338	145	50
60.3	109.8	8.01	879	42.3	0.1139	274.5	17.44	2250	1.197	355.1	432	154	50
90.3	112.5	8.00	900	42.3	0.1159	279.4	17.66	2324	1.179	366.8	526	163	50
120.3	115.0	8.00	920	42.3	0.1166	281.1	17.48	2385	1.156	376.5	617	173	50
180.1	118.1	7.99	944	42.3	0.1176	283.3	17.32	2507	1.108	395.8	784	184	50
240.2	120.0	8.00	960	42.3	0.1190	286.7	17.42	2595	1.084	409.6	922	196	50
481.0	122.9	8.02	986	42.3	0.1174	282.8	16.52	2669	1.040	421.3	938	196	50
521.1	122.4	8.02	982	42.3	0.1172	282.5	16.55	2669	1.038	421.3	936	196	50
598.4	122.8	8.00	982	42.3	0.1157	278.7	16.09	2673	1.023	422.0	938	196	50

TEST NO. AJ1K005
DATE 11/5/86

TIME (SECS)	ARC VOLTAGE (VOLTS)	ARC CURRENT (AMPS)	ARC POWER (WATTS)	GAS FLOW (MGS/S)	THRUST (N)	ISP (SECS)	EFF (%)	C* (M/S) X10	Cf	P in (kPa)	T body (K)	P tank (MICRS)	MAG CURRENT (AMPS)
THhQ110) > 90 F													
TAS(101) > 1500 F													
6.4	87.6	8.41	736	41.5486	.0544	133.7	4.84	9848	.598	218.9	321	89.4	50.1
12.2	97.1	8.40	815	41.5486	.0793	194.9	9.29	12484	.687	277.5	325.5	168	50.1
18.1	101.1	8.32	841	41.5749	.0889	218.4	11.31	13870	.693	308.5	337.5	153.6	50.1
23.7	104.0	8.12	844	41.6012	.0932	228.8	12.38	14481	.696	322.3	351.1	184.1	50.1
29.4	105.6	8.07	852	41.6275	.0957	234.8	12.92	14813	.698	329.9	367.8	195.5	50.1
34.9	106.9	8.07	862	41.6275	.099	242.9	13.67	15029	.711	334.7	384	195.5	50.1
40.8	107.9	8.04	867	41.6275	.0997	244.6	13.78	15213	.708	338.8	403.3	207.7	50.1
46.7	108.5	8.01	869	41.6537	.0995	243.9	13.68	15360	.699	342.3	421	207.7	50.1
52.1	109.2	8.02	875	41.6537	.1011	247.9	14.03	15481	.705	345	438.4	207.7	50.1
57.6	109.8	8.02	880	41.6537	.1035	253.8	14.63	15607	.716	347.8	455.5	207.7	50.1
63.4	110.6	8.01	885	41.6537	.1024	251.1	14.23	15733	.702	350.6	471.9	207.7	50.1
68.8	111.0	8.01	889	41.6537	.1013	248.4	13.87	15854	.69	353.3	490.2	207.7	50.1
74.2	111.7	8.01	894	41.68	.1055	258.5	14.95	15970	.713	356.1	505.6	220.6	50.1
106.9	114.8	8.02	920	41.68	.1113	272.7	16.16	16557	.725	369.2	604.5	220.6	50.1
157.9	117.0	8.01	937	41.7063	.1137	278.4	16.55	17317	.708	386.4	748.8	234.4	50.1
209.4	119.2	8.01	954	41.7326	.1167	285.6	17.12	17987	.699	401.6	877.6	248.9	50.1
260.3	120.6	8.01	966	41.7326	.1218	298.1	18.42	18449	.711	411.9	981.1	248.9	50.1
311.5	121.7	8.01	974	41.7589	.1225	299.6	18.46	18746	.704	418.8	1057.8	264.4	50.1
362.5	122.3	8.02	980	41.7589	.1267	309.9	19.63	18934	.72	423	1110.6	264.4	50.1
413.3	122.4	8.02	981	41.7851	.1238	302.6	18.71	19074	.698	426.4	1147.2	264.4	50.1
465.0	122.5	8.02	982	41.7851	.1245	304.3	18.9	19168	.699	428.5	1173.2	280.9	50.1
516.1	122.6	8.03	984	41.7851	.1265	309.2	19.48	19199	.709	429.2	1189.9	280.9	50.1
567.4	122.8	8.03	986	41.7851	.125	305.5	18.98	19231	.699	429.9	1200.9	280.9	50.1
618.6	122.9	8.03	986	41.8114	.1283	313.4	19.98	19277	.716	431.2	1208.7	280.9	50.1
669.9	122.9	8.03	986	41.8114	.1276	311.7	19.76	19308	.711	431.9	1213.6	280.9	50.1
721.0	122.7	8.03	985	41.8114	.127	310.2	19.6	19339	.706	432.6	1216.9	280.9	50.1
771.9	122.9	8.03	986	41.8114	.1258	307.3	19.21	19339	.699	432.6	1219.1	280.9	50.1
823.4	123.1	8.03	988	41.8377	.1247	304.4	18.82	19390	.691	434	1220.8	280.9	50.1

TEST NO. AJ1K005
DATE 11/5/86

TIME (SECS)	ARC VOLTAGE (VOLTS)	ARC CURRENT (AMPS)	ARC POWER (WATTS)	GAS FLOW (MGS/S)	THRUST (N)	ISP (SECS)	EFF (%)	C* (M/S) X10	Cf	P in (kPa)	T body (K)	P tank (MICRS)	MAG CURRENT (AMPS)
874.7	123.1	8.03	988	41.8377	.1218	297.3	17.96	19390	.675	434	1222.4	280.9	50.1
925.6	123.5	8.03	991	41.8377	.1234	301.2	18.38	19484	.681	436.1	1223.8	280.9	50.1
976.8	123.3	8.03	990	41.8377	.1214	296.3	17.8	19452	.671	435.4	1225.2	280.9	50.1
1028.1	123.9	8.03	994	41.8377	.1203	293.7	17.42	19452	.665	435.4	1226.8	298.4	50.1
1079.7	124.1	8.03	996	41.864	.1214	296.2	17.69	19529	.668	437.4	1228.3	298.4	50.1
1131.1	124.2	8.04	998	41.864	.1203	293.5	17.33	19529	.661	437.4	1229.7	298.4	50.1
174.9	-0.1	0.02	-1	0	.0104	****	****	504	2.215	11.3	288.9	20.2	0.03
214.4	-0.1	0.01	-1	0	.0676	****	****	504	14.398	11.3	288.8	20.2	0.03
254.7	-0.1	0.01	-1	0	.1012	****	****	504	21.555	11.3	288.8	20.2	0.03
285.1	-0.1	0.01	-1	0	.178	****	****	504	37.914	11.3	288.8	20.2	0.02
299.8	-0.1	0.01	-1	0	.2026	****	****	504	43.153	11.3	288.8	20.2	0.02
317.3	-0.1	0.01	-1	0	.2634	****	****	504	56.104	11.3	288.8	20.2	0.02
323.2	-0.1	0.01	-1	0	.2645	****	****	504	56.338	11.3	288.8	20.2	0.03
352.4	-0.1	0.01	-1	0	.2977	****	****	504	63.41	11.3	288.7	20.2	0.02
374.5	-0.1	0.01	-1	0	.3515	****	****	504	74.869	11.3	288.7	20.2	0.02
400.2	-0.1	0.01	-1	0	.2897	****	****	504	61.706	11.3	288.7	20.2	0.03
406.0	-0.1	0.01	-1	0	.2904	****	****	504	61.855	11.3	288.7	20.2	0.03
427.7	-0.1	0.01	-1	0	.253	****	****	504	53.888	11.3	288.7	20.2	0.03
446.9	-0.1	0.01	-1	0	.2066	****	****	504	44.005	11.3	288.7	20.2	0.03
465.6	-0.1	0.01	-1	0	.1615	****	****	24	34.399	11.3	288.7	20.2	0.03
494.9	-0.1	0.01	-1	0	.1266	****	****	24	26.965	11.3	288.7	20.2	0.02
516.5	-0.1	0.01	-1	0	.062	****	****	24	13.206	11.3	288.7	20.2	0.02
522.3	-0.1	0.01	-1	0	.0622	****	****	24	13.248	11.3	288.7	20.2	0.03
543.8	-0.1	0.01	-1	0	.0248	****	****	24	5.282	11.3	288.6	20.2	0.02
70.5	678.4	0.00	0	0	4.1E-03	****	****	22	.93	10.6	288.5	21.1	50.28
IA(128) < 1 AMP													
6.1	679.4	0.00	0	41.0756	.0328	81.5	****	5378	.667	118.2	288.4	47.6	50.28
12.0	232.8	0.00	0	40.3397	.0355	89.8	****	5574	.71	120.3	288.4	112	50.28

TEST NO. AJ1K016
DATE 11/24/86

TIME (SECS)	ARC VOLTAGE (VOLTS)	ARC CURRENT (AMPS)	ARC POWER (WATTS)	GAS FLOW (MGS/S)	THRUST (N)	ISP (SECS)	EFF (%)	C* (M/S) X10	Cf	P in (kPa)	T body (K)	P tank (MICRS)	MAG CURRENT (AMPS)
DATE: 11/24/86 TIME: 16:23:11													
6.4	112.4	8.13	913	40.2083	.0386	98	2.03	9725	.444	209.2	482.2	57	49.91
12.5	131.6	8.02	1055	40.2083	.0552	140.2	3.59	12547	.492	269.9	483	112	49.76
18.5	138.8	7.95	1103	40.2346	.0613	155.6	4.23	13756	.498	296.1	489.3	153.5	49.66
25.3	142.1	7.94	1128	40.2346	.0654	166	4.71	14332	.51	308.5	500.5	183.9	49.61
32.2	143.0	7.93	1133	40.2346	.0683	173.3	5.12	14620	.522	314.7	515.9	201.2	49.60
38.5	144.4	7.93	1145	40.2609	.0703	178.3	5.36	14773	.531	318.2	530.5	201.2	49.59
45.5	144.8	7.93	1148	40.2872	.0705	178.7	5.37	14888	.528	320.9	548.5	144.6	49.56
52.9	145.1	7.93	1150	40.2872	.071	180	5.44	15018	.527	323.7	566.4	201.2	49.55
60.1	145.5	7.93	1153	40.3135	.071	179.8	5.42	15101	.524	325.7	584.2	201.2	49.55
107.2	147.1	7.94	1167	40.3397	.0707	179	5.31	15666	.503	338.1	696.5	144.6	49.55
158.0	151.6	7.89	1196	40.366	.0712	180.1	5.25	16170	.49	349.2	805.3	201.2	49.54
208.9	152.6	7.87	1200	40.3923	.0719	181.8	5.33	16604	.482	358.8	894.1	201.2	49.51
259.7	153.6	7.88	1210	40.4449	.0722	182.3	5.33	16901	.475	365.7	962.8	201.2	49.48
310.5	154.4	7.91	1221	40.4974	.0725	182.8	5.31	17133	.47	371.2	1014.2	201.2	49.49
361.4	152.6	7.93	1210	40.3923	.0722	182.5	5.33	17372	.462	375.4	1052.4	144.6	49.47
412.2	152.7	7.93	1210	40.3923	.0717	181.3	5.26	17469	.457	377.5	1079.8	144.6	49.46
463.1	152.7	7.93	1210	40.3923	.0728	184	5.42	17561	.461	379.5	1099.2	144.6	49.47
514.0	152.9	7.93	1212	40.3923	.0731	184.8	5.46	17626	.461	380.9	1113.3	144.6	49.47
564.8	153.0	7.93	1213	40.3923	.073	184.6	5.44	17659	.46	381.6	1123.1	144.6	49.47
615.7	153.0	7.93	1213	40.4186	.0733	185.2	5.48	17680	.461	382.3	1130.1	144.6	49.47
666.9	152.9	7.93	1212	40.4186	.0736	186	5.53	17712	.462	383	1134.8	144.6	49.46
717.8	152.8	7.93	1211	40.4186	.0743	187.7	5.64	17744	.466	383.7	1138.4	144.6	49.45
769.0	153.2	7.93	1214	40.4186	.0746	188.5	5.67	17744	.467	383.7	1141	144.6	49.46

TEST NO. AJ1K017
DATE 11/25/86

TIME (SECS)	ARC VOLTAGE (VOLTS)	ARC CURRENT (AMPS)	ARC POWER (WATTS)	GAS FLOW (MGS/S)	THRUST (N)	ISP (SECS)	EFF (%)	C* (M/S)	Cf X10	P in (kPa)	T body (K)	P tank (MICRS)	MAG CURRENT (AMPS)
DATE: 11/25/86 TIME: 15:54:46													
6.6	106.6	8.14	867	38.8943	.0447	117.3	2.96	9126	.566	189.9	306.6	52	50.00
12.6	125.6	8.04	1009	38.9469	.0577	151.3	4.24	11628	.573	242.3	309	97.8	49.98
18.9	133.0	7.98	1061	38.9732	.0638	167.2	4.92	12810	.574	267.1	317.5	128.2	49.93
24.9	136.7	7.94	1085	38.9732	.0683	179	5.52	13405	.588	279.5	329.8	153.5	49.92
31.0	138.7	7.91	1097	38.9995	.0707	185.1	5.84	13760	.592	287.1	344.7	160.6	49.90
37.1	139.8	7.91	1105	38.9995	.0715	187.2	5.93	13995	.589	292	361.1	160.6	49.89
44.8	140.9	7.89	1111	39.0257	.0723	189.2	6.03	14182	.587	296.1	382.3	168	49.88
51.9	141.6	7.89	1117	39.052	.0723	189.1	5.99	14335	.581	299.5	402.5	168	49.88
59.7	142.2	7.88	1120	39.0783	.0727	190	6.04	14459	.578	302.3	425.4	160.6	49.88
102.1	145.6	7.86	1144	39.1309	.0737	192.3	6.07	15133	.559	316.8	541.2	160.6	49.86
153.4	149.2	7.84	1169	39.1834	.074	192.9	5.98	15804	.537	331.3	669.4	160.6	49.86
204.6	151.8	7.83	1188	39.2097	.0738	192.2	5.85	16385	.516	343.7	781.5	153.5	49.85
255.9	153.3	7.82	1198	39.2097	.0744	193.8	5.89	16876	.505	354	875.2	153.5	49.85
317.0	154.8	7.81	1208	39.236	.0746	194.2	5.87	17293	.494	363	962.5	153.5	49.86
417.9	156.9	7.80	1223	39.2623	.0751	195.3	5.87	17772	.484	373.3	1053.5	153.5	49.84
518.7	14.5	0.01	0	0	5.5E-03	****	****	9448	.212	62.3	1082	201.2	49.99

TEST NO. AJ1K018
DATE 11/26/86

TIME (SECS)	ARC VOLTAGE (VOLTS)	ARC CURRENT (AMPS)	ARC POWER (WATTS)	GAS FLOW (MGS/S)	THRUST (N)	ISP (SECS)	EFF (%)	C* (M/S) X10	Cf	P in (kPa)	T body (K)	P tank (MICRS)	MAG CURRENT (AMPS)
DATE: 11/26/86 TIME: 11:06:31													
6.6	70.9	8.23	583	37.6592	.0347	94.1	2.74	7678	.539	154.7	303.2	62.3	49.79
12.7	72.4	8.24	596	37.6855	.0426	115.4	4.04	8630	.589	174	303.8	140.3	49.79
18.7	74.0	8.24	609	37.7117	.0456	123.5	4.53	8966	.606	180.9	309.7	201.2	49.79
25.0	75.0	8.24	618	37.738	.0471	127.4	4.75	9202	.61	185.8	317.6	173.3	49.79
32.1	74.9	8.24	617	37.738	.048	129.9	4.95	9371	.61	189.2	328.8	207.7	49.79
39.0	73.3	8.24	603	37.7643	.0492	133	5.31	9538	.614	192.7	340	207.7	49.79
46.0	73.6	8.24	606	37.7643	.0492	133	5.29	9671	.606	195.4	352.5	220.6	49.79
53.9	74.4	8.24	613	37.7906	.0495	133.7	5.29	9803	.601	198.2	366.7	220.6	49.79
61.3	75.1	8.24	618	37.7906	.0499	134.8	5.33	9971	.595	201.6	378.9	220.6	49.79
107.9	76.1	8.24	627	37.8431	.052	140.3	5.7	10876	.568	220.2	459.8	207.7	49.79
159.1	77.6	8.24	639	37.8694	.0542	146.1	6.07	11826	.544	239.6	542	207.7	49.79
210.1	78.8	8.24	649	37.922	.0551	148.4	6.17	12657	.516	256.8	616.9	207.7	49.79
261.0	80.1	8.24	660	37.9483	.0569	153.1	6.46	13461	.501	273.3	685.8	207.7	49.79
327.0	81.9	8.24	674	37.9745	.0582	156.5	6.62	14402	.478	292.6	764.1	207.7	49.79
427.8	83.3	8.24	686	38.0271	.0597	160.3	6.83	15641	.451	318.2	860.1	207.7	49.78
528.9	85.0	8.24	700	38.0534	.0599	160.7	6.73	16607	.426	338.1	927.1	207.7	49.78
629.7	84.9	8.24	699	38.0797	.0606	162.5	6.9	17308	.413	352.6	969.9	207.7	49.79
730.6	86.0	8.24	708	38.1059	.0605	162.1	6.78	17772	.401	362.3	996.5	207.7	49.78
831.5	86.6	8.24	713	38.1322	.0597	159.9	6.56	18063	.389	368.5	1012.6	220.6	49.78
932.3	86.1	8.24	709	38.1322	.0603	161.5	6.73	18264	.389	372.6	1022.4	220.6	49.78
1033.1	85.9	8.24	707	38.1585	.0602	161.1	6.72	18389	.385	375.4	1027.8	220.6	49.78
1134.3	0.6	0.00	0	0	-3E-03	****	****	11446	-.149	48.6	1007.8	112	49.79

TEST NO. AJ1K019
DATE 11/26/86

TIME (SECS)	ARC VOLTAGE (VOLTS)	ARC CURRENT (AMPS)	ARC POWER (WATTS)	GAS FLOW (MGS/S)	THRUST (N)	ISP (SECS)	EFF (%)	C* (M/S) X10	Cf	P in (kPa)	T body (K)	P tank (MICRS)	MAG CURRENT (AMPS)
PDF2(123) < 25 PSIG													
PDF2(123) < 25 PSIG													
6.8	72.3	8.20	592	37.6066	.0355	96.4	2.83	7967	.533	160.3	334.8	57	49.80
12.9	71.5	8.20	586	37.6329	.0438	118.8	4.35	9020	.58	181.6	335.7	128.2	49.80
19.1	74.1	8.20	607	37.6592	.0472	128	4.87	9390	.6	189.2	340.7	183.9	49.81
25.4	74.6	8.20	611	37.6855	.0478	129.5	4.96	9592	.594	193.4	349.6	153.6	49.81
32.3	74.6	8.20	611	37.6855	.0487	131.9	5.15	9761	.595	196.8	359.9	173.3	49.81
39.4	74.7	8.21	613	37.7117	.0491	132.9	5.21	9923	.59	200.2	372.1	184.1	49.81
46.4	75.3	8.21	618	37.7117	.0495	134	5.26	10027	.588	202.3	384	184.1	49.81
53.6	75.4	8.21	619	37.7117	.0499	135.1	5.33	10200	.583	205.8	396.2	184.1	49.81
60.5	75.9	8.21	623	37.738	.0503	136.1	5.38	10327	.58	208.5	408.6	195.5	49.81
112.0	77.4	8.21	635	37.7643	.0525	142	5.75	11310	.553	228.5	494.2	184.1	49.81
163.0	79.2	8.21	650	37.7906	.0544	147	6.02	12222	.529	247.1	572.5	184.1	49.82
214.2	81.1	8.21	665	37.8431	.0563	151.9	6.3	13059	.512	264.4	645.6	184.1	49.82
265.2	82.0	8.21	673	37.8957	.0573	154.4	6.44	13855	.49	280.9	712	184.1	49.82
316.3	83.3	8.21	683	37.922	.0584	157.3	6.59	14629	.473	296.8	770.6	184.1	49.81
402.4	85.3	8.21	700	37.9745	.0594	159.7	6.64	15692	.448	318.8	852	184.1	49.80
503.4	86.3	8.21	708	38.0271	.0603	161.9	6.75	16688	.427	339.5	920.7	184.1	49.80
604.3	88.1	8.21	723	38.0534	.0604	162.1	6.63	17388	.41	354	965.7	184.1	49.80
705.1	87.6	8.21	719	38.0534	.0609	163.4	6.78	17899	.402	364.4	993.7	184.1	49.80
805.9	88.3	8.21	724	38.0797	.061	163.6	6.75	18221	.395	371.2	1010.7	184.1	49.80
907.1	88.8	8.21	729	38.0797	.0608	163	6.66	18427	.389	375.4	1020.2	195.5	49.81
1008.2	88.7	8.21	728	38.1059	.0617	165.3	6.86	18517	.393	377.5	1026.3	195.5	49.82
1109.0	89.1	8.21	731	38.1059	.0622	166.7	6.95	18581	.395	378.8	1029.7	195.5	49.82

TEST NO. AJ1K023
DATE 11/5/86

TIME	ARC VOLTAGE (VOLTS)	ARC CURRENT (AMPS)	ARC POWER (WATTS)	GAS FLOW (mgm/S)	THRUST (N)	ISP (SEC)	EFF (%)	C* (M/S)	Cf	P in (kPA)	T body (K)	P tank (MICRS)	MAG CURRENT (AMPS)
1.2	56.6	8.28	469	10.0	0.0082	83.6	0.72	2152	0.381	80.3	287	77	50
59.4	95.0	8.19	778	37.2	0.0708	194.0	8.66	1909	0.997	265.0	375	156	50
120.1	95.9	8.19	785	36.6	0.0721	200.8	9.04	2027	0.972	276.8	494	156	50
181.3	95.7	8.19	784	36.4	0.0725	203.0	9.21	2094	0.951	284.4	602	158	50
242.4	99.6	8.19	816	37.1	0.0747	205.2	9.22	2174	0.926	300.9	698	160	50
298.7	101.6	8.19	832	38.1	0.0760	203.3	9.11	2228	0.895	316.8	777	162	50
359.1	107.8	8.19	883	39.9	0.0844	215.6	10.11	2304	0.918	343.0	854	164	50
419.7	115.4	8.19	945	42.5	0.0906	217.3	10.22	2380	0.896	377.5	922	165	50
480.2	118.8	8.19	973	42.7	0.0950	226.8	10.86	2455	0.906	391.2	981	166	50
540.7	122.5	8.18	1002	44.3	0.0994	228.7	11.13	2505	0.896	414.0	1027	165	50
601.2	123.4	8.19	1011	44.5	0.1012	231.8	11.39	2518	0.903	418.1	1062	167	50
661.7	125.3	8.13	1019	45.1	0.1056	238.7	12.14	2550	0.918	429.2	1087	166	50
722.3	126.6	8.12	1028	45.7	0.1082	241.3	12.46	2569	0.922	438.1	1107	167	50
782.9	126.2	8.13	1026	45.9	0.1091	242.3	12.64	2570	0.925	440.2	1124	168	50
843.4	128.2	8.13	1042	47.0	0.1130	245.1	13.03	2589	0.929	454.0	1130	167	50
904.0	129.7	8.13	1054	48.1	0.1175	249.0	13.61	2747	0.889	493.0	1135	168	50
964.6	130.4	8.14	1061	48.0	0.1183	251.2	13.73	2769	0.890	496.0	1141	166	50
1015.1	129.9	8.14	1057	48.0	0.1201	255.1	14.21	2773	0.902	496.7	1148	167	50
1065.6	130.1	8.11	1055	48.0	0.1207	256.3	14.38	2762	0.910	494.7	1153	168	50
1126.2	130.2	8.12	1057	48.0	0.1215	258.0	14.55	2762	0.916	494.7	1155	167	50
1177.0	132.2	8.12	1073	49.8	0.1287	263.4	15.49	2633	0.982	489.2	1158	168	50
1237.4	134.6	8.18	1101	50.2	0.1300	264.0	15.29	2641	0.981	494.7	1163	168	50
1318.2	132.8	8.13	1080	50.3	0.1316	266.7	15.95	2643	0.990	496.0	1167	168	50
1378.7	132.7	8.19	1087	50.6	0.1311	264.1	15.63	2657	0.975	501.6	1169	168	50
1439.4	134.0	8.11	1087	51.9	0.1364	267.9	16.49	2683	0.980	519.5	1171	168	50
1500.1	136.2	8.14	1109	52.5	0.1403	272.4	16.91	2673	1.000	523.6	1173	168	50
1560.7	134.2	8.15	1094	52.5	0.1417	275.1	17.48	2754	0.980	539.5	1176	168	50
1621.3	135.8	8.16	1108	52.4	0.1416	275.5	17.27	2808	0.962	549.1	1177	168	50
1681.9	138.9	8.08	1122	52.4	0.1421	276.4	17.17	2816	0.963	550.5	1177	167	50
1742.5	135.1	8.19	1106	52.4	0.1505	292.8	19.53	2808	1.023	549.1	1177	168	50
1803.1	132.3	8.23	1089	52.4	0.1447	281.5	18.35	2805	0.985	548.4	1177	168	50
1863.8	132.6	8.24	1093	52.4	0.1429	278.0	17.83	2805	0.972	548.4	1178	167	50
1924.4	132.4	8.24	1091	52.4	0.1420	276.2	17.64	2816	0.962	550.5	1179	168	50
1985.0	125.8	8.19	1030	52.4	0.1429	278.0	18.91	2819	0.967	551.2	1179	167	50
2045.6	129.2	8.18	1057	52.7	0.1442	278.9	18.67	2754	0.993	541.6	1179	166	50
2106.5	128.3	8.18	1049	54.3	0.1526	286.5	20.43	2717	1.034	550.5	1181	167	50
2157.1	129.7	8.18	1061	54.1	0.1522	286.8	20.18	2727	1.032	550.5	1183	167	50
2217.8	129.2	8.18	1057	54.0	0.1530	288.8	20.51	2732	1.037	550.5	1186	167	50
2298.6	127.0	8.19	1040	55.3	0.1564	288.3	21.26	2735	1.034	564.3	1189	167	50
2359.5	125.5	8.18	1027	56.8	0.1621	290.9	22.53	2744	1.040	581.5	1193	167	50
2400.1	125.0	8.18	1023	56.7	0.1623	291.8	22.72	2752	1.040	582.2	1195	166	50
2460.8	123.8	8.19	1014	57.1	0.1627	290.5	22.86	2733	1.043	582.2	1196	166	50
2521.5	125.0	8.19	1024	57.6	0.1631	288.6	22.56	2734	1.036	587.7	1196	166	50
2582.2	123.1	8.20	1009	58.9	0.1671	289.2	23.48	2756	1.029	605.7	1200	167	50
2642.9	123.2	8.21	1011	59.0	0.1671	288.7	23.39	2754	1.028	606.4	1204	166	50
2703.9	124.5	8.21	1022	59.0	0.1666	287.8	23.01	2786	1.014	613.3	1207	167	50
2785.1	124.3	8.20	1019	59.0	0.1647	284.6	22.55	2804	0.995	617.4	1207	168	50
2846.1	121.4	8.21	996	59.1	0.1686	290.8	24.15	2756	1.035	607.7	1208	166	50
2917.2	125.8	8.22	1034	61.0	0.1725	288.3	23.59	2788	1.014	634.6	1212	168	50

TEST NO. AJ1K023
DATE 11/5/86

TIME	ARC VOLTAGE (VOLTS)	ARC CURRENT (AMPS)	ARC POWER (WATTS)	GAS FLOW (mgm/S)	THRUST (N)	ISP (SEC)	EFF (%)	C* (M/S)	Cf	P in (kPA)	T body (K)	P tank (MICRS)	MAG CURRENT (AMPS)
2998.5	123.5	8.22	1015	61.2	0.1728	287.8	24.03	2836	0.995	647.7	1211	168	50
3059.0	124.8	8.22	1026	61.1	0.1759	293.5	24.70	2856	1.008	651.2	1210	167	50
3119.9	124.1	8.22	1020	61.1	0.1745	291.1	24.41	2887	0.989	658.1	1211	167	50
3180.8	123.8	8.18	1013	61.1	0.1743	290.7	24.54	2895	0.985	660.1	1211	164	50
3241.7	117.4	8.22	965	61.1	0.1737	289.7	25.57	3047	0.933	694.6	1211	164	50
3302.8	122.1	8.22	1004	62.3	0.1765	288.7	24.90	3041	0.931	707.0	1211	164	50
3363.8	121.8	8.26	1006	63.3	0.1777	286.1	24.78	2915	0.963	688.4	1213	164	50
3424.8	122.5	8.25	1011	63.3	0.1776	286.0	24.65	2909	0.964	687.0	1214	164	50
3485.9	122.6	8.26	1013	63.3	0.1765	284.2	24.29	2959	0.942	698.8	1215	163	50
3546.8	127.2	8.29	1054	65.4	0.1812	282.4	23.80	3013	0.919	735.3	1216	163	50
3607.8	124.8	8.28	1033	65.4	0.1814	282.7	24.34	3010	0.921	734.6	1218	163	50
3668.7	125.8	8.28	1042	65.4	0.1819	283.5	24.28	3019	0.921	736.7	1220	163	50
3717.7	135.0	8.24	1112	65.4	0.1808	281.8	22.47	3041	0.909	742.2	1222	166	50
3780.7	135.7	8.23	1117	65.4	0.1798	280.2	22.13	3050	0.901	744.3	1221	166	50
3841.5	134.8	8.24	1111	65.4	0.1787	278.5	21.98	3047	0.897	743.6	1221	165	50
3902.3	136.0	8.24	1121	65.4	0.1785	278.2	21.74	3044	0.897	742.9	1221	165	50
3963.1	134.6	8.26	1112	66.1	0.1819	280.5	22.52	2945	0.935	726.3	1220	165	50
4024.0	144.3	8.26	1192	67.4	0.1861	281.5	21.56	2976	0.928	748.4	1221	164	50
4084.9	148.0	8.25	1221	67.2	0.1873	284.2	21.38	3004	0.928	753.2	1222	164	50
4145.8	147.7	8.25	1219	67.1	0.1867	283.7	21.32	3014	0.923	754.6	1221	163	50
4206.9	148.7	8.25	1227	67.1	0.1865	283.4	21.13	3028	0.918	758.1	1221	163	50
4257.6	149.0	8.24	1228	67.1	0.1865	283.4	21.12	3028	0.918	758.1	1220	163	50
4318.6	145.6	8.23	1198	65.6	0.1823	283.3	21.15	3243	0.857	793.9	1220	163	50
4379.6	142.8	8.23	1175	65.5	0.1786	278.0	20.73	3251	0.839	794.6	1217	163	50
4440.7	147.0	8.23	1210	65.5	0.1776	276.5	19.91	3245	0.836	793.2	1216	163	50
4501.7	146.8	8.24	1210	65.5	0.1762	274.1	19.58	3243	0.829	792.5	1216	163	50
4583.1	152.6	8.23	1256	65.5	0.1725	268.4	18.08	3243	0.812	792.5	1216	163	55
4644.2	146.6	8.24	1208	65.5	0.1719	267.5	18.66	3240	0.810	791.8	1216	163	50
4705.3	145.9	8.28	1208	65.5	0.1722	267.9	18.73	3240	0.811	791.8	1215	160	45
4766.3	148.0	8.28	1225	65.5	0.1711	266.2	18.23	3240	0.806	791.8	1214	162	45
4827.4	154.9	8.29	1284	65.5	0.1696	263.9	17.09	3243	0.798	792.5	1213	160	41
4857.9	156.7	8.30	1301	65.5	0.1700	264.5	16.96	3251	0.798	794.6	1213	159	40

TEST NO. AJ1K026
DATE 11/5/86

TIME	ARC VOLTAGE (VOLTS)	ARC CURRENT (AMPS)	ARC POWER (WATTS)	GAS FLOW (mgm/S)	THRUST (N)	ISP (SEC)	EFF (%)	C* (M/S)	Cf	P in (kPA)	T body (K)	P tank (MICRS)	MAG CURRENT (AMPS)
3.9	75.2	8.17	614	31.0	0.0224	73.7	1.32	1219	0.593	141.0	349	88	50
61.8	101.9	8.17	833	35.8	0.0705	200.7	8.34	2358	0.835	315.0	446	154	50
119.8	103.9	8.17	849	35.2	0.0728	210.8	8.87	2497	0.828	328.0	564	156	50
180.5	117.3	8.27	970	41.1	0.0913	226.4	10.45	2655	0.837	407.1	683	155	50
241.3	125.3	8.19	1026	44.9	0.1053	239.1	12.03	2714	0.864	454.7	797	159	50
302.2	129.0	8.19	1057	45.8	0.1121	249.5	12.99	2838	0.862	485.0	899	162	50
360.4	140.3	8.19	1149	51.3	0.1329	264.1	14.98	3027	0.856	579.5	982	159	50
421.5	147.4	8.19	1207	55.3	0.1527	281.5	17.46	3111	0.888	642.0	1056	159	50
479.6	146.7	8.21	1204	55.2	0.1550	286.2	18.07	3141	0.894	647.0	1111	162	50
540.5	147.4	8.21	1210	55.0	0.1559	288.9	18.26	3178	0.892	652.3	1151	160	50
601.5	160.6	8.35	1341	58.9	0.1681	290.9	17.89	3220	0.886	707.7	1183	162	50
659.6	160.1	8.36	1338	58.7	0.1686	292.8	18.09	3247	0.885	711.2	1204	163	50
720.6	158.6	8.57	1359	58.7	0.1699	295.0	18.09	3266	0.886	715.3	1220	163	50
781.5	164.9	8.58	1415	62.1	0.1794	294.5	18.32	3295	0.877	763.6	1231	163	50
839.7	165.4	8.56	1416	62.1	0.1830	300.4	19.04	3331	0.885	771.8	1242	163	50
919.9	167.3	8.33	1394	61.9	0.1839	302.8	19.60	3363	0.883	776.7	1249	163	50
980.8	167.6	8.21	1376	61.7	0.1835	303.2	19.83	3385	0.878	779.4	1250	163	50
1041.7	159.2	8.10	1290	61.5	0.1853	307.1	21.65	3412	0.883	782.9	1250	163	50
1102.6	159.4	8.00	1275	61.4	0.1857	308.3	22.02	3426	0.883	784.9	1249	163	50
1160.8	160.5	8.00	1284	61.4	0.1866	309.8	22.08	3420	0.889	783.6	1248	163	50
1221.8	159.7	8.00	1278	60.4	0.1851	312.4	22.20	3455	0.887	778.7	1248	163	50
1279.9	155.3	7.98	1239	58.3	0.1773	310.0	21.75	3434	0.886	747.0	1246	160	50
1340.9	156.4	7.83	1225	58.1	0.1743	305.8	21.35	3452	0.869	748.4	1243	164	50
1399.1	157.9	7.74	1222	58.2	0.1723	301.8	20.87	3446	0.859	748.4	1241	163	50
1460.0	166.1	7.65	1271	65.0	0.1865	292.5	21.06	3444	0.833	835.3	1239	163	50
1521.0	164.5	7.75	1275	63.5	0.1835	294.6	20.80	3618	0.799	857.3	1241	163	50
1579.2	160.4	7.74	1241	60.5	0.1774	298.9	20.95	3926	0.747	886.3	1242	163	50
1640.2	153.4	7.71	1183	55.8	0.1641	299.8	20.40	4402	0.668	916.6	1239	163	50
1701.2	156.8	7.59	1190	55.8	0.1620	295.9	19.76	4399	0.660	916.0	1235	163	50
1762.2	157.7	7.46	1176	55.8	0.1595	291.4	19.38	4396	0.650	915.3	1231	164	50
1820.4	149.2	7.48	1116	50.7	0.1421	285.7	17.84	5006	0.560	947.0	1227	163	50
1881.4	149.4	7.48	1118	50.7	0.1373	276.1	16.64	5002	0.541	946.3	1222	163	50
1939.7	149.5	7.48	1118	50.7	0.1358	273.0	16.26	4998	0.536	945.6	1220	163	50
2000.7	145.1	7.96	1155	50.7	0.1333	268.0	15.17	4998	0.526	945.6	1220	163	50
2061.8	151.7	8.11	1230	55.5	0.1402	257.5	14.39	4842	0.522	1002.8	1225	163	50
2120.0	165.4	8.11	1341	64.1	0.1748	278.0	17.77	4167	0.654	996.6	1234	163	50
2181.1	163.2	8.28	1351	64.1	0.1714	272.6	16.96	4163	0.642	995.6	1244	163	50
2236.6	160.3	8.68	1391	64.1	0.1704	271.0	16.28	4164	0.638	995.9	1254	163	50

```
]LIST

10  REM  PROGRAM SETS COMPUTER CONTROLS ON 1KW ARCJET
20  REM  "PORELAY4"
30  REM  C.M.GRACEY  11/26/86
32  REM  TURNS VALVE ON & OFF
35  HOME
40  PRINT  CHR$ (4)"BLOAD OPTOMUX.OBJ/$4000,A$4000"
45 ER% = 0:SN% = 4:TD% = 0:RC% = 10: POKE 20506,0: HIMEM: 16383
50  POKE 49366,128: POKE 49366,128
52 T$ = "1KW ARCJET CONTROLLER"
100 T1 = 1000
130 DN =  INT (T1 / 10): GOSUB 1000:Z1$ = "Z0001H" + Z$
290 X =  FRE (0)
295  PRINT : PRINT "HIT ";: FLASH : PRINT "<SPACE BAR> KEY ";: NORMAL : PRINT
     "TO START"
297  GET A$: PRINT  CHR$ (1)
298  IF A$ <  > " " THEN 297
299  PRINT  CHR$ (1)
300  GOSUB 3000
305  HOME : PRINT T$: PRINT : PRINT "SYSTEM AWAITING START COMMAND..."
308  PRINT : PRINT "TO ACTIVATE SYSTEM PRESS ";: FLASH : PRINT "START SWI
     TCH": NORMAL
309  PRINT  CHR$ (1)
310  IF  PEEK (49251) > 127 THEN 310
311  PRINT T$: PRINT
312  HOME : PRINT "SYSTEM AWAITING CURRENT START..."
313 X =  PEEK (49361)
314  IF  PEEK (49361) > 200 THEN  VTAB 5: HTAB 1: FLASH : PRINT "RESET CU
     RRENT ALARM": NORMAL : GOTO 313
315  VTAB 5: HTAB 1: PRINT "                    "
318  IF  PEEK (49361) < 200 THEN 318
319  IF  PEEK (49251) > 100 THEN 312
320  HOME : PRINT T$: PRINT : PRINT "SYSTEM NOW OPERATING..."
340  GOSUB 4000
350  HOME : PRINT T$: PRINT : PRINT "SYSTEM NOW SHUTDOWN..."
360  IF  PEEK (49360) > 200 THEN  VTAB 5: HTAB 1: FLASH : PRINT "ALARMS I
     NDICATED": NORMAL
370 CM$ = "L0001": GOSUB 5000
380  GOTO 295
1000  REM  CONVERT NUMBER TO HEX
1010 Y1 =  INT (DN / 4096):Y = Y1: GOSUB 2000:X1$ = Z$
1020 Y2 =  INT ((DN - Y1 * 4096) / 256):Y = Y2: GOSUB 2000:X2$ = Z$
1030 Y3 =  INT ((DN - Y1 * 4096 - Y2 * 256) / 16):Y = Y3: GOSUB 2000:X3$ =
     Z$
1040 Y4 =  INT (DN - Y1 * 4096 - Y2 * 256 - Y3 * 16):Y = Y4: GOSUB 2000:X
     4$ = Z$
1050 Z$ = X1$ + X2$ + X3$ + X4$
1060  RETURN
2000  IF Y = 0 THEN Z$ = "0": RETURN
2010  IF Y < 10 THEN Z$ =  STR$ (Y): RETURN
2020  IF Y = 15 THEN Z$ = "F": RETURN
2030  IF Y = 14 THEN Z$ = "E": RETURN
2040  IF Y = 13 THEN Z$ = "D": RETURN
2045  IF Y = 12 THEN Z$ = "C": RETURN
2050  IF Y = 11 THEN Z$ = "B": RETURN
2060  IF Y = 10 THEN Z$ = "A": RETURN
3000 AD% = 253:CM$ = "A": GOSUB 5000:CM$ = "G0001": GOSUB 5000
```

```
3010 CM$ = Z0$: GOSUB 5000
3110  RETURN
4000 CM$ = "K0001": GOSUB 5000
4002  FOR X = 1 TO 1000
4004  IF  PEEK (49360) < 200 THEN  VTAB 5: HTAB 1: PRINT "NO ALARMS INDIC
     ATED"
4006  IF  PEEK (49360) > 200 THEN  VTAB 5: HTAB 1: FLASH : PRINT "ALARMS
     INDICATED": NORMAL
4008  NEXT X
4010  IF  PEEK (49360) > 200 THEN 4030
4020  IF  PEEK (49251) > 100 THEN 4030
4025  GOTO 4010
4030  RETURN
5000  CALL 16384: IF ER% = 0 THEN  GOTO 5010: PRINT "ERROR MESSAGE= "ER%
5010 ME$ = "": FOR C = 0 TO RC%
5020 ME$ = ME$ +  CHR$ ( PEEK (20576 + C)): NEXT C
5030  RETURN

]
```

```
]LIST

10  REM  PROGRAM SUMMARIZES 1KW ARCJET DATA IN METRIC UNITS
20  REM   "ARCSUML3"
30  REM  C..GRACEY  12/18/86
35  HIMEM: 40000
40  DIM CD$(50),CD(50),A$(10)
42  HOME
44  INPUT "VOLUME NO. ";VN
45  FOR N = 1 TO 3:A$(N) = "": NEXT N
46  PRINT  CHR$ (4)"BLOAD READWRIT.OBJ,S7,V2"
48  POKE 769,VN: POKE 773,2
49  CALL 768
50 NC = 8:K = 1:KK = 1:JJ = 1
52 W$ = "TIME      ARC       ARC       ARC       GAS       THRUST    ISP
          EFF       C*        Cf        P in      T body    P tank    MA
    G"
55 X$ = "          VOLTAGE   CURRENT   POWER     FLOW
                                                                       CU
    RRENT"
60 Y$ = "(SECS)    (VOLTS)   (AMPS)    (WATTS)   (MGS/S)   (N)       (SEC
    S)    (%)       (M/S)               (kPa)     (K)       (MICRS)   (A
    MPS)"
64  INPUT "TEST NO. ";TN$
65  INPUT "DATE ";DA$
68  PRINT  CHR$ (4)"PR#2"
70  PRINT  CHR$ (9)"1D"
72  PRINT  CHR$ (9)"7P"
74  PRINT  CHR$ (9)"1T"
76  PRINT  CHR$ (9)"Z"
78  PRINT  CHR$ (27)"E"
80  PRINT  CHR$ (27)"&l10"
82  PRINT  CHR$ (27)"(s16.66H"
84  PRINT  CHR$ (27)"&s0C"
88  PRINT  CHR$ (12)
90  CALL 768:I = 511
95  IF J = 192 THEN  PRINT  CHR$ (4)"PR#0": END
96  PRINT  SPC( 80)"PAGE NO. "KK: PRINT : PRINT "TEST NO. "TN$: PRINT "DA
    TE "DA$
97  PRINT
98  PRINT  SPC( 3)W$: PRINT  SPC( 3)X$: PRINT  SPC( 3)Y$
100  PRINT
105  FOR N = 1 TO 3
110 A$(N) = ""
115  IF I = 767 THEN I = 511: CALL 786
120 J =  PEEK (I + 1): IF J = 192 THEN  PRINT  CHR$ (12): PRINT  CHR$ (4)
    "PR#0": END
122  IF J = 135 THEN I = I + 1: GOTO 105
125  IF J = 141 THEN I = I + 1: GOTO 200
130 A$(N) = A$(N) +  CHR$ (J - 128):I = I + 1: GOTO 115
200  IF  LEN (A$(N)) = 72 THEN 220
201  IF  LEN (A$(N)) <  > 128 THEN D$ = A$(N): GOTO 105
206  IF  LEN (A$(N)) <  > 128 THEN 105
210  NEXT N
220  IF N < 3 THEN 105
230 A$ = A$(1) +  LEFT$ (A$(2),40)
235  GOSUB 1000
236  IF CD(1) < 1 THEN  PRINT D$:C$ = "START": GOTO 255
```

```
237  IF C$ <  > "START" THEN 105
238 JJ = JJ + 1: IF JJ < 11 THEN 105
239 JJ = 1
240 A$ = CD$(1) + "  " + CD$(32) + "  " + CD$(31) + PW$ + "  " + WG$ + "
      " + FV$ + "  " + IV$ + "  "
242 B$ = EF$ + "  " + CS$ + "  " + CF$ + "  " + PI$ + "  " + CD$(2) + "
    " + PT$ + "  " + CD$(30) + "  "
250  PRINT A$ + B$
255  IF K =  > 30 THEN K = 1:KK = KK + 1: PRINT  CHR$ (12): GOTO 95
258 K = K + 1
260 X =  FRE (0)
300  GOTO 105
1000  FOR N = 1 TO 16:M = (N - 1) * 8 + 1
1010 CD$(N) =  MID$ (A$(1),M,8):CD(N) =  VAL (CD$(N))
1020  NEXT N
1030  FOR N = 17 TO 32:M = (N - 17) * 8 + 1
1040 CD$(N) =  MID$ (A$(2),M,8):CD(N) =  VAL (CD$(N))
1050  NEXT N
1060  FOR N = 33 TO 36:M = (N - 33) * 8 + 1
1070 CD$(N) =  MID$ (A$(3),M,8):CD(N) =  VAL (CD$(N))
1072  NEXT N
1074  IF CD(27) < 6 THEN 1078
1076 PT =  INT ( EXP ((17.7735 - CD(27)) / 2.21947) * 10) / 10:PT$ = "
        " +  STR$ (PT):PT$ =  RIGHT$ (PT$,8)
1077  GOTO 1082
1078 PT =  INT ( EXP ((14.1415 - CD(27)) / 1.65685) * 10) / 10:PT$ = "
        " +  STR$ (PT):PT$ =  RIGHT$ (PT$,8)
1082 FS =  - CD(1) * (.0002 - .0006) / 784.3 + .0002
1090 PW =  INT ((CD(31) * CD(32))):PW$ = "       " +  STR$ (PW):PW$ =  RIGHT$
    (PW$,8)
1100 FV =  INT ((0.900 * (CD(35) - FS) + 0.04155 * PT * 0.00001933) * 4.4
    5 * 10000) / 10000:FV$ = "       " +  STR$ (FV):FV$ =  RIGHT$ (FV$,
    8)
1105  IF CD(21) <  = 0 THEN WG$ = "       0": GOTO 1120
1110 WG =  INT ((0.219 * (CD(21) + 14.7)) * 1.2 * 10000) / 10000:WG$ = "
         " +  STR$ (WG):WG$ =  RIGHT$ (WG$,8)
1120  IF  VAL (WG$) <  = 0 THEN IV$ = "    *****":EF$ = "    *****":WG$ = "
          0": GOTO 1145
1130 IV =  INT (FV / WG / 0.0000022 / 4.45 * 10) / 10:IV$ = "       " +
     STR$ (IV):IV$ =  RIGHT$ (IV$,8)
1135  IF  VAL (PW$) <  = 0 THEN EF$ = "    *****": GOTO 1145
1140 EF =  INT (21.810 * FV * IV / 4.45 / PW * 10000) / 100:EF$ = "
      " +  STR$ (EF):EF$ =  RIGHT$ (EF$,8)
1145 PI =  INT ((CD(25) + 14.65) * 6.895 * 10) / 10:PI$ = "       " +  STR$
    (PI):PI$ =  RIGHT$ (PI$,8)
1147  IF WG <  = 0 THEN CS$ = "    *****":CF$ = "    *****": GOTO 1210
1150 CS =  INT (6068.9 * PI / WG * .308):CS$ = "       " +  STR$ (CS):CS
    $ =  RIGHT$ (CS$,8)
1155 CF =  INT (FV / PI * 2406.9 * 1000) / 1000:CF$ = "       " +  STR$
    (CF):CF$ =  RIGHT$ (CF$,8)
1160  IF FV > .1 THEN FV$ = "    *****":IV$ = "    *****":EF$ = "    *****":
    CF$ = "    *****"
1170 CD(2) =  INT ((CD(2) + 460) / 1.8 * 10) / 10:CD$(2) = "       " +  STR$
    (CD(2)):CD$(2) =  RIGHT$ (CD$(2),8)
1210  RETURN

]
```